Interface frictional characteristics of non-woven geotextile - Sabkha and - sand using pull-out tests.

Syed Muhammad Ali

Civil Engineering

September 1999

Abstract

Sabkha soil is widely spread along the Arabian Gulf and Red Sea coasts and is found to be a problematic soil due to its acute water sensitivity and chemical aggressiveness. In many situations, there is a need to improve the load carrying capacity of sabkha and the use of geotextile for such purpose was found appropriate. The lack of information regarding pull-out resistance of locally available geotextiles embedded within local soils including sand and sabkha led to this experimental research program. The objectives of this research were to study frictional characteristics of sand-geotextile-sand and sabkha-geotextile-sand interfaces and to compare the pull-out resistance of locally available non-woven geotextiles taking into account different test parameters. A detail literature review was carried out to determine the parameters that strongly affect the pull-out characteristics. An experimental setup was then developed in soil laboratory at KFUPM to conduct the pull-out tests. Normal applied pressure, geotextile type, geotextile length, water content and soil type were the five parameters that were considered in this investigation.

Strength test results indicated that the strength of sabkha decreases with the increase in moisture content where the angle of internal friction decreases by up to 8° upon soaking. Pull-out test results have indicated the existence of three stages of deformation in the geotextile under pull-out testing, which ultimately leads to the slippage of the entire length of the geotextile. This condition was labeled the residual state. The Interface characteristics were determined for this state, which is considered a limit for the pull-out resistance at failure. The use of the pull-out plate reduces the effects of the lateral earth pressure developed on the front wall of the pull-out box. Furthermore, the plate insures that the free geotextile is kept within the box and thus under the applied confinement, throughout the test. The pull-out tests results also indicated that the geotextile having high tensile strength takes large pull-out force in the case of sand-geotextile-sand interface whereas, the least extensible geotextile takes the maximum pull-out force in the case of sabkha-geotextile-sand interface. It was also found that the surface texture and extensibility of the geotextile are the two main factors, in addition to the mass per unit area of the geotextile, in the case of sabkha-geotextile-sand interface. The results indicated that the interface interaction factor is not constant but depends on the normal pressure, the geotextile type and the moisture content of the sabkha soil. Furthermore, the results indicated that soaking of the bottom sabkha layer improved the shear stresses mobilized on the sabkha-geotextile interface.

Interface Frictional Characteristics of Non-woven Geotextile – Sabkha and Sand using Pull-out Tests

by

Syed Muhammad Ali

A Thesis Presented to the

FACULTY OF THE COLLEGE OF GRADUATE STUDIES

KING FAHD UNIVERSITY OF PETROLEUM & MINERALS

DHAHRAN, SAUDI ARABIA

In Partial Fulfillment of the
Requirements for the Degree of

MASTER OF SCIENCE

In

CIVIL ENGINEERING

September, 1999

INFORMATION TO USERS

This manuscript has been reproduced from the microfilm master. UMI films the text directly from the original or copy submitted. Thus, some thesis and dissertation copies are in typewriter face, while others may be from any type of computer printer.

The quality of this reproduction is dependent upon the quality of the copy submitted. Broken or indistinct print, colored or poor quality illustrations and photographs, print bleedthrough, substandard margins, and improper alignment can adversely affect reproduction.

In the unlikely event that the author did not send UMI a complete manuscript and there are missing pages, these will be noted. Also, if unauthorized copyright material had to be removed, a note will indicate the deletion.

Oversize materials (e.g., maps, drawings, charts) are reproduced by sectioning the original, beginning at the upper left-hand corner and continuing from left to right in equal sections with small overlaps.

Photographs included in the original manuscript have been reproduced xerographically in this copy. Higher quality 6" x 9" black and white photographic prints are available for any photographs or illustrations appearing in this copy for an additional charge. Contact UMI directly to order.

Bell & Howell Information and Learning
300 North Zeeb Road, Ann Arbor, MI 48106-1346 USA

UMI®
800-521-0600

Interface Frictional Characteristics of Non-woven Geotextile - Sabkha and - Sand using Pull-out Tests

BY

Syed Muhammad Ali

A Thesis Presented to the

DEANSHIP OF GRADUATE STUDIES

KING FAHD UNIVERSITY OF PETROLEUM & MINERALS

DHAHRAN, SAUDI ARABIA

In Partial Fulfillment of the
Requirements for the Degree of

MASTER OF SCIENCE

In

Civil Engineering

September 1999

KING FAHD UNIVERSITY OF PETROLEUM AND MINERALS
DHAHRAN 31261, SAUDI ARABIA

DEANSHIP OF GRADUATE STUDIES

This thesis, written by **Mr. Syed Muhammad Ali** under the direction of his Thesis Advisor and approved by his Thesis Committee, has been presented to and accepted by the Dean of Graduate Studies, in partial fulfillment of the requirements for the degree of **MASTER OF SCIENCE** in **Civil Engineering (Geotechnical)**

Thesis Committee

Dr. Saad A. Aiban (Chairman)

Dr. Omar S. B. Al-Amoudi (Member)

Dr. S. N. Abduljauwad (Member)

Dr. S. N. Abduljauwad
Department Chairman

Dr. Abdallah M. Al-Shehri
Dean of Graduate Studies

16-10-99
Date


بسم الله الرحمن الرحيم

This Humble work is Dedicated to:

My Parents, Sisters and Brothers

Acknowledgments

All praise and thanks be to Allah, the Most Gracious, the Most merciful; the Almighty, whose blessings and help are all the time with me and He is the only one who helps and His help is the best of all. Peace and blessings of Allah be upon the messenger of Allah prophet Muhammad (peace be upon him).

I am deeply thankful to KFUPM and the Department of Civil Engineering for providing facilities to conduct this research. I wish to express my sincere gratitude and thanks to my thesis advisor Dr. Saad A. Aiban for his valuable guidance, support and encouragement during this research. I would also like to thank my other committee members, Dr. Omar S. B. Al-Amoudi and Dr. S. N. Abduljauwad, for their valuable suggestions and support in the course of this work.

I would like to express special thanks to the KFUPM library staff, Dr. Moid A. Siddiqui and Syed Mansoor Shah of Reference and Information section, for providing me help in finding literature on inter-library loan basis. My special thanks are due to Mr. Hassan Zakariya, the technician in the Geotechnical laboratory of the civil engineering department, for his continuous help in the construction of the experimental setup and during the execution of the experimental work. I would also like to thank all my seniors Asad-ur-Rehman, Kalim sahib and friends Khuram, Imran, Zaki for their continuous help. Last, but not the least, I extend my thanks to all my family members for their moral support, patience, encouragement, and prayers throughout my studies.

Table of Contents

List of Tables

List of Figures

Abstract

Name: Syed Muhammad Ali

Title: Interface Frictional Characteristics of Non-woven Geotextile - Sabkha and - Sand using Pull-out Tests

Major Field: Civil Engineering (Geotechnical)

Date of Degree: September 1999

Sabkha soil is widely spread along the Arabian Gulf and Red Sea coasts and is found to be a problematic soil due to its acute water sensitivity and chemical aggressiveness. In many situations, there is a need to improve the load carrying capacity of sabkha and the use of geotextile for such purpose was found appropriate. The lack of information regarding pull-out resistance of locally available geotextiles embedded within local soils including sand and sabkha led to this experimental research program. The objectives of this research were to study frictional characteristics of sand–geotextile–sand and sabkha–geotextile–sand interfaces and to compare the pull-out resistance of locally available non-woven geotextiles taking into account different test parameters. A detail literature review was carried out to determine the parameters that strongly affect the pull-out characteristics. An experimental setup was then developed in soil laboratory at KFUPM to conduct the pull-out tests. Normal applied pressure, geotextile type, geotextile length, water content and soil type were the five parameters that were considered in this investigation.

Strength test results indicated that the strength of sabkha decreases with the increase in moisture content where the angle of internal friction decreases by up to 8° upon soaking. Pull-out test results have indicated the existence of three stages of deformation in the geotextile under pull-out testing, which ultimately leads to the slippage of the entire length of the geotextile. This condition was labeled the residual state. The Interface characteristics were determined for this state, which is considered a limit for the pull-out resistance at failure. The use of the pull-out plate reduces the effects of the lateral earth pressure developed on the front wall of the pull-out box. Furthermore, the plate insures that the free geotextile is kept within the box and thus under the applied confinement, throughout the test. The pull-out tests results also indicated that the geotextile having high tensile strength takes large pull-out force in the case of sand–geotextile–sand interface whereas, the least extensible geotextile takes the maximum pull-out force in the case of sabkha–geotextile–sand interface. It was also found that the surface texture and extensibility of the geotextile are the two main factors, in addition to the mass per unit area of the geotextile, in the case of sabkha–geotextile–sand interface. The results indicated that the interface interaction factor is not constant but depends on the normal pressure, the geotextile type and the moisture content of the sabkha soil. Furthermore, the results indicated that soaking of the bottom sabkha layer improved the shear stresses mobilized on the sabkha–geotextile interface.

Master of Science Degree
Department of Civil Engineering
King Fahd University of Petroleum and Minerals
Dhahran, Saudi Arabia

September 1999

الخلاصة

الاسم: سيد محمد علي
عنوان البحث: الخواص الاحتكاكية بين الأنسجة (الألياف) الاصطناعية باستخدام اختبارات الشد
التخصص: الهندسة المدنية (جيوتقنية)
تاريخ نيل الدرجة: سبتمبر ١٩٩٩م

تنتشر تربة السبخة بصورة واسعة على ساحلي الخليج العربي والبحر الأحمر، وهـــذه التربـــة معروفـــة بمشاكلها العديدة بسبب حساسيتها المفرطة للماء، وتفاعلاتها الكيميائية القوية مع المنشآت، وفي كثير مـــن الأحيان تكون هناك حاجة لتحسين قوة التحمل للسبخة، وقد وُجد أن استخدام الأنسجة الاصطناعيـــة غـــير المحاكة، مناسباً لهذا الغرض. ونظراً لقلة المعلومات عن الخواص الاحتكاكية بين بعـــض أنـــواع التربـــة المحلية في شرق المملكة مثل السبخة والرمال، والأنسجة الاصطناعية غير المحاكة، فقد تقرر القيام بعمـــل دراسة لإيجاد هذه الخواص. وتتلخص أهداف البحث في دراسة الخواص الاحتكاكية بين الرمل-الأنســـجة-الرمل، والسبخة-الأنسجة-الرمل، ومن ثم مقارنة مقاومة السحب لعدد من الأنسجة المتوفرة محلياً. وقد تـــم تحديد العوامل المؤثرة على خواص الاحتكاك بعد إجراء بحث أدبي مستفيض، كما تم استحداث وتصنيـــع التجهيزات المخبرية في معامل الهندسة المدنية بجامعة الملك فهد للبترول والمعـــادن، وقـــد أخـــذ بعيـــن الاعتبار تأثير العوامل الخمسة التالية: مقدار الضغط الطبيعي، ونوع النسيج وطوله، ونسبة الماء، ونـــوع التربة.

وقد أظهرت نتائج الاختبارات أن قوة تحمل السبخة تتناقص كلما زادت نسبة الماء فـــي العينـــات وأن زاوية الاحتكاك الداخلي قد تتناقص بمقدار ثمان درجات عندما يتم غمر العينات بالماء. كما أظـــهرت نتائج الاختبارات وجود ثلاث مراحل للتشويه الناتج عن اختبارات الاحتكاك عن طريـــق الســـحب، التـــي تنتهي عادة إلى الانزلاق التام للنسيج، وهذا ما يسمى بالحالة القصوى التي تعد الحد الأقصى لمدى التحمـــل أثناء الشد بعد حدوث الانزلاق، وقد تم استخدام صفيحة معدنية تمتد داخل صندوق الاختبار لتثبيت النســـيج عليها، ووجد أنها تقلل تأثير الضغط الجانبي الناتج من الوجه الأمامي للصندوق، إضافة إلى ذلـــك، فـــإن الصفيحة تضمن وجود النسيج كاملا دائماً داخل الصندوق وتحت تأثير الضغط الطبيعي أثناء عملية الشـــد. وقد دلت نتائج اختبارات الشد على أن النسيج القوي يتحمل قوة سحب أكثر من النسيج الضعيـــف، عندمـــا يكون النسيج بين طبقتين من الرمل. بينما يكون النسيج ذو الاستطالة الأصغر أكـــثر تحمـــلاً عندمـــا يتـــم وضعه بين طبقة من السبخة وأخرى من الرمل، مقارنة بالنسيج الأقوى، الذي له استطالة أكبر. كما دلـــت النتائج على أن طبيعة سطح النسيج واستطالته هما العنصران الهامان إضافة إلى الثقل، والسماكة، وذلـــك عندما يتم استخدام النسيج بين تربة السبخة والرمل. كما أظهرت النتائج أن معامل التفـــاعل ليـــس ثابتـــاً، ولكن يتأثر بمقدار الضغط الطبيعي، ونوع النسيج، ونسبة الماء في تربة السبخة، إضافة إلى ذلـــك دلـــت النتائج على أن غمر طبقة السبخة السفلى بالماء يُحسن من قوة تحمل الأنسجة التي على السطح.

درجة الماجستير
قسم الهندسة المدنية
جامعة الملك فهد للبترول والمعادن
الظهران، المملكة العربية السعودية
سبتمبر ١٩٩٩م

CHAPTER 1

INTRODUCTION

During the last two decades, the Arabian Gulf countries have gone through a spectacular phase of both industrialization and infrastructure establishment. Due to the lack of proper quality soils and unfamiliarity with the inferior properties of the available soils, unexpected constructional and post constructional problems have been observed in some projects. Some of the problems reported in the literature include depressions and settlement in roads, loss of subgrade support, penetration of base material into weak subgrade, high collapse potential and low bearing capacity of sabkha and marl soils. (Aiban et al., 1994). Paved roads constructed on sabkha subgrade in the Eastern Province of Saudi Arabia suffered from major damages due to the poor load bearing capacity of sabkhas and the dissolution of salt upon saturation (Abduljauwad et al., 1994). The increasing number of construction projects and the lack of good quality soil for use in these projects in eastern

Saudi Arabia necessitate the improvement of the available marginal soils prior to any construction. (Abduljauwad et al., 1994).

The large extent of sabkha in eastern Saudi Arabia emphasizes its uses for road construction and foundations. Russell (1974) indicated that sabkha had been used for unpaved road construction in the Arabian peninsula. Akili et al. (1978) reported that many parts within the sabkha area were designated as construction sites because of their proximity to industrial areas or population centers. In Saudi Arabia, large investment has been placed in constructing high quality roads. Inevitably, some of these roads were located in sabkha area and, therefore, the pavements were subjected to many problems of cracking, rutting, and depression due to the variability of sabkha from one location to another (Aiban et al., 1994). The problems associated with these soils are highly challenging and their consequences are not yet fully understood. Such a situation presents an unacceptable risk in normal practice and calls for the improvement of geotechnical properties of such soils prior to any construction. (Al-Amoudi et al., 1995)

Different ground improvement techniques have been used in large-scale construction projects in eastern Saudi Arabia to avoid the constructional and post constructional problems. The techniques used include mechanical modification, hydraulic modification, chemical stabilization and modification by inclusion and confinement. Aiban et al. (1994) reported that reinforcement by means of geosynthetic materials, fibers, strips, bars, meshes, soil nailing and anchors have been used in many projects throughout the world. However, geotextiles are mostly used in Saudi Arabia for shore protection, to prevent the erosion of fines along the shoreline or undermining of coastal slope.

1.1 Improvement Using Geosynthetic Materials

During the last twenty years there has been an increasing demand for the use of different geosynthetic materials in separation, reinforcement, erosion control, filtration, drainage and waterproofing. These materials gain popularity due to the relative ease and quick construction as well as for their economic advantages. The acceptance of these materials as improvement techniques necessitates further research on their properties, uses, and performance evaluation. There have been many conferences and publications discussing issues related to geosynthetics. The major ones include the six International Conferences on Geosynthetics, since 1982.

Geotextiles, as known and used today, were first used in connection with erosion control applications in early 1950s (Koerner, 1997). They are defined by ASTM D 4439 as any permeable textile material used with soil, rock or any other geotechnical engineering related material, as an integral part of a man-made project, structure or system. With the availability of competent geotextiles, the use of geotextile in many engineering applications has become more apparent and proven to be an effective means of soil improvement (Espinoza, 1994). These materials are used worldwide in many areas of civil engineering such as transportation infrastructures, coastal protection, retaining walls, earth dams, embankments, silt-fences, clay liners, landfills, railroads, drainage, sport fields and vertical drains, etc.

1.2 Statement of the Problem

Sabkha is a term generally used to describe salt-encrusted surfaces and the material that forms these flats (Ellis, 1973). Sabkha is widely distributed in the Arabian peninsula, especially in the well populated cities along the Arabian Gulf and the Red Sea coasts (Al-Amoudi et al., 1992b). Saudi Arabia has a large number of sabkhas. Both coastal and continental sabkhas are found in the eastern province of Saudi Arabia. Sabkha terrain constitutes roughly about one fourth of the eastern Saudi surfacial soils (Aiban et al., 1998). Sabkha soils are generally viewed as unconsolidated, heterogeneous, cemented sedimentological framework, bathed in highly concentrated sub surface brines. The strength of sabkha soil is generally very low with a standard penetration test (SPT) number as low as 0 to 8. Moreover, due to the presence of water-soluble cements such as halite, gypsum, and anhydrite, sabkha soil is susceptible to collapse upon wetting. Sabkha is found to be a problematic soil due to its water sensitivity. However, its use cannot be avoided, especially for road construction, because it is difficult to replace it with other soil due to its wide spread and the shallowness of the ground water.

Imtiaz (1997) has recently performed a limited number of experiments regarding the improvement of sabkha soil using geotextile and found out that geotextile can improve the load carrying capacity of sabkha by 415% under saturated conditions and by 145% under as molded (at the molding moisture content) conditions. Currently, there is no information available regarding the pull-out resistance of locally available geotextile embedded within local soils including sand and sabkha. Moreover, there is a lack of

knowledge about sabkha–geotextile interface frictional parameters. This study is intended to find out the frictional characteristics for sand-geotextile-sand and for sabkha-geotextile-sand interfaces. Sabkha-geotextile-sabkha interface is not practical since backfill material is usually of free draining or good quality material and sabkha is known for its acute water sensitivity and poor drainage. Usually, the backfill material in case of earth structures is sand, which gives rise to the investigation of sand–geotextile–sand interface characteristics. On the other hand, the geotextile can be placed directly on the sabkha soil and backfilled with the sand, and that gives rise to the investigation of sabkha–geotextile–sand interface characteristics. Such a study is necessary to properly understand the interaction mechanism of sabkha and geotextile and to monitor the strain developed in the geotextile during pull-out tests. This study will help in understanding the effect of different parameters on the pull-out resistance of geotextile when it is used for shore protection, embankments, roadways and foundations on sabkha or locally available sand. Such a study can help the construction industry in properly designing reinforced soil structures and shore protection systems.

1.3 Research Objectives

The main objectives of this experimental research program are:

- To study the frictional characteristics of sand-geotextile-sand and sabkha-geotextile-sand interface taking into account the effect of the following parameters on the pull-out resistance:

  1 - Level of applied normal pressure

2 - Geotextile type

3 - Water content of the soil

4 - Length of geotextile

5 - Soil type

- To compare the pull-out resistance of locally available non-woven geotextiles when used with local sand and sabkha soils.

The outcome of such research project will be a first step towards the use of geotextile as reinforcement in road construction over sabkha soil, design of embankments, landfill clay liners, reinforced wall, silt-fences and shore protection. Interface frictional characteristics are not available for local Saudi soils and locally manufactured geotextiles. This study will contribute to the database of local soils and also will be helpful for the local geotextile industry.

1.4 Thesis Organization

In order to accomplish the above mentioned objective a through literature review was done keeping in mind the factors that effect the pull-out resistance of geotextile. Chapter 2 is devoted to the literature review. In Chapter 3, the experimental program is discussed. It also discusses the experimental setup and procedures, and the materials used in this investigation (sand, sabkha and geotextile). Chapter 4 presents the experimental results and discussion. The conclusions and recommendations derived from this research are presented in Chapter 5. At the end, the collected data in the form of graphs for pull-out testing are provided in the appendices.

CHAPTER 2

LITERATURE REVIEW

The chapter presents a summary of the previous work related to soil-fabric interaction and Eastern Saudi soils. In order to study the effect of various parameters on the shear strength of soil-geotextile interface, the properties of soil, its engineering behavior and related problems must be recognized alongwith the properties of geotextiles. This chapter also presents the study of different factors affecting the pull-out resistance of geotextiles, on the basis for which the parameters were selected for the experimental program.

2.1 Problematic Sabkha in Eastern Saudi Arabia

The term sabkha is originally defined as saline flats that are underlain by sand, silt or clay and are often encrusted with salts (Al-Amoudi, 1994). There are two main types of sabkha; 1) continental sabkha and 2) coastal sabkha. Both sabkha types usually form in hot, arid climates and are associated with shallow ground water table. Sabkha surfaces when dry, are usually hard enough to support a medium weight vehicle, however, they

become impassable when become wet in a way where a person would sink in, nearly, to knee depth (Aiban, 1994).

Saudi Arabia has a large number of sabkha, both continental and inland. Johnson et al. (1978) reported a summary of these sabkhas in the coastal plains of the Eastern Province, based mainly, on reconnaissance visits. Sabkhas also exist along the western shores of Saudi Arabia. Sabkha soil is generally viewed as unconsolidated, hetrogenous layered or unlayered sedimentological framework bathed in highly concentrated subsurface brine. The principal cementing materials in sabkhas are aragonite, calcite, gypsum and sometimes anhydrite, as well as halite (Johnson et al., 1978; Al-Amoudi et al., 1992a). Stipho (1985) discussed various geotechnical problems associated with saline sabkha indicating the presence of weak cementation due to the crystallization of soluble salts in the upper parts of sabkha profiles.

Many geotechnical problems do occur when sabkha soil is utilized in construction. This is mainly due to their high salt content, high natural moisture content, the proximity of ground water tables to the surface, their susceptibility to severe settlements or swelling. Problems arises due to the periodic changes in moisture content, compressibility variations, rise of ground water and the presence of highly corrosive salts and brines. Different types of preventive measures are taken to control these problems. One of the methods is the utilization of geotextiles. The use of geotextile for sabkha is cost-effective and multi-functional. Abduljauwad et al. (1994) conducted a research program to investigate the load carrying capacity of soil-fabric-aggregate system and found that the use of geotextile can significantly enhance the load carrying capacity of sabkha specially

when it is saturated. However, there is a lack of knowledge regarding sabkha-geotextile interface.

In addition to the soil reinforcement, geotextile had been used previously in many geotechnical applications in the form of separators and filters. The information obtained from local contractors pointed out its application along the Dammam and Khobar corniches. More than 100,000 m^2 of geotextile were used for shore protection. It had been used for soil stabilization (reinforcement) in King Abdul Aziz Street Dammam. More than 100,000 m^2 of geotextile had been used as reinforcement in Al-Qaseem ring road, Riyadh ring road, and Shaybha road (Al-Sheikh, 1998). It had also been used for soil stabilization in King Fahd International Airport and few other muncipality roads in Dammam area.

2.2 Geotextiles

Geotextiles are defined by Swan (1987) as a textile structure produced from non-woven synthetic fibers or woven and/or knitted synthetic yarns made of polypropylene, polyester, polyamide or fiberglass. These permeable textiles are used in conjunction with soil or rocks, as an integral part of a man-made project. It is believed that the first application of geotextile was for a woven industrial fabric used beneath concrete block revetments in the late 1950s and in water front structure built in Florida in 1958 (John, 1986). Their growth over the past twenty years has been nothing short of awesome. Their use in major projects become necessary in many applications. They are indeed textiles in traditional sense, but consists of synthetic fibers rather than natural ones such as cotton, wool or silk. Thus biodegradation is not a major problem (Koerner, 1997). These fibers are made into

flexible, porous fabric by standard weaving machinery or are matted together in a random or non-woven manner.

2.2.1 Types of Geotextiles

All types of geotextiles are made up of four main polymer families, used as raw materials for geotextiles; polyester, polyamide, polypropylene, and polyethylene. Geotextiles can be subdivided into the following categories (see Fig. 2.1) depending on the method of manufacture.

a - Woven Geotextiles

These geotextiles are manufactured using techniques adopted from those used to weave clothing textile (John, 1986). The weaving process gives these geotextile their characteristic appearance which consists of two sets of parallel yarn, interlaced at right angles to each other. The term warp and weft are used to distinguish between the two different directions of yarn. The yarn running along the length of the loom or length of the geotextile roll is known as the warp. The yarn running in the transverse direction, across the width of both the loom and geotextile is known as weft.

b - Non-Woven Geotextiles

There are three subdivision of non-woven geotextiles, based on the way in which the geotextile fibers are bonded together (John, 1986). These fibers could be thermally bonded, chemically bonded or mechanically bonded (Koerner, 1997). Thermally bonded non-woven geotextiles are produced by spraying polymer filament on a moving belt

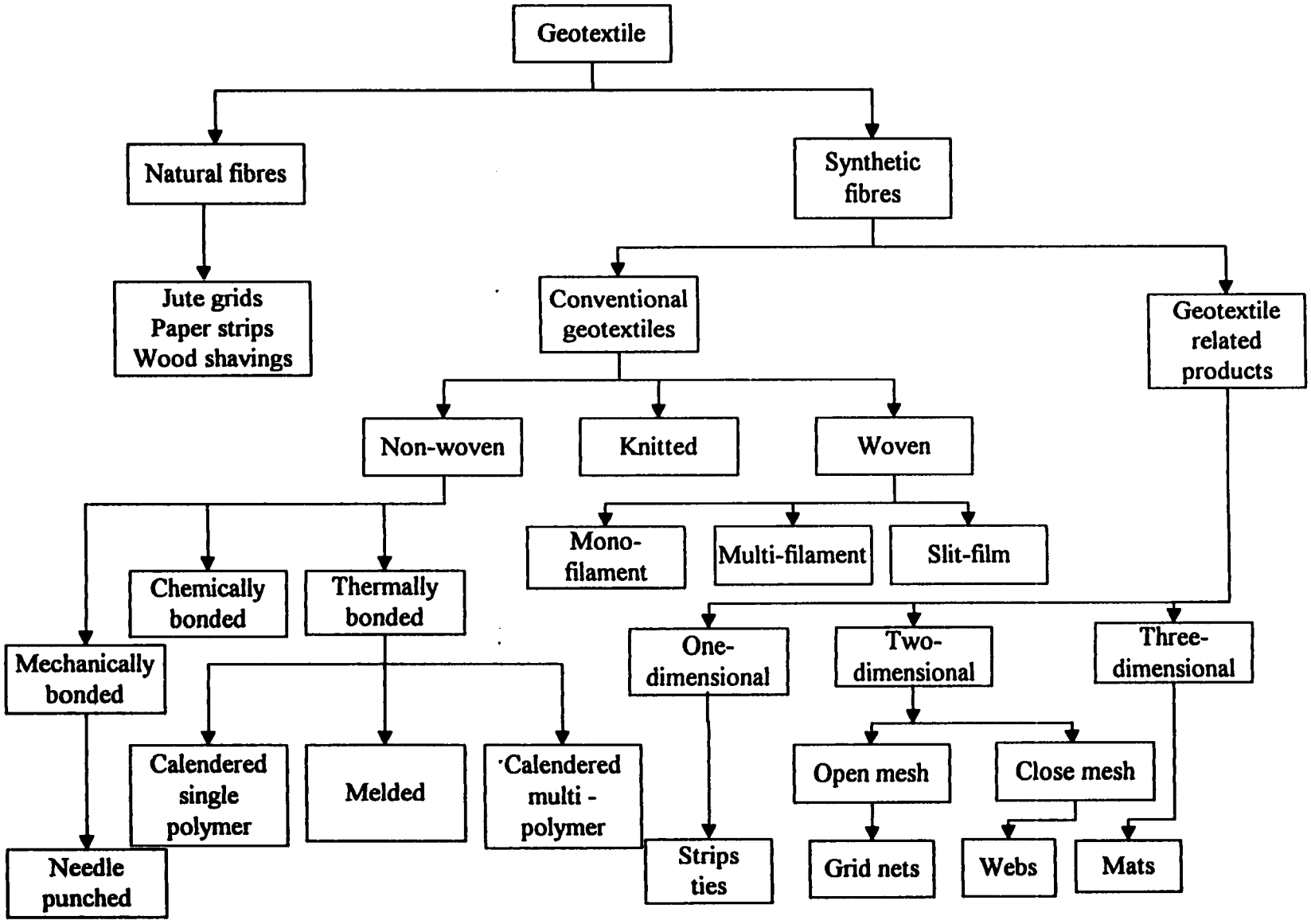

Fig. 2.1: Geotextile classification (John, 1986)

passing through a heated roller, leading to thermal bonding at filament cross-over points. There is no warp or weft direction in such type of geotextiles. The term spun bonded is also used for heat bonded.

Chemically bonded geotextile are also formed by spraying polymer filament onto a moving belt in a random manner, but the next stage involves dipping or spraying the sheet of filament with a chemical binder called acrylic resin. The mechanically bonded geotextiles are formed by deliberately entangling the filaments to form comparatively loose bonds. These geotextiles are referred as needle punched geotextiles. Needle punching involves repeatedly driving thousands of barbed needles into loose sheet of polymer filament so a quicker entanglement of filament is achieved. These geotextiles are usually 2 to 5 mm in thickness (John, 1986).

2.3 Functions of Geotextiles

There are at least 100 specific application areas for geotextiles (Koerner, 1997). The main functions performed by geotextiles are separation, filtration, drainage, and reinforcement.

2.3.1 Separation

The separation function refers to the separation of two dissimilar materials. The primary function of the geotextile is to prevent intermixing of two different materials through-out the design life of the structure. Geotextile can be used as a separator on soft subgrade and graded base course, between foundation soils and rigid retaining wall.

2.3.2 Filtration

When liquids flow across the plane of geotextile, the geotextile acts as a filter. Filtration is one of the most widely used function of geotextile. A geotextile used for filtration serves the same role, as the various graded filters. It allows the water to go through but prevents the migration of fine particles. This is widely used in shore protection, between backfill soil and pervious retaining wall, around perforated drain pipe.

2.3.3 Drainage

In-plane flow of liquid through geotextile is called drainage. When placed in a soil of low permeability, the geotextile is acting as drain where it gathers the water and moves it towards the outlet. Examples are the use of geotextile as a chimney drain in an earth dam, and behind retaining wall where it works also as a filter.

2.3.4 Reinforcement

Reinforcement function is defined by Koerner (1997) as " the synergistic improvement of a total system's strength created by the introduction of a geotextile (good in tension) into a soil (good in compression but poor in tension) or other disjointed or separated material". Geotextiles are used to reinforce many structures such as embankments, retaining walls, etc.

2.4 Soil Fabric Interaction

One of the primary functions of geotextile is reinforcement, whereby the geotextile is

subjected to a sustained tensile force or load. Soils are known for their ability to withstand high compressive force and their relatively low capacity for sustaining tensile forces. In almost the same way that tensile forces are taken up by steel in reinforced concrete flexural members, the geotextile supports tensile force that cannot be carried out by soil in a soil-geotextile system, as shown in Fig. 2.2. The tensile forces in the geotextile are carried by friction between the soil and the geotextile provided that the geotextile is properly anchored into the soil.

As the backfill material deforms under the load, relative movement develops between the reinforcement and the soil, and thus mobilizing the bond stresses on the soil-reinforcement interface. The relative movement may generate tensile forces and thus elongation of the reinforcement. If these tensile forces in the reinforcement can be transferred to the surrounding soil, then the overall load carrying capacity of the reinforced soil can be increased (Fourie and Fabian, 1987). The soil-reinforcement interaction has two different failure modes: the shearing (bond) mode and the pull-out (anchoring) mode. In the shearing (bond) mode the soil moves relative to the reinforcement and this movement is constant along the interface as shown in Fig. 2.3. This mode is modeled in the laboratory through direct shear test. Whereas in the pull-out mode, the reinforcement is in tension and mobilizes the shear stresses on the interface and therefore the relative movement between the reinforcement and soil is not constant along the interface and depends on the distance from the point of application of the tensile load on the reinforcement.

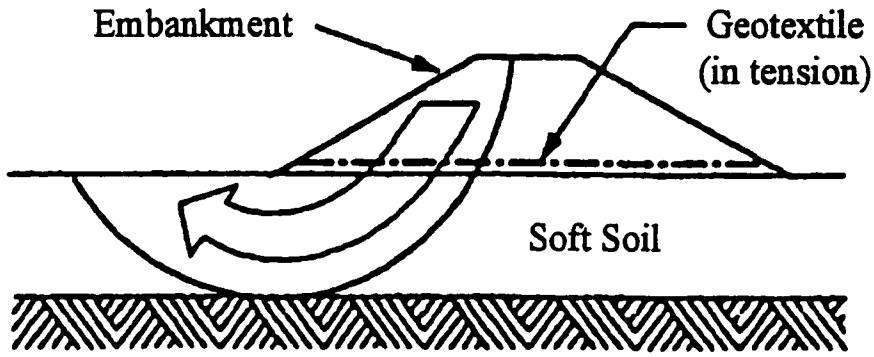

Fig. 2.2: Reinforcement function of geotextiles (Amoco, 1993)

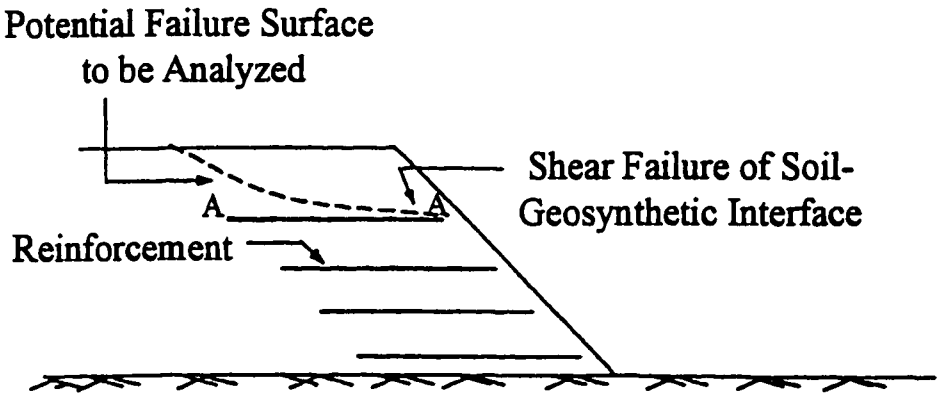

Fig. 2.3: Shear failure mode in soil reinforcement application (Zhai et al., 1996)

When a geotextile is used as reinforcement, it is necessary to evaluate the soil-geotextile shear strength characteristics in order to: (i) quantify the ability of the geotextile to act as a reinforcement and (ii) determine whether the geotextile could act as a slip surface inside the earth mass (Collios et al., 1980). The shear stresses developed at the interface due to the friction between the soil and the geotextile lead to the concept of soil-fabric interaction. These stresses are not uniformly distributed over the length of geotextile due to the progressive elongation of the geotextile, which indicates the non-linear behavior under the pull-out action (Long et al., 1997). Friction between the soil and fabric depends on many parameters including the geotextile type, soil placement and compaction, and the surface texture of soil and geotextile. According to Koerner (1997) there are three reinforcement mechanisms (or types) when geotextiles are used to reinforce soils. These mechanisms are discussed in the following paragraphs.

2.4.1 Membrane Type

Membrane reinforcement mechanism occurs when a vertical load is applied to a geotextile resting on a deformable soil. According to Koerner (1997), the applied vertical load produces tension on the horizontal plane beneath it. This tension is taken by the geotextile, which is acting as reinforcement. Many situations, in which geotextiles are placed on the soft soil, simulate this reinforcement mechanism. Espinoza (1993) has provided closed-form solutions for design purposes. In his paper, he used circular and parabolic shapes to simulate geotextile deformation. He stated that circular support model furnishes larger values of membrane support as compared to the parabolic one.

2.4.2 Shear Type

A geotextile placed on a soil is loaded by backfill material. When shear failure at the soil-geotextile interface occurs, the two materials are sheared at their interface A-A, as shown in Fig. 2.3. In this case, the failure surface does not pass through the geotextile but the soil-geotextile interface acts as the failure plane and the soil mass above the geotextile slides over the geotextile. The shear strength parameters at the soil-geotextile interface can be determined by means of direct shear tests. These values can be compared to the shear strength parameters of the soil itself. This will enable the determination of the efficiency of shear strength mobilization which ranges between zero and unity (Koerner, 1997).

2.4.3 Pull-out or Anchorage Type

Anchorage reinforcement is similar to the shear type, but in this case the soil on both sides of the geotextile, acts to produce tensile force tending to pull the geotextile out of the soil, as shown in Fig. 2.4. In this case, the failure surface passes through the geotextile and the shear strength of soil is low enough such that part of the soil mass becomes unstable. This type of mechanism can be modeled in the laboratory using pull out tests. The pull-out test is thought to be a realistic model in those circumstances where field pull-out resistance might be the criterion governing the design (Ingold, 1982). Yehia et al. (1994) indicated that the pull-out test simulates the applications where geotextiles are anchored within the soil mass. The difficulty in interpreting the pull-out test data revolves around the

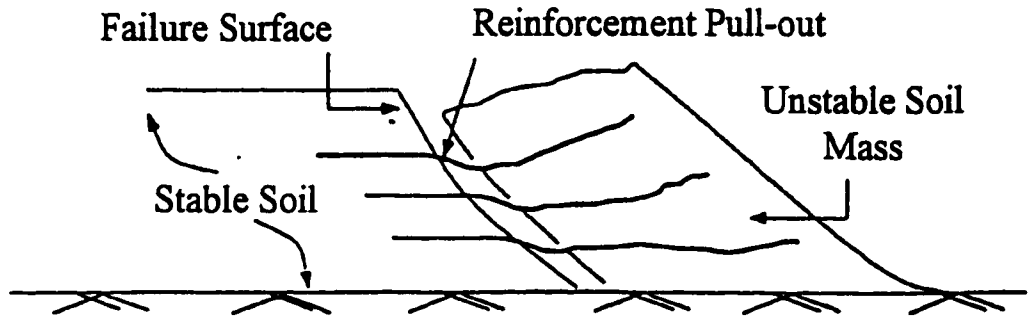

Fig. 2.4: Pull-out failure of reinforcement in soil reinforcement application (Zhai et al., 1996)

extensibility of the geotextile, which gives rise to a highly non-uniform distribution of shear stress along the geotextile.

Geotextiles are used as reinforcing materials within earth structures like reinforced wall, embankment and unpaved pavements on weak subgrade, for which two types of failures can occur. One is slippage of geotextile and other is the tensile failure of the reinforcement (geotextile). In both cases, the interface friction remains the governing factors for satisfactory design of reinforced earth structure.

The geotextiles are also used in coastal protection instead of a multilayer granular graded filters to prevent erosion of fines along coastlines or undermining of coastal slopes. In these applications, both rip-rap rock and precast concrete blocks are placed on the geotextile which acts as a filter. Sand cushion layer or fine aggregates layer is provided to prevent the geotextile puncture during installation. Although the main function of the geotextile is filteration, anchoring the geotextile is required at the top and at the toe of the slope to avoid slippage or pull-out. Various kinds of anchorages of geotextile for such purposes are shown in Fig. 2.5 and Fig. 2.6.

2.5 Interfacial Soil-Geotextile Frictional Tests

Design of soil structures reinforced with planar reinforcing material such as geotextiles is undergoing revolutionary changes with rapidly developing testing technologies and analytical approaches (Bergado et al. 1992; Wilson-Fahmy et al. 1994; Alfaro et al. 1995). In all soil reinforcement applications the ability of the geosynthetics to interact with the soil to get anchored, is a key element in the performance of reinforced earth structures.

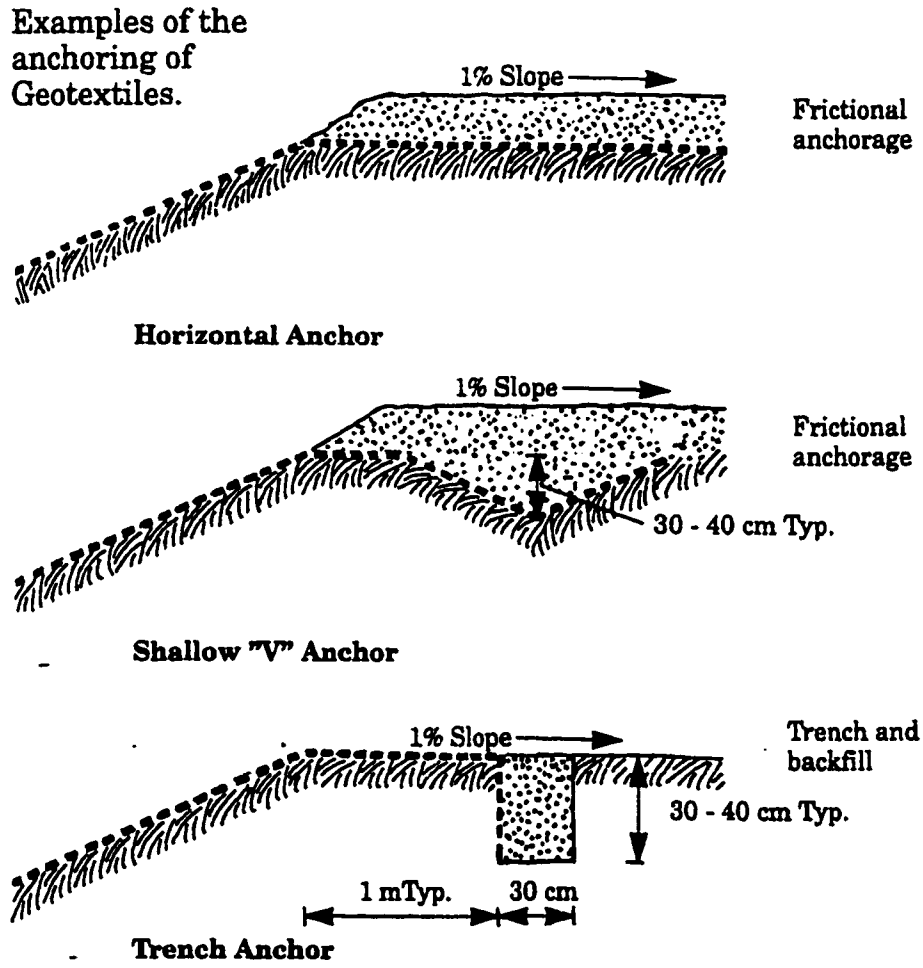

Fig. 2.5: Typical anchorage types of geotextile in shore protection applications (Fibertex, 1995)

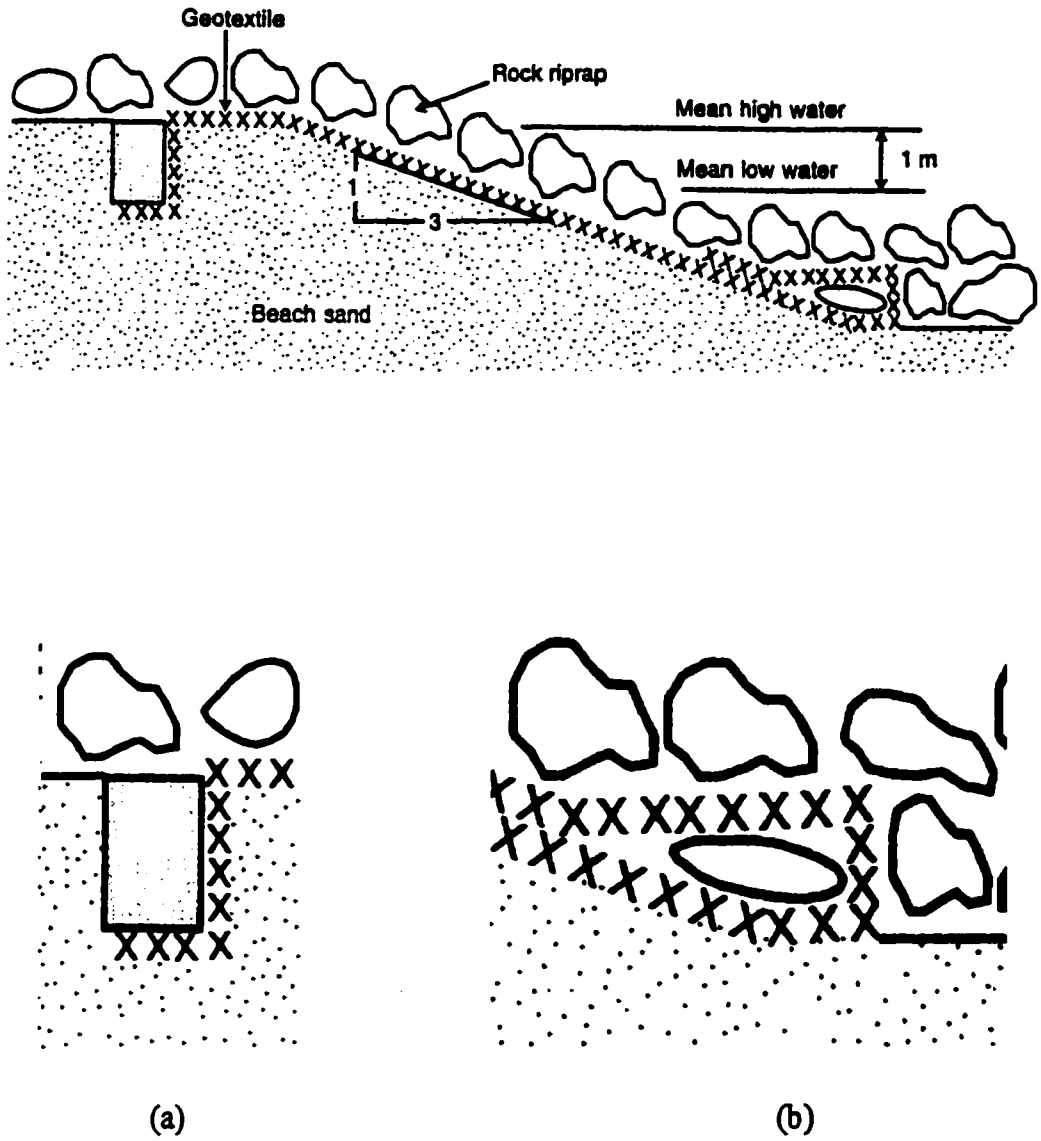

Fig. 2.6: Typical geotextile anchorage (a) at top of the slope (b) at toe of slope (Koerner, 1997)

The required embedment lengths are computed based on the interface frictional characteristics.

The two prominent techniques for testing planar reinforcements are the direct shear test and the pull out test, where each yields different interaction parameters. These two mechanisms are shown schematically in Fig. 2.7. The direct shear test is conducted according to ASTM D 5321. However, there is, presently, no ASTM standard procedure for the pull out test (Mallick, 1996). These two tests are fundamentally different in terms of geometric configuration, stress paths and boundary conditions. Published data have demonstrated that the interface shear strength parameters determined by the two tests are often different (Collios et al. 1980; Ingold 1984; Richards and Scott 1985; Rowe et al. 1985; Juran et al. 1989). It is generally recognized that the direct shear test is more appropriate for evaluating a sliding failure occurring between the reinforcement and soil above it. However the pull out test gives a better representation of a pull out failure at the far end (i.e. the free end) of an embedded reinforcement. It is known that the pull-out test simulates the field condition and allows for better strain monitoring as the pull-out test progresses. The relationship between pull-out test and field situation is given by Collios (1980). In the pull-out test the characteristics of geotextile are changing with the increase in strain, i.e.; apparent opening size and surface roughness are changing with the extension of the geotextile. Such changes are not accounted for in the direct shear test.

2.5.1 Direct Shear Test

In the direct shear test, the geotextile is placed between the two halves of the shear box,

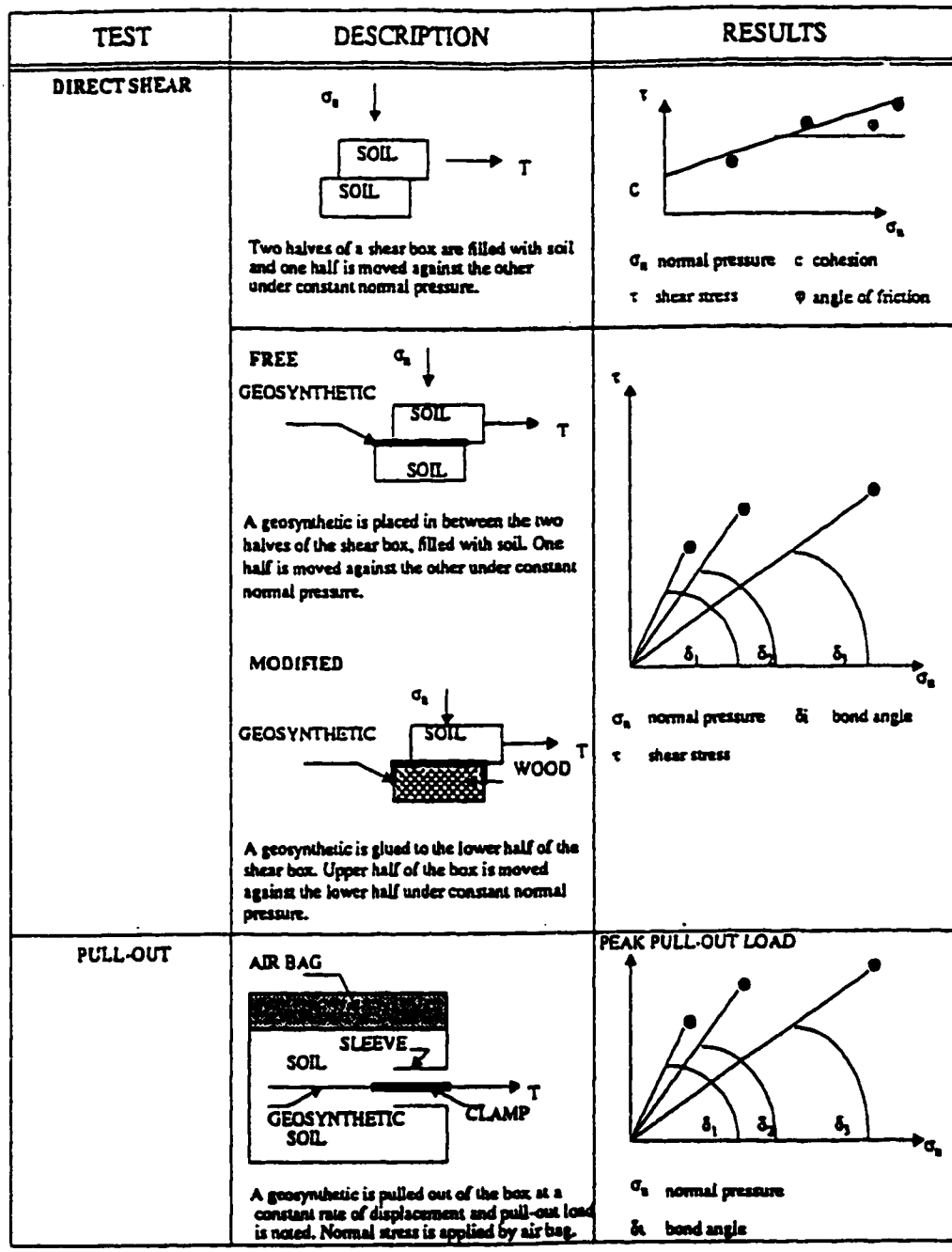

Fig. 2.7: Direct shear and pull-out tests (Mallick, 1996)

or alternatively the geotextile is firmly fixed to the lower half while the soil is in the upper half as shown in Fig. 2.7. One half is, then moved against the other after the application of the normal stress. A shear force is gradually mobilized until sliding occurs between the geotextile and the soil with no further increase in the shear force.

Frictional resistance in the direct shear test is largely function of the surface roughness of the geotextile and the interlocking of the soil and geotextile (Mallick, 1996). There are two types of direct shear testing of geotextiles; free geosynthetic and modified geosynthetic. In the modified geosynthetic direct shear test, a geotextile is glued to the lower half of the shear box and the upper half is pushed against the lower box at an applied normal pressure. Thus, the extensibility of the geotextile is not permitted in this test.

According to Williams and Houlihan (1987), the deformation required to mobilize sand geotextile residual shear stress is in range of 2 to 7 cm. Therefore, in order to mobilize the residual shear stress at the soil-geotextile interface in the direct shear test, the contact area needs to be much larger than the contact area of the conventional shear box. Most direct shear test devices that are used to measure the interface friction parameters have contact area of at least 300 by 300 mm.

2.5.2 Pull-out Test

In the pull-out test, the geotextile is sandwiched within a soil or between two different soils from both sides. A normal force is applied to the soil surrounding the geotextile and the geotextile is then subjected to a pull-out force. The pull-out resistance depends on the

applied normal force, the properties of the geotextile and the type of soil. Mallick (1996) stated that the pull-out resistance in the test is function of surface roughness of soil-geotextile interface, geotextile extensibility, soil type and interlocking between the soil particles and the geotextile. For design purposes, the general practice is to take the direct shear test results for both sides of the geotextile and add them together. However, this may not be a conservative approach. On the other hand, pull-out test resistance is less than the sum of the direct shear test resistance (Koerner, 1997). The reason for this reduction is the extensibility of the geotextile and its axial deformation during the pull-out test due to which smaller relative displacement occurs between the soil and the geotextile. Such deformation decreases as the point moves away from the point of application of the pull-out load. The full frictional strength does not develop along the entire length of the geotextile. The extensibility also causes the soil particles to reorient themselves into a reduced shear strength situation at the soil-geotextile interface. In addition, the elongation of the geotextile alters the geotextile roughness. Furthermore, the reduction in the thickness of the geotextile will result in a reduction in the dilation effects and thereafter in the total pull-out resistance.

2.6 Pull-out Resistance and Interface Frictional Characteristics

Frictional resistance between soils and geotextiles must be known for the design of reinforced slopes or earth structures utilizing geotextiles for reinforcement, filteration or

other purposes. The pull-out resistance of geotextile is the result of complex phenomena occurring at the soil-geotextile interface (Karmokar, 1998). This is mainly due to the interactions at the interface and the changes of the geotextile characteristics upon elongation. The data obtained from the pull-out test is used to determine the interface interaction coefficient (c_i), which is a measure of the reinforcement efficiency in transferring stresses from the reinforcing geotextile layer to the adjacent soil (Koutsourais, 1998). The c_i is given by

$$c_i = \frac{\tau_i}{\tau_s} = \frac{(c_a + \sigma_n \tan\psi)}{(c + \sigma_n \tan\phi)} \tag{2.1}$$

Where;

τ_i = Shear stress at the interface

τ_s = Shear strength of soil

ψ = Interface friction angle

ϕ = Internal friction angle of the soil

c_a = Interface adhesion

c = Soil cohesion

σ_n = Normal pressure

Koutsourais (1998) stated that the interface interaction coefficient could range from 0.9 to 1.0 in sand and from 0.6 to 0.9 in clay. However, Mallick (1996) reported the values of coefficient of friction at soil-geotextile interface to be 0.7 to 1.6 in pull-out test. Rao and Pandey (1988) and Cheng et al. (1993) demonstrated that the coefficient of friction at soil-geotextile interface could exceed the coefficient of friction of the soil itself.

Pull-out test performed by Rowe et al. (1985) on non-woven geotextiles in loose fill (sawdust) gave interface friction angles of 35 - 37°.

2.7 Application of Pull-out Test Results to Design of Reinforced Earth Structures

In the design of reinforced soil structures, there are two issues that are related to the use of pull-out test and need to be considered. These are:

1) The development length (L) required beyond a given failure plane to mobilize the allowable tensile strength of the reinforcement.
2) The maximum pull-out force that can be used to limit the strain within the structure to a certain limit. It must be determined for designs where limiting strains are critical to the structure's long - term performance.

Cowell and Sprague (1993) recommended the use of the interface interaction coefficient values, which are associated with a stress level at which the shear stress within the sample tends to be more uniform. Soil-reinforcement pull-out tests are essential for evaluating the strength, integrity, and effectiveness of soil-reinforcement system (Madhav, 1998). The pull-out test is important for the soil geotextile shear strength parameter used in the design of reinforced wall, reinforced embankment or reinforced clay liners. The analysis of such structures requires data on the limiting shear strength along the interface between soil and geotextile, which is determined by pull-out tests.

The parameters measured in a pull-out test corresponds to longer anchorage length in the prototype because soil displacement in the pull-out box is small whereas in full scale structure, the displacement is usually more. Furthermore, the length of the geotextile is small in the test as compared to the full scale structure. Therefore, severe progressive failure along the interface, during the pull-out test, can be considered a simulation for real full scale structure (Lo, 1998).

2.8 Factors Influencing the Frictional Resistance

Direct shear test and pull out test results are significantly affected by the soil parameters, geotextile properties, and testing procedures. The pull-out resistance depends on many factors including the applied normal pressure, soil properties, reinforcement properties, water content, strain rate, and aspect ratio of the pull-out box, testing procedure and sample preparation. Soil properties include soil gradation, composition, plasticity, in-place density, stress history, whereas the reinforcement properties include fabric mass per unit area, surface roughness, strength, extensibility, thickness and opening size, etc. The pull-out resistance depends on many other factors including length of geotextile, compaction procedure, width of specimen, and the gripping mechanism. The effect of the main parameters will be discussed in the following sections.

2.8.1 Effect of Soil Properties and Loading Condition

a - Normal pressure and related soil dilatancy

The effect of normal pressure has been studied in terms of the coefficient of friction of the soil (μ) and of the soil-geotextile interface (ν) and efficiency factor (μ / ν) of the geotextile soil interface, where:

$\mu = \tan\phi$ = Coefficient of internal friction of soil

$\nu = \tan\psi$ = Coefficient of interface friction for soil geotextile interface.

ϕ = Angle of internal friction of soil.

ψ = Interface friction angle of soil geotextile interface.

For geotextile in direct shear and pull out tests, the soil reinforcement interaction has two contributing factors:

1- Frictional resistance between the reinforcement surface and the soil layer.

2- Interlocking between the soil and the reinforcement because of indentation of soil particles into the reinforcement that results in a complex stress state due to the development of a composite material. Yehia et al. (1994) suggested that this interlocking results in adhesion component which is overcome before soil/fabric friction mobilization.

Many researchers have studied the effect of different parameters. Mallick (1995) stated that the peak pull out load decreases with increasing the shear rate at high normal pressures. In addition, the coefficient of friction is shown to decrease with an increase in the normal pressure. Normally, a higher pull out load is expected at higher normal stress

levels. This is mainly due to the restrained dilatancy of the soil in the vicinity of soil geotextile interface and the resultant soil geotextile interlock. Shingenori et al. (1996) indicated that the sheet-like reinforcement scheme corresponds to the case of free dilatancy while strip reinforcement scheme corresponds to the case of restrained dilatancy. Lo (1998) stated that in the case of restrained dilatancy, the pull-out resistance at the soil-geotextile interface increases due to the increase of normal stress in the surrounding soil. The increased shear resistance can be modeled by an increase in the coefficient of friction defined as the ratio of average shear stress to normal stress. He also pointed out that the increase in friction factor due to constrained dilatancy would be significant at low overburden stress level. Ingold (1984) reported that the interface friction angle at a soil–geotextile interface exceeds the coefficient of friction of soil at low normal pressure levels.

Mallick (1996) stated that the interface shear strength in a pull out test may decrease significantly because of the large deformation of the soil at high normal pressure. Peak pull out resistance was obtained at low normal pressure values and the corresponding deformations were low. Moreover, the reduction of shear strength at high normal pressure is due to extensibility of the geotextile and the non-uniform stress distribution along the geotextile in the pull out test. Under the effect of shear stresses, mobilized at the soil geotextile interface, granular soils tend to dilate, but its dilatancy is restrained by the surrounding soil. This restrained soil dilatancy has significant effect on the efficiency factor estimated from the pull out test result.

The normal load encountered in the field is highly dependent on the type of structure and loading conditions. Hari et al. (1997) pointed out that normal stress ranges

from as low as 6.0 kPa to 24 kPa which are typical values for landfill covers. On the other hand, a pressure as high as 480 kPa simulates the surcharge loads on the base and side slopes of liners or embankments. Mallick (1997) conducted the pull out tests at normal pressures of 7, 21, 35 and 49 kPa. Ingold (1982) reported coefficient of interface friction greater than 1 for sand for normal stress less than 20 kPa in pull-out tests. He also indicated that as the normal load is increased the mobilized bond stress occurs at the point of load application with relatively little strain at free end for extensible geotextile. Yehia et al. (1994) observed that for low normal stress ranges (up to 5 kPa), there is a non-linear relationship between $\tan\psi$ and normal stress. This means that Mohr-Coloumb law is not valid. He also stated that for visco-elastic material such as polymeric fabric, the law of friction depends on the level of normal stress, surface roughness and deformational mode of fabric. The deformational modes suggested by Yehia et al. (1994) are pure slippage of the geotextile, complete rupture and combined slippage and longitudinal deformation.

b - Effect of dry density of the soil

The shear resistance of geotextile - sand interface increases with the increase in the dry density of sand in the direct shear tests. Similarly, an increase in the peak pull out resistance and the interface stiffness modulus with an increase in soil density was observed by Mallick (1996). For a woven fabric, the efficiency of loose sand-geotextile friction is high (close to one), while that of dense sand-geotextile friction varies between 0.61 to 0.98. The drop in the efficiency appears to be related to construction of the fabric (Richards and Scott, 1985).

c - Effect of the water content of the soil

Farrag (1995) shows that the changes in moisture content at the soil geotextile shearing zone affects the interface shear resistance. He showed that an increase in the soil moisture content above its optimum value caused a decrease in the pull out resistance for a clay due to the development of excess pore water pressure during pull-out testing. Such changes of water contents are usually attained after rainfall or when compacting the soil at water contents higher than their optimum water content values. Miyamori et al. (1986) performed direct shear test on sand-geotextile interface and found that the frictional resistance between the non-woven fabric and the wetted sand is smaller than that between the fabric and air-dried sand. William and Houlihan (1987) pointed out that for highly cohesive soils which are near complete saturation, the rate of deformation during testing should be slow enough to allow complete dissipiation of excess pore pressure.

A decrease in the pull-out resistance of a grid reinforcement in cohesive soil with an increase in water content has been reported by Farrag (1995). Moreover, for dry sand, no difference between peak and residual shear strength was observed in the direct shear test where as for wet sand a distinct peak and residual shear strength were reported by Mallick (1996).

2.8.2 Effect of Reinforcement Properties

a - Effect of reinforcement extensibility and stiffness

Reinforcement extensibility significantly affects the pull-out and direct shear resistance of geotextiles. In free geosynthetic direct shear test, the reinforcement extensibility resulted

in higher peak shear displacement as compared to that in modified direct shear test. However, Mallick (1996) found that the peak shear strength in the direct shear test is independent of extensibility.

In the pull-out tests, geotextile extensibility results in a non-uniform distribution of shear stress and thus shear displacement along the geotextile. Due to the extensibility of the geotextile, the pull-out test on low modulus and very extensible geotextile produces much lower peak strength compared to the strength obtained from direct shear test. In pull-out tests, the bond stress is mobilized over a comparatively short section of the specimen that is close to the point of pull out load application. This results in a non-uniform distribution of shear stress along the geotextile (Long et al., 1997). In the case of more flexible geotextile, failure occurred by rupture. For more rigid and stronger geotextile, the peak nature of the load displacement curves is characterized by an abrupt failure due to the lack of adherence between the geotextile and the soil (Long et al., 1997).

Geotextile stiffness also has a significant effect on the pull-out test. A higher stiffness and tensile strength of the geotextile may result in a slippage failure between the soil and the geotextile at the interface. The interface interaction factor or geotextile efficiency is inversely proportional to the stiffness of the geotextile (Fourie and Fabian, 1987). Lower stiffness materials deform under the normal load and the soil particles can be squeezed into the surface of the fabric. This increases the contact efficiency through interlocking. However, the displacement required to mobilize the bond strength is much lower in the case of geotextile with large stiffness compared to that with low stiffness.

b - Effect of structural geometry of the geotextile

It has been demonstrated that the fabric texture or structure of the woven geotextile affects the shear strength parameters. The shear strength of soil-geotextile interface increases with the increase in warp thickness. This increase was associated with increase in bearing resistance due to displacement of warp yarn.

Swan (1987) had shown that geotextiles having similar strength, construction and yarn geometries, but different fabric geometries, can mobilize significantly different shear strength for the same soil. Surface roughness has been found to have a significant effect on the friction angle obtained from the pull-out tests. The coefficient of friction increases with an increase in the surface roughness. The interlocking of soil particles depends on ratio of apparent opening size of the geotextile to the diameter of soil particles. Mallick (1996) found that the friction angle between geotextile and soil increases with an increase in the opening size.

c - Effect of width and depth of placement of the geotextile

Khera et al. (1997) studied the effect of width and depth of placement of the geotextile on the pull-out resistance of geotextiles embedded in an anchor trench in sandy soil. They showed that for depths less than 1.0 m (3 ft.), failure occurred in the sand mass with apparent heaving of soil beyond the geotextile boundaries, while at greater depths, failure occurred at the sand-geotextile interface. They also showed that angle of interface friction decreases with increasing depth of anchor trench and become constant at 1.2 m (4 ft.) depth. Khera (1997) also indicated that the angle of interface friction dropped as the width

of specimen increases. This result was also supported by Schlosser and Elias (1978) who reported from field test data a decrease in coefficient of friction as the width of the specimen increases.

d - Effect of geotextile opening size

Collios et al. (1980) performed pull-out tests on woven and non-woven geotextiles and found that if the soil particles are finer than the geotextile openings, the contact efficiency can be as large as one. They also found that the contact efficiency is smaller for a pull-out test than for a direct shear test performed on the same soil and geotextile. They stated that this is due to the large displacement of the geotextile sample in the pull-out test which causes reorientation of soil particles into a reduced shear face.

2.8.3 Effect of Test Parameters

a - Effect of test procedure

Two types of test procedures are used in pull-out test; the controlled displacement rate and the controlled load. The controlled displacement rate tests are usually used to investigate the performance of geotextile under short term pull out loads. In such tests, the shear deformation along the soil geotextile interface has been found the main contributing factor in the pull-out mechanism. However, in the load controlled pull-out tests, the creep deformation of a geotextile in the sand has been found to be the most significant factor in pull-out resistance. It predicts the critical creep load below which creep failure of geotextile is unlikely to occur.

Fannin and Raju (1991) reported that tests performed at a constant rate of displacement and constant rate of loading yield similar relationship between mobilized pull out resistance and displacement in case of geogrid. It has also been suggested by Fannin and Raju (1991) that the interface interaction factor for dynamic loading in seismic design should be taken as 80% of that for static loading, which was found to range between 0.7 and 1.6 in pull-out tests.

b - Effect of displacement rate

Boyle et al. (1996) studied the effect of strain rate on the geotextile properties and found that the response of woven geotextile was very sensitive to the strain rate. The effect of displacement rate was found to be different for direct shear and pull-out tests. In the direct shear test, a critical shear rate has been defined. The use of a shear rate greater than the critical shear rate in direct tests, for moist sand, resulted in negative pore pressure, which increased the shear strength as reported by Mallick (1996). Whereas, the peak pull-out load decreases with an increase in the rate of displacement. It was also found that higher displacement rates results in lower strain values along the geotextile.

c - Effect of pull-out box front wall roughness

The pull-out resistance of the geotextile is affected by the friction between the soil and the front wall. According to Palmeira and Milligan (1989) the pull-out resistance increases due to the increase in the normal pressure, which is caused by the vertical component of lateral earth pressure acting on the front wall of the box. The results obtained by Palmeira and Milligan (1989) show that the zone of the increased normal pressure extends up to 15

times the thickness of the geotextile, after which no increase in normal stress was observed. Other factors that affect the interaction between the soil-geotextile and the front wall of the pull-out box are the type of soil, effective stress increase, pore pressure build up, cavitation, rigidity of wall and the position of the slit. When the geotextile is pulled out, there is an increase in the lateral earth pressure against the front wall, which in turn leads to an apparent increase of pull out resistance. According to Lopes and Ladeira (1996), the placement of 0.2 m long sleeve around the slit in the front wall of the pull-out box minimizes the effect of friction due to the roughness of the front wall. On the other hand, the absence of a sleeve leads to an increase in maximum pull out force by approximately 10%. Zhai (1996) used a sleeve, which has a length equal to 25% of length of geotextile sample. This was done to avoid the effect of roughness of the front wall on pull-out resistance. Tzong (1987) used sheet metal clamps for pulling the geosynthetic. Fannin and Raju (1993) used the clamp assembly operated by hydraulic jack. All such mechanisms reduce the effect of wall friction on the pull-out resistance. These methods also keep the geotextile within the confinement of soil throughout the test.

2.9 Importance of Pull-out Resistance and Interface Frictional Parameters

One of the primary causes of geotextile failure in reinforced slope, clay liner anchor trench, and in foundation is the slippage of geotextile under the resulting axial or pull-out load, as shown in Fig. 2.8. The soil geotextile interface frictional parameters are used in

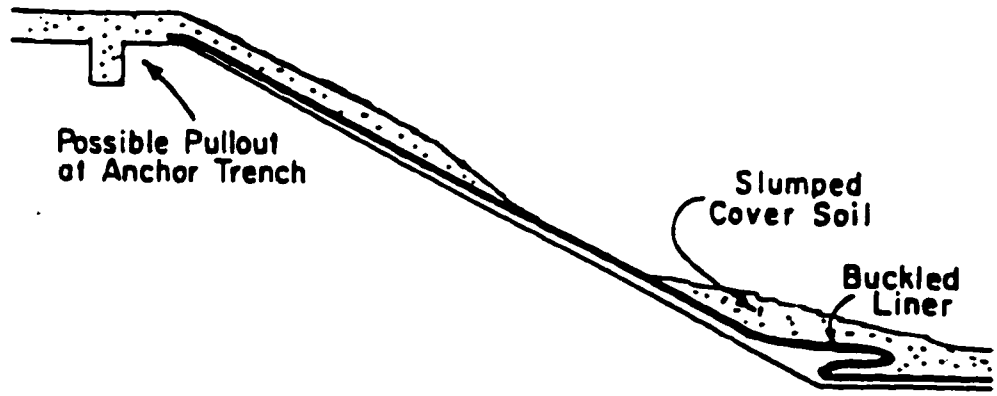

Fig. 2.8: Liner slippage failure (Martin et al., 1984)

the design of landfill side slopes, road and railroad embankments, embankments over weak soils, reinforced walls, and unpaved roads (Martin et al., 1984). The interface interaction factor c_f is used to calculate the required bond length of the reinforcement that is required beyond a critical failure plane.

The use of interface frictional parameters help in optimizing the design. Once these parameters are accounted for, failures of structures due to the pull-out of the geotextile are minimized. Such failures usually result from the lack of enough embedded lengths. There are five discrete design considerations used in safe design of embankments reinforced with geotextiles (Koerner, 1997).

1) Bearing capacity check

   In this case, the embankment is checked against bearing capacity (shear) failure. Any conventional geotechnical engineering theory can be used directly to limit the maximum height of embankment.

2) Global stability check

   The overall stability of the embankment is checked by performing slope stability analysis. The effect of the geotextile is taken just as an anchor. The tension carried by the geotextile adds to the stabilizing moments, hence increases the overall stability.

3) Elastic deformation control

   The amount of the elastic deformation allowed by the geotextile will govern the deformation of the embankment. Hence, this check is important for the design of reinforced embankments. This check calculates the required modulus of the geotextile.

4) Lateral spreading control

Lateral spreading control is the check against the active earth pressure developed within the soil due to the development of tension cracks on the surface of the embankment.

5) Pull-out or anchorage length

2.9.1 Pull-out or Anchorage length

A potential failure scenario for an embankment is shown in Fig. 2.9. The required anchorage length of geotextile can be calculated for different applications. The soil behind potential slip zone resists the pull-out of the geotextile. For high strength geotextiles, Koerner (1997) reported that long anchorage lengths are usually required. Considering the problem in Fig. 2.9, the required anchorage length can be calculated as given by Koerner (1997).

$$T_{act} = 2\tau L = 2(c_a + \sigma_n \tan\psi)L \tag{2.2}$$

$$L_{reqd} = \frac{T_{act}}{2(c_a + \sigma_n \tan\psi)} = \frac{T_{act}}{2c_i(c + \sigma_n \tan\phi)} \tag{2.3}$$

Where:

T_{act} is the axial force developed in geotextile per unit length

L_{reqd} is the required geosynthetic anchorage length

c is the cohesion of soil

c_a is the adhesion of soil to the geosynthetic

ϕ is the angle of internal friction of soil

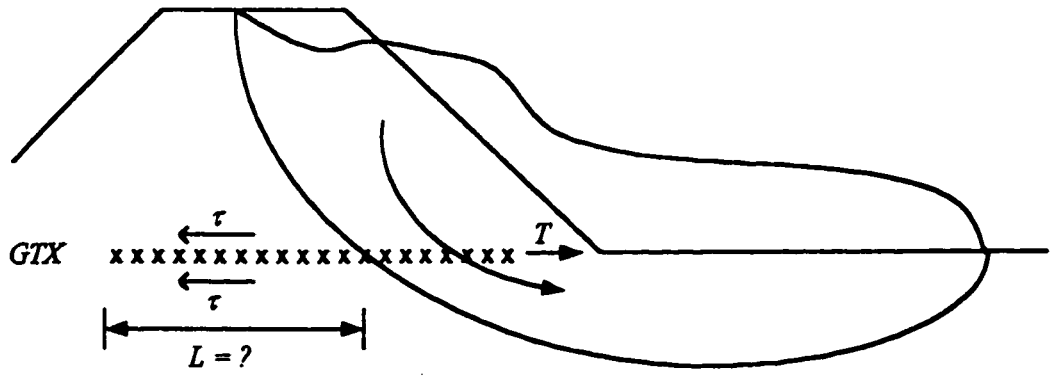

Fig. 2.9: Pull-out or anchorage model (Koerner, 1997)

ψ is the friction angle of the soil to geosynthetic

σ_n is the average vertical stress

c_i is the interface interaction factor

The calculation shows that the anchorage length depends on the strength of the geotextile, the properties of soil, the normal overburden pressure and the interface interaction factor. When there is insufficient anchorage capacity, failure will occur at the soil-reinforcement interface as the reinforcement is being pulled out of the soil. This type of failure mode is known as the pull-out mode (Rowe et al., 1985). It involves the displacement of the reinforcement relative to the soil on both sides of reinforcement. This is the mechanism which controls the anchorage of the geotextile and hence limits the maximum force that is developed in the geotextile.

CHAPTER 3

EXPERIMENTAL PROGRAM

The problems associated with sabkha soil and its use in construction, as discussed in the literature review, are many and requires serious efforts to minimize their consequences. The utilization of geotextile for the improvement of sabkha has shown practical potential due to its lower cost and better effectiveness compared to chemical treatment. Knowledge of the pull-out characteristics of geotextiles, when used with problematic soil such as sabkha soil, becomes extremely important. Therefore it is necessary to have a proper understanding of the anchorage requirements at a given factor of safety or at a given percentage of strain in the geotextile when used with different soils. In order to achieve the objectives of this research, an experimental program was developed to study the frictional characteristics of geotextiles embedded in a local sand and sabkha soil.

This Chapter discusses the procedures followed to fulfill the objectives of this research program. The experimental program consisted of three phases, as shown in Fig. 3.1. General characterization of the sabkha and sand used in this investigation was carried

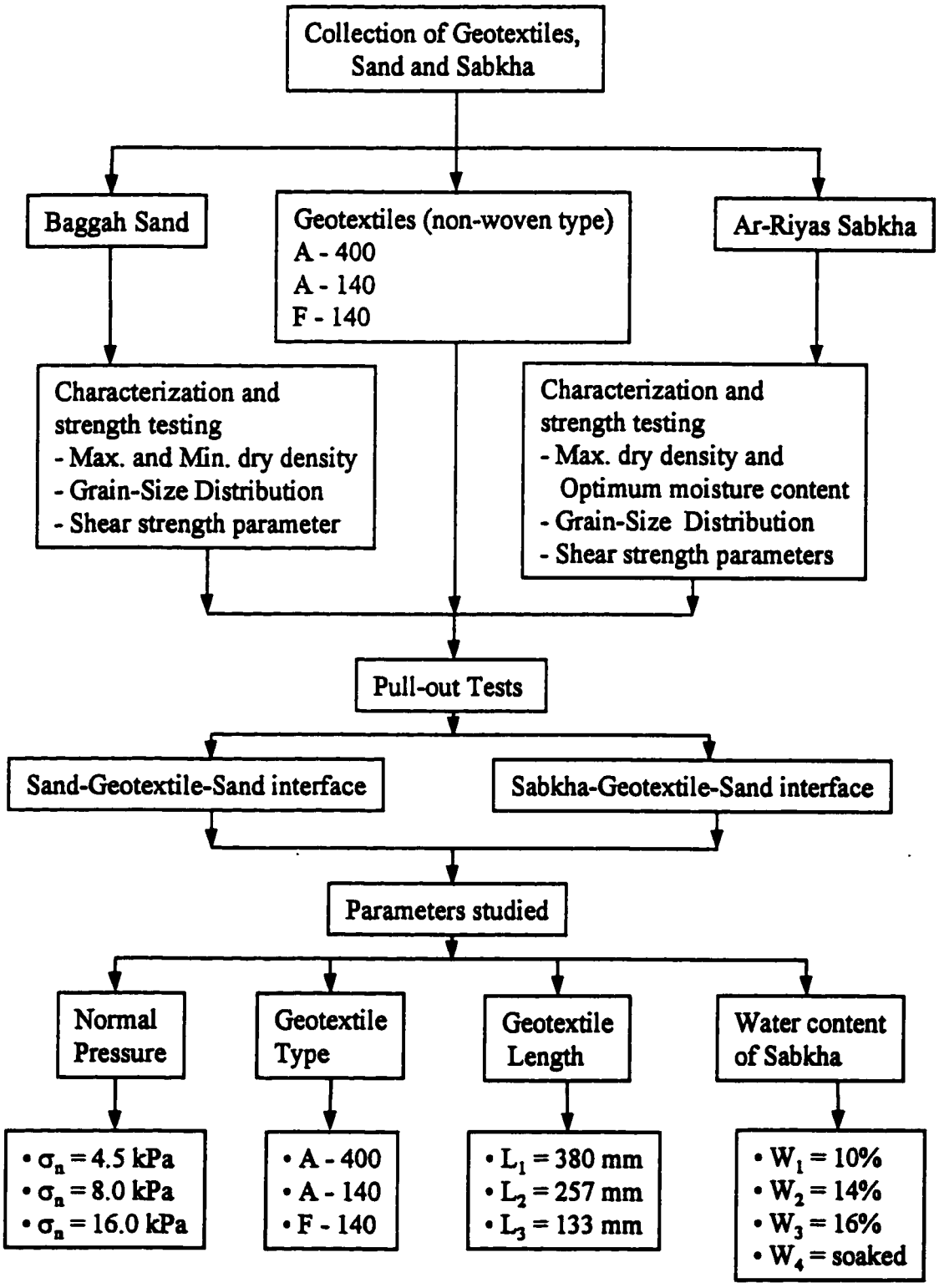

Fig. 3.1: Flow chart for experimental program

out and constituted the first phase. The second phase consisted of performing the pull-out tests of geotextile on local sand to study the effects of various parameters on sand-geotextile-sand interface. To observe the effects of different parameters on sabkha soil, pull-out tests were performed on sabkha–geotextile-sand interface that constituted the third phase.

3.1 Collection of Sand and Sabkha Soils and Geotextiles

3.1.1 Collection of Sand

The sand used in this investigation was brought from Baggah area, which is located in southwest of Dhahran as shown in Fig. 3.2. The site is located along the Dammam-Riyadh Highway. This sand has recently been extensively used in the research conducted at KFUPM (Aiban et al., 1999) and it is considered as a typical eastern Saudi sand. The soil is dune sand, light yellowish in color and have a smooth texture and uniform gradation.

3.1.2 Collection of Sabkha

The Sabkha soil used in the testing program was collected from Ar-Riyas sabkha (Pit # 9). This sabkha soil has also been used in the research conducted by Aiban et al. (1999) and found to be one of the most problematic sabkhas in the area. The Ar-Riyas sabkha is located approximately 55 km NNW of Dhahran and extends for about 30 km SSE of Al-Jubail as shown in Fig. 3.2. The materials were retrieved from all layers above the ground

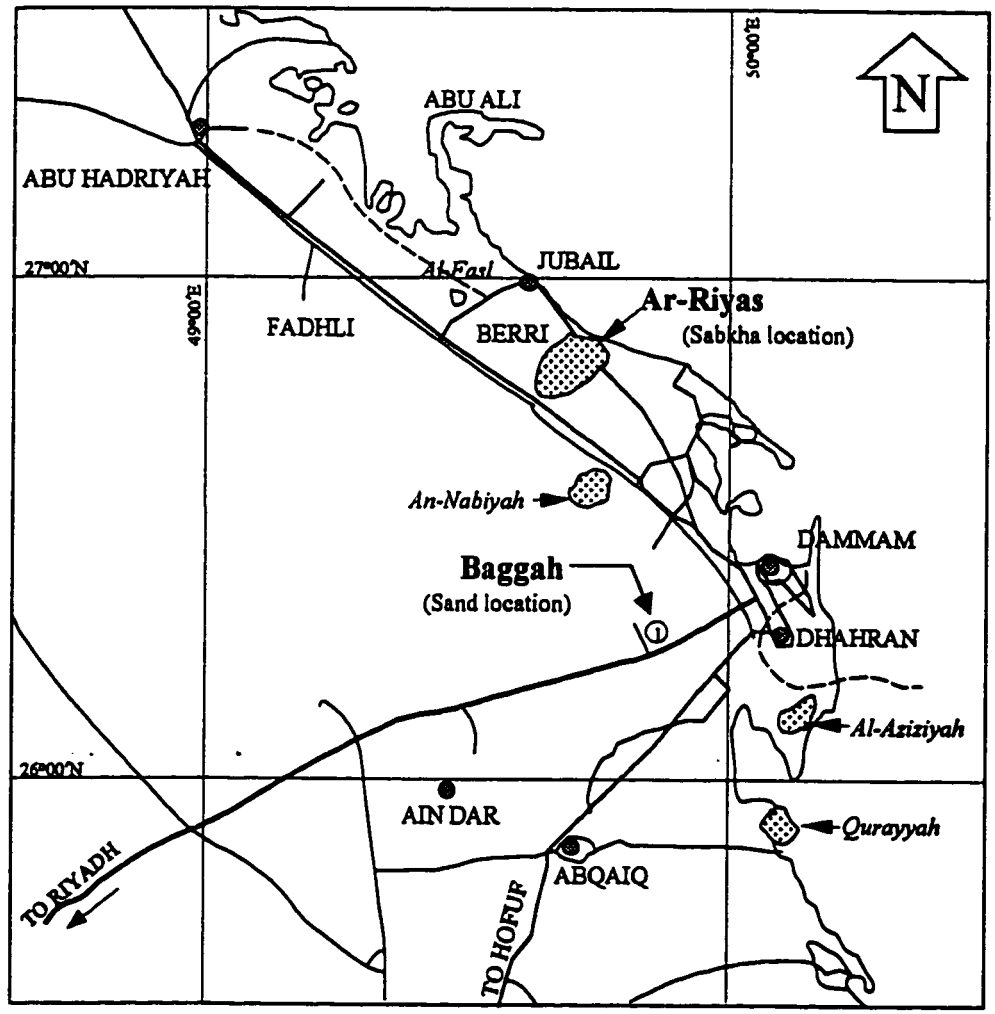

Fig. 3.2: Map of eastern Saudi Arabia showing the locations of the Baggah sand and Ar-Riyas sabkha (Aiban et al. 1999)

water table excluding the salt crust. At that particular site, the surface was observed to be covered with non crystallized halite, which extends 3 to 4 cm. The ground water table was found at a depth of about 200 mm in this pit.

3.1.3 Collection of Geotextiles

As reported in the literature review, there are two types of geotextile: woven and non-woven. The non-woven geotextiles are usually needle-punched or heat-bonded and are manufactured from polypropylene and polyester as their raw material. The main characteristic of polypropylene geotextile is its low sensitivity to chemicals of low and moderate concentration. The non-woven needle-punched geotextiles are normally used for soil reinforcement purposes. Needle-punched, non-woven, polypropylene geotextiles are manufactured locally due to its excessive use in the region for reinforcement, separation and filtration purposes. In this research program, three different non-woven geotextiles were used. These were named "generically" as A-400, A-140 and F-140. The A-400 and A-140 geotextiles are non-woven and needle-punched. These are manufactured locally in Saudi Arabia and have a mass per unit area of 400 g/m^2 and 140 g/m^2, respectively. Whereas, the F-140 geotextile is a non-woven geotextile needle-punched on one face and thermally bonded on the other face. It is an imported product, supplied by a local dealer. It has a mass per unit area of 140 g/m^2. The technical properties and specifications of these geotextiles, as provided by the suppliers, are shown in Table 3.1.

Table 3.1: Technical specification of geotextiles used in pull-out tests

Characteristics	Standard	Units	Geotextile Type (Non-woven)		
			A-400	A-140	F-140
Mass per unit area	ASTM D 5261	g/m^2	400	140	140
Thickness (under 2 kN/m^2)	ASTM D 5199	mm	4.0	2.0	0.95
Tensile strength (MD/CD)	EN 29073-3	kN/m	20/28	7/9	7/8
Elongation (MD/CD)	EN 29073-3	%	>70/>80	>70/>80	>50/>60
Grab Strength (MD/CD)	ASTM D 4632	N	1100/1500	380/500	-
Grab Elongation (MD/CD)	ASTM D 4632	%	>80/>90	>80/>90	-
Permeability	ASTM D 4491	cm/sec	0.45	0.5	0.08
Transmittivity (at 2kN/m^2)	ASTM D 4716	10^{-6} x m^2/s	70	39	-
Apparent Opening Size (O_{95})	ASTM D 4751	micron	75	106	85

MD: Machine Direction

CD: Cross-machine Direction

EN: European standards

3.2 Characterization of Baggah Sand and Ar-Riyas Sabkha Soils

Relevant ASTM and AASHTO tests were used to characterize the two soils, namely Baggah sand and Ar-Riyas sabkha, and determine their compaction characteristics. Furthermore, the conventional triaxial compression testing was performed to quantify the shear strength parameters of both soils. The procedures followed for each type are presented in the following sections.

3.2.1 Grain-Size Distribution

The grain-size distribution test was performed for the collected soils (Baggah sand and Ar-Riyas sabkha) according to ASTM D 422 and D 423. Dry sieve analysis was done for the Baggah sand, whereas for Ar-Riyas sabkha washed sieve analysis was performed. Sabkha was washed with both distilled water and sabkha brine. A set of sieve including ASTM No. 10, 20, 30, 40, 60, 60, 100, 140 and 200 sieves was used for both soil types.

3.2.2 Atterberg's Limit

The liquid limit and plastic limit were determined for the sabkha soil passing ASTM sieve No. 40. The tests were performed according to ASTM D 4318. Liquid limit and plastic limit tests were performed with distilled water and sabkha brine. The plasticity index obtained using sabkha brine only was used for the classification of sabkha soil. The grain-size distribution curve for the Baggah sand shows that less than 5% of its particles pass

sieve No. 200 therefore, plasticity tests are not required for Baggah sand according to Unified Soil Classification System.

3.2.3 Compaction Characteristics

The compaction test type is dependent on the soil type. For cohesionless soils such as sands, the relative density tests (ASTM D 4253 and D 4254) are performed to find the maximum and minimum dry densities. For the maximum dry density determination, there are two methods: one is called dry method and other is called wet method. In dry method, the sand is poured into the mold, with the collar attached, using a method that minimizes segregation such as the pluviation method. The side of the mold is struck few times using a rubber hammer to densify the soil. A surcharge weight is then placed on the top of the soil and the mold is vibrated using the vibrating table. Vibration is carried out for 8 minutes at 60 Hz. The total mass of the surcharge weight is equivalent to a surcharge pressure of 2.0 psi. Whereas in the case of the wet method, sand is poured into the mold attached to the collar. The mold is placed on the vibrating table and fixed to it. Enough water to soak the sample, was added to the sand in the mold during densification (vibration) process. Knowing the wet weight of sand in the standard mold and dry weight of sand after oven drying, the maximum dry density can be determined.

For the determination of minimum dry density, sand is poured in the standard mold maintaining a free fall of sand of about ½ in. or just high enough to maintain continuous flow of the soil particles. The pouring device is moved in a spiral path to minimize the

segregation. Knowing the weight of sand in the mold and the volume of the mold, the minimum density of sand is found.

On the other hand, the Proctor compaction test is used for cohesive soils. The Proctor compaction tests provide a relationship between the molding moisture content and the dry density of the soil. The modified proctor test was performed in this investigation to determine the moisture-density relation of the sabkha soil. The test was conducted according to ASTM D 1557.

3.2.4 Triaxial Test

In order to compare the shear strength of the soil with the shear stresses developed at sand-geotextile-sand or sabkha-geotextile-sand interface, the shear strength parameters of Baggah sand and Ar-Riyas Sabkha were determined. Triaxial tests were performed on Baggah sand in dry condition at a relative density of 75%, which is usually required in the field. These tests were performed according to ASTM D 2850. Similarly undrained triaxial tests were conducted on as molded sabkha samples at 10% and 14% moisture content. In addition, consolidated-undrained triaxial tests were conducted on soaked samples, in order to simulate the field condition of the rising water table.

3.3 Pull-out Experimental Setup

The pull-out test had been conducted on various type of geosynthetics by previous researchers (Collios et al., 1980; Ingold, 1982 and 1984; Rowe et al., 1985, Fourie and Fabian, 1987; Rao and Pandey, 1988; Palmeira and Milligan, 1989; Fannin and Raju, 1991

and 1993; Kharchafi and Dysli, 1993; Murthy et al., 1993; Yehia et al., 1994; Farrag, 1995; Zhai et al., 1996; Lopes and Ladeira, 1996; Mallick, 1996; Shingenori et al., 1996; Long et al., 1997; Karmokar, 1998; Koutsourais, 1998; Lo, 1998). They used different sizes of pull-out boxes and different normal load application mechanisms. In order to carry out the pull-out tests on sand and sabkha soil, a pull-out apparatus was manufactured in the Geotechnical Engineering Laboratory at KFUPM. The schematic diagram of the setup is shown in Fig. 3.3. The setup consisted of a pull-out box, normal loading plate, pull-out gear box system with adjustable speed. The pull-out gear box is operated through an electrical motor.

3.3.1 Pull-out Box

The pull-out box is made of plexiglas sheets 25 mm thick. All sides are bolted together such that all pieces can be dismantled for cleaning purposes including removal of soil after testing. The box has an internal length of 500 mm and an internal width of 100 mm. The clear internal height of the shear box is 250 mm. The front wall has a horizontal slit at an elevation of 100 mm from the bottom. The thickness of the slit is 8 mm. The slit was provided for pulling the geotextile during the pull-out tests. Each side of the box is attached to the adjacent sides by means of ten – 10-mm diameter screws, 5 on each end. The base is attached to the four sides using 12 – 10-mm diameter screws on each of the long sides and by 3 – 10-mm diameter screws on each of the short sides. In the back wall of the box, three holes, 2.5 mm in diameter were drilled to accommodate the three inextensible steel rods (1.5 mm in diameter) that are used for the measurement of

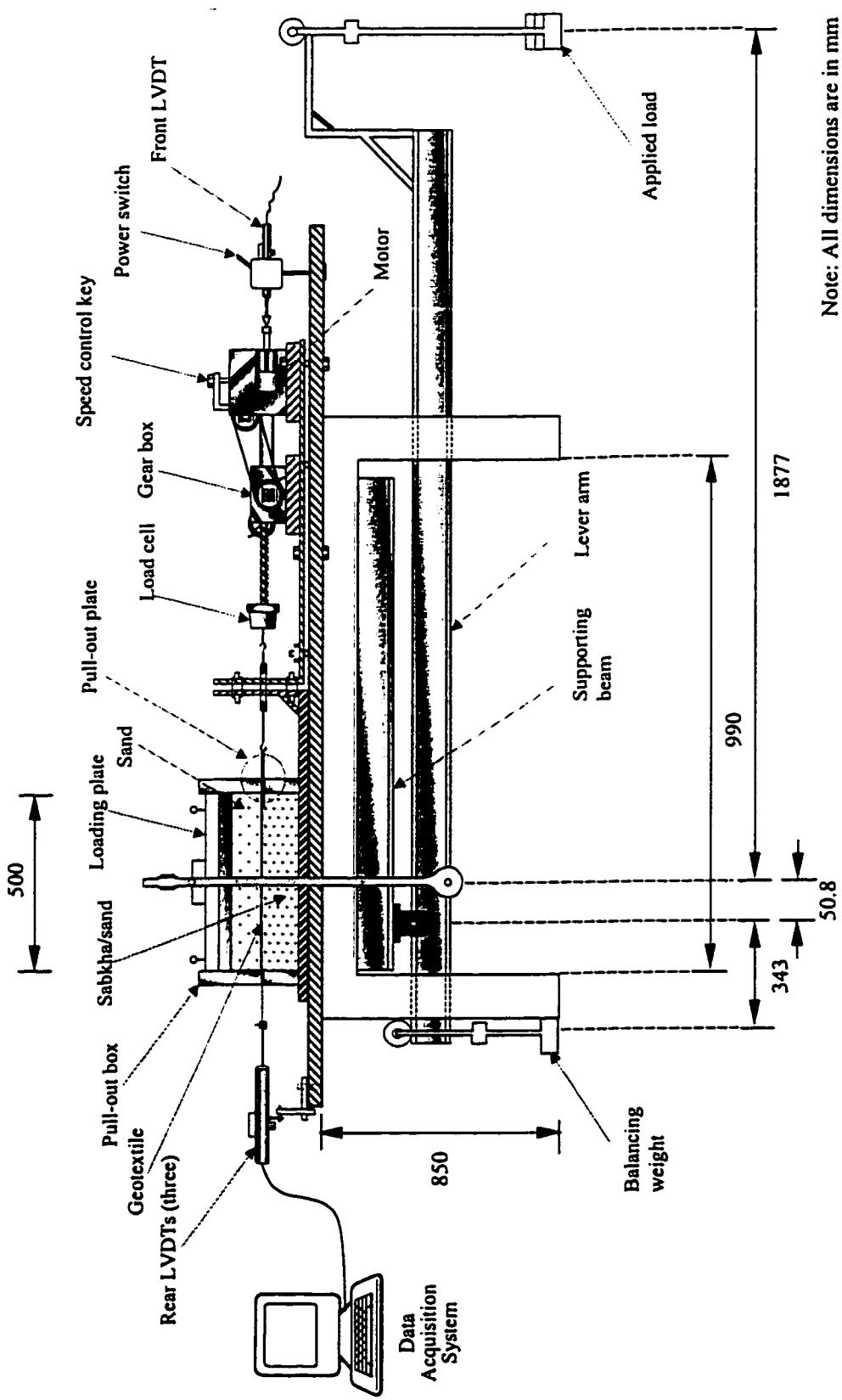

Fig. 3.3: Schematic diagram of experimental set up

displacement. These holes are at the same level as the front slit, which is 100 mm above the base of the box.

3.3.2 Application of the Normal Load

Different researchers used different mechanisms for applying the normal load. Some of them had used pressurized air /or water bag to provide a flexible top boundry (Fannin and Raju, 1991; Kharchafi, 1993; Alfaro, 1995; Zhai et al., 1996; Lo, 1998). Others had applied direct load from the top using rigid plate to provide rigid top boundary (Palmeira and Milligan, 1989). In present case, the concept of conventional oedometer system was used, on a larger scale, for normal load application. This system consists of a loading plate, supporting beam, lever arm, balancing weight and the applied load or surcharge, as shown in Fig. 3.3. It works on the principle of fulcrum. High couple moment is produced because of the longer lever arm for applied load. The high moment results in heavy load at the center of pull-out box, which is transferred to the soil through a thick steel loading plate placed above the compacted sand layer. The steel loading plate has the same dimensions as the cross section of the box (little smaller to fit in) and has a thickness of 50 mm.

The procedure for applying the normal load involves placing the thick steel plate over the compacted and leveled top sand layer in the box. The loading rod is bridging over the steel plate and the load is transferred by means of a ball. The lever arm is kept horizontal by means of balancing weight and positioning nut in the loading rod. Once the lever arm becomes horizontal, the load is then applied as shown, in Fig. 3.4. The resulting

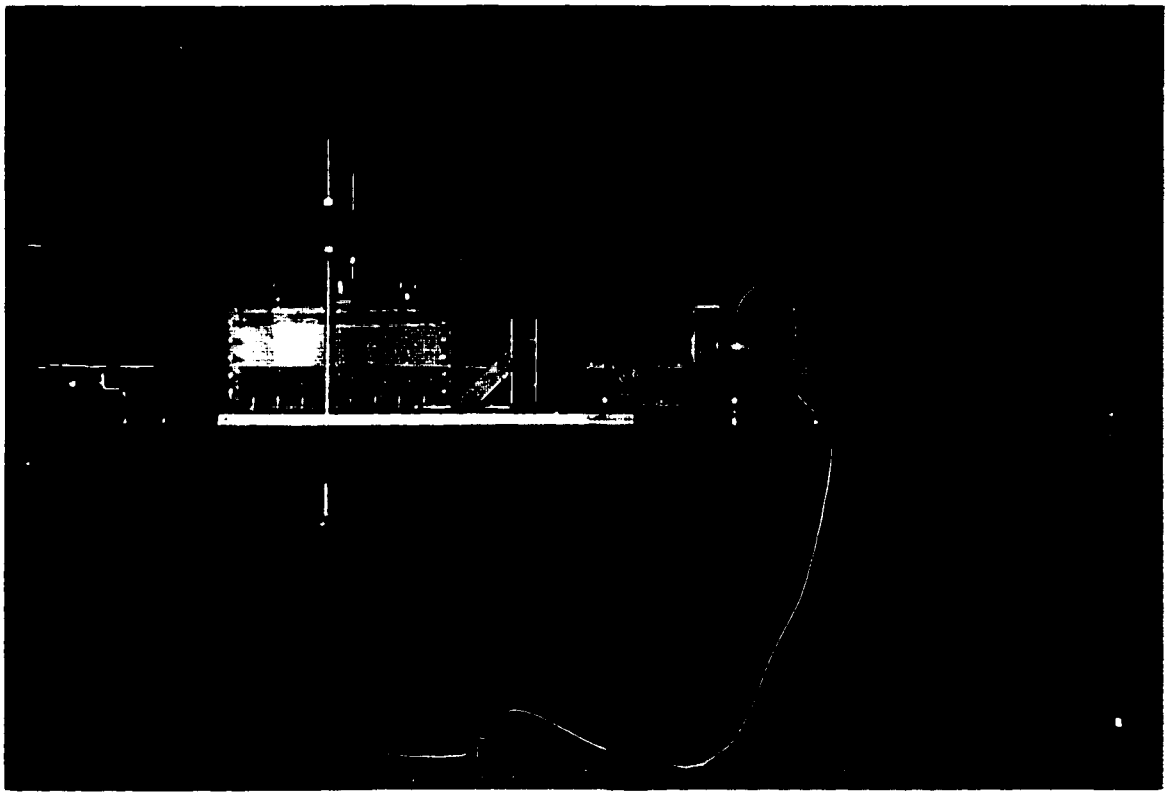

Fig. 3.4: Pull-out test apparatus

load on the loading rod (subsequently on the loading plate) is 34.3 times the applied load. This mechanism was intended to magnify the load and thus small loads can be utilized to produce high normal stresses.

3.3.3 Pull-out Load Mechanism

The mechanism that pulls the geotextile from its embedded condition must be able to detect the magnitude of the pull-out force, while the pulling out operation is in progress. Such mechanism was discussed by Kabeya (1993), and Alfaro et al. (1995). In the present case, the pullout mechanism consists of an electric motor with a 0.3 ampere capacity delivering a torque of 20 lb. in, a gear box, a speed change knob, a threaded rod and a housing cylinder for the threaded rod. The procedure for applying the pull-out load involves switching the electric motor on. This will rotate the gears in the gear box that are connected to another gear attached at the housing cylinder by means a of steel chain. The rotation of this gear moves the threaded rod in/or out of the housing cylinder. Whenever it is required to apply the pull-out load, the threaded rod was taken out completely by means of a manual handle that is attached to the gear on the housing cylinder. The calibrated load cell is attached at the head of threaded rod, which is capable of measuring the tensile load. The double headed hook is used to connect the load cell attached on the threaded rod with the steel plate emerging out of the box on which the geotextile is glued. When the electric motor is switched on, it rotates the gear on the housing cylinder, which causes the threaded rod to move away at a constant speed thus pulling the plate and attached geotextile. The load cell will then measure the pull-out load. The pull-out system is

displacement controlled with adjustable speed. During the experimental work, the threaded rod moves at a constant speed of 1.27 mm per minute and it is capable of pulling the geotextile for maximum of 120 mm displacement at its front end.

3.3.4 Displacement Monitoring System

The method adopted for measuring the displacement resembles that of Forsman (1994), Bourdeau et al. (1994), Alobaidi et al. (1997) and Long et al. (1997). The displacement along the geotextile during the pull-out testing was monitored at different points. The geotextile was divided into three equal parts and marked at each position. The three inextensible steel rods, of 1.5 mm diameter, were bent at one end to form a hook and these rods were firmly attached to the geotextile using cotton yarn knitting at one-third points of the geotextile. These rods were placed at an equal distance away in transverse direction, as shown in Fig. 3.5. These rods were protruded out of the box through the three holes drilled in the back wall of the box. In order to measure the displacement at one-third point, each rod was connected to a linear variable differential transducer (LVDT) which was placed at the back of the box, as shown in Fig. 3.6. The displacement at the front end of the geotextile was recorded by the LVDT connected to the threaded rod. This enabled displacement monitoring at four points along geotextile, front end (df), rear end (d end) and at two one-third points (d1 and d2).

3.3.5 Data Acquisition System

All the LVDTs, three at the back of shear box and one at the front, and the load cell measuring the pull-out load, were attached to a portable datalogger model TDS 303

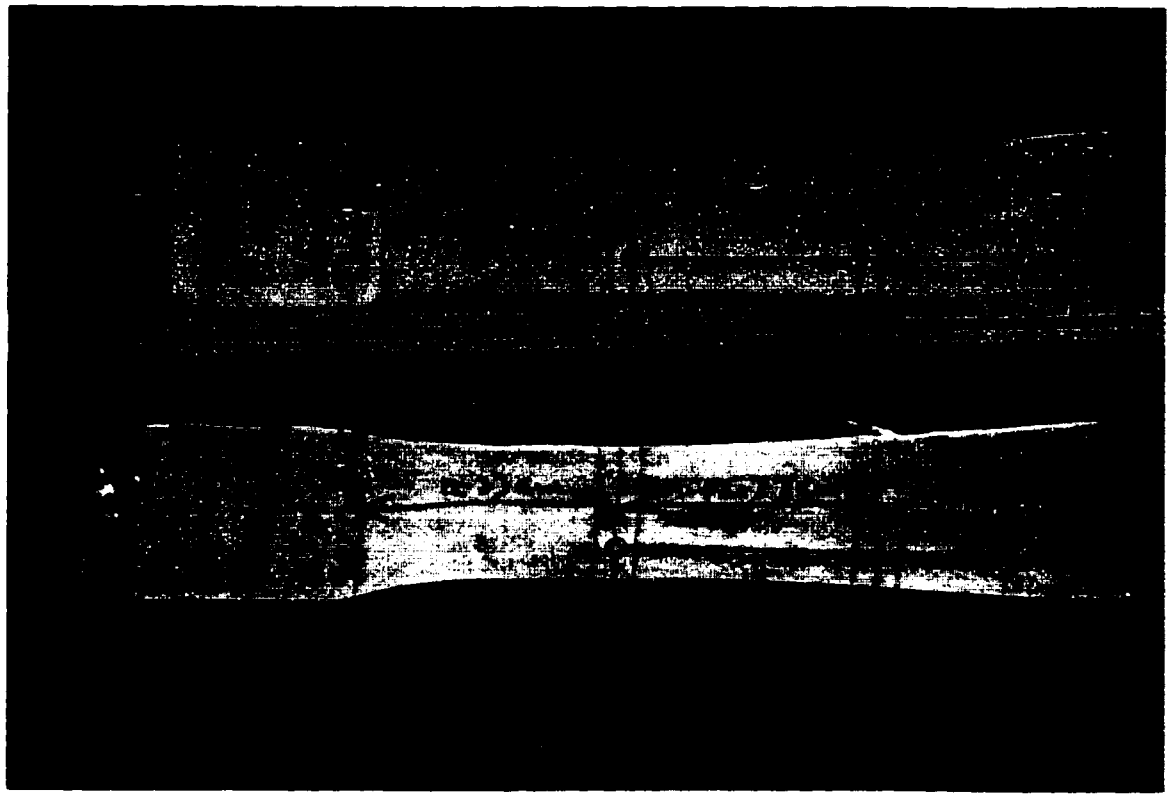

Fig. 3.5: Placement of inextensible steel rods for measuring displacement at different points along the geotextile

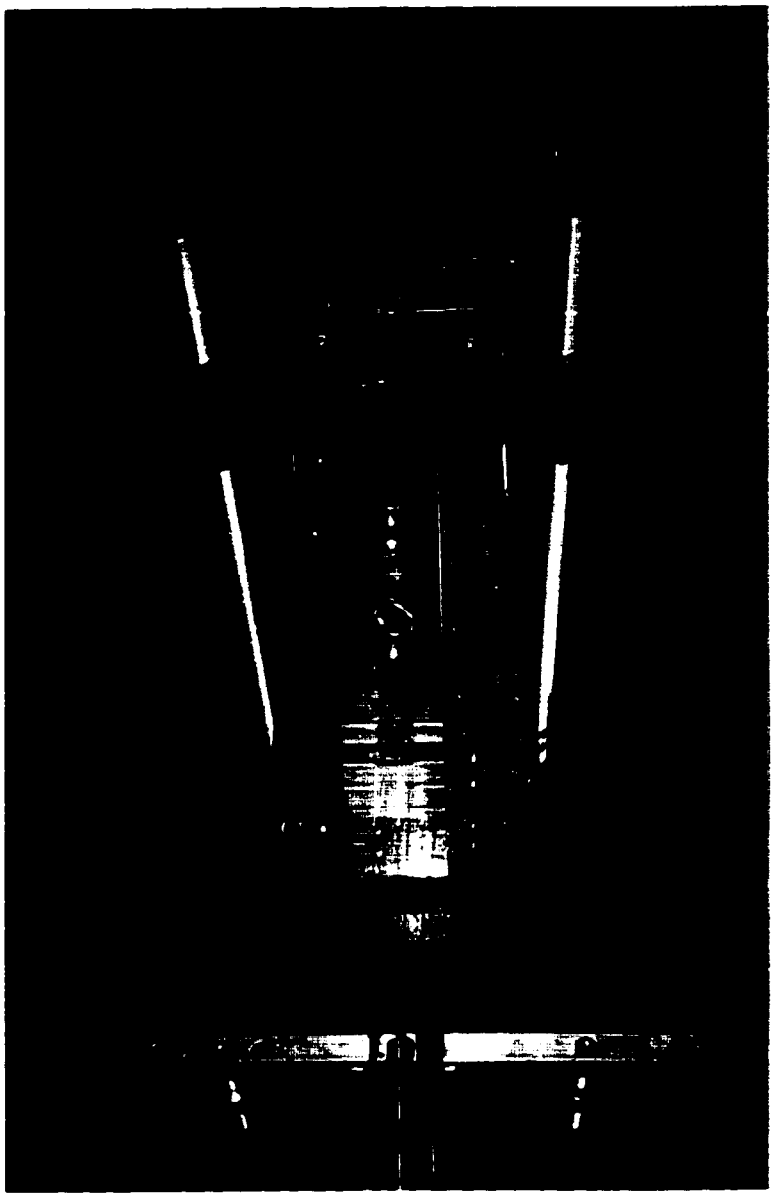

Fig. 3.6: Connection of displacement rods emerging out of pull-out box with LVDTs at the back of pull-out box (Top rear view)

manufactured by Tokyo Sokki Kenkyujo Co. Ltd. which has a built-in memory for storing data. The data was copied from the datalogger to a PC after the completion of each test.

3.4 Sample Preparation and Testing Procedure

3.4.1 Compaction of the soil below the geotextile

In the case of sand-GTX-sand interface testing, the bottom sand layer (100 mm thick) was placed by means of pluviation from a funnel and compacted to a relative density of 75% by striking the box with a rubber hammer. Different trials were performed to adjust the pluviation height such that a relative density of 75% is achieved.

In the case of sabkha-GTX-sand interface, the bottom layer below the geotextile consisted of 100 mm thick sabkha compacted at the required moisture content. The compaction of sabkha was carried out in two layers, 50 mm thick each. Each layer was compacted by applying a static load of 62.3 kN (14000 lb.) which resulted in a pressure of 1250 kPa. The compaction was done through a steel plate placed over the sabkha. The static load was applied using Tinius Olsen compaction machine (Fig 3.7).

3.4.2 Preparation of Geotextile Specimens

The geotextiles used were provided in the form of square sheets, 1 m x 1 m in size. All geotextile specimens in the experimental work have a width of 100 mm but different lengths. The specimens were cut from the 1 m x 1 m sheets, where the length of geotextile is perpendicular to the machine direction. Three different lengths were used in the experimental program with the dimensions shown in Fig. 3.8. A mark line was made at

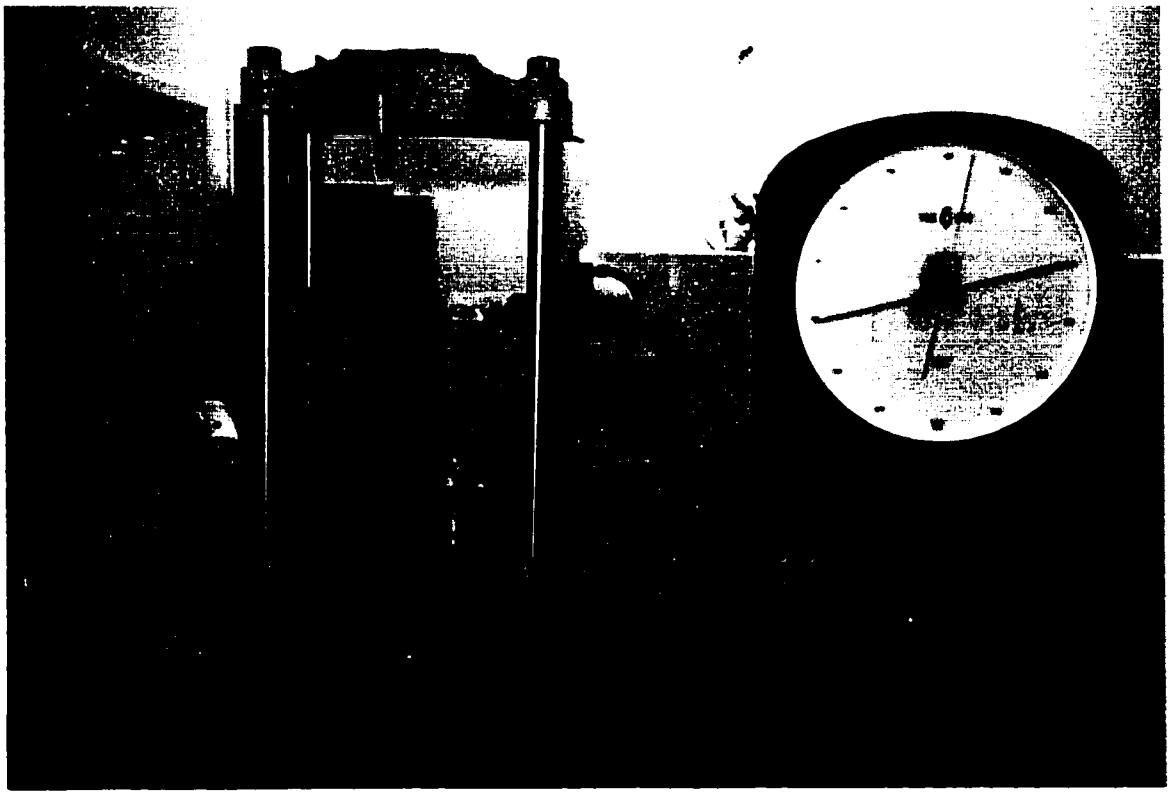

Fig. 3.7: Static compaction of sabkha using Tinius Olsen compaction machine

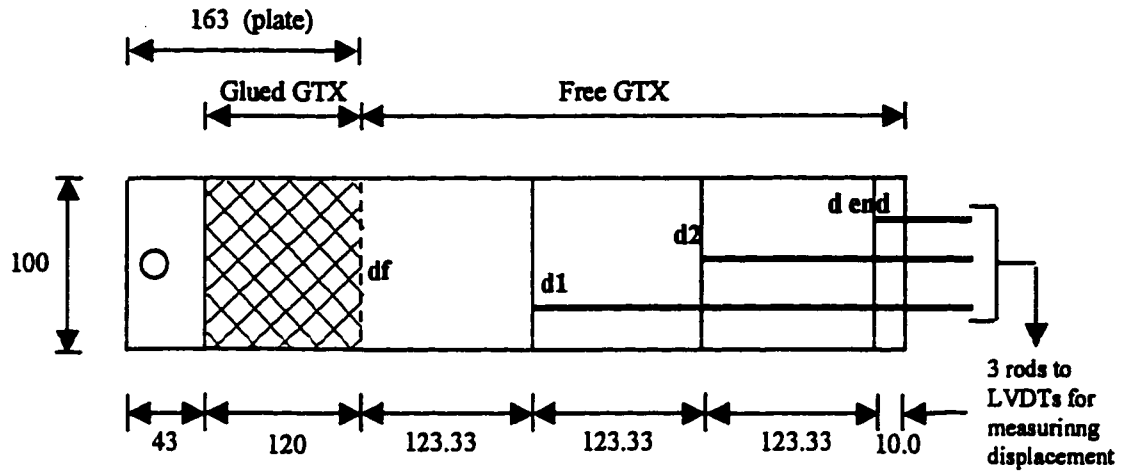

Total length of specimen = 380 mm

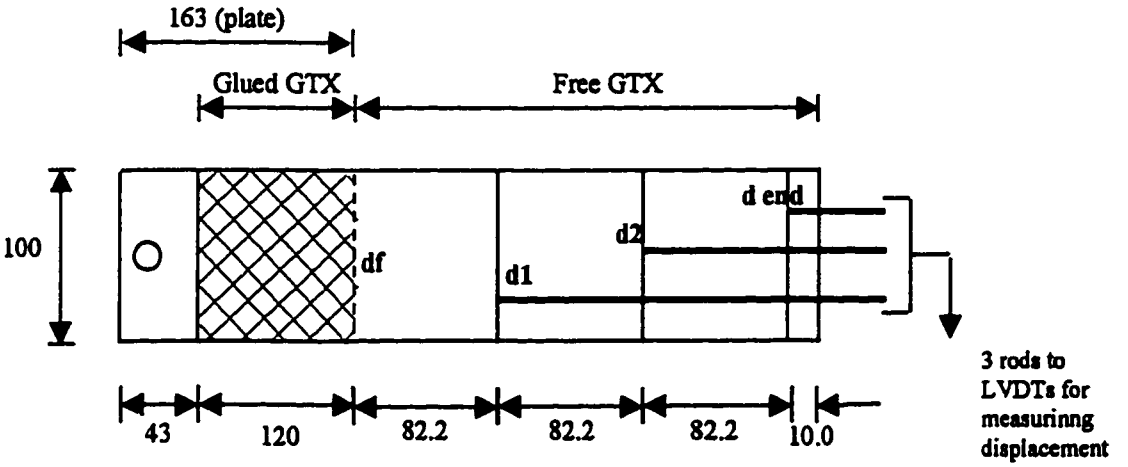

Total length of specimen = 257 mm

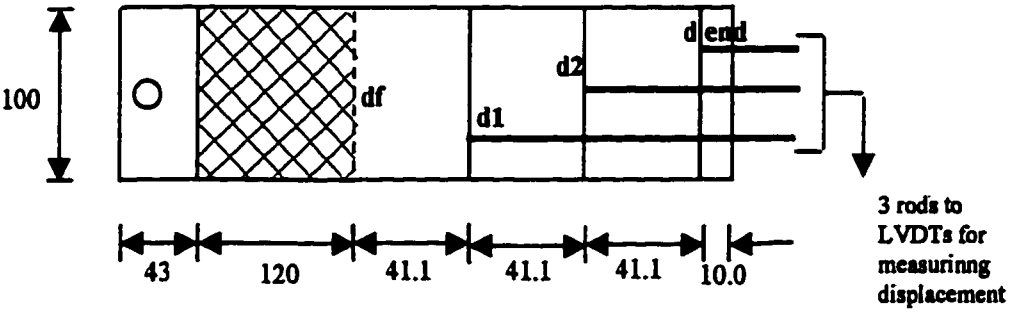

Total length of specimen = 133 mm

Note: All Dimensions are in mm

Fig. 3.8: Various lengths of geotextile used in the experimental program

120 mm from one end. That portion of the geotextile (120 mm long) was glued to the 1.0 mm thick steel plate which would be attached to the pulling mechanism. The remaining geotextile length is divided into three equal parts leaving 10 mm from the other end. Similar procedure was also described by Zhai et al. (1996).

3.4.3 Gluing of Geotextile with Pull-out Steel Plate

For each pull-out test, the front 120 mm portion of the geotextile sample was glued to the stainless steel plate which is 100 mm in width and 163 mm long. The thickness of the plate is 1.0 mm. The remaining portion of the geotextile was left free. Special adhesive was used for gluing the geotextile to the stainless steel plate over the 120 mm length. This was done to ensure that the bond remains perfect throughout the test. The glue was applied to one side of the steel plate that has been made rough by grinding. The 120 mm length of the geotextile specimen was then placed over the steel plate in a proper alignment. The steel plate has a hole of 9 mm diameter near its front end. The hook from the pulling system will be attached to this hole.

The geotextile attached, with the displacement rods and steel plate, was placed over the compacted bottom soil layer. The steel plate emerged from the horizontal slit which was made in the front wall of the box. The 120 mm long glued geotextile steel plate remains inside the pull-out box with its beginning at the interior face of the front wall. Therefore, the remaining free geotextile was also inside the box. The pull-out system has a maximum displacement capacity of 120 mm. This means that the front end of the free geotextile remains inside the shear box during the whole test. This has the consequence

that the entire geotextile length remains under normal pressure throughout the pull-out testing.

3.4.4 Compaction of upper Sand Layer (Overburden material)

After placing the geotextile, the top 100 mm sand layer was backfilled and compacted by pluviation and striking the side wall of the box with rubber hammer as described earlier. The top surface was properly leveled and the steel plate was placed on the top of the leveled surface. Extra care was taken to maintain the plate horizontal so that a uniform pressure is applied over the whole surface.

The box filled with sand, geotextile and sabkha is placed on the table and the normal loading rod is adjusted during the leveling of the lever arm. The steel plate was connected to the pulling system with the help of a double headed hook. A calibrated load cell was then attached to the threaded rod. The LVDTs and the load cell were connected to the data logger that was programmed to take reading every 4 seconds. The anticipated load was applied at the far end of the lever arm such that it develops the required normal pressure at the geotextile layer. Once the normal pressure is applied, the pull-out motor is switched on while the load cell measures the pull-out resistance of the geotextile and steel plate during the test. The LVDTs record the displacement along the geotextile at the specified locations.

3.4.5 Soaking of Samples

The effect of sabkha soaking on the pull-out resistance was of primary concern. It was, therefore, decided to soak the sabkha layer to quantify the effect of soaking in sabkha–

GTX–sand interface. In addition, pull-out test was performed while soaking the bottom sand layer in sand–GTX–sand interface. For such tests, the box was water proofed by applying a silicon compound at all joints to prevent leakage. The sample was then prepared in the same way.

In order to soak the soil, three holes, 6.25 mm diameter each were drilled in the sides of the bottom plate of the box, across the length, such that the water is discharged to the centerline of the bottom plate. Before placement of the bottom soil layer, 10 mm thick layer of sand was placed on top of a filter fabric sheet placed directly on the bottom plate to prevent the soil from plugging the three holes. The 10 mm sand layer acts as a drain where water can flow upward throughout the bottom soil layer. Distilled water was used for soaking, and the necessary head was provided by means of water tank placed at a level of 1.14 m above the box bottom plate. Soaking of sabkha was carried out for 4.5 hours. The water tank was connected to the box by means of rubber tubing and connections.

3.5 Experimental Design Matrix

In order to investigate the interfacial soil geotextile frictional parameters, two types of local interface soils were selected because of their abundance in eastern Saudi Arabia. The parameters investigated for each soil are discussed below:

a - Sand-GTX-Sand Interface

Sand-GTX-sand interface consisted of a bottom sand layer 100 mm in thickness, which is compacted to a relative density of 75%. The geotextile layer was placed over the

compacted sand layer. Another 100 mm thick compacted sand layer was placed over the geotextile. This layer simulates the subbase in roads or the backfill below the foundations. The experimental design matrix for the pull-out tests on sand-GTX-sand interface is shown in Table 3.2.

b - Sabkha-GTX-Sand Interface

In this interface, the bottom layer consisted of a 100 mm compacted sabkha layer at a given moisture content. The sabkha is overlain by a geotextile layer which is overlain by 100 mm compacted sand layer over which the normal load is applied. The experimental design matrix for the pull-out tests on sabkha - GTX - sand interface is shown in Table 3.3.

For both interfaces, the tests were carried out with 120 mm of geotextile glued to the steel plate. The remaining geotextile length is the free geotextile which simulates the geotextiles in the field. The strip of geotextile including the steel plate is placed inside the box and is sandwiched between the top and bottom soil layers. The pull-out resistance obtained from this is contributed by the steel plate with the geotextile glued to it and the free geotextile. As the test proceeds, the steel plate comes out of the box, thus the pull-out load is gradually transferred to the free geotextile and ultimately the steel plate will have no contribution when the pull-out deformation reaches 120 mm at the front end. At this point, the pull-out load is carried entirely by the free geotextile. With this concept in mind, the pull-out test was repeated with stainless steel plate glued to the geotextile only without any free geotextile. The pull-out measured in this test is the resistance offered by the steel plate (with 120 mm long geotextile glued to it) only. Therefore, the difference between the

Table 3.2 Experimental design matrix for pull-out tests on sand-GTX-sand interface

Normal Pressure (kPa)	Moisture Content	Geotextile Type and Length							
		A-400				F-140		A-140	
4.5	Dry	380 mm		Plate*		380 mm	Plate*	380 mm	Plate*
8	Dry	133 mm	257 mm	380 mm	Plate*	380 mm	Plate*	380 mm	Plate*
	Soaked**	380 mm		Plate*		-		-	
16	Dry	380 mm		Plate*		380 mm	Plate*	380 mm	Plate*
24	Dry	380 mm		Plate*		-		-	

* Test is performed with only stainless steel plate glued with 120 mm geotextile, and without free geotextile.

** Test was performed with only bottom sand layer being soaked.

Table 3.3 Experimental design matrix for pull-out tests on sabkha-GTX-sand interface

Normal Pressure (kPa)	Moisture Content of Sabkha(%)	Geotextile Type and Length							
		A-400				F-140		A-140	
4.5	14	380 mm		Plate*		380 mm	Plate*	380 mm	Plate*
8	10	380 mm		Plate*		-		380 mm	Plate*
	14	133 mm	257 mm	380 mm	Plate*	380 mm	Plate*	380 mm	Plate*
	16	380 mm		Plate*		-		-	
	Soaked**	380 mm		Plate*		-		-	
16	14	380 mm		Plate*		380 mm	Plate*	380 mm	Plate*

Note: Sand layer on top of the geotextile was dry for all the tests except the soaked ones.

* Test is performed with only stainless steel plate glued with 120 mm geotextile, and without free geotextile.

** Test was performed with only sabkha layer (below the geotextile) being soaked.

readings from the two tests gives the pull-out resistance of the free geotextile only as described by Palmeira and Milligan (1989), Mallick et al. (1996) and Long et al. (1997). In fact, each test that involves a change in normal pressure or a change in geotextile type or a change in moisture content of soil is repeated for the plate only to enable the determination of the pull-out load taken by free geotextile only.

3.6 Parameters Studied

The main objective of this study is to investigate the effect of various parameters on the pull-out resistance of geotextiles. The applied normal pressure is the most important parameter since the pull-out resistance is highly dependent on the normal stress level. Normal pressure in the field is usually coming from the overlying soil and the supported structures, if any. Generally, the thickness of the pavement layers in local roads varies between 0.26 m to 1.0 m. It was therefore proposed to use normal pressure values of 4.5, 8, 16 kPa and higher values if needed.

The other main parameter is the geotextile type. Three different types of geotextiles were selected on the basis of tensile strength and percentage elongation of the geotextiles. A-400 and A-140 geotextiles are manufactured locally and these are polypropylene non-woven needle punched geotextile. These two grades of geotextiles have many applications in erosion control, road stabilization, and drainage. The A-400 geotextile is three times stronger than A-140 geotextile in tensile strength but both have about 70% elongation at rupture. The third geotextile type is F-140. This is also needle punched polypropylene geotextile, but it is less extensible as compared to the other two

geotextiles. One face of this geotextile was thermally bonded while the other face was needle-punched. It has about 50% elongation at rupture. Moreover it is thinner as compared to other geotextiles.

The third main parameter is the length of the geotextile. Three different geotextile lengths were selected, as shown in Fig. 3.8. The effect of each parameter was studied by keeping the other parameters fixed and varying only that particular parameter. Varying the length of the geotextile will provide useful information regarding the deformational modes from which the pull-out resistance in geotextile is developed. For each geotextile specimen, the front 120 mm of geotextile is glued into the stainless steel plate. The remaining portions are 380, 257 and 133 mm of free geotextile length.

The fourth parameter is the moisture content of the sabkha layer. This is the moisture content at which compaction was performed. Three different moisture contents (10, 14, and 16%) were used. In addition, one sample was soaked to investigate the effect of soaking. These parameters were investigated for two types of interface soils. The tests were performed for both sand-GTX-sand and sabkha-GTX-sand interfaces.

CHAPTER 4

RESULTS AND DISCUSSIONS

This Chapter presents the results obtained from the experimental program described in Chapter 3. Firstly, the characterization test results of sabkha and sand soils are discussed. Then, the preliminary investigation used for the selection of pull-out plate size is presented. The results of pull-out tests on both sand–geotextile–sand and sabkha–geotextile–sand interface are presented and discussed in detail.

4.1 Material Properties of Soils used in Pull-out Tests

4.1.1 Baggah Sand

Baggah sand is light yellowish dune sand with uniform gradation. The grain-size distribution curve is presented in Fig. 4.1. This curve shows that 88% of the soil passes ASTM sieve No. 40 and most of the particles lie in the range of 0.1 to 0.9 mm. The effective diameter D_{10} is 0.16 mm and D_{50} is 0.27 mm. The coefficient of uniformity (C_u) is

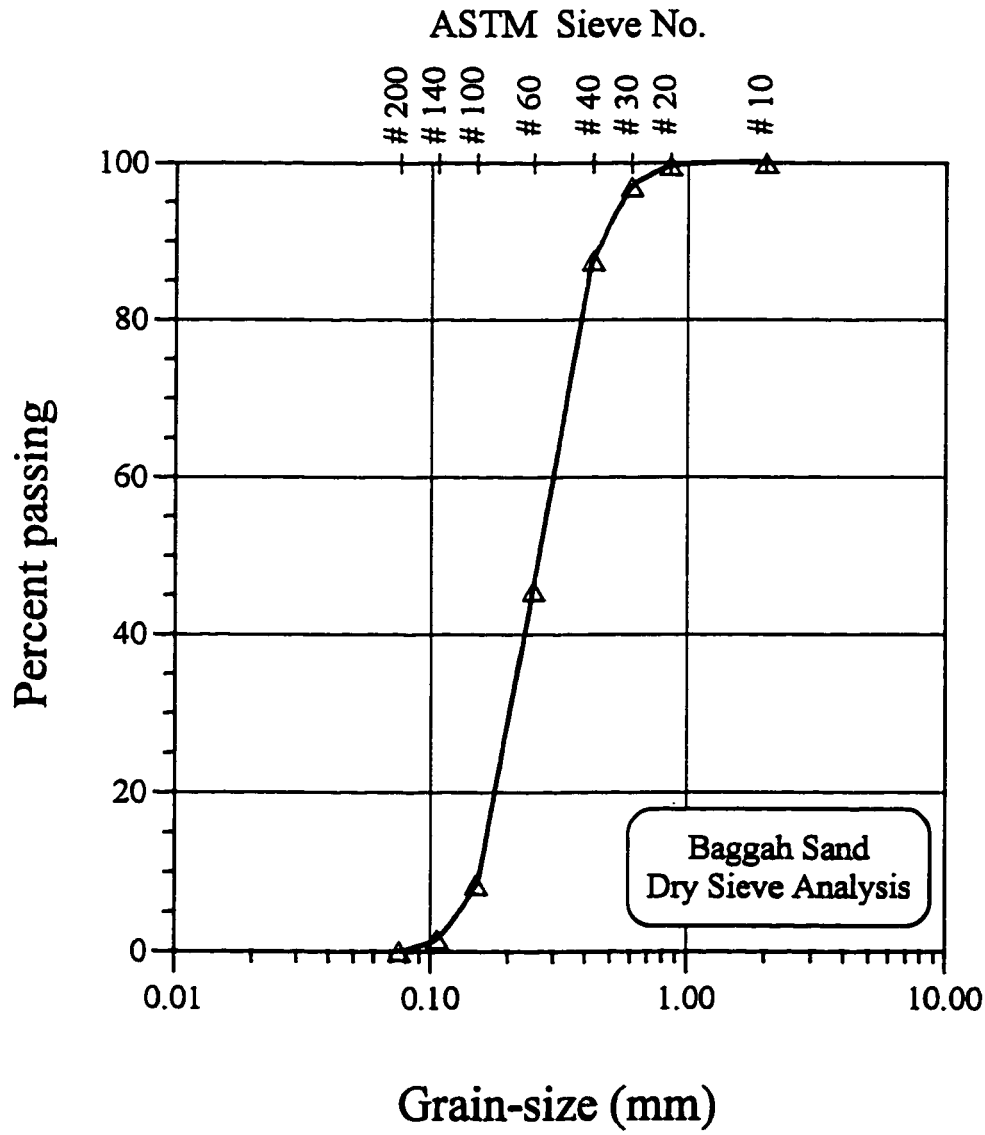

Fig. 4.1: Grain-size distribution curve for Baggah sand

1.88, and coefficient of curvature (C_c) is 0.83. Therefore, the soil can be classified as poorly graded sand (SP) according to the Unified Soil Classification System and A-3 on the basis of AASHTO classification system. The maximum dry density is 1.81 g/cm^3 using both wet and dry methods. The minimum dry density of the sand is 1.59 g/cm^3. The properties of Baggah sand are summarized in Table 4.1.

Triaxial tests were performed on air–dry Baggah sand samples. The samples were densified by pluviation until 75% relative density is reached. The triaxial test was performed at three different cell pressures (20, 50, and 100 kPa). The variation of the deviator stress with axial deformation is shown in Fig. 4.2. It has been observed that clear peaks were obtained in these three tests and the peak values occurred within 5% axial strain. Residual values were also observed at higher percentage of axial strain. The Mohr's circles of the peak stress are shown in Fig. 4.3. The angle of internal friction at peak stress level (ϕ_p) is 46° for relative density of 75%. The Mohr's circles of stress for the residual stress conditions are shown in Fig. 4.4. The angle of internal friction for the sand at residual state (ϕ_R) is 39° at relative density of 75%.

4.1.2 Ar-Riyas Sabkha

Washed sieve analysis was performed on Ar-Riyas sabkha using both distilled water and sabkha brine. The soil consisted of fine-grained particles, as shown in the grain-size distribution curves in Fig. 4.5. It was found that the percentage passing the ASTM sieve No. 200 is 97 when washed with distilled water, and is 92 when washed with sabkha brine.

Table 4.1: Properties of Baggah sand used in pull-out tests

Properties		Unit	Value
Particle size range		mm	0.1 - 0.9
D_{10}		mm	0.16
C_u		-	1.88
C_c		-	0.83
AASHTO Classification		-	A – 3
USCS Classification		-	SP
Maximum dry density (ASTM D 4253)		g/cm^3	1.81
Minimum dry density (ASTM D 4254)		g/cm^3	1.59
Angle of internal friction*	Peak	degree	46
	Residual	degree	39

* Triaxial tests were performed for the dry sand at 20, 50 and 100 kPa confining pressure and 75% relative density.

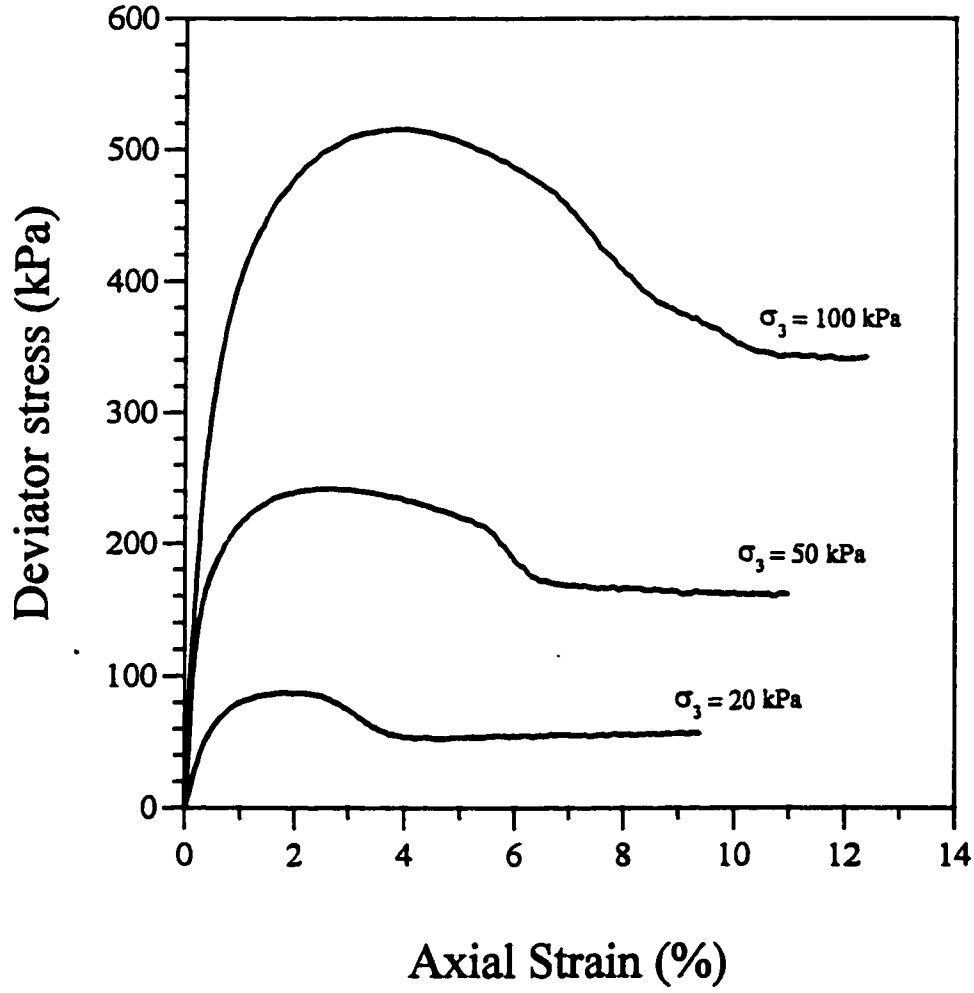

Fig. 4.2: Variation of deviator stress with axial strain for Baggah sand tested at 75% relative density

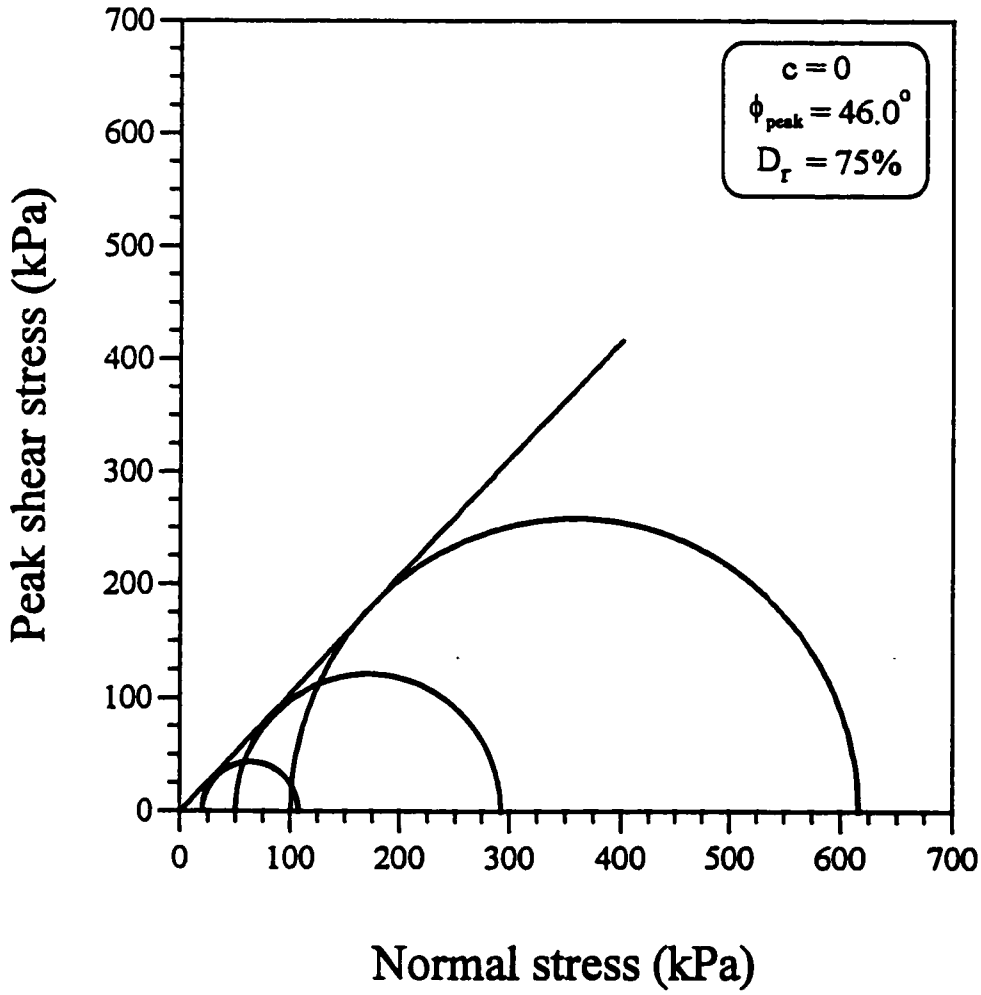

Fig. 4.3: Mohr-Coulomb failure envelop at peak stress condition for Baggah sand tested at 75% relative density

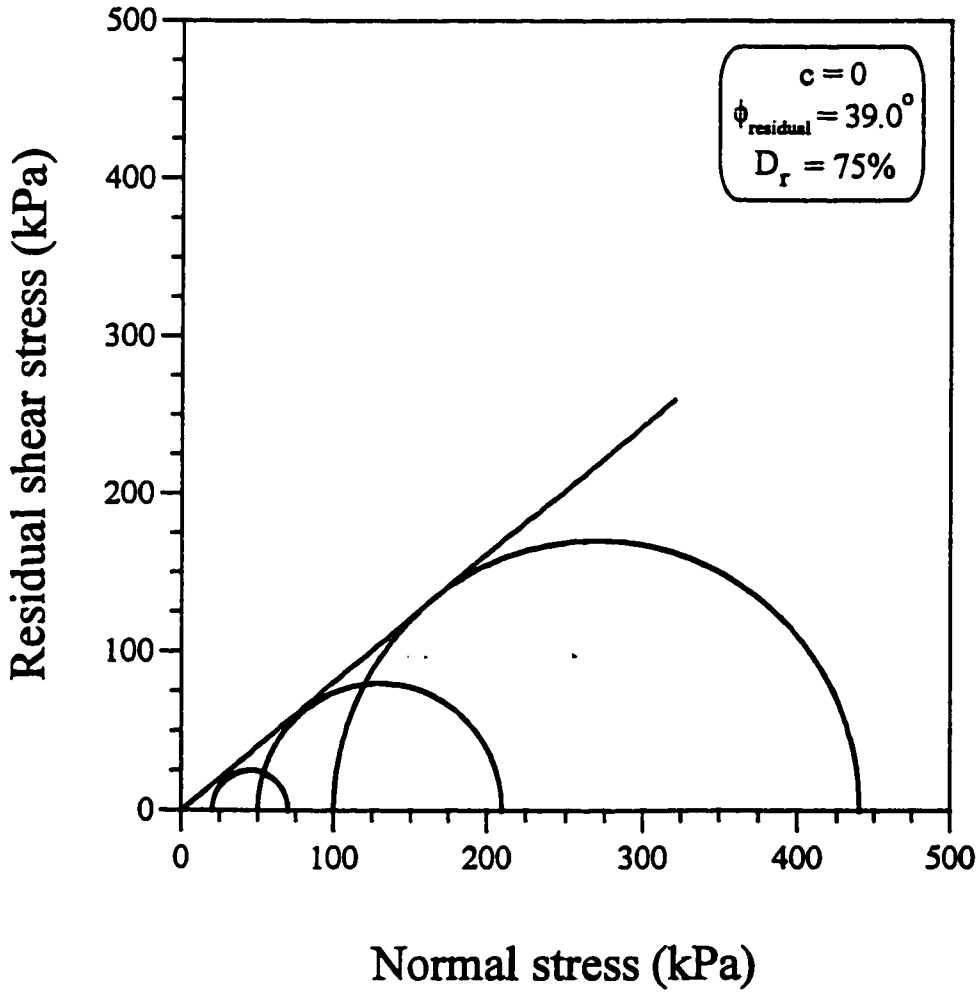

Fig. 4.4: Mohr-Coulomb failure envelop at residual stress condition for Baggah sand tested at 75% relative density

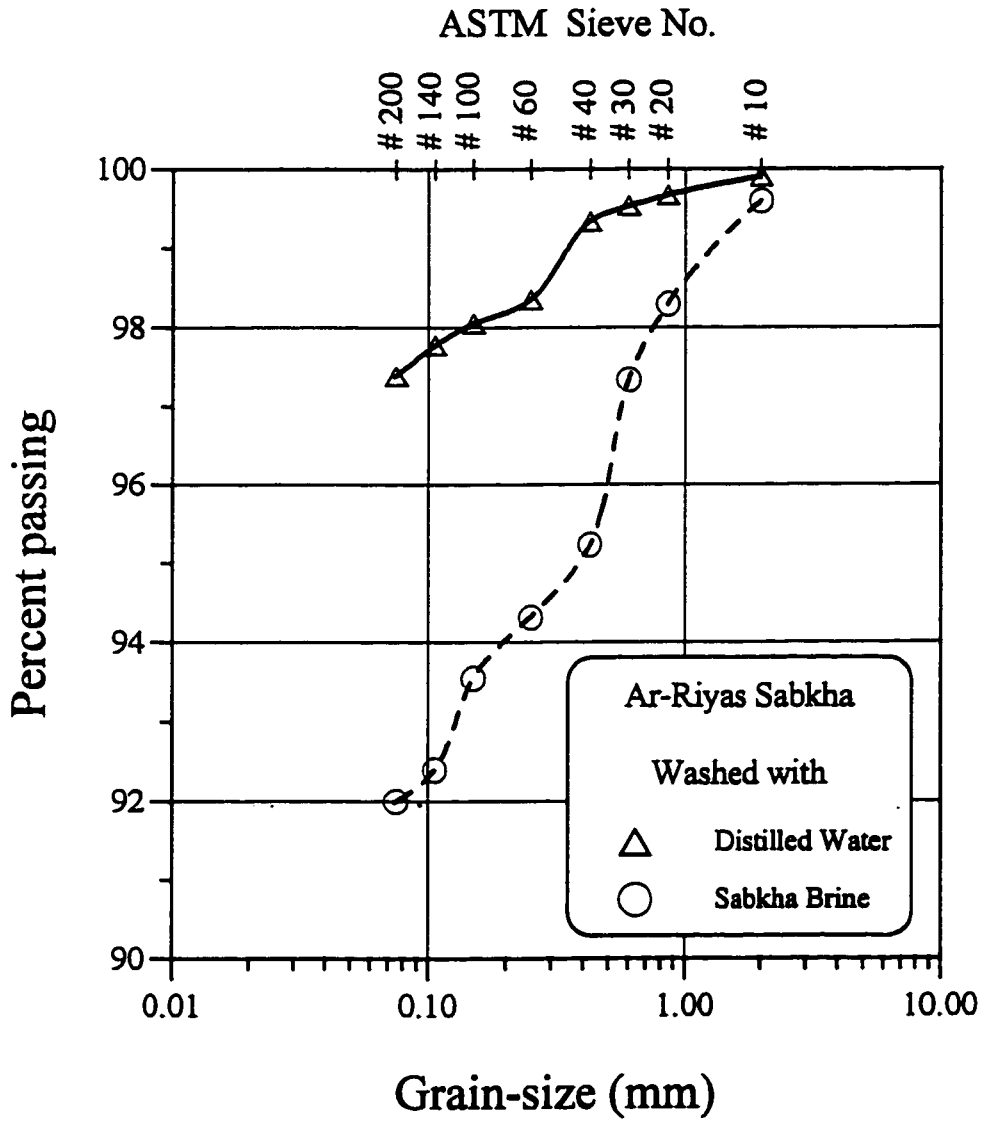

Fig. 4.5: Grain-size distribution curve for Ar-Riyas sabkha soil

The liquid limit for this sabkha was found to be 42.5 and 33 when using distilled water and sabkha brine, respectively. The plastic limits are 26.3 and 20.4 when using distilled water and sabkha brine, respectively. Thus the plasticity index is 16.2 for distilled water and 12.6 for sabkha brine. The soil is classified as CL (a clay of low plasticity) according to Unified Classification System and as A-6 (clayey soil and rated as fair to poor for subgrade) according to AASHTO classification system. Little variation is present in these results compared to the results obtained by Aiban et al. (1999). This variation is due to the heterogeneity and variability of sabkha and due to the cycles of rise and fall in water table during the year of sample collection. The properties of Ar-Riyas sabkha are presented in Table 4.2.

The higher value of the plasticity index obtained using distilled water, as compared with that using sabkha brine, can be ascribable to the dissolution of salts in distilled water. Furthermore, when sabkha brine is used part of the added fluid contains salt, which precipitates upon drying and thus increases the solid weight on the expense of reducing the evaporated water.

In order to determine the moisture-dry density relationship, the modified proctor compaction tests were carried out at different percentages of moisture content. The results are shown in Fig. 4.6. The optimum moisture content for the sabkha is 14% and corresponding maximum dry density is 1.80 g/cm^3.

Undrained triaxial tests were performed on as molded samples of Ar-Riyas sabkha prepared at 10% moisture content and at the optimum moisture content (14%). Samples for both sets were compacted to 90% of the maximum dry density using static compaction. Figs. 4.7 and 4.8 show the plots of the deviator stress versus axial strain for

Table 4.2: Properties of Ar-Riyas sabkha used in pull-out tests

Properties		Unit	Value
Particle size range		-	> 50% passing ASTM seive 200
Liquid Limit	With distilled water	%	42.5
	With sabkha brine	%	33.0
Plastic Limit	With distilled water	%	26.3
	With sabkha brine	%	20.4
Plasticity Index	With distilled water	-	16.2
	With sabkha brine	-	12.6
AASHTO Classification		-	A – 6
USCS Classification		-	CL
Maximum dry density (Modified Proctor Test)		g/cm^3	1.80
Optimum Moisture Content (OMC)		%	14
Cohesion	at 10% moisture content	kPa	90.0
	at 14% moisture content	kPa	60.0
	Soaked	kPa	52.0
Angle of internal friction	at 10% moisture content*	degrees	32.0
	at 14% moisture content**	degrees	31.2
	Soaked***	degrees	22.8

*Undrained triaxial tests at σ_3 of 100, 200, 300 and 500 kPa and 90% compaction of sabkha.

**Undrained triaxial tests at σ_3 of 100, 300 and 500 kPa and 90% compaction of sabkha.

***Consolidated undrained triaxial tests at σ_3 of 100, 300 and 500 kPa and 90% compaction of sabkha.

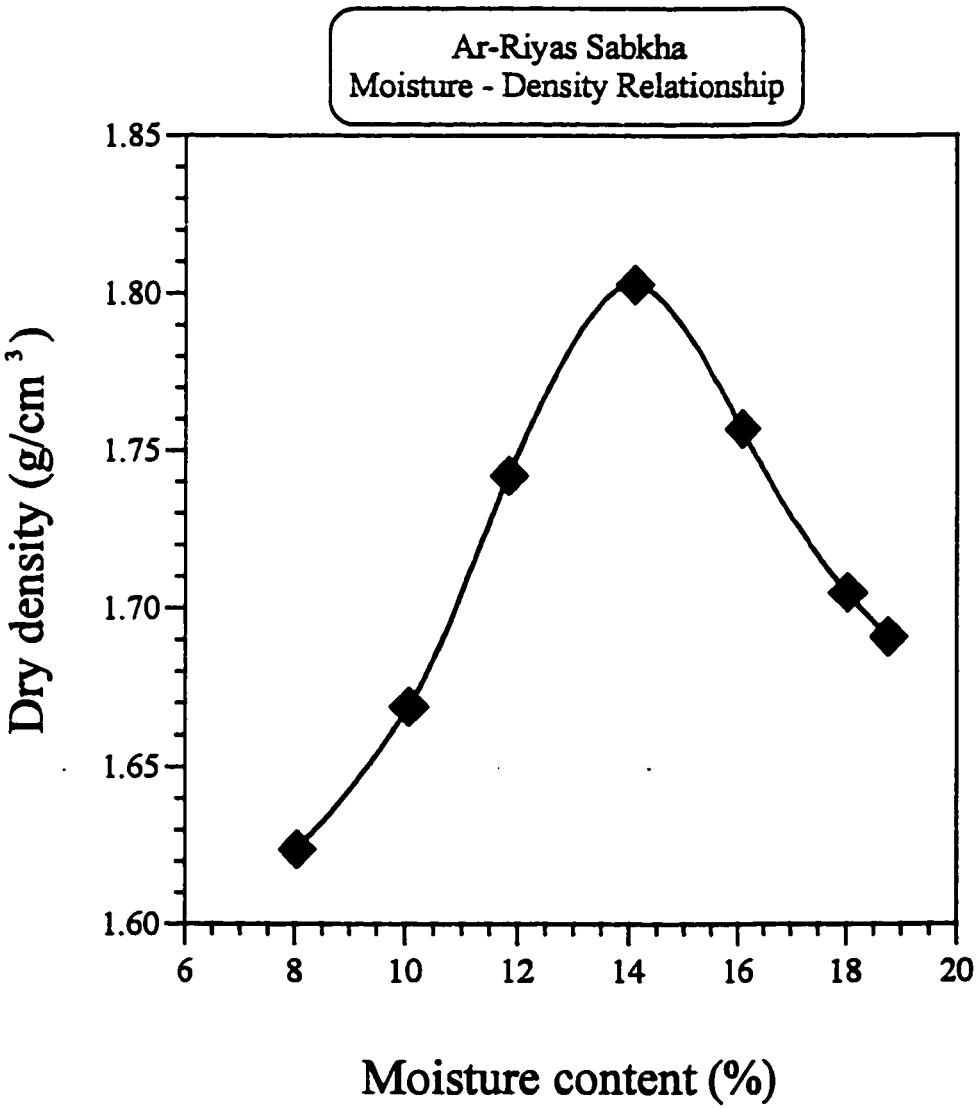

Fig. 4.6: Variation of the dry density with molding moisture content for Ar-Riyas sabkha soil

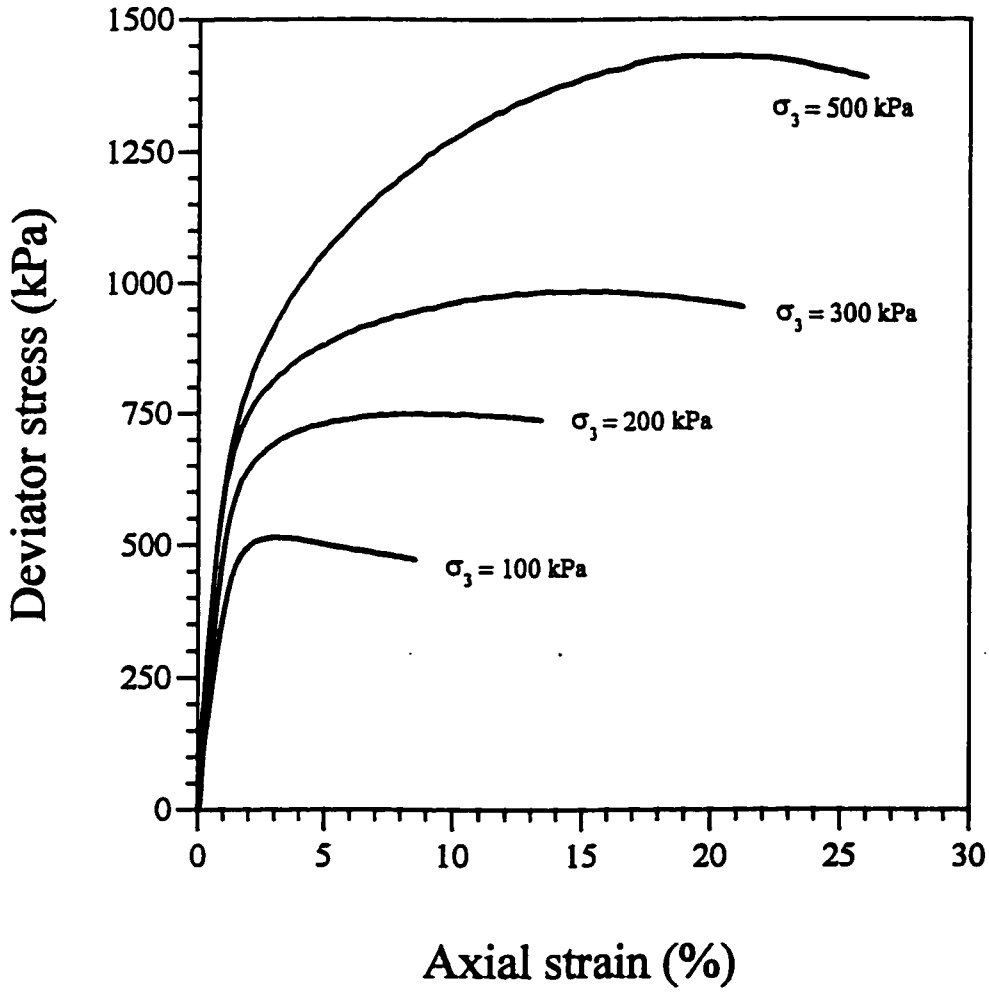

Fig 4.7: Variation of deviator stress with axial strain for Ar-Riyas sabkha compacted at 10% moisture and 90% relative compaction and tested under as mold condition

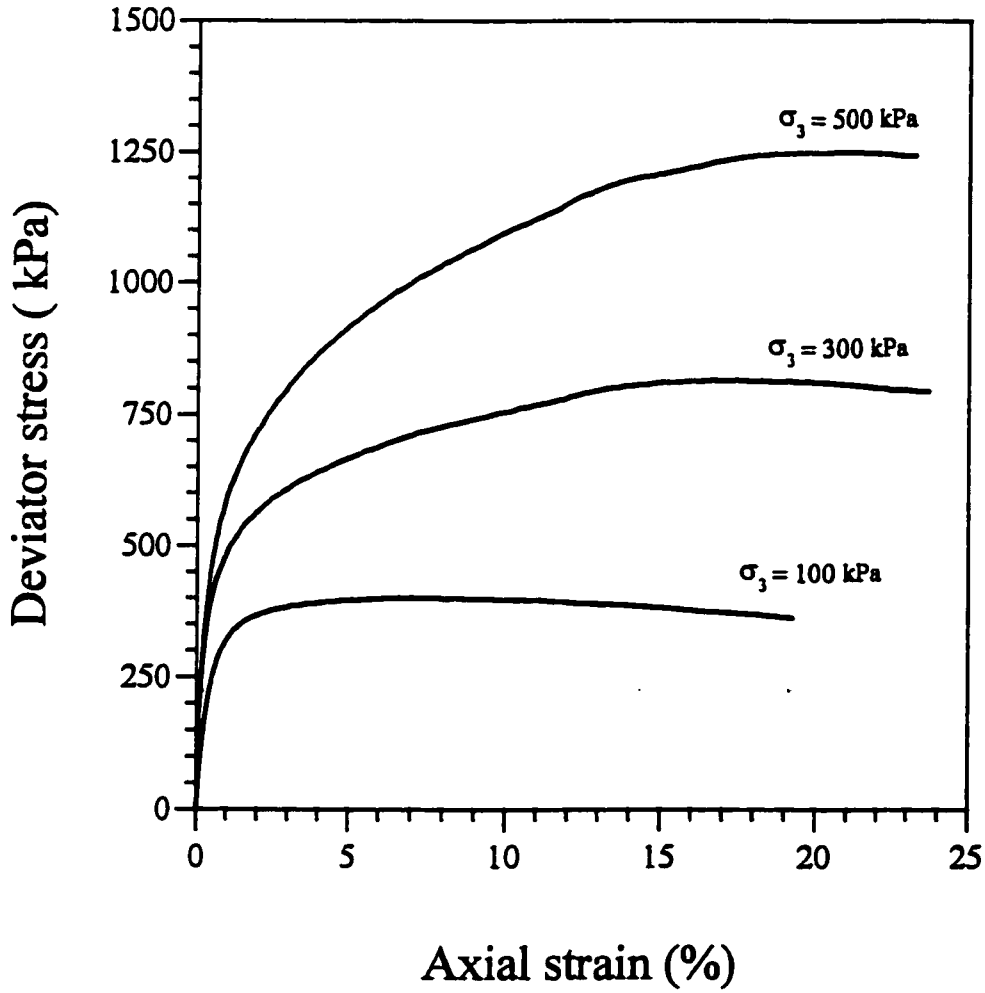

Fig. 4.8: Variation of deviator stress with axial strain for Ar-Riyas sabkha compacted at 14% moisture and 90% relataive compaction and tested under as mold condition

samples compacted at 10% and 14%, respectively. The corresponding Mohr's circles of stress are shown in Figs. 4.9 and 4.10. The total shear stress parameters for samples compacted at 10% are 90.0 kPa for the cohesion and 32° for the angle of internal friction whereas, the total shear stress parameters for samples compacted at 14% are 60.0 kPa for the cohesion and 31.2° for the angle of internal friction.

In order to compare the shear strength of sabkha–geotextile–sand interface when the sabkha was flooded, with the shear strength of sabkha itself; consolidated undrained triaxial tests were performed on soaked (flooded) samples of sabkha without pore pressure measurement. The soaking was achieved by applying back pressure. The tests were performed at confining pressures of 100, 200 and 300 kPa. The results of the tests are shown in Fig. 4.11 and Fig. 4.12. The total shear stress parameters are 52.0 kPa for the cohesion and 22.8° for the angle of internal friction.

4.2 Selection of the Size of the Pull-out Plate

Different researchers used different clamping mechanisms for pulling out the geotextile as discussed in the literature review. In this experimental work, it was decided to use stainless steel plate 1.0 mm thick, 100 mm wide and 163 mm long. The size of the plate was selected such that the front end of the geotextile remains within the box and thus subjected to the normal load during the pull-out test. Since the pull-out system allows a maximum movement of 120 mm, it was decided to glue 120 mm of geotextile to the plate and leave the remaining length as free geotextile. The plate was placed inside the box alongwith the free geotextile. The front part of the glued geotextile was positioned to be

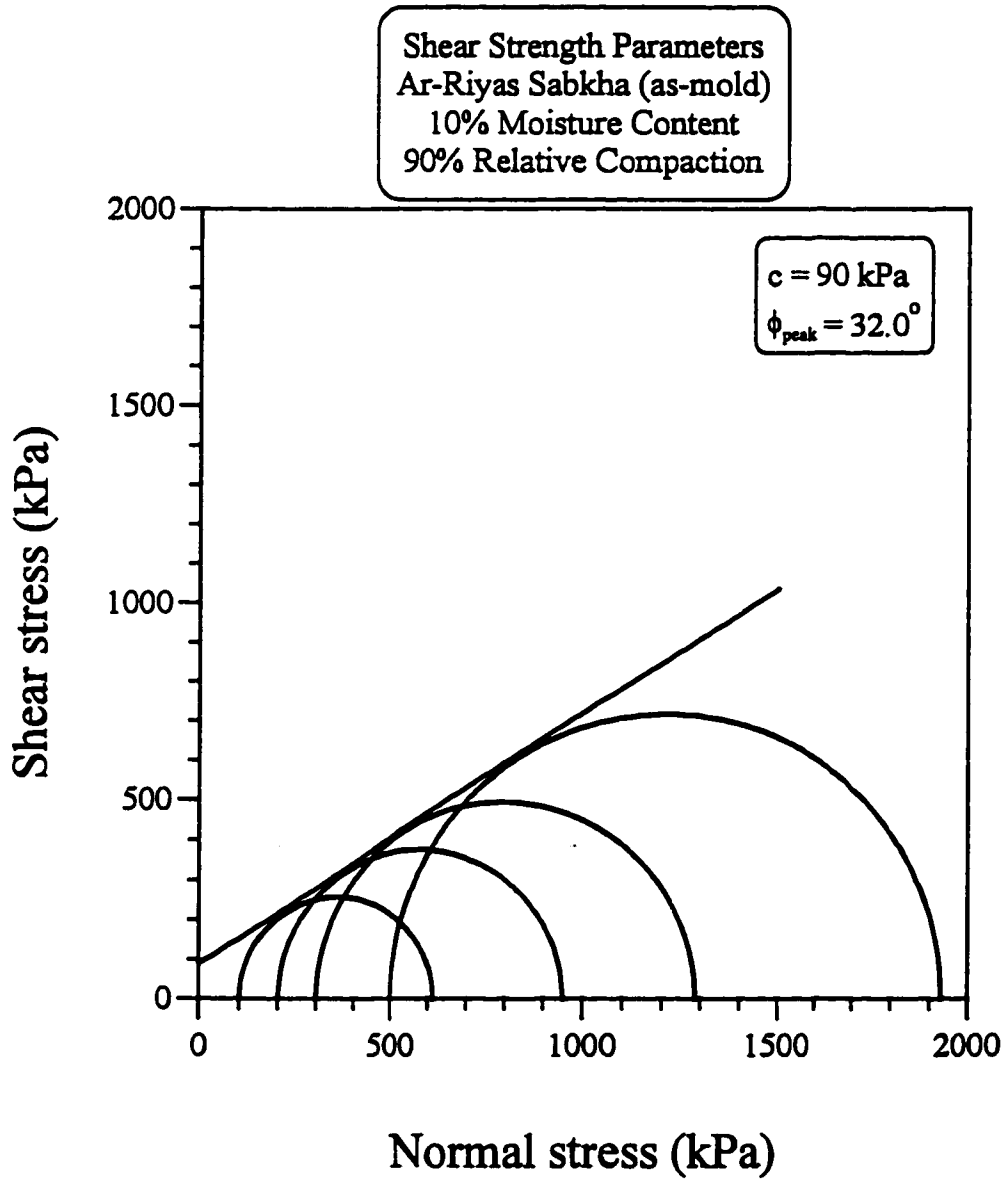

Fig. 4.9: Mohr-Coulomb failure envelop for Ar-Riyas sabkha compacted at 10% moisture and 90% relative compaction and tested under as-mold condition

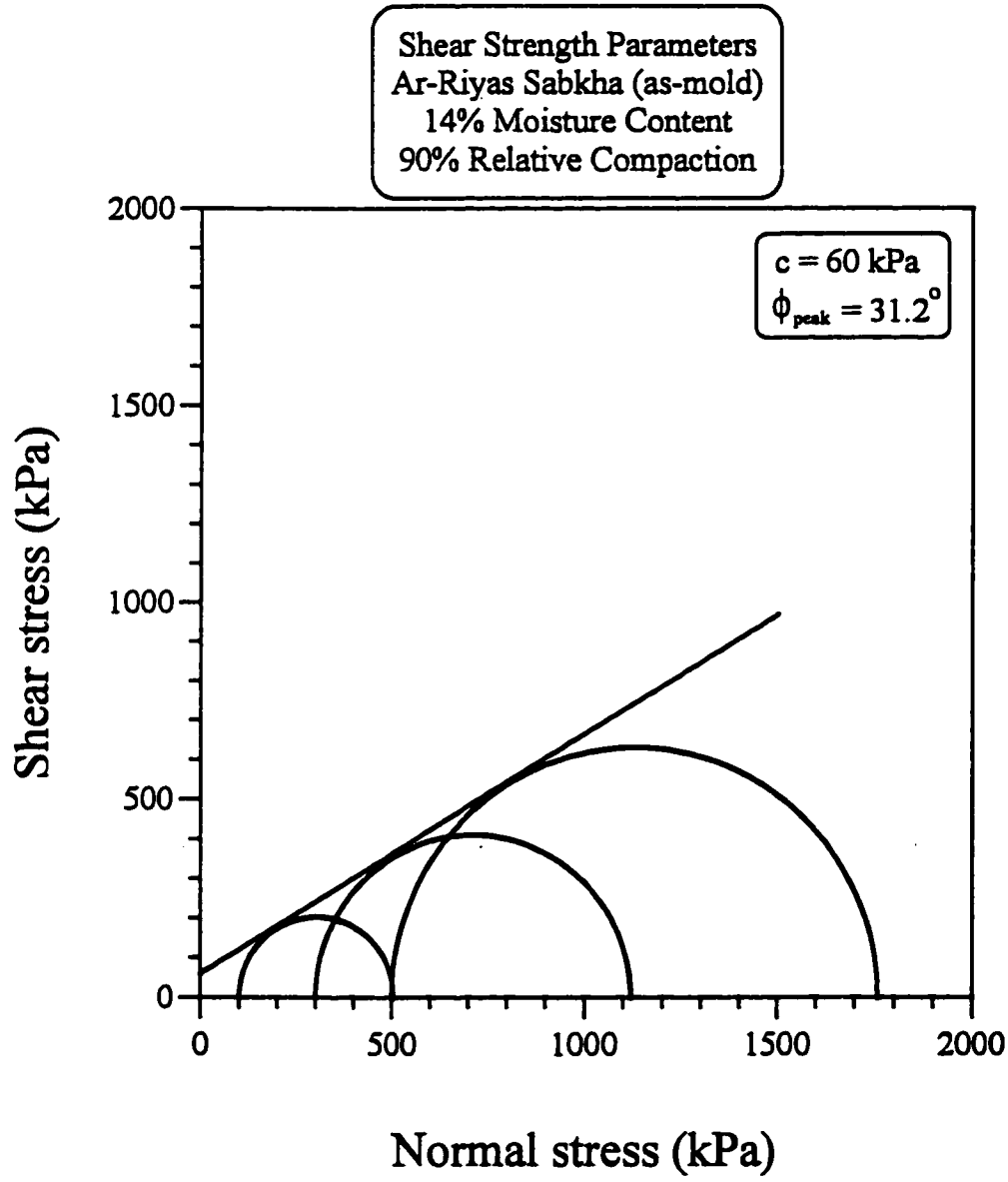

Fig. 4.10: Mohr-Coulomb failure envelop for Ar-Riyas sabkha compacted at 14% moisture and 90% relative compaction and tested under as-mold condition

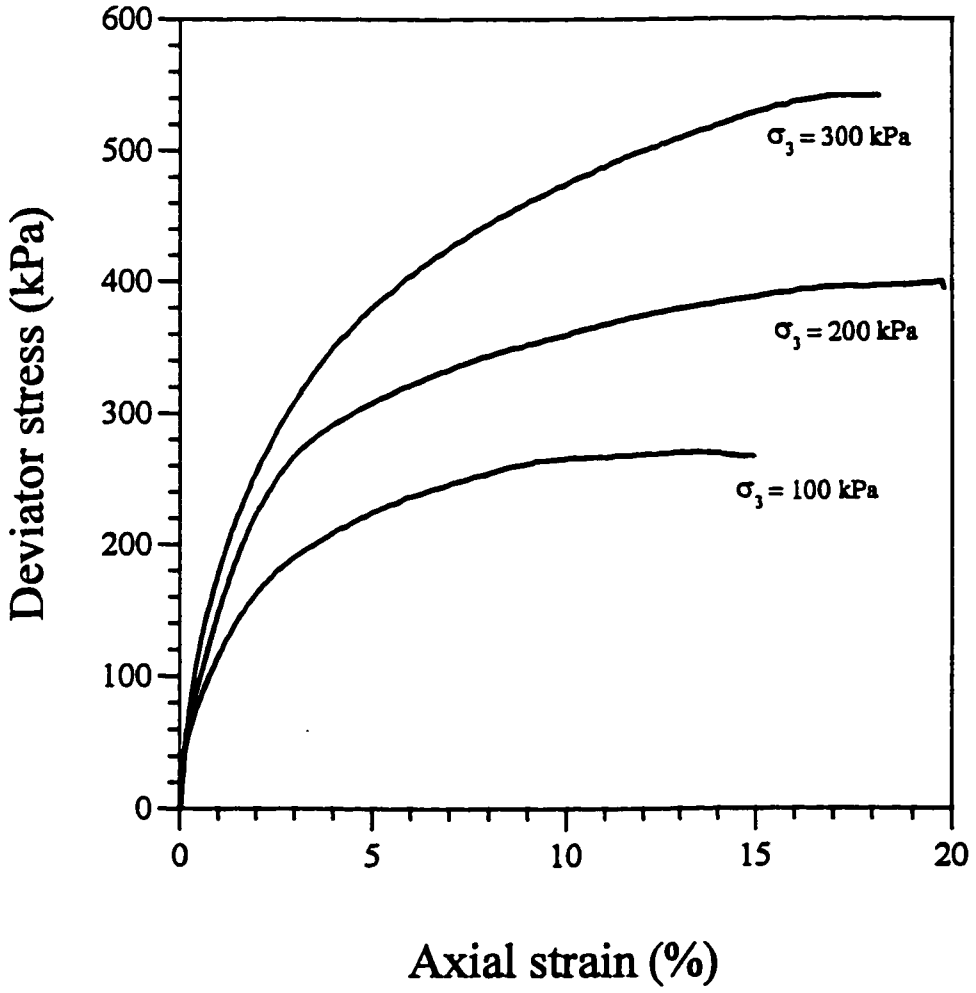

Fig. 4.11: Variation of deviator stress with axial strain for Ar-Riyas sabkha prepared at 90% relative compaction and tested in soaked condition

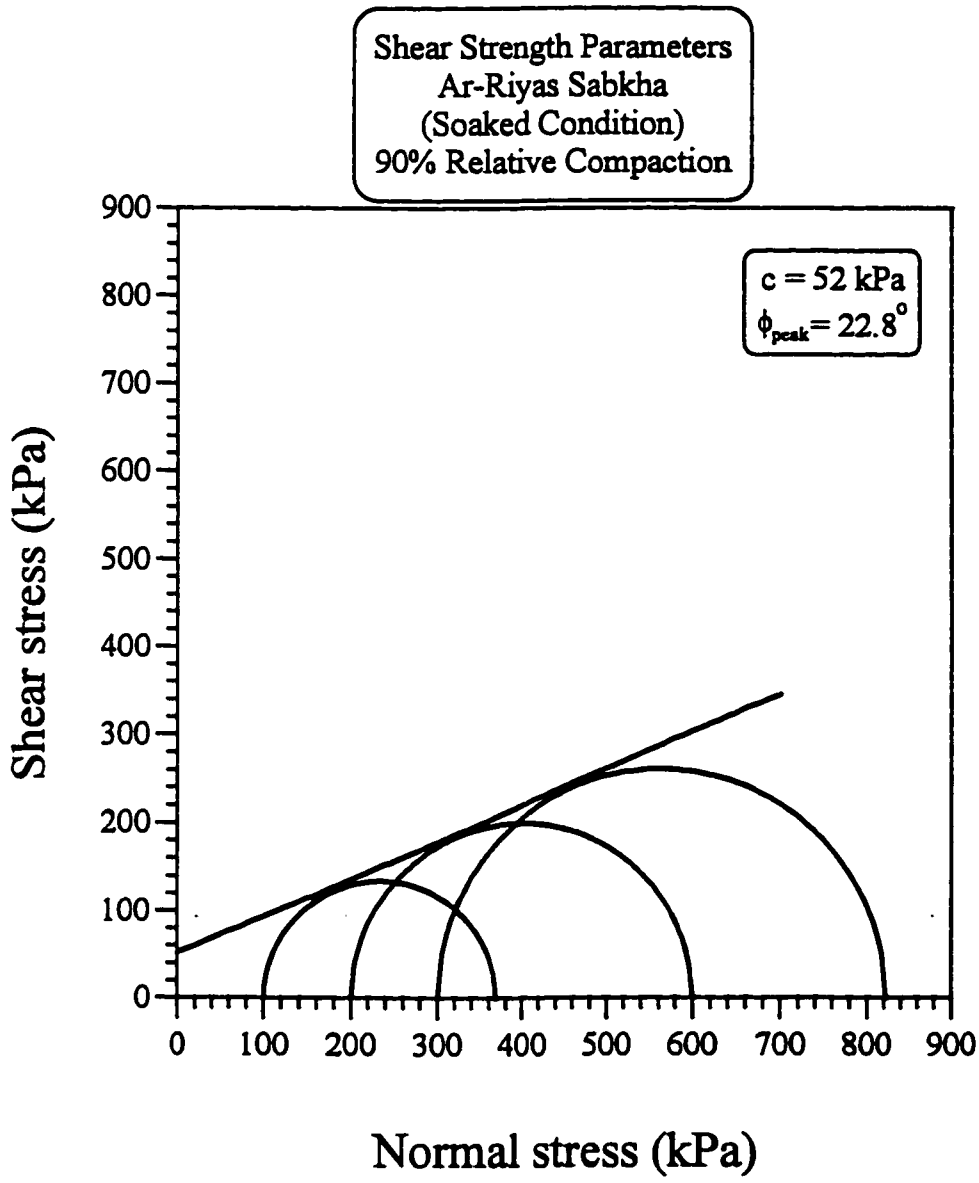

Fig. 4.12: Mohr-Coulomb failure envelop for Ar-Riyas sabkha prepared at 90% relative compaction and tested in soaked condition

in contact with the front wall of the box at the beginning of the test. As the test proceeds the glued geotextile comes out of the slit while the front part of the free geotextile remains inside the box. In such case all the free geotextile remains under the normal pressure through out the test, whereas for the other researchers portion of geotextile is coming out of slit and will no longer be under normal pressure or confinement. This will have the consequence that part of the geotextile deforms under normal load while other parts deform under no confinement and that will intensify the necking of the geotextile and the non-homogeneity of strains.

The selection of the plate size was also supported by preliminary stress monitoring tests. In the tests, the variation of lateral earth pressure was monitored at different distances from the front wall. The variation of the lateral earth pressure with the front end displacement is shown in Fig. 4.13. The pressure cells were placed at the front wall and at 60, 120, 180, 240 mm away from the front wall. The results show that the lateral pressure is very high at the front wall but it drops quickly to one-thirds its value, at 60 mm away from the front wall. The results also show that the lateral earth pressure decreases with increasing the distance from the front wall. Thus, the geotextile away from the front wall of the box, will be affected to a lesser degree by the front wall roughness. Trial pull-out experiment was also performed with a longer pull–out steel plate glued to the geotextile. In that case 180 mm of geotextile was glued to the steel plate leaving the remaining length (257 mm) as free geotextile. Pull-out results obtained from this test are similar to that obtained from the test in which 120 mm of geotextile was glued to the steel plate leaving

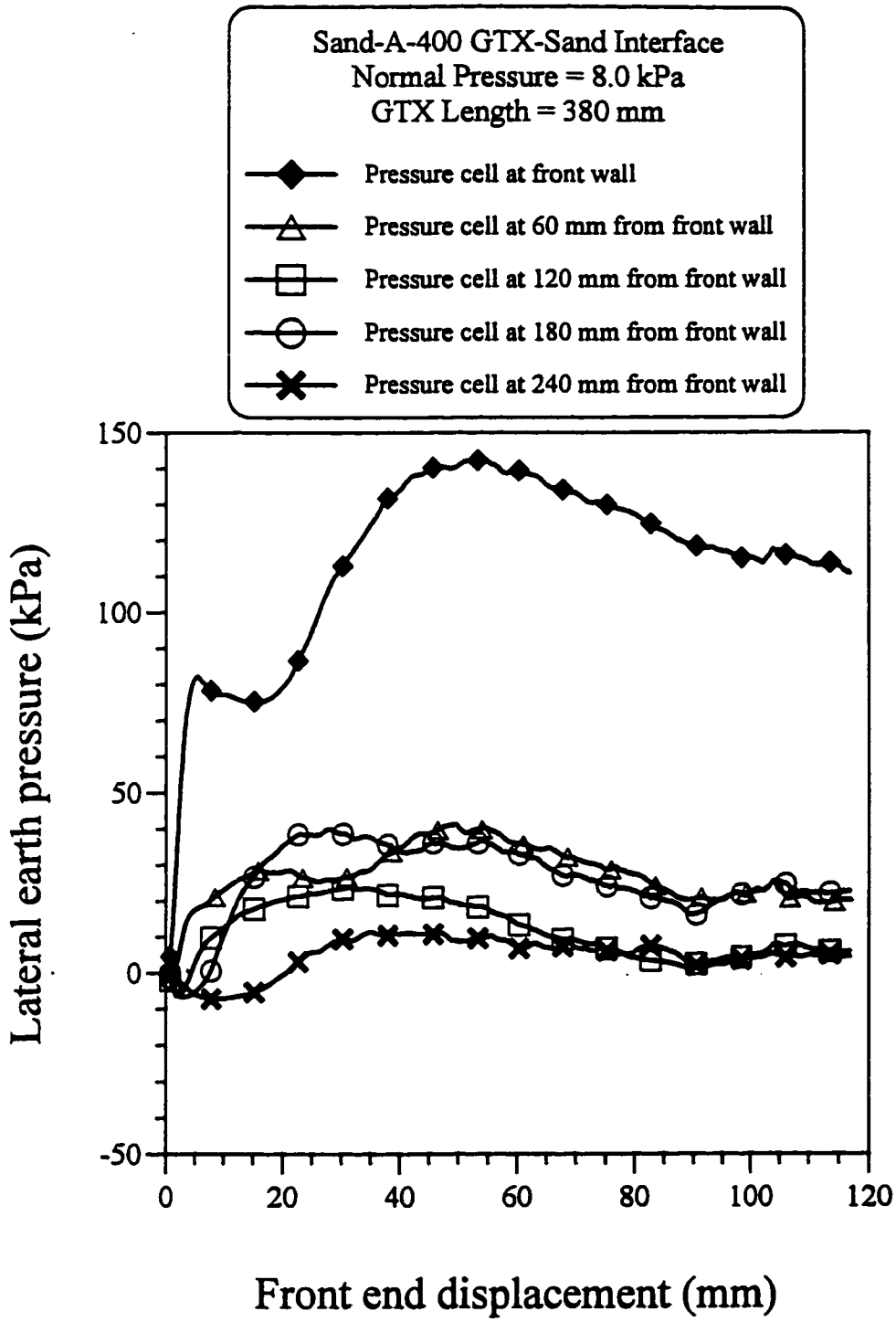

Fig. 4.13: Variation of the lateral earth pressure with the front end displacement at 3 cm above sand-GTX-sand interface, 8.0 kPa normal pressure, and 380 mm long geotextile

257 mm long free geotextile. All subsequent tests were performed using 120 mm of geotextile glued to the steel plate and leaving the remaining length as free geotextile.

4.3 Typical Results of Pull-out Tests

In this section, typical results obtained from pull-out tests will be presented, to illustrate the features of load displacement curves. The selected test was performed on sand–GTX–sand interface under 4.5 kPa normal pressure. The geotextile used was A-400 and the free length of geotextile was 380 mm. As explained earlier, each test involving the change of normal pressure, change of geotextile type or change in moisture content of sabkha required a separate pull-out test on geotextile glued to the pull-out plate with no free geotextile. This was done to quantify the contribution of the plate alone. When the pull-out test is carried out on plate and free geotextile, the plate moves forward and comes out of the box and the load is transferred gradually into the free geotextile. Typical results are shown in Fig. 4.14, which presents the pull-out test on the plate alone i.e. plate with geotextile glued to one side with no free geotextile. As the displacement increases, the pull-out resistance increases until it is fully mobilized after which it decreases as the plate starts coming out of the slit. The pull-out resistance will finally reach zero at a front end displacement of 120 mm.

Fig 4.15 presents the variation of pull-out resistance offered by A-400 geotextile. It should be noted here that in Fig. 4.15, the pull-out resistance offered by the plate alone was subtracted from the combined pull-out resistance of the plate and the free geotextile. This gives the net force on the free geotextile which is plotted against the front end

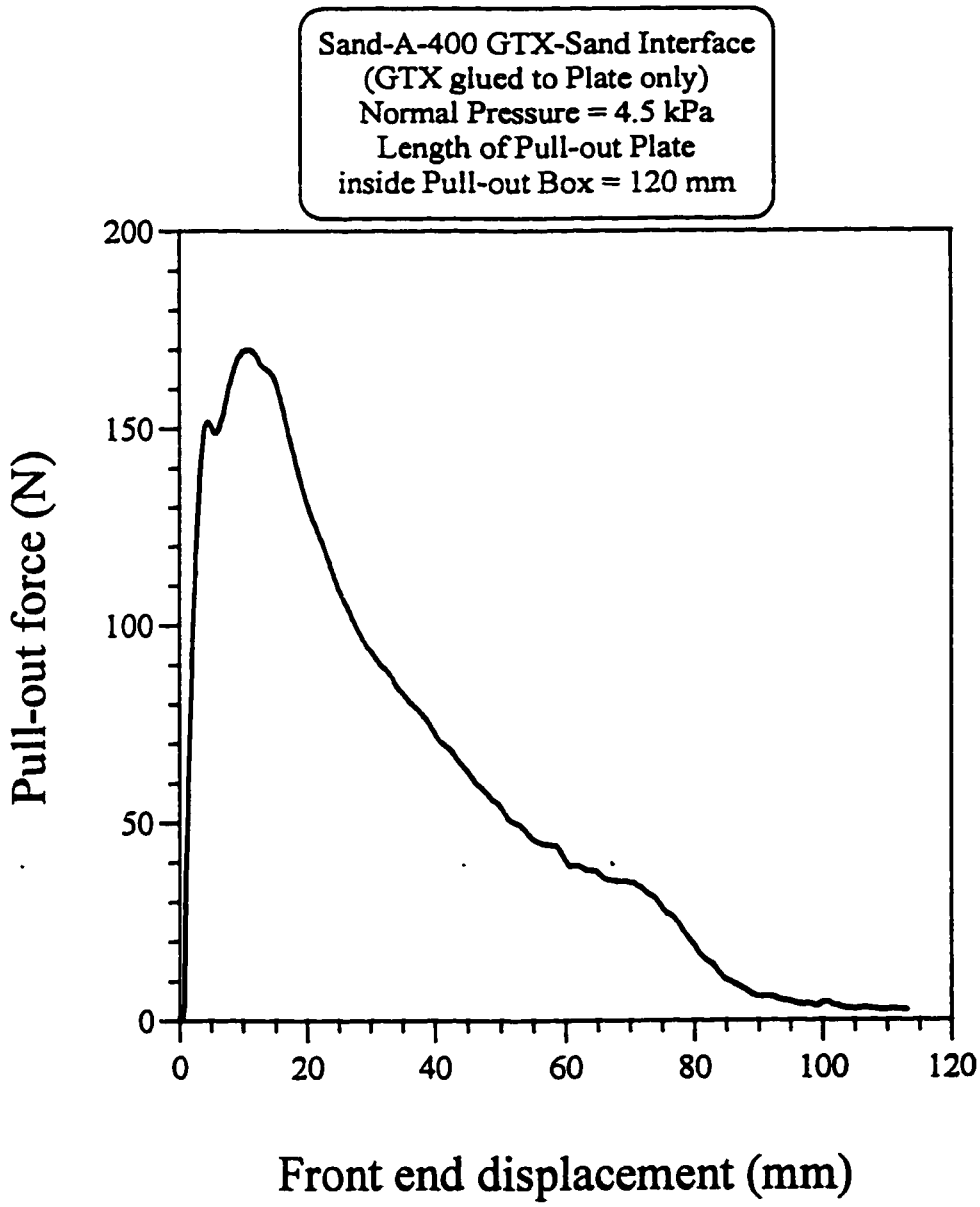

Fig. 4.14: Variation of the pull-out force on the pull-out plate with the front end displacement for sand-GTX-sand interface, at 4.5 kPa normal pressure, and with geotextile glued to plate only (no free geotextile)

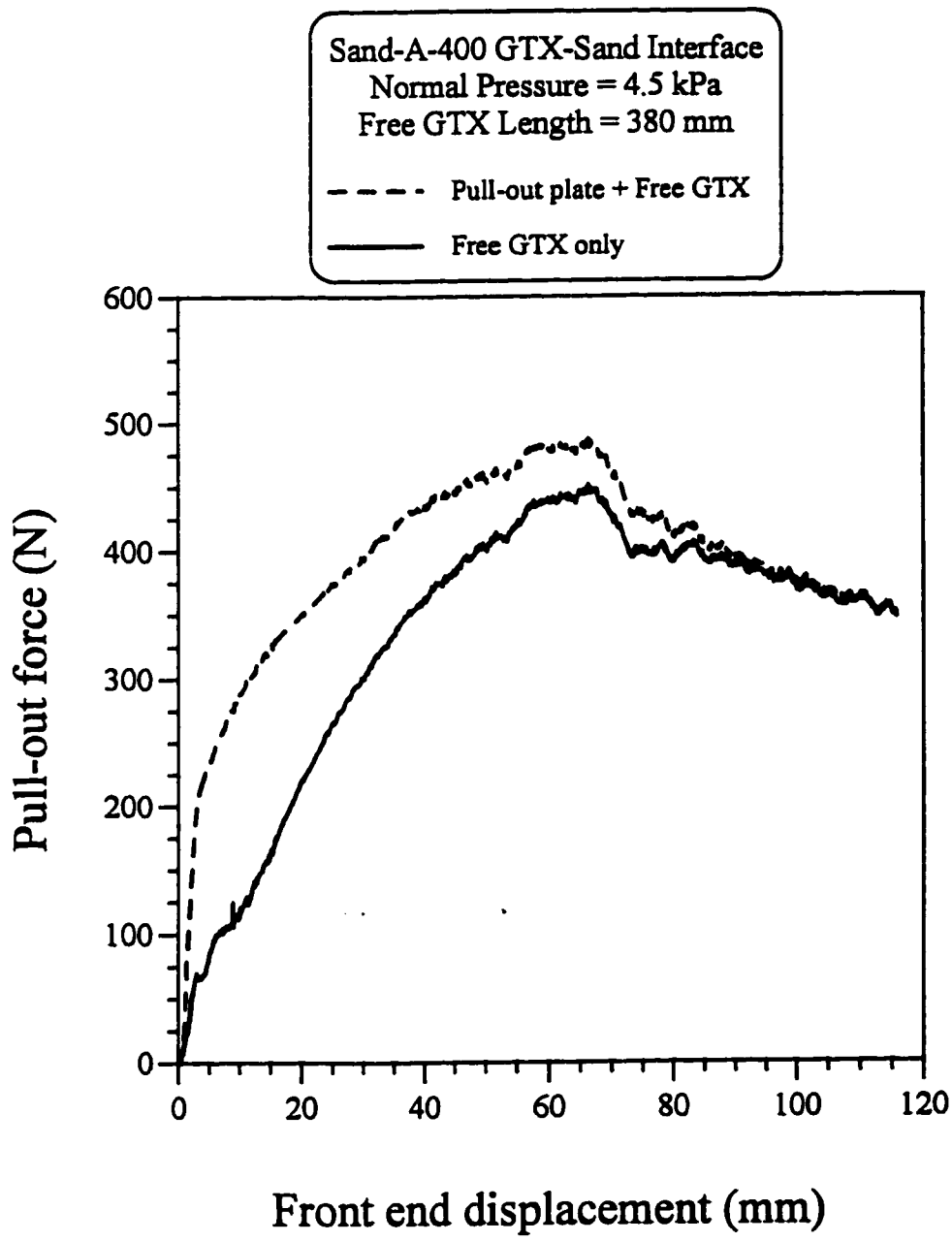

Fig. 4.15: Variation of the pull-out force on A-400 geotextile with the front end displacement for sand-GTX-sand interface, at 4.5 kPa normal pressure, and 380 mm long free geotextile

displacement. This data shows a peak value representing the maximum mobilized shear force. Here, it was assumed that the lateral earth pressure that got developed up in the case of plate alone was same as that in the case of combined plate and free geotextile. This assumption may not be correct because of the difference in the length of samples in the two cases.

Fig. 4.16 presents the average axial tensile strain developed in the different portions of the geotextile. This Figure also presents the overall average strain for the geotextile. It is clear that the strain in the front one-third is higher than that in the middle one-third. Similarly, the strain in the middle one-third is higher than the strain in the rear one-third at any given front end displacement value. Fig. 4.16 shows also that the average strain in any of the three parts becomes constant after a specific value of front end displacement. It is clearly seen in Fig. 4.16 that after a front displacement of 72 mm, the overall average strain approaches a constant value of 17.4%. This means that the geotextile is slipping under the pull-out load with no further extension in any part of the geotextile. This implies that when the geotextile becomes under pure slippage, the shear stress would be uniform over the entire length. This shear stress can be regarded as the residual value and will be called the residual shear stress throughout this thesis.

Fig. 4.17 presents the variation of the displacement measured at different points on the geotextile, with time. Since the pull-out testing device is displacement controlled with a constant rate of 1.27 mm/min., the displacement can be obtained directly by multiplying the time scale by 1.27. It should be noted that the frequency of the symbols used in Fig. 4.16 and 4.17 is 90 i.e. each symbol is shown every 90 data points. The figure depicts the

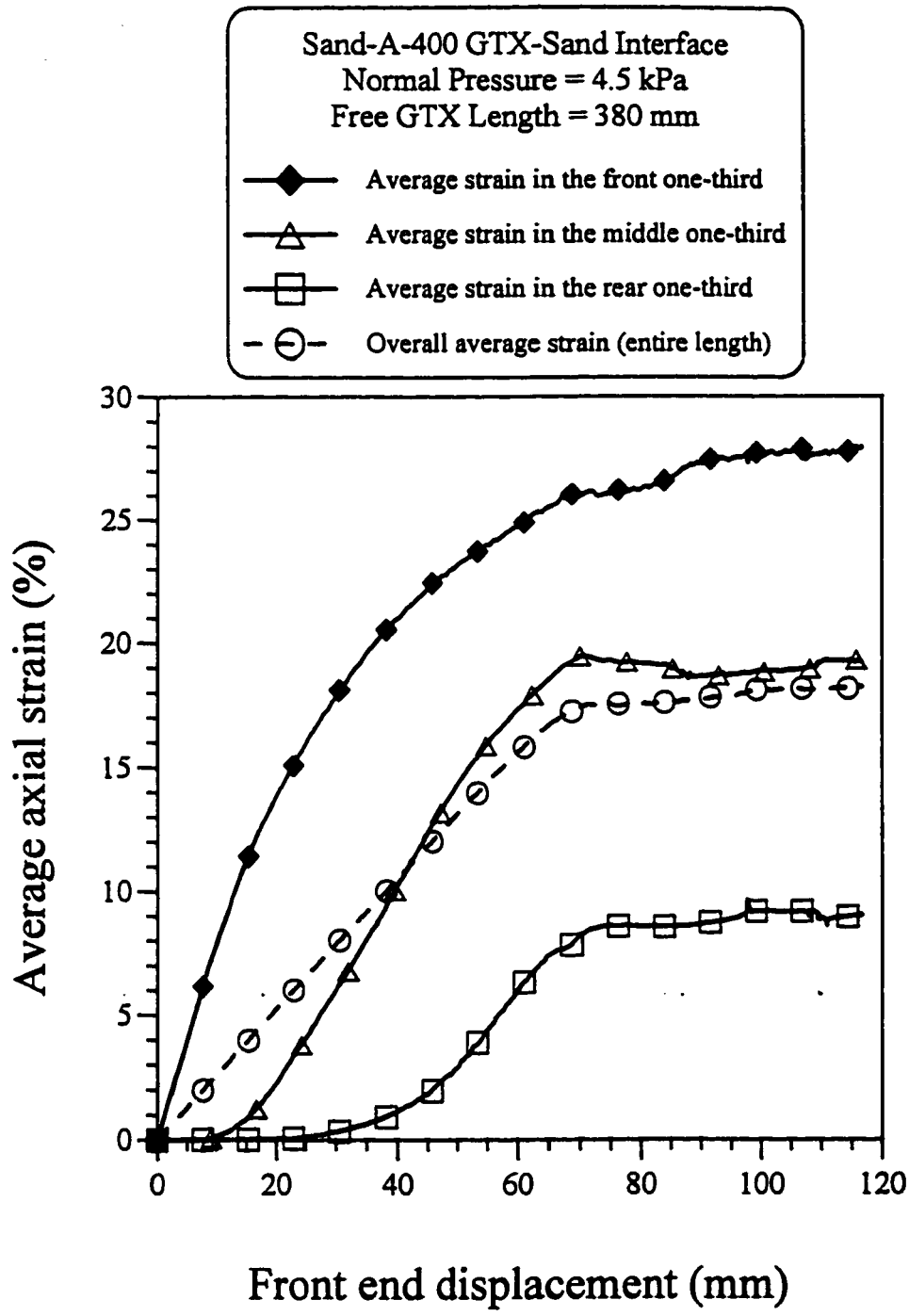

Fig. 4.16: Variation of the average axial strain of A-400 geotextile with the front end displacement for sand-GTX-sand interface, at 4.5 kPa normal pressure, and 380 mm long free geotextile

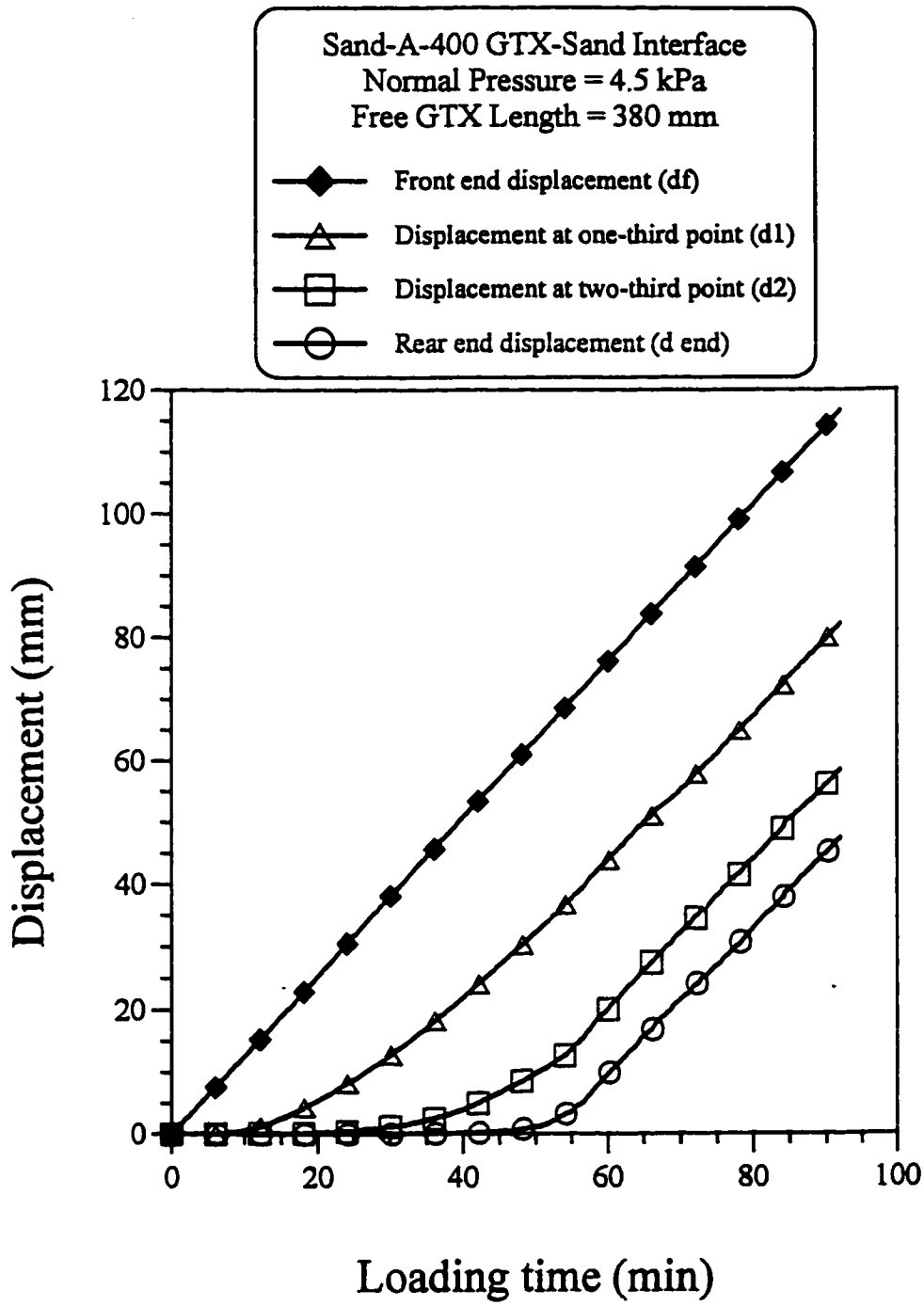

Fig. 4.17: Variation of the displacement of A-400 geotextile with loading time for sand-GTX-sand interface, at 4.5 kPa normal pressure, and 380 mm long free geotextile

various deformational stages that develop the pull-out resistance of geotextile in sand–GTX–sand interface. These stages are discussed in the following sections.

4.4 Deformation Stages of the Geotextile during the Pull-out Testing

The results presented in Fig. 4.17, which are typical for all tests, clearly show the following three displacement stages in these pull-out experiments.

- Stage 1 Progressive extension in the geotextile
- Stage 2 Extension in the geotextile and slippage in some parts
- Stage 3 Slippage of the entire length of the geotextile

The front portion of the geotextile is under stage 1 as the pull-out test starts. Stage 2 exists in the geotextile when the front part of the geotextile is in slippage and the rear part of geotextile is in extension. Stage 2 continues until the rear end starts moving. Once the rear end starts moving, the entire geotextile is in stage 3. When the difference between the front end displacement and the rear end displacement becomes constant, i.e. when the line for front end displacement and the line for rear end displacement become parallel, the third stage of displacement (slippage) starts. This constitutes the residual state.

4.5 Definitions of the Terminology Used

4.5.1 Peak Shear Stress

The peak shear stress is the stress corresponding to the peak pull-out force of the geotextile. This is not the actual stress on the geotextile since it is an average value where different parts of the geotextile are subjected to a stress less than that at the front end. It is calculated on an average basis assuming a uniform stress over the entire geotextile length. The peak value is given by:

$$\text{Peak shear stress (kPa)} = \frac{P_{max}}{2 * w * L * (1 + \varepsilon_p)} \qquad (4.1)$$

Where:

P_{max} = Peak Pull-out force on the geotextile (N)

w = Width of the geotextile sample (m) = 0.1 m

L = Free length of the geotextile (mm)

ε_p = Overall average strain at peak stress defined as:

$$\frac{\text{(Front end displacement - Rear end displacement)}}{\text{Length of the geotextile}}$$

4.5.2 Residual Shear Stress

Residual shear stress occurs at a stage in which the geotextile is under pure slippage mode.The residual state is defined as the point at which no more strain takes place. However, it was observed that in the geotextiles with large extensibility and low tensile strength, the strains are concentrated in the front portion and the overall average strain

does not become constant even at the end of the test. In such cases, the stress at the end of the test is assumed to be the residual stress. This is given by:

$$\text{Residual shear stress (kPa)} = \frac{P_{residual}}{2 * w * L * (1 + \varepsilon_R)} \quad (4.2)$$

Where:

$P_{residual}$ = Pull-out force on geotextile corresponding to residual state defined above

ε_R = Overall average strain at residual stress

The other parameters were defined earlier.

4.5.3 Peak Angle of Interface Friction (ψ_p)

The angle of interface friction at peak stress conditions (ψ_p) can be defined only for sand–GTX–sand interface since sabkha–GTX–sand interface has more than one soil type in contact with the geotextile.

$$\psi_p = \tan^{-1} \frac{\text{Peak shear stress on the interface}}{\text{Normal stress on the interface}} \quad (4.3)$$

4.5.4 Angle of Interface Friction at Residual State (ψ_R)

The angle of interface friction at residual stress condition (ψ_R) can also be defined for only sand–GTX–sand interface since sabkha–GTX–sand interface has more than one soil type in contact with the geotextile.

$$\psi_R = \tan^{-1} \frac{\text{Shear stress on the interface at residual state}}{\text{Normal stress on the interface}} \quad (4.4)$$

4.5.5 Interface Interaction Factor (c_i)

The interface interaction factor (c_i) is defined as the ratio of shear stress that develops between the soil and the geotextile at the interface to the shear strength of the soil alone, at the residual state. According to Collios et al. (1980) and Koutsourais (1998) the c_i for sand–GTX–sand interface is defined as:

$$c_i = \frac{\tan \psi_R}{\tan \phi_R} \tag{4.5}$$

where ϕ_R is the angle of internal friction of the sand at the residual state

However for sabkha–GTX–sand interface, the c_i can be defined as:

$$c_i = \frac{2\tau_i}{(\tau_{sand} + \tau_{sabkha})} \tag{4.6}$$

where:

τ_{sand} = $\sigma_n \tan\phi_R$

τ_{sabkha} = $c_{sabkha} + \sigma_n \tan\phi_{sabkha}$

τ_i = Shear stress on the sabkha–GTX–sand interface at residual state

τ_{sand} = Shear strength of sand at residual state

τ_{sabkha} = Shear strength of sabkha soil

σ_n = Applied normal pressure

ϕ_{sabkha} = Angle of internal friction of sabkha soil

4.5.6 Average Axial Strain at Residual State

The displacement of the free geotextile at every one-third point is measured using the attached displacement rods. The difference between the reading of any two consecutive points divided by the corresponding original length gives the average strain for the individual portion (one-third) of the geotextile. This will give three different strain values in the three portions of the free geotextile, for every value of the front end displacement. The values of these strains, at the residual state, are plotted at the center of their corresponding portion to obtain the variation of average axial strain with position along the free geotextile.

4.6 Results of Pull-out Tests on Sand–GTX–Sand Interface

The data of the pull-out tests performed on sand–GTX–sand interface at varying normal pressure, geotextile type and geotextile length are shown in Appendix - A. These data are the raw data presented in the form of graphs (pull-out force on geotextile vs. front end displacement, average axial strain vs. front end displacement, displacement vs. loading time). The frequency of the symbols used in the figures presented in Appendix – A is every 90 points i.e. each symbol is shown after 90 data points. In this section, the results obtained for the different parameters are presented.

4.6.1 Effect of Normal Pressure

The results of pull-out tests performed on sand–GTX–sand interface are summarized in Tables 4.3, 4.4 and 4.5 for A-400, F-140, and A-140 geotextiles, respectively. Fig. 4.18 presents the variation of the pull-out force on geotextile with the front end displacement for A-400 geotextile with different normal pressures. It is clear from the figure that as the normal pressure increases on the surface of the geotextile, the pull-out force, or the resistance mobilized, increases. The reason for this behavior can be obtained directly from the basic shear strength equation ($\tau = \sigma_n \tan\psi$). As the applied normal pressure increases, the shear stress on the interface increases, resulting in larger pull-out resistance. Table 4.3 shows that at the normal pressure of 24 kPa, the peak and the residual interface characteristics are similar for A-400 geotextile, and are also close to the end of the test characteristics. This means that at 24 kPa normal pressure it is difficult to differentiate between peak and residual state since both values are very close to the values at the end of the test.

Fig. 4.19 presents the variation of the shear stress at the residual state with the applied normal pressure for the three geotextiles. Results show that the sand–GTX–sand interface shear stress does not obey the Mohr's Coulomb law, and the shear stresses are not linearly proportional to the normal stress. The results also show that the shear stress increases as the normal pressure increases, that means pull-out load increases with the increase in normal stress. This increase is due to the high restrains on dilatancy in the vicinity of soil-geotextile interface with the increase in the normal pressure, as described by Shingenori et al. (1996), and due to geotextile soil interlocking. It can also be observed

Table 4.3: Interface characteristics for sand-A-400 GTX-sand interface and 380 mm long geotextile with varying normal pressure

At peak pull-out state					
Normal pressure (kPa)	Pull-out force (N)	Shear stress (kPa)	ψ_p	Overall average strain (%)	Front end displacement (mm)
4.50	448.32	5.04	48.30	16.95	66.40
8.00	541.51	5.98	36.80	19.20	73.00
16.00	767.14	8.62	28.30	17.10	65.00
24.00	722.99	7.38	17.10	28.90	111.80
At residual pull-out state					
Normal pressure (kPa)	Pull-out force (N)	Shear stress (kPa)	ψ_R	Overall average strain (%)	Front end displacement (mm)
4.50	409.07	4.58	45.50	17.40	72.10
8.00	514.04	5.52	34.60	22.50	87.10
16.00	668.35	7.06	23.80	25.07	95.30
24.00	722.99	7.38	17.10	28.90	111.80
At the end of the test					
Normal pressure (kPa)	Pull-out force (N)	Shear stress (kPa)	ψ_{End}	Overall average strain (%)	Front end displacement (mm)
4.50	350.22	3.90	40.90	18.20	115.30
8.00	502.27	5.37	33.80	23.20	117.30
16.00	602.33	6.27	21.40	26.30	117.50
24.00	722.99	7.27	16.90	30.87	118.53
Axial strain in geotextile at residual state					
Normal pressure (kPa)	Average strain in the front one-third (%)	Average strain in the middle one-third (%)		Average strain in the rear one-third (%)	Overall average strain (%)
4.50	27.40	18.70		8.60	17.40
8.00	30.90	26.30		12.00	22.50
16.00	37.27	29.30		8.90	24.60
24.00	41.70	30.50		13.50	28.90
Axial strain in geotextile at the end of the test					
Normal pressure (kPa)	Average strain in the front one-third (%)	Average strain in the middle one-third (%)		Average strain in the rear one-third (%)	Overall average strain (%)
4.50	27.40	18.70		8.60	18.20
8.00	34.10	25.50		12.50	23.20
16.00	39.70	30.70		10.00	26.30
24.00	45.80	31.60		14.60	30.80

Table 4.4: Interface characteristics for sand-F-140 GTX-sand interface and 380 mm long geotextile with varying normal pressure

At peak pull-out state					
Normal pressure (kPa)	Pull-out force (N)	Shear stress (kPa)	ψ_p	Overall average strain (%)	Front end displacement (mm)
4.50	367.09	4.24	43.30	13.97	53.10
8.00	576.83	6.60	39.50	15.00	57.00
16.00	516.01	5.61	19.30	21.10	80.00
At residual pull-out state					
Normal pressure (kPa)	Pull-out force (N)	Shear stress (kPa)	ψ_R	Overall average strain (%)	Front end displacement (mm)
4.50	199.14	2.14	25.44	22.40	105.00
8.00	414.96	4.40	28.60	24.13	95.14
16.00	468.92	4.75	16.50	29.80	116.40
At the end of the test					
Normal pressure (kPa)	Pull-out force (N)	Shear stress (kPa)	ψ_{End}	Overall average strain (%)	Front end displacement (mm)
4.50	181.49	1.94	23.30	23.20	114.50
8.00	339.43	3.60	23.26	24.13	112.00
16.00	468.92	4.75	16.50	29.80	116.40
Axial strain in geotextile at residual state					
Normal pressure (kPa)	Average strain in the front one-third	Average strain in the middle one-third (%)		Average strain in the rear one-third (%)	Overall average strain (%)
4.50	39.20	19.60		10.34	22.40
8.00	36.30	27.81		10.35	24.13
16.00	39.85	37.10		14.60	29.80
Axial strain in geotextile at the end of the test					
Normal pressure (kPa)	Average strain in the front one-third	Average strain in the middle one-third (%)		Average strain in the rear one-third (%)	Overall average strain (%)
4.50	39.20	19.60		12.86	23.20
8.00	36.30	27.81		10.35	24.13
16.00	39.85	37.10		14.60	29.80

Table 4.5: Interface characteristics for sand-A-140 GTX-sand interface and 380 mm long geotextile with varying normal pressure

At peak pull-out state					
Normal pressure (kPa)	Pull-out force (N)	Shear stress (kPa)	ψ_p	Overall average strain (%)	Front end displacement (mm)
4.50	117.33	1.32	16.30	17.30	65.70
8.00	281.55	3.24	22.02	14.47	56.25
16.00	267.81	2.71	9.60	30.13	114.50
At residual pull-out state					
Normal pressure (kPa)	Pull-out force (N)	Shear stress (kPa)	ψ_R	Overall average strain (%)	Front end displacement (mm)
4.50	106.83	1.07	13.33	31.60	120.00
8.00	260.95	2.64	18.20	30.26	117.10
16.00	267.81	2.71	9.60	30.13	114.50
At the end of the test					
Normal pressure (kPa)	Pull-out force (N)	Shear stress (kPa)	ψ_{End}	Overall average strain (%)	Front end displacement (mm)
4.50	106.83	1.07	13.30	31.60	120.00
8.00	260.95	2.64	18.20	30.26	117.10
16.00	267.81	2.71	9.60	30.13	114.50

Axial strain in geotextile at residual state				
Normal pressure (kPa)	Average strain in the front one-third	Average strain in the middle one-third (%)	Average strain in the rear one-third (%)	Overall average strain (%)
4.50	42.10	37.10	18.50	31.60
8.00	42.80	33.80	17.12	30.26
16.00	57.80	33.20	1.58	30.13
Axial strain in geotextile at the end of the test				
Normal pressure (kPa)	Average strain in the front one-third	Average strain in the middle one-third (%)	Average strain in the rear one-third (%)	Overall average strain (%)
4.50	42.10	37.10	18.50	31.60
8.00	42.80	33.80	17.12	30.26
16.00	57.80	33.20	1.58	30.13

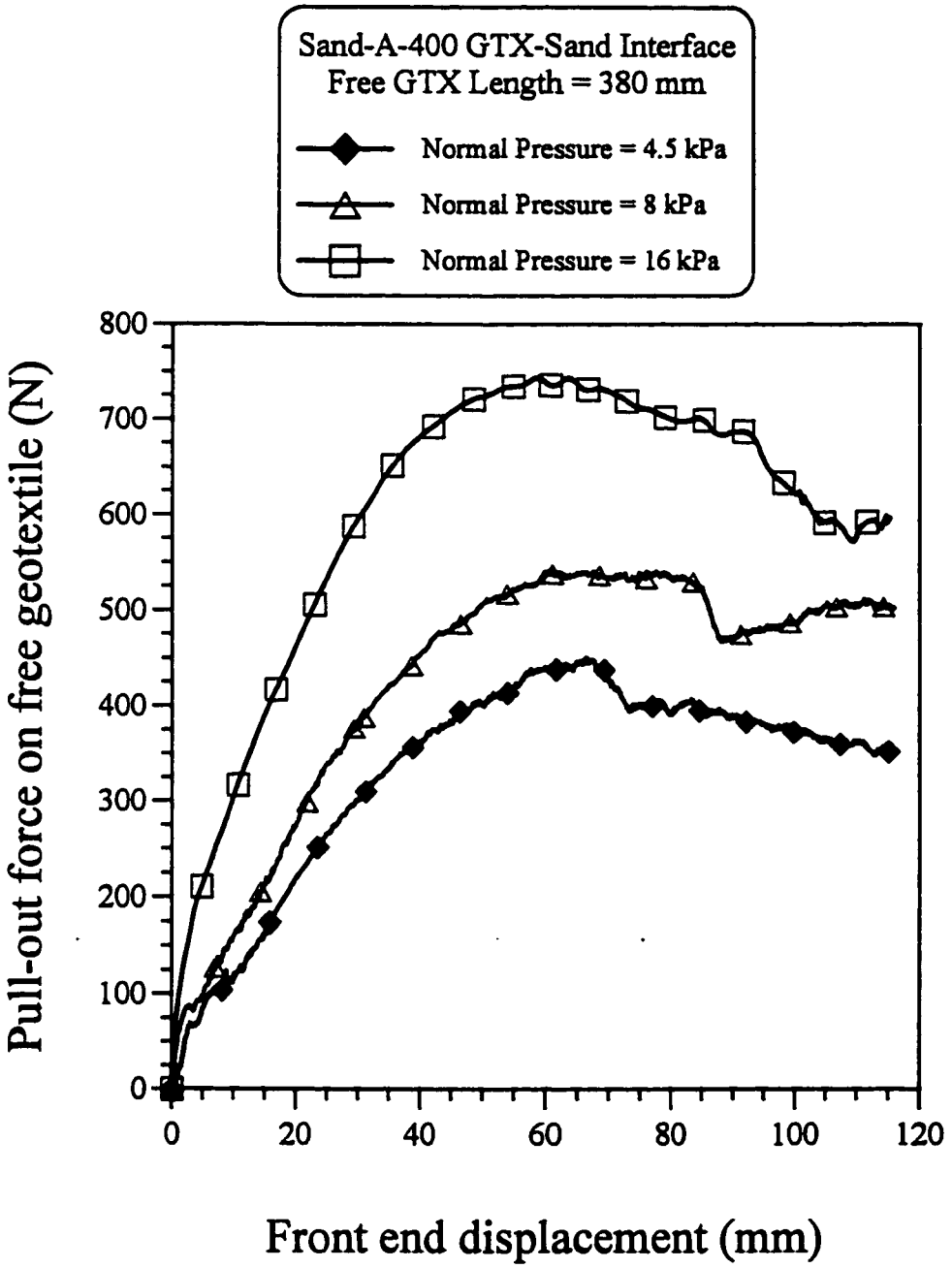

Fig. 4.18: Variation of the pull-out force on A-400 geotextile with the front end displacement for sand-GTX-sand interface, and 380 mm long geotextile

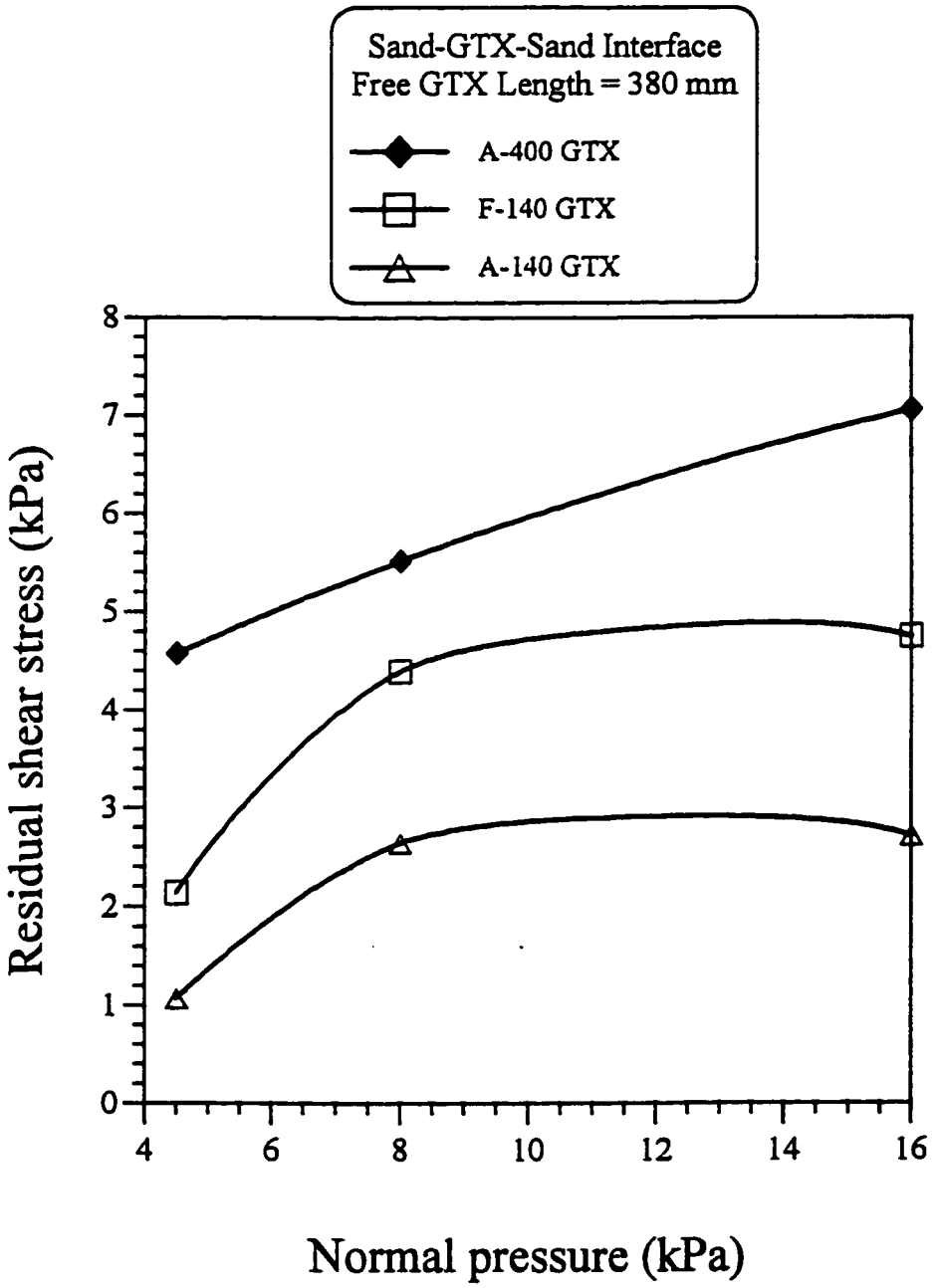

Fig. 4.19: Variation of the shear stress at the residual state with the applied normal pressure for sand-GTX-sand interface, and 380 mm long free geotextile

that the increase in the residual shear stress decreases with the increase in the normal pressure level. The figure also shows that A-400 geotextile offers largest pull-out resistance for sand–geotextile–sand interface since it can take more shear stress as compared with other two geotextiles.

Table 3.1 shows that F–140 and A-140 geotextiles have the same tensile strength, however, F-140 geotextile is 20% less extensible than A-140 geotextile (60% versus 80%). This is confirmed by results in Fig. 4.19 which shows that less extensible geotextile (F-140) is more efficient than the A-140 geotextile in the pull-out load capacity for soil–geotextile interface (reinforcement). Such results were also observed by Zhai (1996), who stated that inextensible geotextile behaves effectively in reinforcement function. The results in Fig. 4.19 show that A-400 geotextile has a pull-out resistance of at least twice that of the A-140 geotextile in sand–GTX–sand interface. This is expected since A-400 and A-140 geotextile have the same elongation percentage at rupture, but A-400 geotextile is 2.9 times stronger (tensile strength) than A-140 geotextile.

Fig. 4.20 shows the variation of the interface friction angle at the residual state with the applied normal pressure for sand–GTX–sand interface. The angle of interface friction decreases with the increase in normal pressure for A-400 geotextile. However, for F-140 and A-140 geotextiles, the angle increases when the normal pressure is increased from 4.5 kPa to 8 kPa, then it decreases when normal pressure is increased from 8 kPa to 16 kPa. It can be observed here that the behavior of A-140 and F-140 geotextiles is similar but F-140 geotextile is stronger than A-140 geotextile. The higher extensibility of A-140 geotextile as compared to F-140 geotextile makes it offering lower pull-out resistance.

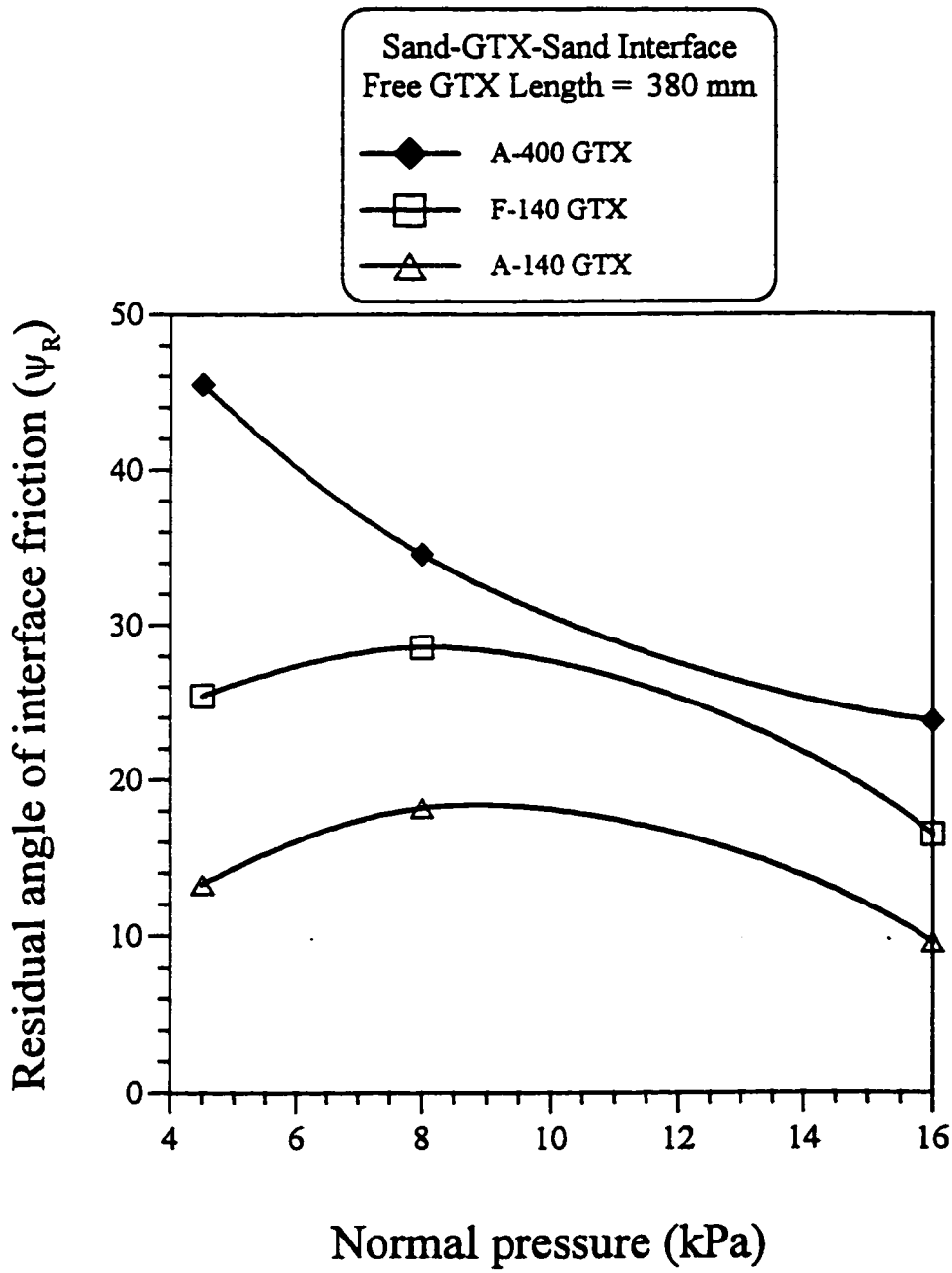

Fig. 4.20: Variation of residual angle of interface friction (ψ_R) with the applied normal pressure for sand-GTX-sand interface, and 380 mm long free geotextile

Furthermore, at 16 kPa normal pressure, F-140 and A-140 geotextiles show necking of samples after the test. The necking extends upto two-third of the total length in the case of 380 mm long geotextile samples. The necking reduces the surface area of geotextile, which in turn reduces the contact area between the geotextile and sand, resulting in lower pull-out resistance. It was observed that the A-140 geotextile samples showed more necking as compared to the F-140 geotextile samples for the same value of applied normal pressure. This was due to the higher extensibility of A-140 as compared to F-140 geotextile.

Table 4.6 presents the interface interaction factors c_i for sand–GTX–sand interface. The results show that the value of c_i is dependent on the applied normal pressure and it decreases with increasing the applied normal pressure for the A-400 geotextile. For A-140 and F-140 geotextiles, the c_i value is found to increase in magnitude with increase in the normal pressure from 4.5 kPa to 8 kPa. After normal pressure value of 8 kPa, c_i value decreases with further increase in normal pressure. Its value is greater than 1.0 for the A-400 geotextile at 4.5 kPa normal pressure. Mallick (1996) also found that in the case of sand, coefficient of friction of soil-geotextile interface can range between 0.7 to 1.6 in pull-out tests. Rao and Pandey (1988) and Chang et al. (1993) have found that the coefficient of friction of a soil-geotextile interface can exceed the coefficient of friction of soil itself. Practically, the value of c_i cannot exceed 1.0 because the soil in the vicinity of the geotextile will fail in shear as soon as the shear strength of the soil is reached.

The results in Fig. 4.21 show the variation of overall average strain with normal pressure. For the F-140 geotextile, the overall average strain at both the peak shear stress

Table 4.6: Interface interaction factor c_i for sand-GTX-sand interface and 380 mm long free geotextile

Normal Pressure (kPa)	c_i		
	A-400 GTX	F-140 GTX	A-140 GTX
4.50	1.26	0.59	0.29
8.00	0.85	0.67	0.41
16.00	0.54	0.37	0.21

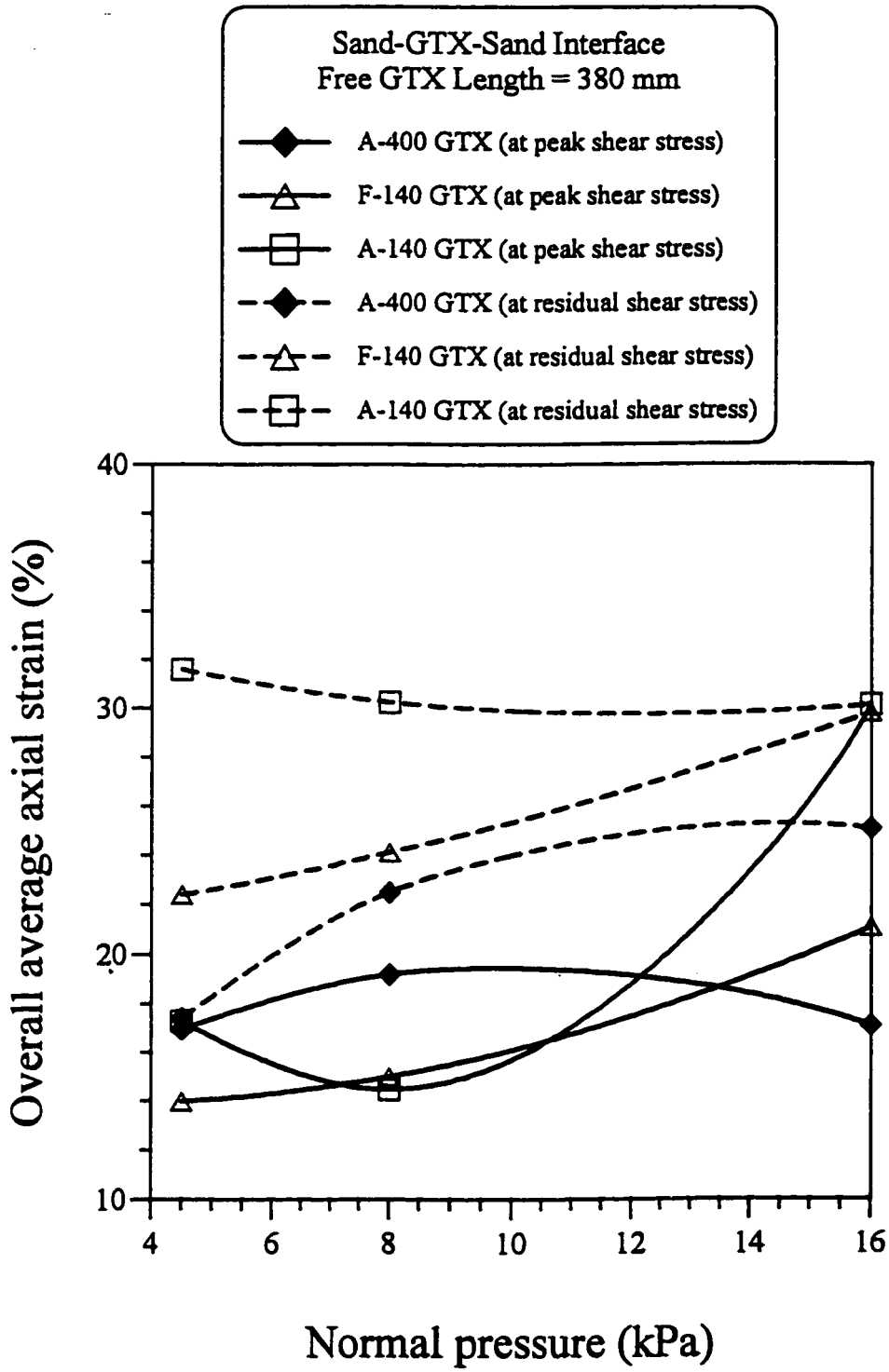

Fig. 4.21: Variation of the overall average axial strain with the applied normal pressure for sand-GTX-sand interface, and 380 mm long free geotextile

and residual conditions increase with the increase in normal pressure. Whereas for the A-140 geotextile the overall average strain, at peak condition, increases when the normal pressure exceeds 8 kPa. However, the overall average strains at peak shear stress conditions are not so sensitive to normal pressure for A-400 geotextile. This is due to the fact that both F-140 and A-140 geotextiles are thinner than A-400 geotextile and have also less tensile strength.

It should be clear that the maximum possible experimental strain for 380 mm long geotextile sample is about 30 – 31% at the end of the test. Therefore it can be seen from Fig. 4.21 that A-140 geotextile reached the maximum possible strain at the end of the test while it was still straining and did not reach the residual state at the end of the test. For such case the end of the test was declared as the residual state. Whereas A-400 and F-140 geotextiles show the increase in overall strain with increase in normal pressure for residual state. Figs. 4.22, 4.23 and 4.24 are representing the variation of the average axial strain for different portions along the geotextile. For A-400 and F-140 geotextiles, it can be seen that the strain at any point along the geotextile increases with the increase in the normal pressure. However, in the case of A-140 geotextile, the strains are concentrated more at the front portion for high normal pressure values and little strain was measured at the rear portion. However, for the low normal pressure values (i.e. 4.5 and 8 kPa) the difference in axial strain at front end and rear end is smaller than that for the normal pressure of 16 kPa. It is noticed that the variations of axial strain along the A-140 geotextile were identical for the normal pressure of 4.5 and 8 kPa. This is mainly due to the necking at the 16 kPa normal pressure.

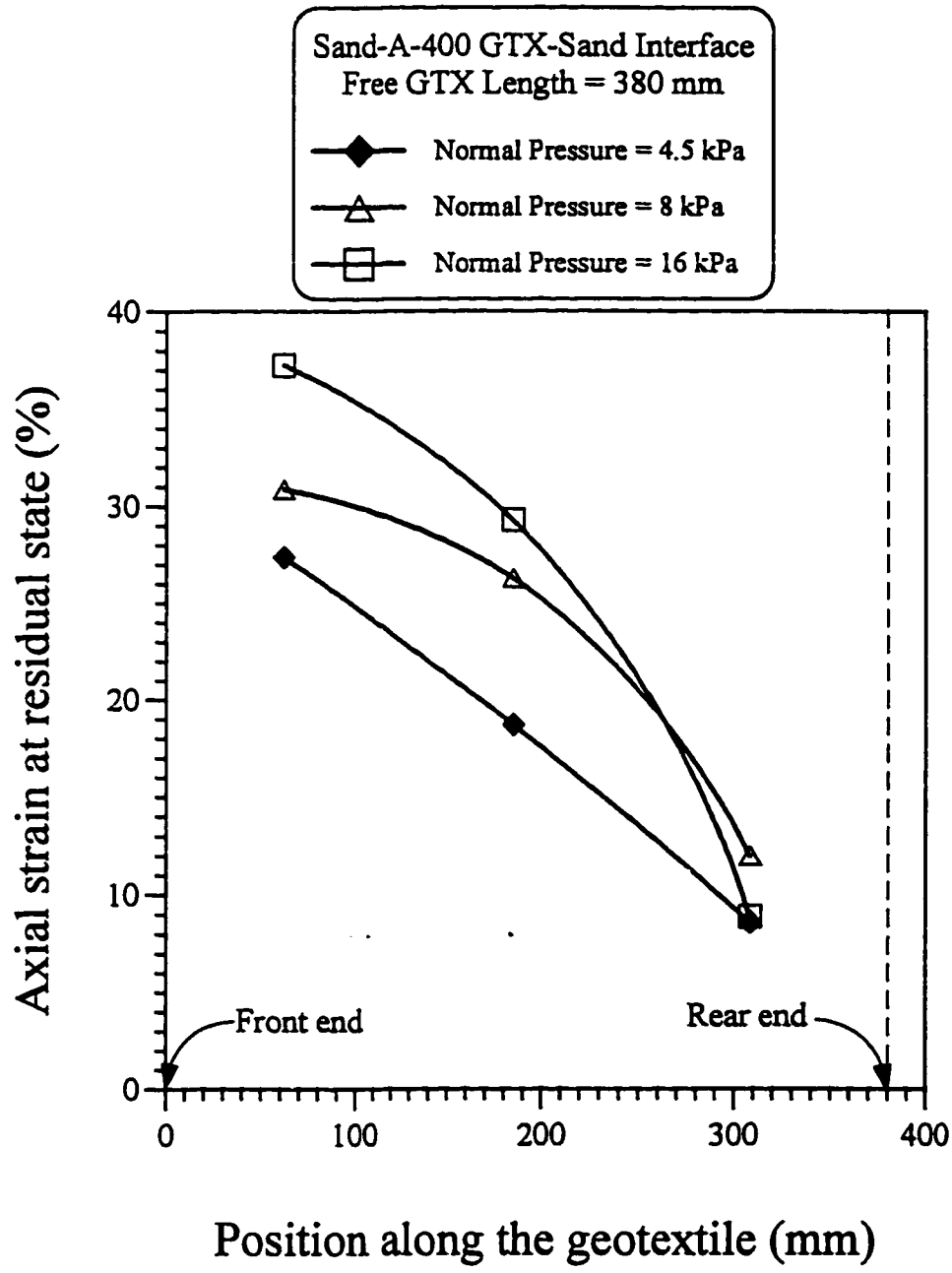

Fig. 4.22: Variation of the average axial strain at the residual state with the postion along geotextile for sand-A-400 GTX-sand interface and 380 mm long free geotextile

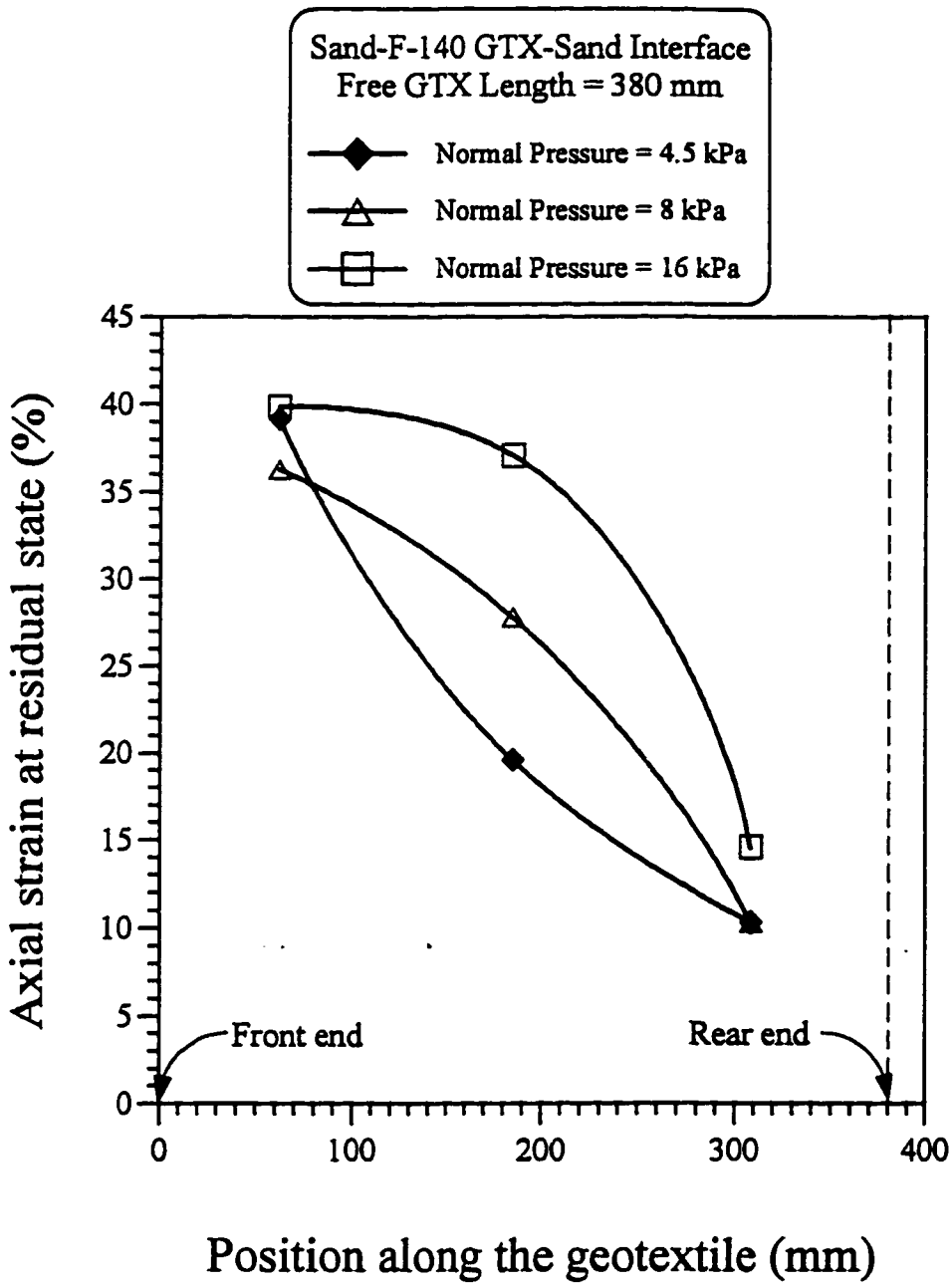

Fig. 4.23: Variation of the average axial strain at the residual state with the postion along geotextile for sand-F-140 GTX-sand interface and 380 mm long free geotextile

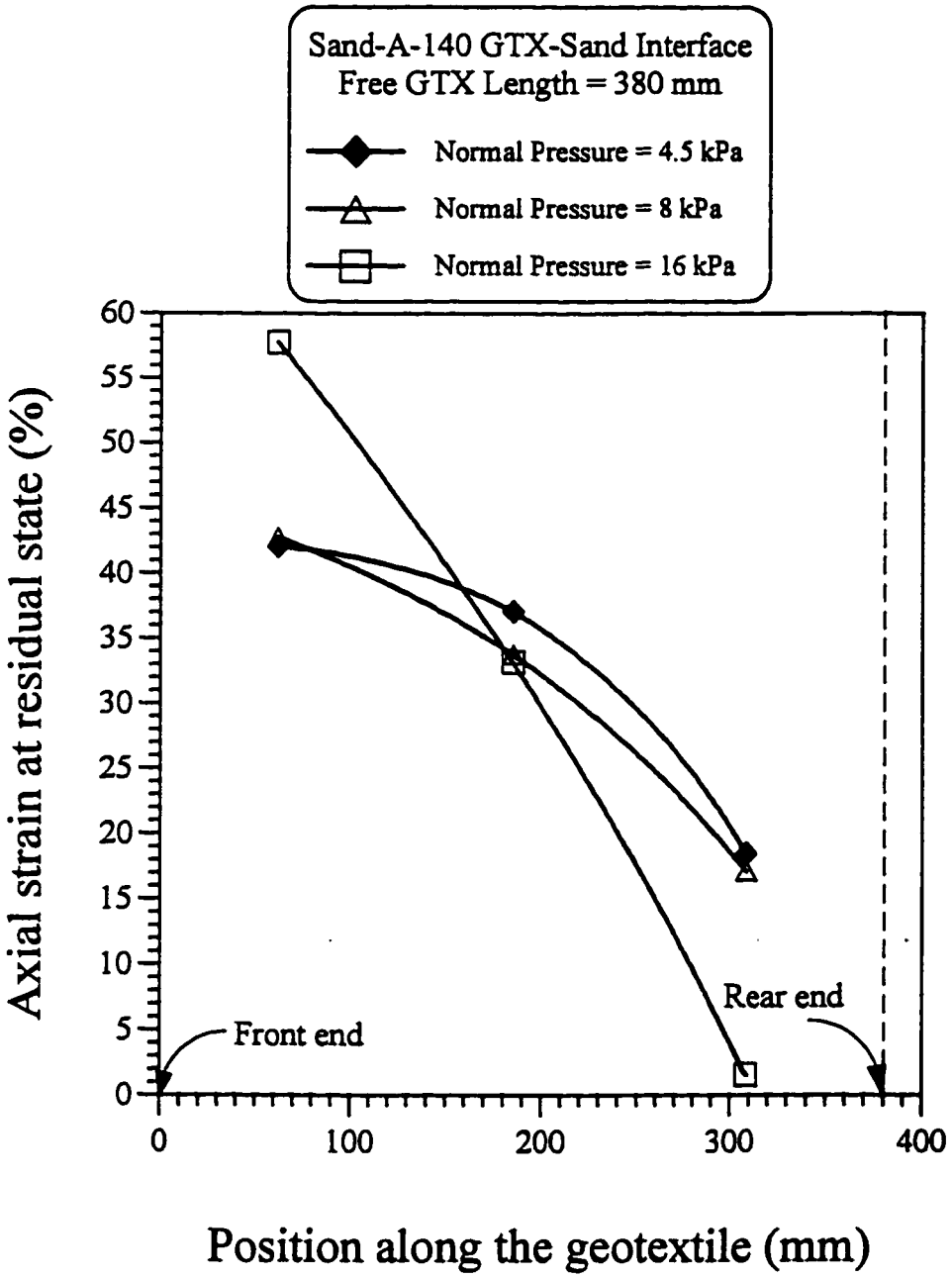

Fig. 4.24: Variation of the average axial strain at the residual state with the postion along geotextile for sand-A-140 GTX-sand interface and 380 mm long free geotextile

4.6.2 Effect of Geotextile Type

The technical specifications of the three geotextiles are shown in Table 3.1. The A-140 and F-140 geotextiles have the same tensile strength but have different extensibility. The F-140 is less extensible as compared with A-140 and A-400 geotextiles. The A-400 geotextile has higher tensile strength, compared with other two geotextiles and have the same extensibility as the A-140 geotextile.

The interface characteristics for sand–GTX–sand interface at 8 kPa normal pressure and 380 mm long geotextile is shown in Table 4.7. The test results plotted in Figs. 4.25, 4.26, and 4.27 show that A-140 is the weakest while A-400 is the strongest geotextile regarding the sand–GTX–sand interface. From Figs. 4.25 and 4.26 it is clear that the F-140 geotextile has higher initial tangent modulus as compared with other two geotextiles. This is mainly due to the low extensibility as compared with other geotextiles. However, with the increase in normal pressure to 16 kPa, the initial tangent modulus of both A-400 and F-140 geotextile becomes almost similar, as shown in Fig. 4.27. This is due to the fact that the large normal stresses are resulting in a proper anchorage of the F-140 geotextile and thus it will elongate. The geotextile reached the maximum possible strain at the end of the test and it was still straining. Therefore, the end of the test was declared as the residual state.

Fig. 4.28 presents the variation of peak shear stress with the geotextile type. It shows that peak shear stress value at 16 kPa is less than the peak shear stress value at 8 kPa for A-140 and F-140 geotextile. Figs. 4.29 and 4.30 show, respectively, the variation of shear stress and axial strain at residual state with the geotextile type. It is clear that for

Table 4.7: Interface characteristics for sand-A-400 GTX-sand interface, 8 kPa normal pressure, and 380 mm long free geotextile with different geotextiles

At peak pull-out state					
Type of Geotextile	Pull-out force (N)	Shear stress (kPa)	ψ_P	Overall average strain (%)	Front end displacement (mm)
A-400	541.51	5.98	36.80	19.20	73.00
F-140	576.83	6.60	39.50	15.00	57.00
A-140	281.55	3.24	22.02	14.47	56.25
At residual pull-out state					
Type of Geotextile	Pull-out force (N)	Shear stress (kPa)	ψ_R	Overall average strain (%)	Front end displacement (mm)
A-400	514.04	5.52	34.60	22.50	87.10
F-140	414.96	4.40	28.60	24.13	95.14
A-140	260.95	2.64	18.20	30.26	117.10
At the end of the test					
Type of Geotextile	Pull-out force (N)	Shear stress (kPa)	ψ_{End}	Overall average strain (%)	Front end displacement (mm)
A-400	502.27	5.37	33.80	23.20	117.30
F-140	339.43	3.60	23.26	24.13	112.00
A-140	260.95	2.71	9.60	30.13	114.50
Axial strain in geotextile at residual state					
Type of Geotextile	Average strain in the front one-third	Average strain in the middle one-third (%)		Average strain in the rear one-third (%)	Overall average strain (%)
A-400	30.90	26.30		12.00	22.50
F-140	36.30	27.81		10.35	24.13
A-140	42.80	33.80		17.12	30.26
Axial strain in geotextile at the end of the test					
Type of Geotextile	Average strain in the front one-third	Average strain in the middle one-third (%)		Average strain in the rear one-third (%)	Overall average strain (%)
A-400	34.10	25.50		12.50	23.20
F-140	36.30	27.81		10.35	24.13
A-140	42.80	33.80		17.12	30.28

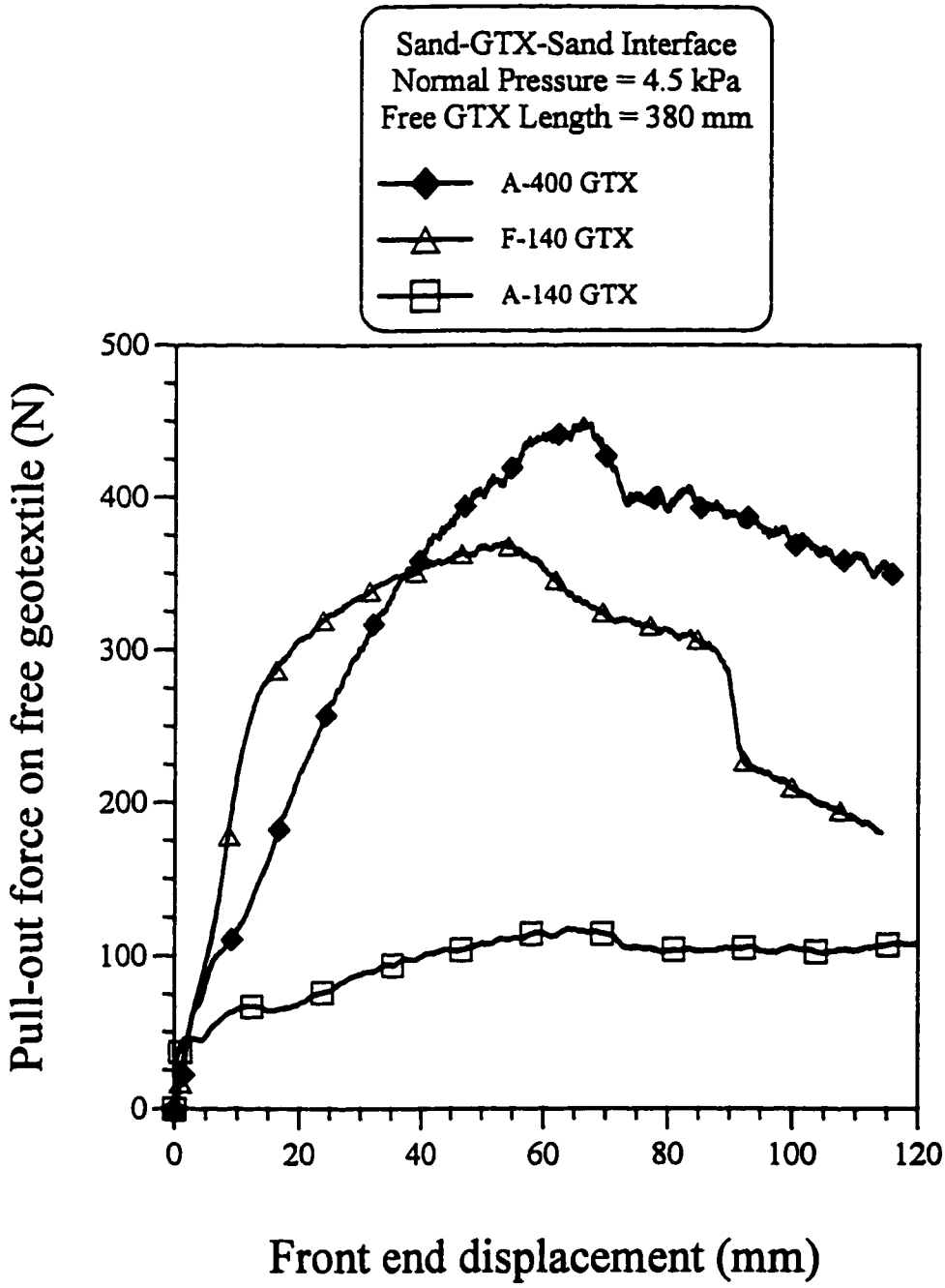

Fig. 4.25: Variation of the pull-out force on the geotextile with the front end displacement for sand-GTX-sand interface, under 4.5 kPa normal pressure, and 380 mm long free geotextile

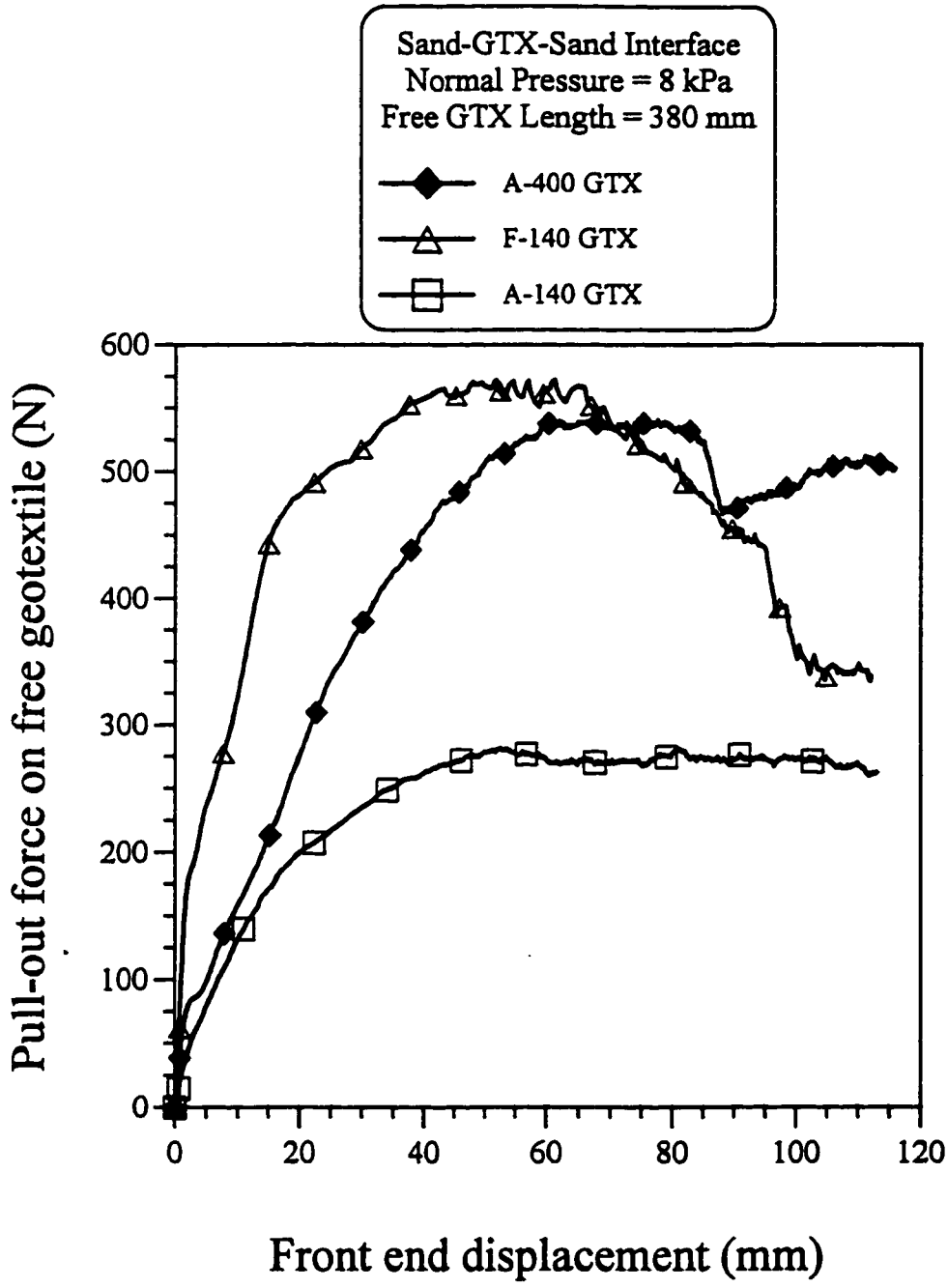

Fig. 4.26: Variation of the pull-out force on the geotextile with the front end displacement for sand-GTX-sand interface, under 8 kPa normal pressure, and 380 mm long free geotextile

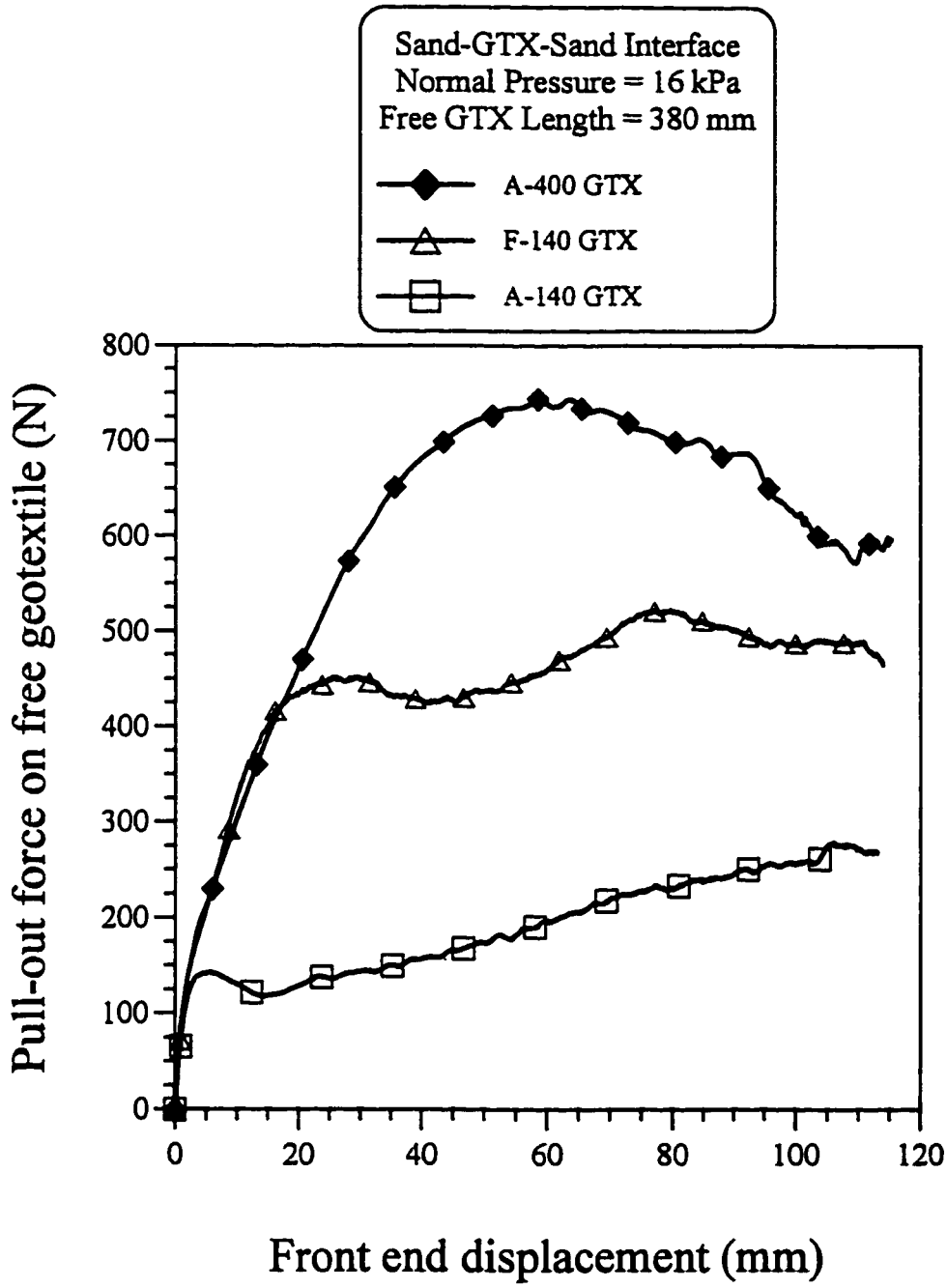

Fig. 4.27: Variation of the pull-out force on the geotextile with the front end displacement for sand-GTX-sand interface, under 16 kPa normal pressure, and 380 mm long free geotextile

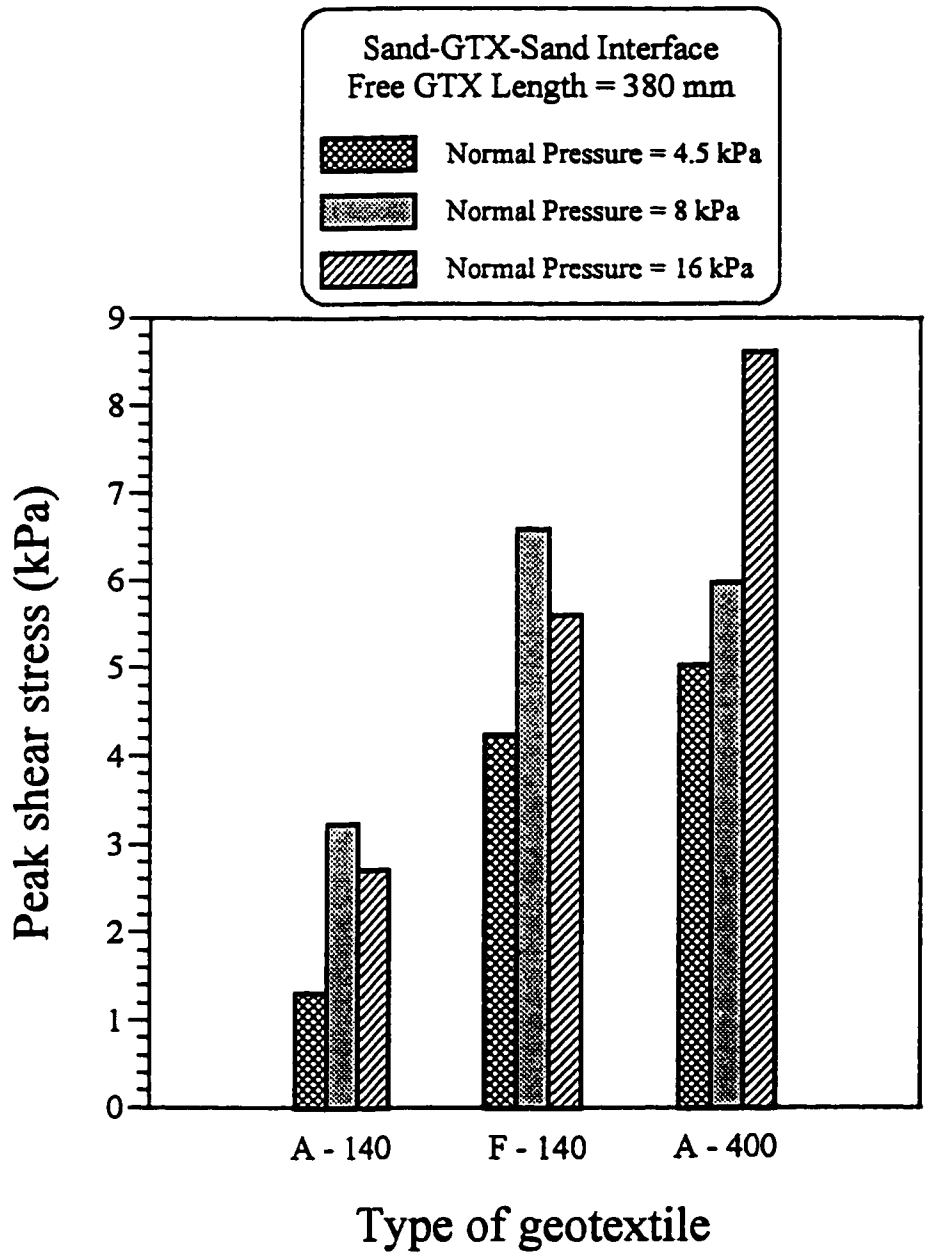

Fig. 4.28: Variation of the peak shear stress with geotextile type for sand-GTX-sand interface and 380 mm long free geotextile

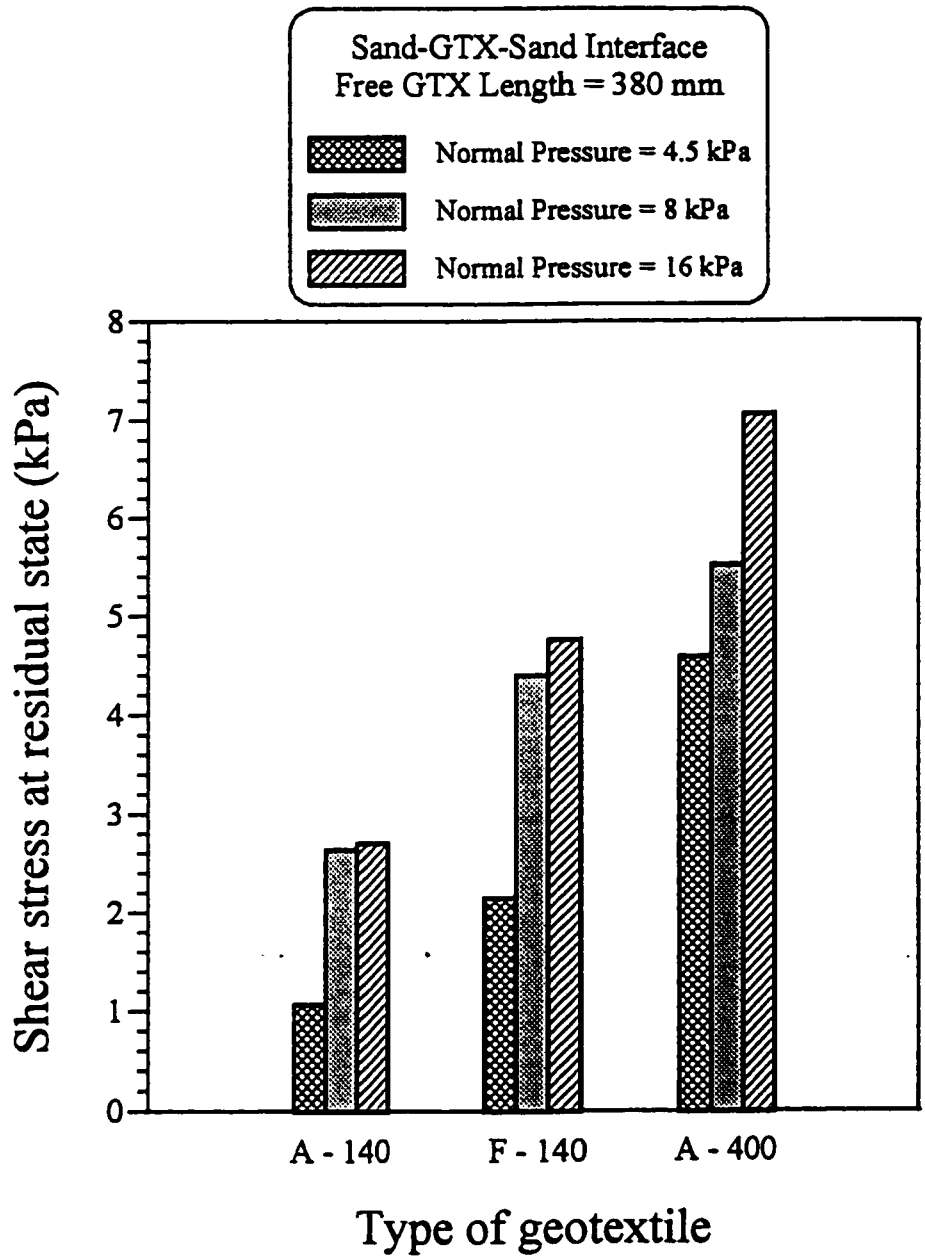

Fig. 4.29: Variation of the shear stress at the residual state with the geotextile type for sand-GTX-sand interface and 380 mm long free geotextile

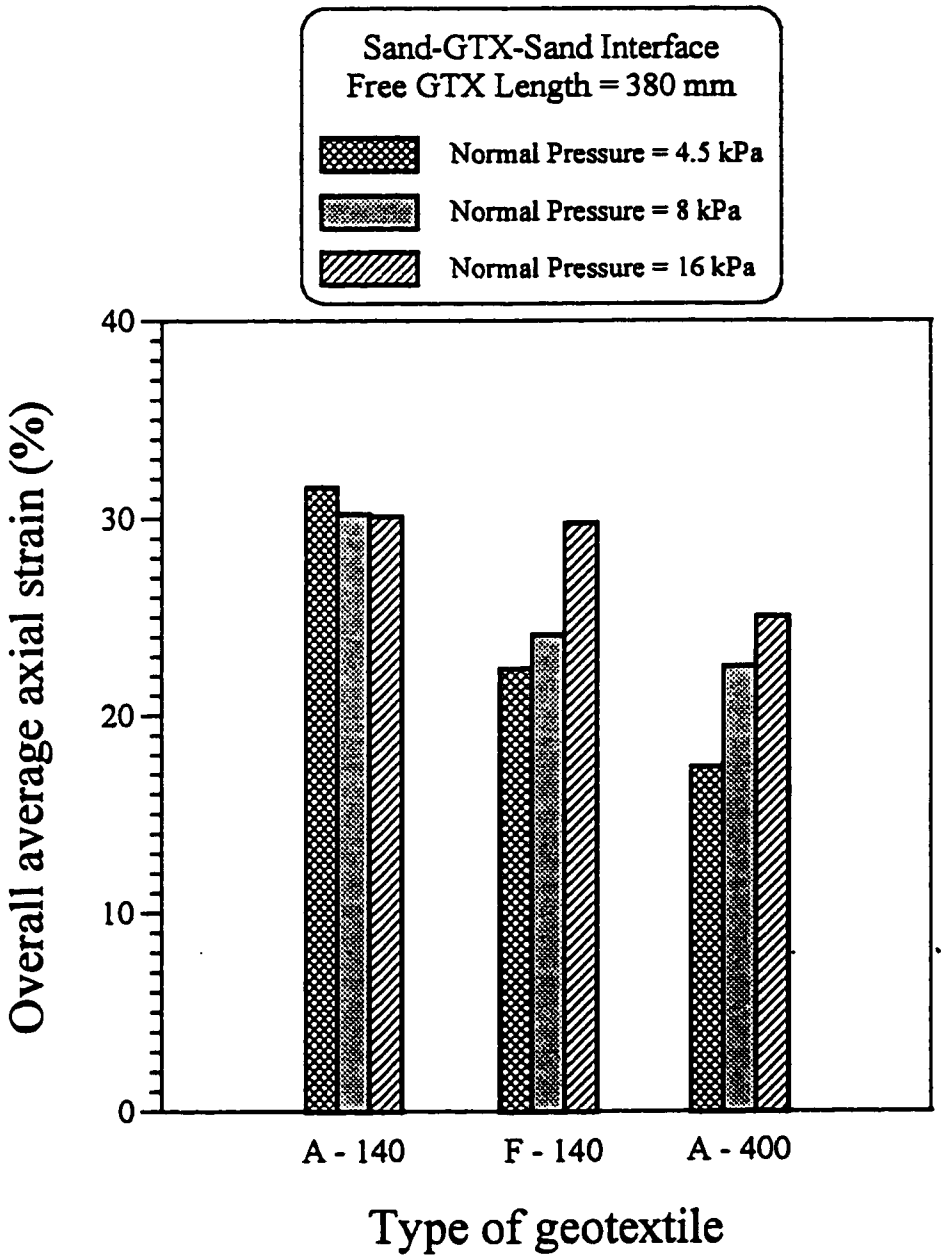

Fig. 4.30: Variation of the overall average axial strain at the residual state with geotextile type for sand-GTX-sand interface and 380 mm long free geotextile

A-140 geotextile, the percentage of strain is high when compared with A-400 and F-140 geotextiles. Therefore, low values of shear stresses are developed in the A-140 geotextile as shown in Fig. 4.29. This means that the stiffer (less extensible) the geotextile, the higher the shear stresses it can carry. For example, at a normal pressure of 4.5 kPa, the strain values at residual conditions are 31.6%, 22.4% and 17.4% for A-140, F-140, and A-400 geotextile, respectively. On the other hand, the shear stresses carried by A-400, at 17.4% strain, are the highest and thus it is the most efficient geotextile regarding the sand–GTX–sand interface.

Figs. 4.31, 4.32, and 4.33 show the variation of the average strain along the geotextile for different geotextile types. It can be seen from these figures that the A-140 geotextile is strained more throughout the length of the geotextile as compared with A-400 and F-140 geotextiles. However, for 16 kPa normal pressure, the A-140 geotextile showed more concentration of strain in the front part as shown by the data and by the necking observed after the test was over. Moreover, the trend of these lines shows that the strain is not uniformly distributed along the geotextile and the variation depends on the applied normal pressure as well as the on geotextile type. From these figures, it is clear that the strain along the geotextile decreases progressively towards its free end. As the pull-out load is applied to the geotextile, a combination of frictional and tensile stresses develop along its length. It should be clear, however, that the zero strain at any point of the geotextile indicates that no tensile stress has been generated in that area. This could be the case near the free end when the geotextile at that portion did not move.

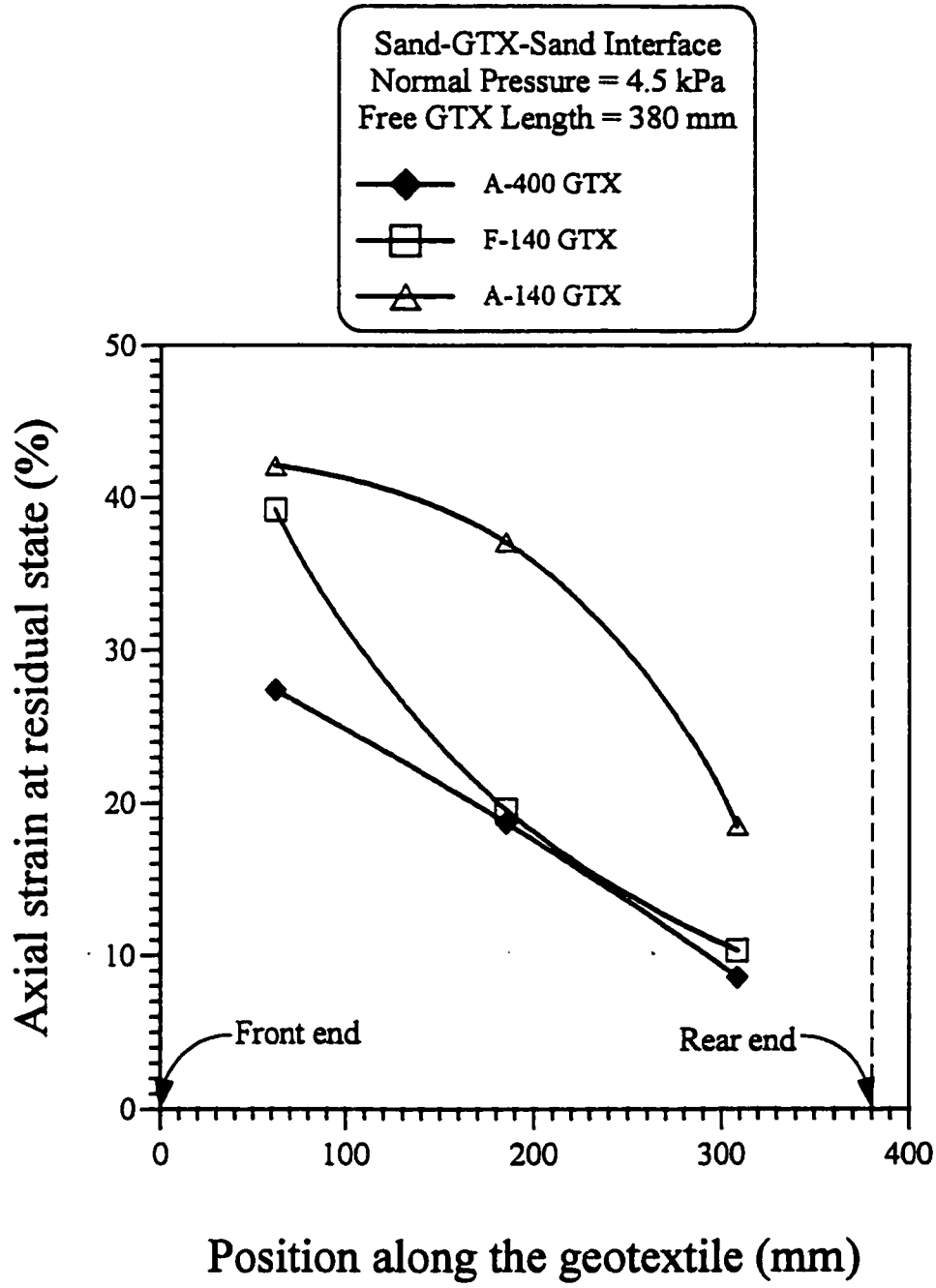

Fig. 4.31: Variation of the average axial strain at the residual state with the postion along the geotextile for sand-GTX-sand interface under 4.5 kPa normal pressure, and 380 mm long free geotextile

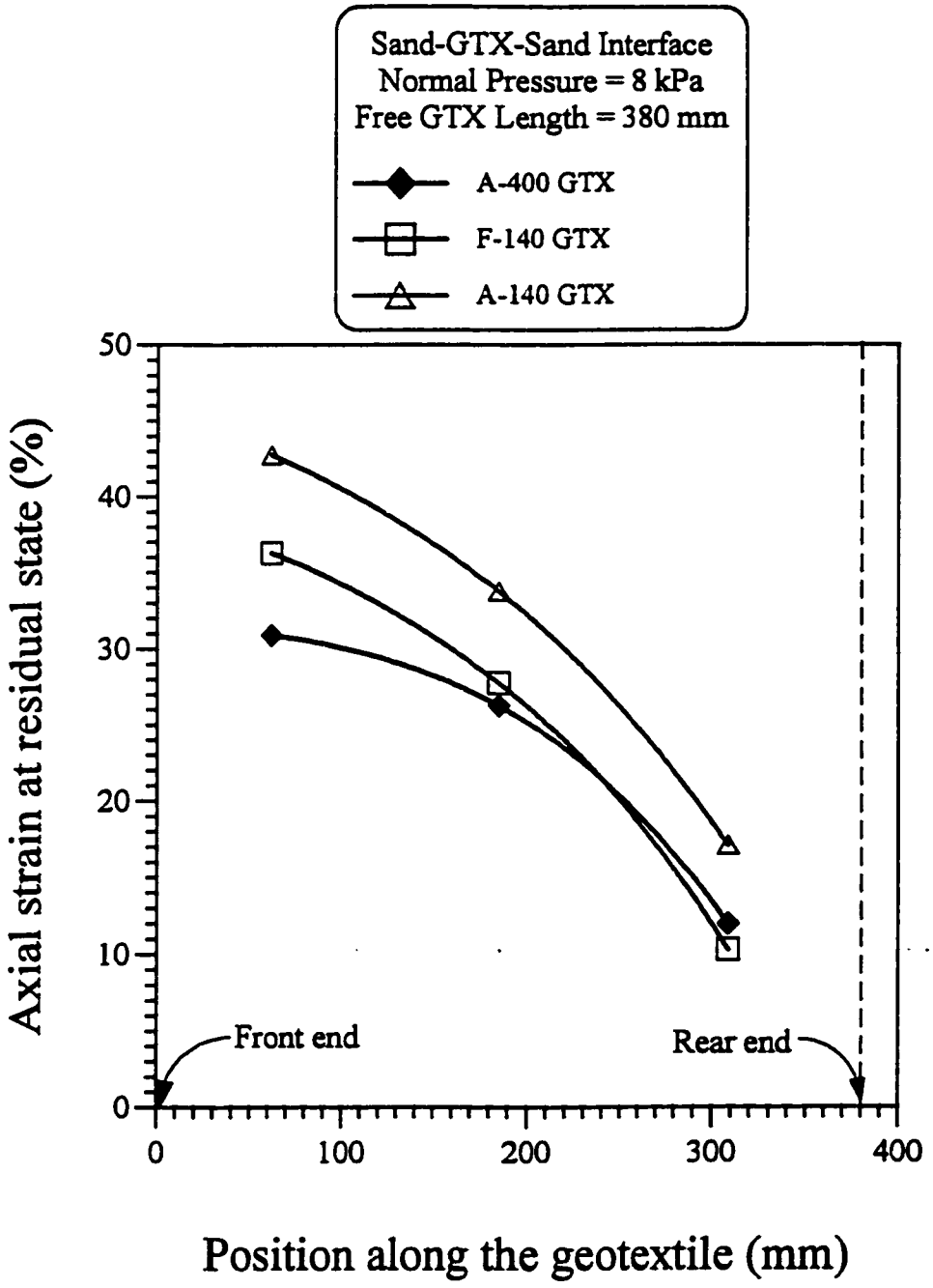

Fig. 4.32: Variation of the average axial strain at the residual state with the postion along the geotextile for sand-GTX-sand interface at 8 kPa normal pressure, and 380 mm long free geotextile

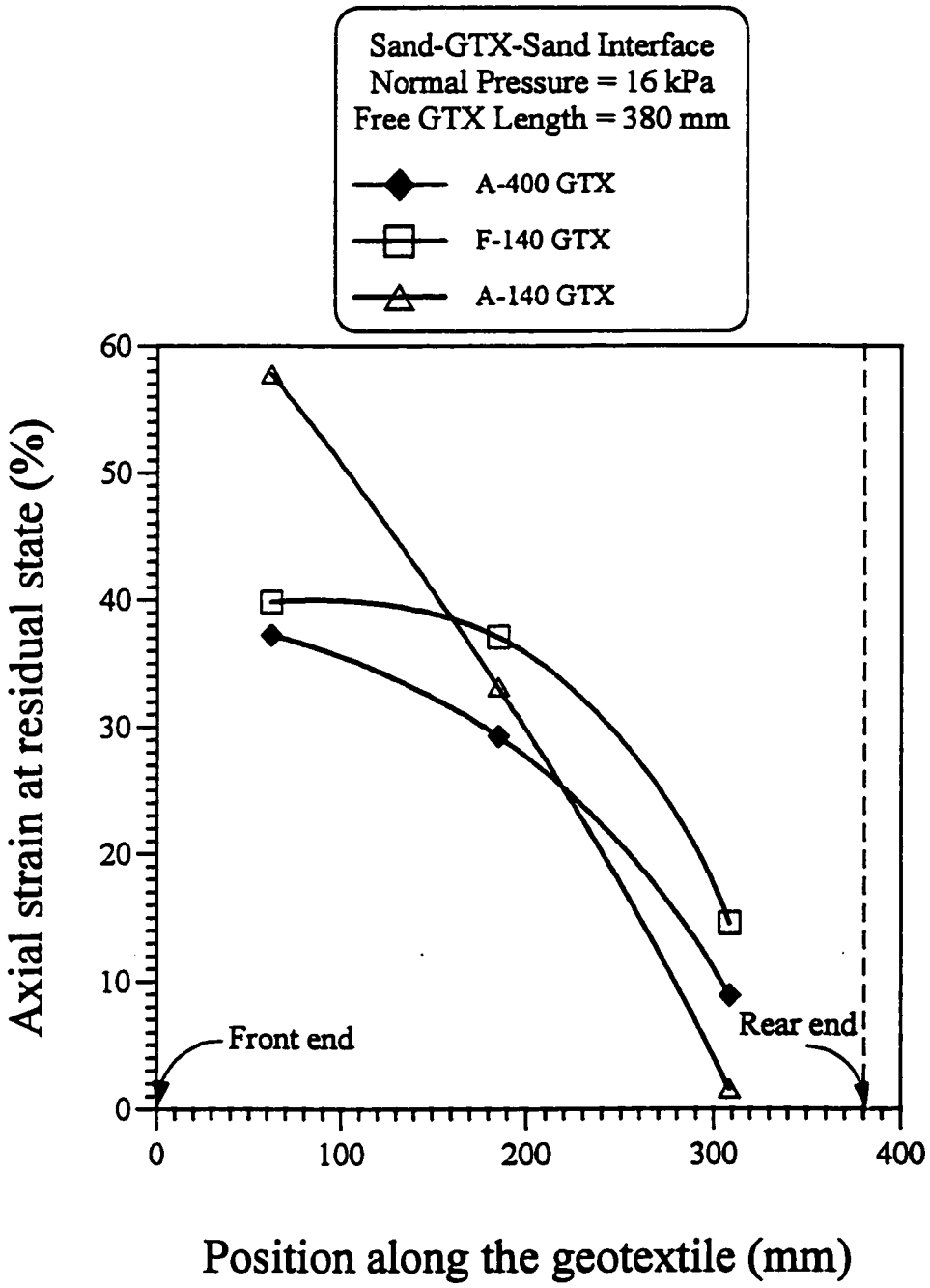

Fig. 4.33: Variation of the average axial strain at the residual state with the postion along the geotextile for sand-GTX-sand interface at 16 kPa normal pressure, and 380 mm long free geotextile

4.6.3 Effect of Geotextile Length

Three different lengths of A-400 geotextile were used in this experimental program at a normal pressure of 8 kPa. The results are summarized in Table 4.8. Fig. 4.34 presents the pull-out force versus displacement curves while Fig. 4.35 presents the variation of shear stress with geotextile length. It is clearly seen that as the geotextile length increases the shear stress decreases. Similar findings were reported by Imaizumu (1994) based on pull-out tests performed on Toyoura sand. The overall average strain is also plotted against the geotextile length in Fig. 4.35. It is observed that as the length of geotextile increases the overall axial strain increases. This means that as the length is increased, the geotextile is anchored more strongly into the sand, whereas for short lengths of geotextile, less strain is required to cause slippage due to lack of proper anchorage. It is known that increasing the length will provide proper anchorage and that is what counts in field applications since the geotextile will perform its intended functions as long as it is properly anchored.

The variation of the residual angle of interface friction for sand–GTX–sand interface with geotextile length is shown in Fig. 4.36. The figure shows that the angle of interface friction (ψ_R) can be as high as 56° for the 133 mm long geotextile. The reason for this high ψ_R value is the progressive shear stress development on the interface. The shear stresses are higher at locations close to the geotextile front end, compared to those close to the rear end. Therefore, when using smaller geotextile lengths, the stresses in most of the geotextile are high and the average of these high shear stresses is calculated to get the average shear stress on the interface. This can be seen from Fig. 4.37. On the other hand, for the larger geotextile sample length, the average shear stress on the interface

Table 4.8: Interface characteristics for sand-A-400 GTX-sand interface, and 8 kPa normal pressure with varying

At peak pull-out state					
Length of geotextile (mm)	Pull-out force (N)	Shear stress (kPa)	ψ_p	Overall average strain (%)	Front end displacement (mm)
380	541.51	5.98	36.80	19.20	73.00
257	579.08	9.39	49.60	20.10	75.60
133	413.00	13.71	59.70	12.80	79.20
At residual pull-out state					
Length of geotextile (mm)	Pull-out force (N)	Shear stress (kPa)	ψ_R	Overall average strain (%)	Front end displacement (mm)
380	514.04	5.52	34.60	22.50	87.10
257	552.70	8.94	48.20	20.30	83.50
133	358.07	11.76	55.77	14.18	94.70
At the end of the test					
Length of geotextile (mm)	Pull-out force (N)	Shear stress (kPa)	ψ_{End}	Overall average strain (%)	Front end displacement (mm)
380	502.27	5.37	33.80	23.20	117.30
257	430.66	6.82	40.50	22.98	115.00
133	308.03	10.02	51.40	15.20	114.70
Axial strain in geotextile at residual state					
Length of geotextile (mm)	Average strain in the front one-third	Average strain in the middle one-third (%)		Average strain in the rear one-third (%)	Overall average strain (%)
380	30.90	26.30		12.00	22.50
257	35.90	19.70		9.12	20.30
133	28.60	4.70		14.30	14.15
Axial strain in geotextile at the end of the test					
Length of geotextile (mm)	Average strain in the front one-third	Average strain in the middle one-third (%)		Average strain in the rear one-third (%)	Overall average strain (%)
380	34.10	25.50		12.50	23.20
257	36.50	19.70		12.17	22.98
133	32.90	3.00		13.20	15.20

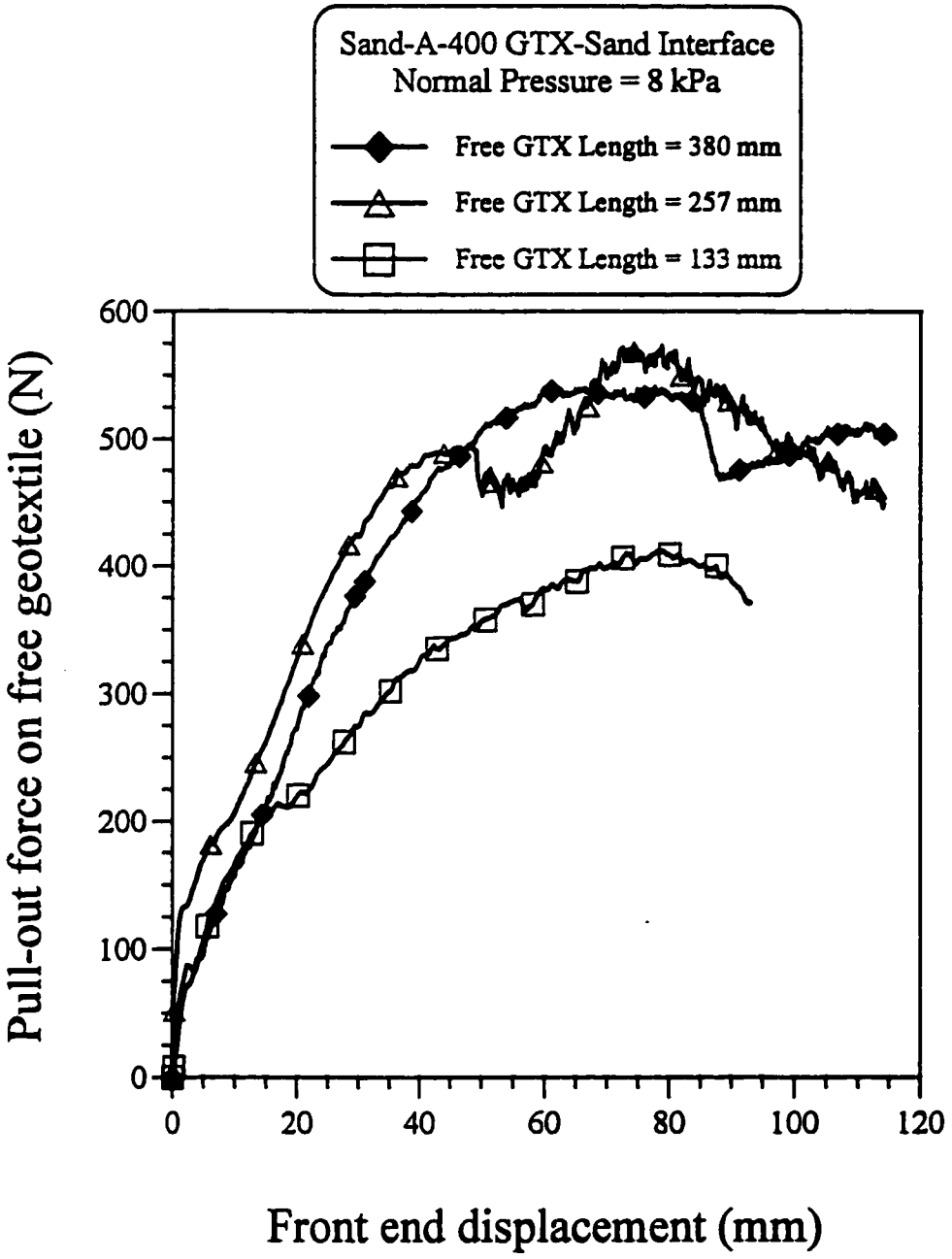

Fig. 4.34: Variation of the pull-out force on A-400 geotextile with the front end displacement for sand-GTX-sand interface, at a normal pressure of 8 kPa

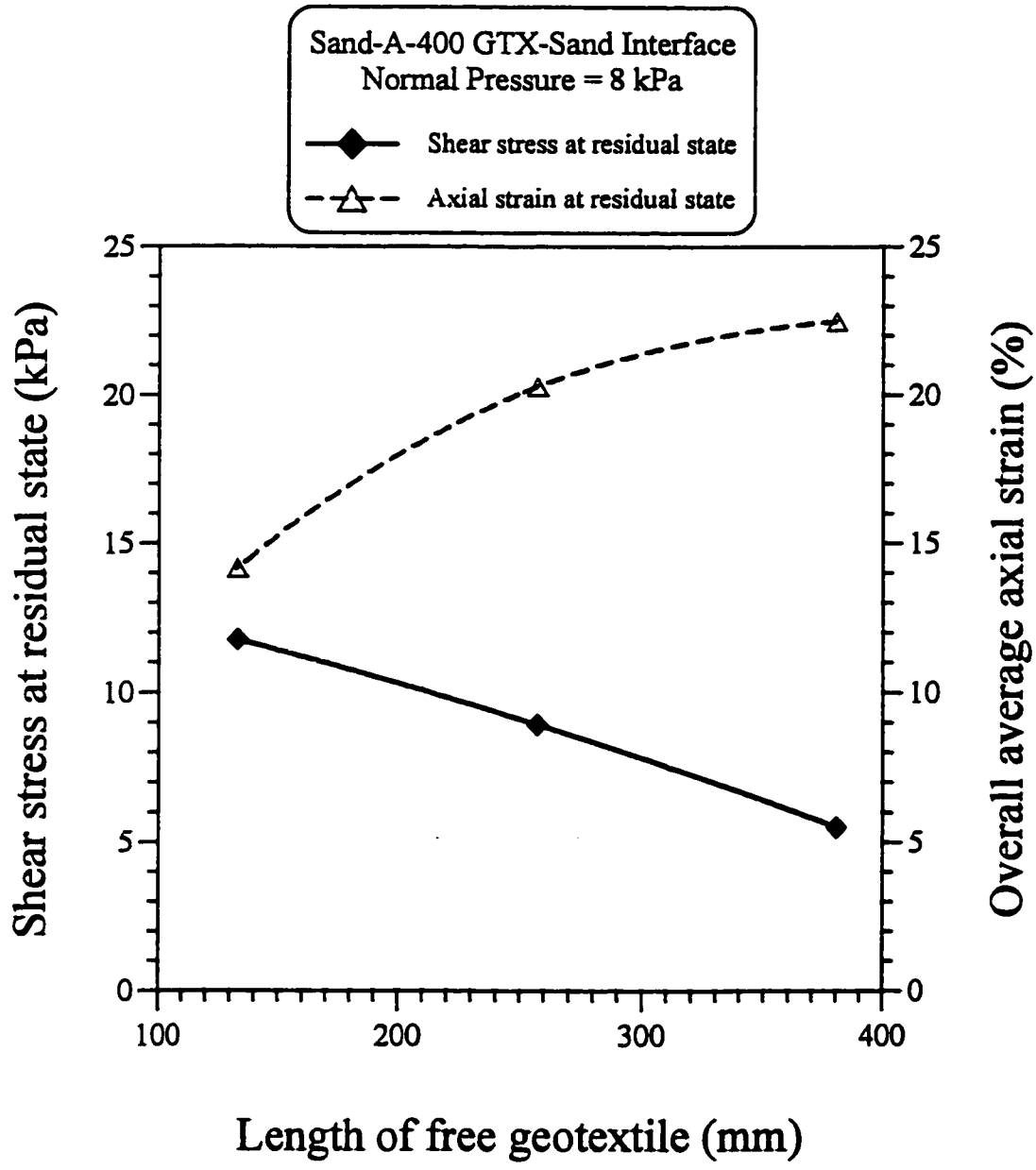

Fig. 4.35: Variation of the shear stress at residual state and the overall average axial strain at residual state with geotextile length for Sand- A-400 GTX-Sand interface at a normal pressure of 8 kPa

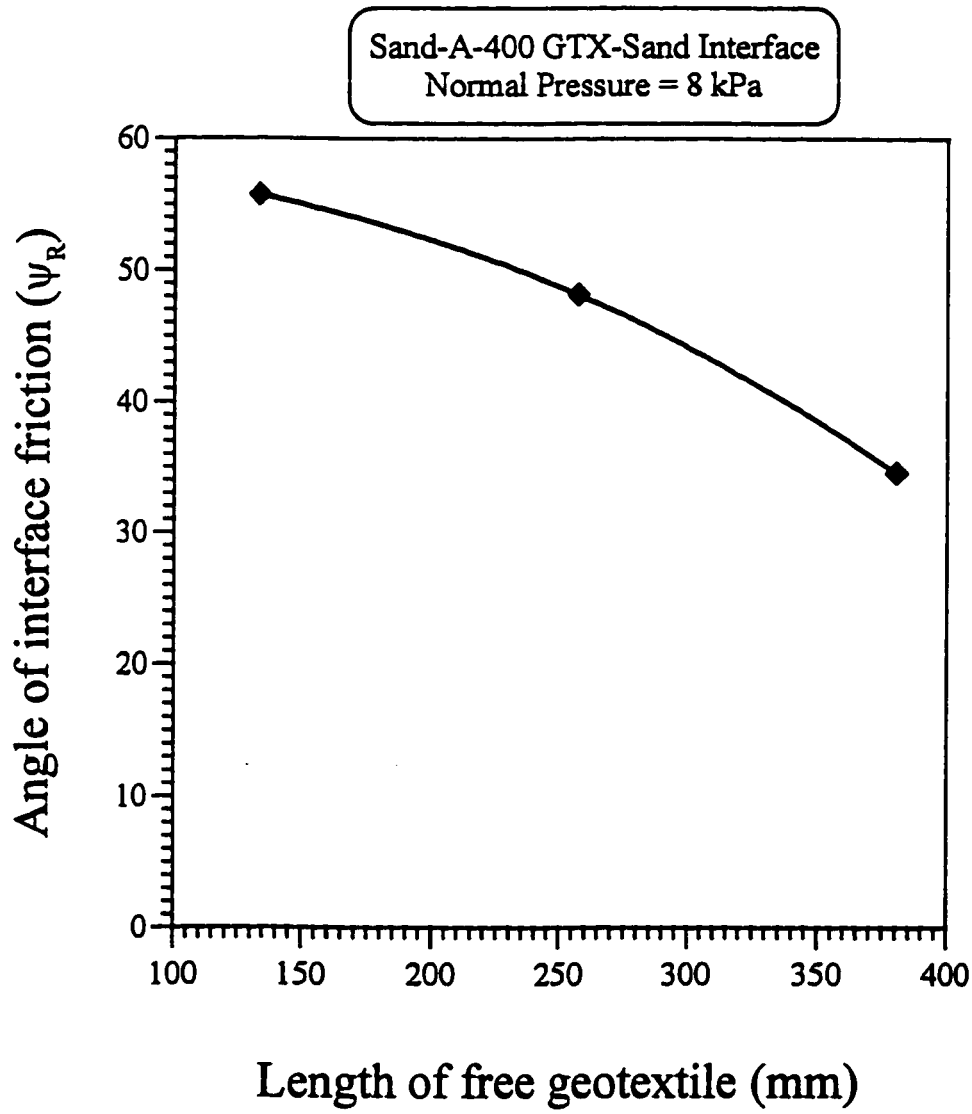

Fig. 4.36: Variation of the angle of interface friction at residual state (ψ_R) with the geotextile length for sand-A-400 GTX-sand interface at a normal pressure of 8 kPa

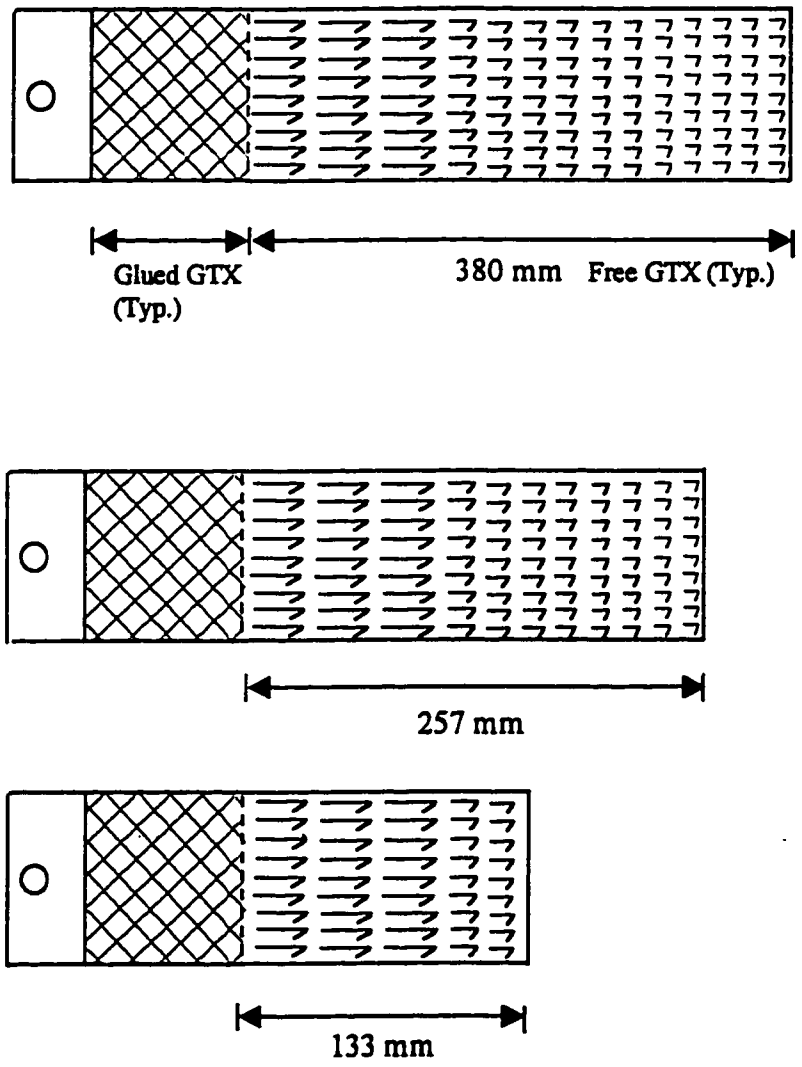

Fig. 4.37: Assumed shear stress distribution along the geotextile during the pull-out test

would include low shear stress values at the rear end. Another reason for high value of angle of interface friction can be attributed to the high vertical pressure built up due to front wall roughness. In the case of short samples, the glued portion of geotextile is 120 mm and when it moves forward, the whole geotextile moves forward and for 133 mm long geotextile sample, the whole geotextile is under high normal pressure due to proximity to the front wall.

It was also observed that there was no necking was observed in the 133 mm long geotextile sample after the pull-out test. However, necking was observed in the front one-third and middle one-third portion of 380 mm long geotextile sample.

Fig. 4.38 presents the variation of strain along the geotextile samples having different lengths. It is shown that the front part of the geotextile is strained to almost the same percentage irrespective of geotextile length. However, for the shortest specimen length (133 mm), the strain is not progressive over the geotextile length and it reduces to very small value within the middle third portion of length. In this case the strain increased towards the end of the geotextile. This test was repeated and similar results were obtained.

4.6.4 Effect of Wetting

The effect of the wetting on sand–GTX–sand interface characteristics was investigated by performing the pull-out test while the bottom sand layer was soaked. The results of the soaked pull-out test are compared with those for the dry pull-out test as shown in Table 4.9. Fig. 4.39 shows the variation of the pull-out force on the geotextile with the front end displacement for both dry and soaked tests. It can be seen that higher values of shear

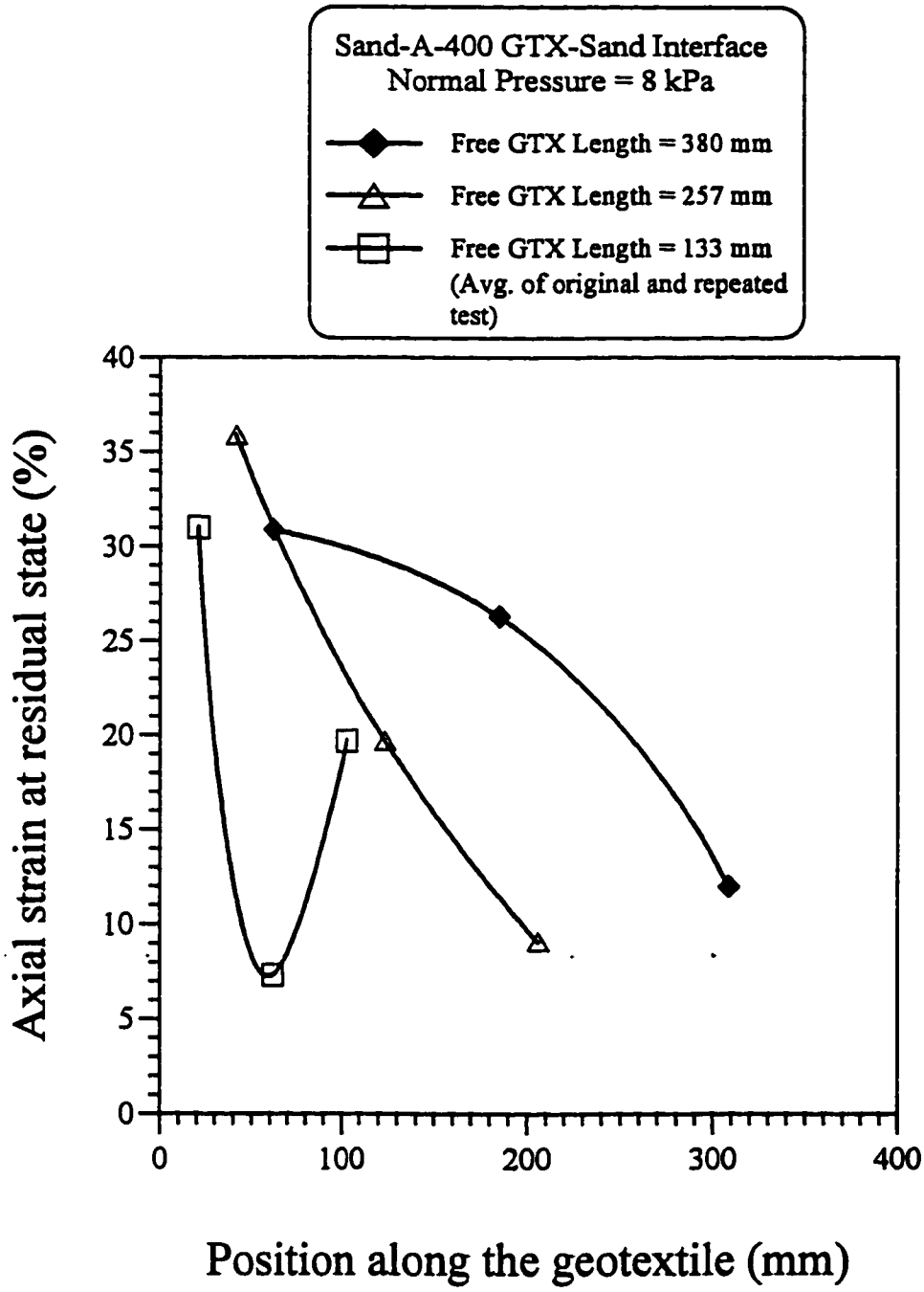

Fig. 4.38: Variation of the average axial strain at the residual state with the postion along the geotextile for sand-A-400 GTX- Sand interface at 8 kPa normal pressure

Table 4.9: Interface charateristics for sand-A-400 GTX-sand interface, 380 mm long free geotextile, and 8 kPa normal pressure with varying moisture content

At peak pull-out state					
Moisture Content	Pull-out force (N)	Shear stress (kPa)	ψ_p	Overall average strain (%)	Front end displacement (mm)
Dry	541.51	5.98	36.80	19.20	73.00
Soaked*	725.00	7.63	43.60	25.00	100.00
At residual pull-out state					
Moisture Content	Pull-out force (N)	Shear stress (kPa)	ψ_R	Overall average strain (%)	Front end displacement (mm)
Dry	514.04	5.52	34.60	22.50	87.10
Soaked*	725.00	7.63	43.60	25.00	100.00
At the end of the test					
Moisture Content	Pull-out force (N)	Shear stress (kPa)	ψ_{End}	Overall average strain (%)	Front end displacement (mm)
Dry	502.27	5.37	33.80	23.20	117.30
Soaked*	725.00	7.54	43.30	26.50	116.00
Axial strain in the geotextile at residual state					
Moisture Content	Average strain in the front one-third (%)	Average strain in the middle one-third (%)		Average strain in the rear one-third (%)	Overall average strain (%)
Dry	30.90	26.30		12.00	22.50
Soaked*	35.00	32.50		9.80	25.00
Axial strain in the geotextile at the end of the test					
Moisture Content	Average strain in the front one-third (%)	Average strain in the middle one-third (%)		Average strain in the rear one-third (%)	Overall average strain (%)
Dry	34.10	25.50		12.50	23.20
Soaked*	35.00	35.00		9.80	26.50

* Only the bottom sand layer was soaked

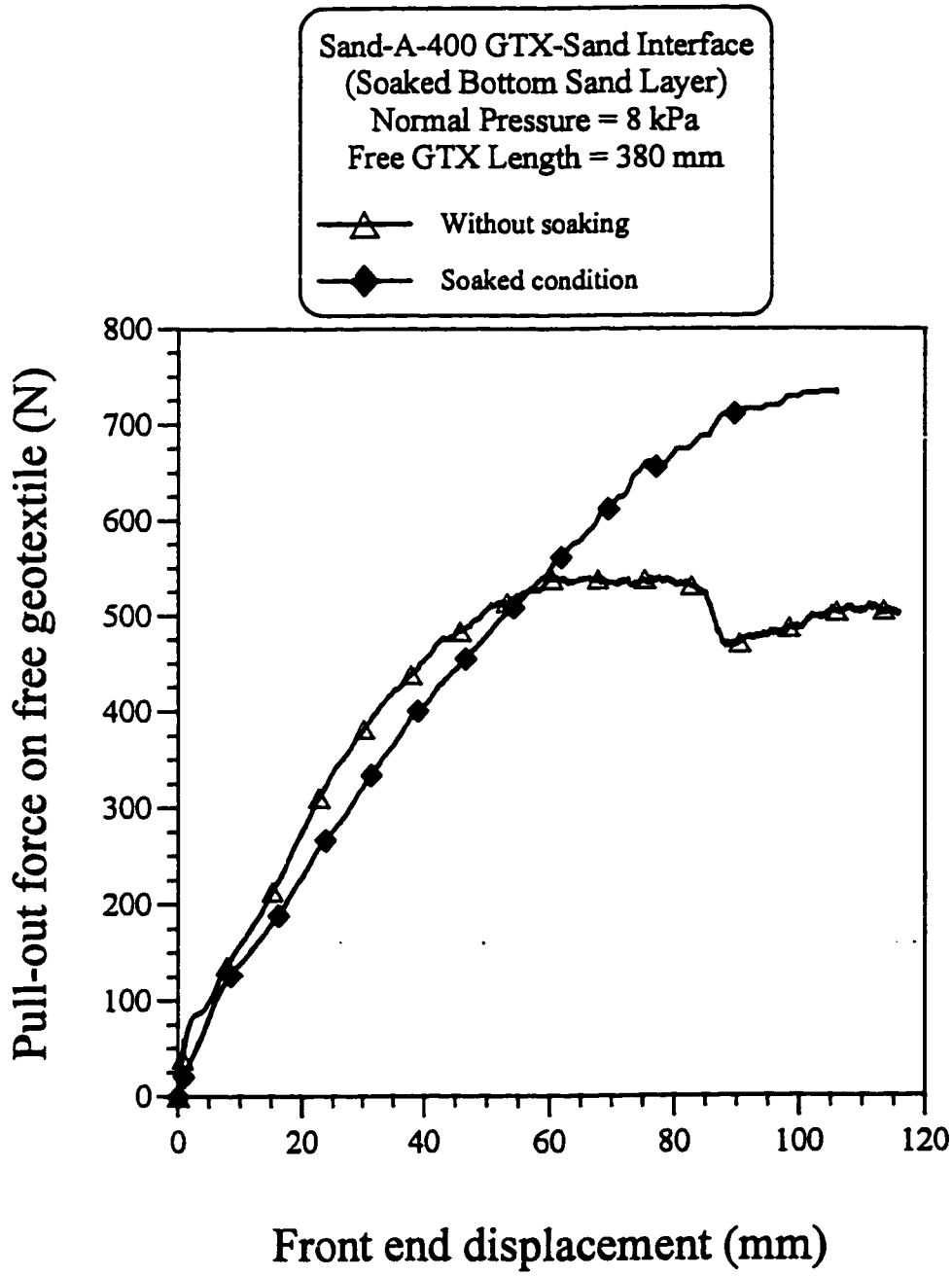

Fig. 4.39: Variation of the pull-out force on A-400 geotextile with the front end displacement for sand-GTX-sand interface, at a normal pressure of 8 kPa, and 380 mm long free geotextile

stress are mobilized on the interface for the soaked condition. It is also observed, during the soaked test, that water rose up in the upper sand layer due to capillary action because the slit in the front wall of the box does not allow the soaking of upper sand layer. This capillary action will increase the shear strength of the sand due to the increase in effective stresses ($\sigma' = \sigma - u$) since u is negative. It can, therefore, be inferred that the increase in shear stresses upon soaking is due to the increase in normal pressure caused by the capillary action (surface tension). Fig. 4.40 presents the variation of the axial strain with the position along geotextile at the residual state, for both dry and soaked tests. It can be observed that the geotextile is strained to a higher value in the case of soaked test as compared to the corresponding values for the dry test. This is expected since the pull-out force is higher for the same geotextile length when tested in soaked condition.

4.7 Results of the Pull–out Tests on Sabkha–GTX–Sand Interface

The second stage of the pull-out testing considers the pull-out tests on sabkha–GTX–sand interface. The data of all tests is presented in Appendix – B in the form of graphs. The frequency of the symbols used in the figures presented in Appendix – B is 90 i.e. each symbol is shown after 90 data points. In this Section, the different test results are presented and discussed to quantify the effect of the various parameters investigated.

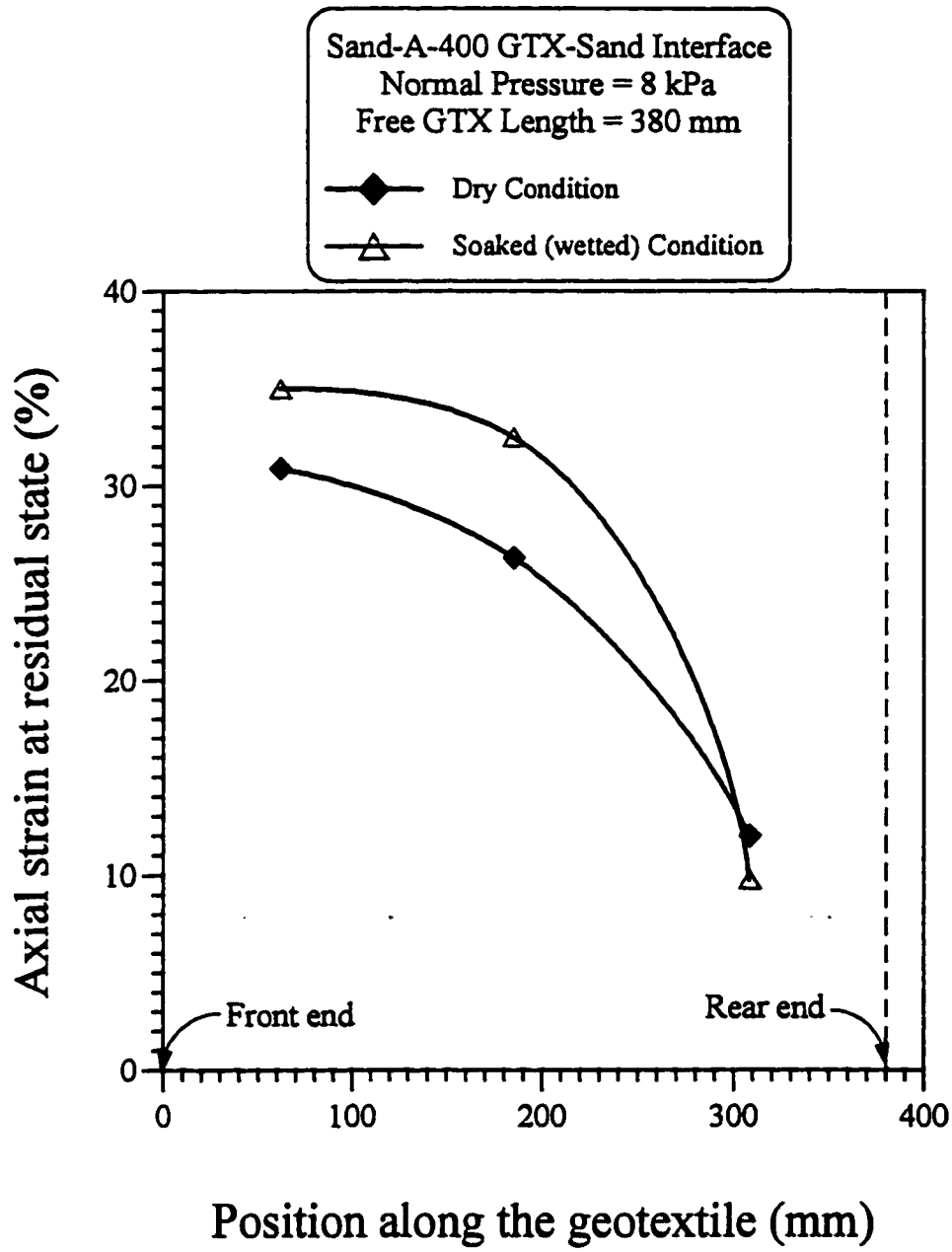

Fig. 4.40: Variation of the average axial strain at the residual state with the postion along geotextile for sand-A-400 GTX-sand interface, for dry and soaked condition

4.7.1 Effect of Normal Pressure

The pull-out tests were performed on sabkha–GTX–sand interface at normal pressure values of 4.5, 8, 16 kPa. The test results are summarized in Tables 4.10, 4.11 and 4.12, for the three geotextiles. The effect of the increase of the normal pressure is shown in Figs. 4.41, 4.42, and 4.43 for A-400, F-140, and A-140 geotextiles, respectively. All figures show that the pull-out resistance increases with the increase in the normal pressure.

Fig. 4.44 summarizes the data presented in Figs. 4.41, 4.42, and 4.43 and shows the variation of the shear stress at residual state with the applied normal pressure for sabkha–GTX–sand interface. It is clearly seen that the A-140 geotextile is the only geotextile conforming to the Mohr's Coulomb law. It can also be seen that the increase in the shear stress with the increase in normal pressure is less for A-140 geotextile, compared to the other two geotextiles. Comparing Fig. 4.19 (sand–GTX–sand interface) with Fig. 4.44 (sabkha–GTX–sand interface), one can find that lower or bottom layer (sabkha soil) in the case of sabkha–GTX–sand interface is not contributing to shear stress mobilized on A-140 geotextile. However, it contributes significantly in mobilizing shear stress when using the F-140 geotextile.

The F-140 geotextile was found to be the strongest in pull-out resistance in the case of sabkha–GTX–sand interface, despite the fact that the tensile strength of the A-400 geotextile is 2.9 times that of the F-140 geotextile. Such findings are not consistent with those of sand–GTX–sand interface. In the sand–GTX–sand interface the geotextile with higher tensile strength gave higher pull-out resistance compared to the one with lower tensile strength. This clearly shows the effect of elongation and surface texture on the pull-

Table 4.10: Interface characteristics for sabkha- A-400 GTX-sand interface, 380 mm long free geotextile and 14% moisture content of sabkha with different normal pressures

At peak pull-out state				
Normal pressure (kPa)	Pull-out force (N)	Shear stress (kPa)	Overall average strain (%)	Front end displacement (mm)
4.50	309.02	3.41	19.20	74.40
8.00	418.89	4.73	16.50	65.00
16.00	521.89	5.46	25.80	101.20
At residual pull-out state				
Normal pressure (kPa)	Pull-out force (N)	Shear stress (kPa)	Overall average strain (%)	Front end displacement (mm)
4.50	217.78	2.41	18.90	89.10
8.00	383.57	4.33	16.50	76.00
16.00	461.07	4.80	26.30	110.00
At the end of the test				
Normal pressure (kPa)	Pull-out force (N)	Shear stress (kPa)	Overall average strain (%)	Front end displacement (mm)
4.50	206.99	2.28	19.20	116.84
8.00	334.62	3.78	16.50	104.00
16.00	461.07	4.80	26.30	110.00
Axial strain in the geotextile at the residual state				
Normal pressure (kPa)	Average strain in the front one-third (%)	Average strain in the middle one-third (%)	Average strain in the rear one-third (%)	Overall average strain (%)
4.50	29.40	21.50	8.77	19.20
8.00	20.27	21.70	8.72	16.50
16.00	39.40	28.80	12.60	26.30
Axial strain in the geotextile at the end of the test				
Normal pressure (kPa)	Average strain in the front one-third (%)	Average strain in the middle one-third (%)	Average strain in the rear one-third (%)	Overall average strain (%)
4.50	29.40	21.50	8.77	19.20
8.00	18.85	21.70	9.73	16.57
16.00	39.40	28.80	12.60	26.30

Table 4.11: Interface characteristics for sabkha-F-140 GTX-sand interface, 380 mm long free geotextile and 14% moisture content of sabkha with different normal pressure

At peak pull-out state				
Normal pressure (kPa)	Pull-out force (N)	Shear stress (kPa)	Overall average strain (%)	Front end displacement (mm)
4.50	412.31	4.71	15.30	58.00
8.00	574.87	6.84	10.53	40.00
16.00	699.94	7.80	18.10	68.80
At residual state				
Normal pressure (kPa)	Pull-out force (N)	Shear stress (kPa)	Overall average strain (%)	Front end displacement (mm)
4.50	220.73	2.35	23.50	97.50
8.00	462.44	4.67	30.30	112.98
16.00	641.67	6.42	31.60	120.00
At end of the the test				
Normal pressure (kPa)	Pull-out force (N)	Shear stress (kPa)	Overall average strain (%)	Front end displacement (mm)
4.50	188.35	2.00	23.50	110.00
8.00	462.44	4.67	30.30	112.98
16.00	641.67	6.42	31.60	120.00
Axial strain in the geotextile at the residual state				
Normal pressure (kPa)	Average strain in the front one-third (%)	Average strain in the middle one-third (%)	Average strain in the rear one-third (%)	Overall average strain (%)
4.50	29.80	28.40	13.30	23.50
8.00	42.50	36.70	15.45	30.30
16.00	49.80	40.55	6.56	31.60
Axial strain in the geotextile at the end of the test				
Normal pressure (kPa)	Average strain in the front one-third (%)	Average strain in the middle one-third (%)	Average strain in the rear one-third (%)	Overall average strain (%)
4.50	29.80	28.40	13.30	23.50
8.00	42.50	36.70	15.45	30.30
16.00	49.80	40.55	6.56	31.60

Table 4.12: Interface characteristics for sabkha-A-140 GTX-sand interface, 380 mm long free geotextile and 14% moisture content of sabkha with different normal pressure

At peak pull-out state				
Normal pressure (kPa)	Pull-out force (N)	Shear stress (kPa)	Overall average strain (%)	Front end displacement (mm)
4.50	150.49	1.76	12.78	49.82
8.00	152.06	1.76	13.80	52.50
16.00	221.12	2.37	22.67	86.13
At residual pull-out state				
Normal pressure (kPa)	Pull-out force (N)	Shear stress (kPa)	Overall average strain (%)	Front end displacement (mm)
4.50	126.35	1.28	30.45	115.71
8.00	148.13	1.49	31.11	118.24
16.00	188.74	1.89	31.11	118.24
At the end of the test				
Normal pressure (kPa)	Pull-out force (N)	Shear stress (kPa)	Overall average strain (%)	Front end displacement (mm)
4.50	126.35	1.28	30.45	115.71
8.00	148.13	1.49	31.11	118.24
16.00	188.74	1.89	31.11	118.24
Axial strain in the geotextile at the residual state				
Normal pressure (kPa)	Average strain in the front one-third (%)	Average strain in the middle one-third (%)	Average strain in the rear one-third (%)	Overall average strain (%)
4.50	43.20	39.00	11.60	30.45
8.00	37.50	39.40	18.50	31.11
16.00	42.10	43.25	10.81	31.11
Axial strain in the geotextile at the end of the test				
Normal pressure (kPa)	Average strain in the front one-third (%)	Average strain in the middle one-third (%)	Average strain in the rear one-third (%)	Overall average strain (%)
4.50	43.20	39.00	11.60	30.45
8.00	37.50	39.40	18.50	31.11
16.00	42.10	43.25	10.81	31.11

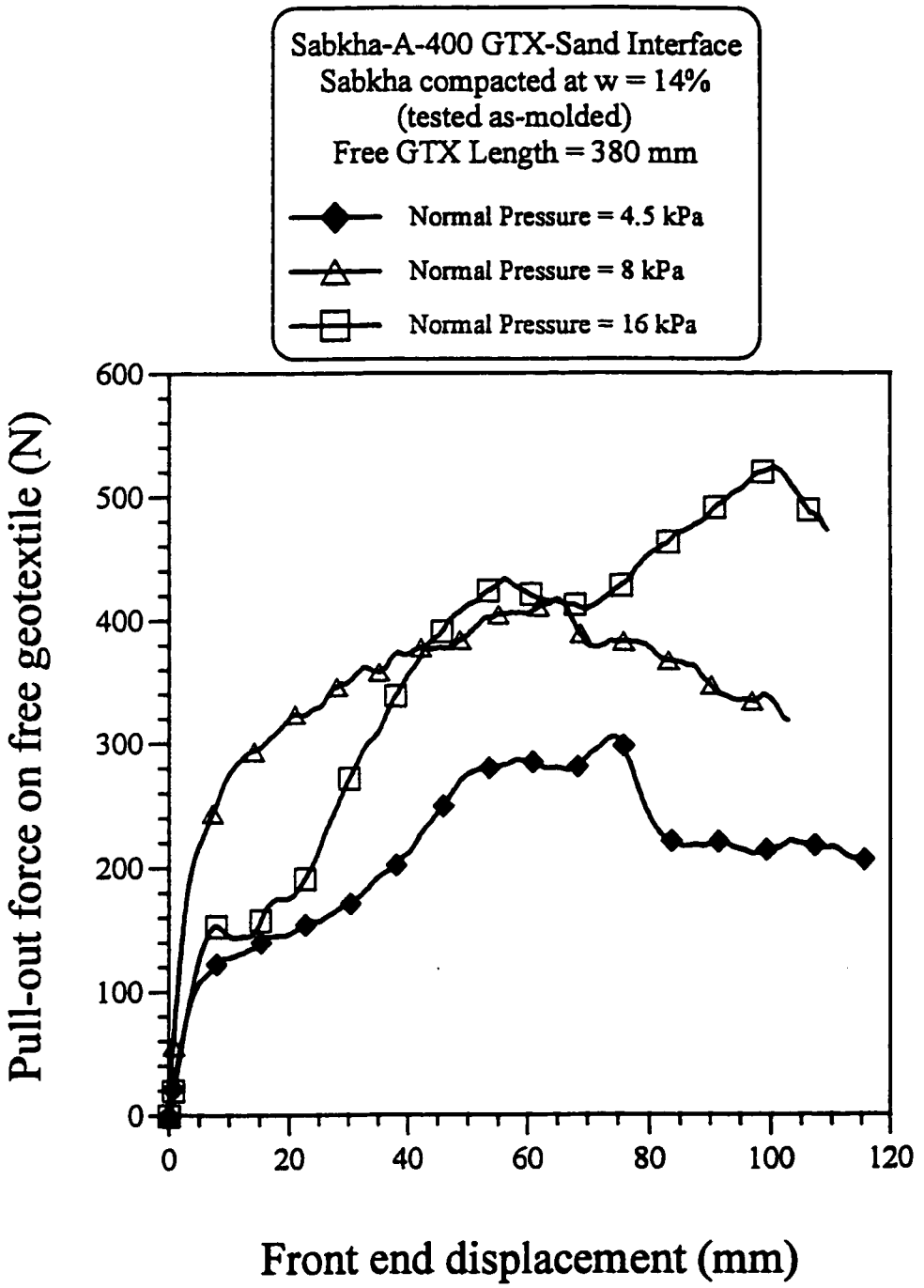

Fig. 4.41: Variation of the pull-out force on A-400 geotextile with the front end displacement for sabkha-GTX-sand interface, 380 mm long free geotextile and 14% moisture content of sabkha (as-molded)

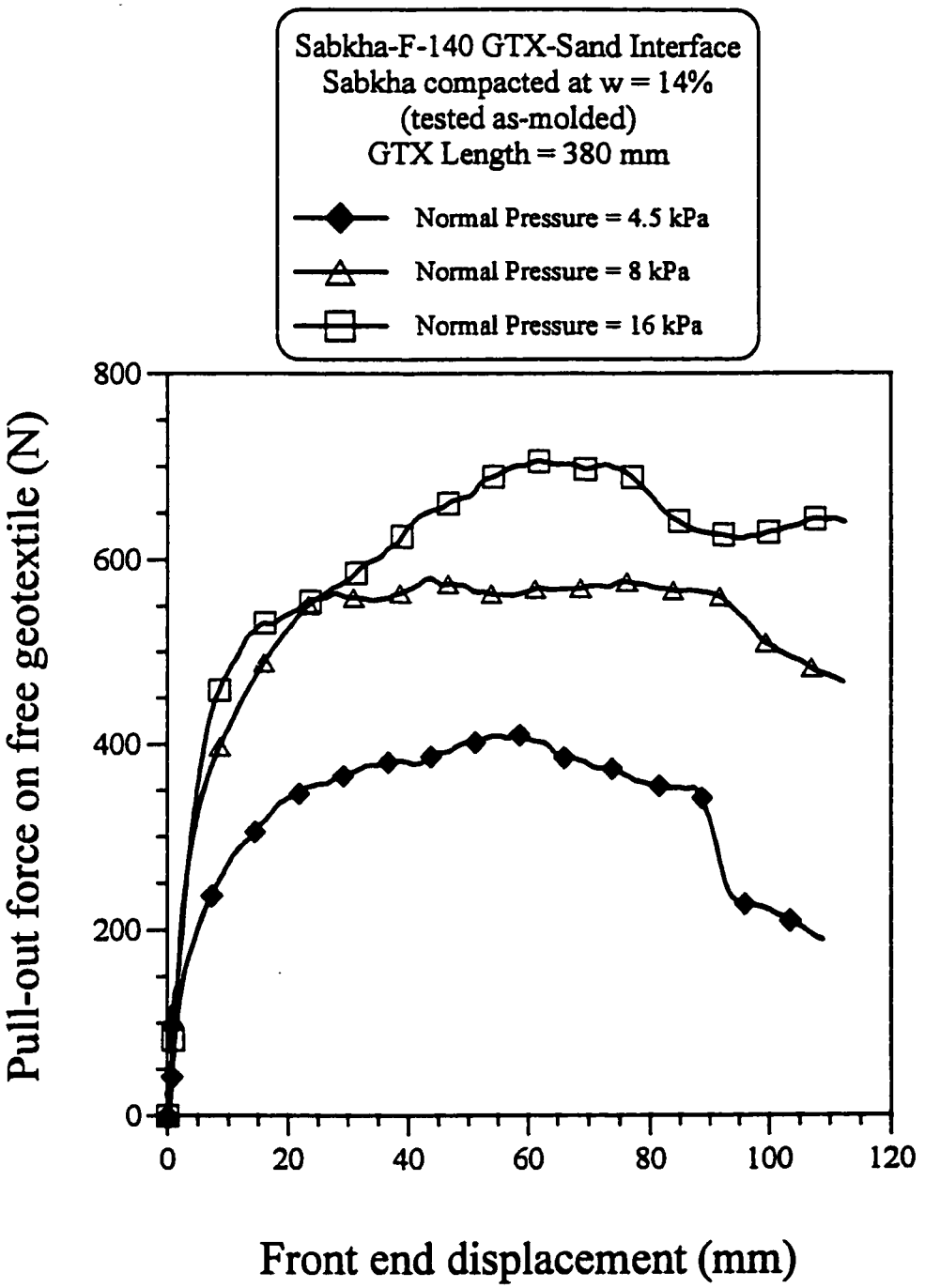

Fig. 4.42: Variation of the pull-out force on F-140 geotextile with the front end displacement for sabkha-GTX-sand interface, 380 mm long free geotextile and 14% moisture content of sabkha (as-molded)

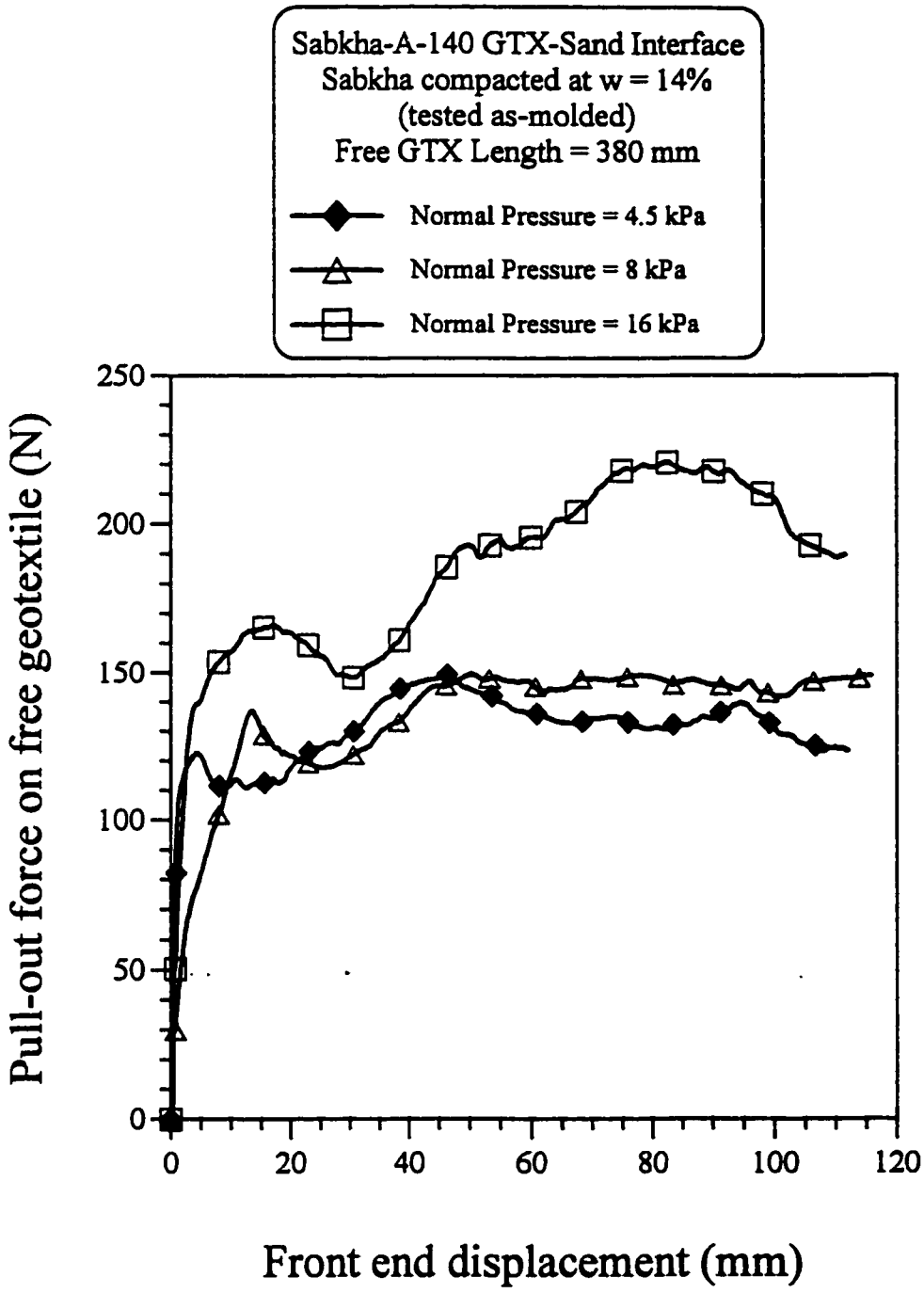

Fig. 4.43: Variation of the pull-out force on A-140 geotextile with the front end displacement for sabkha-GTX-sand interface, 380 mm long free geotextile and 14% moisture content of sabkha (as-molded)

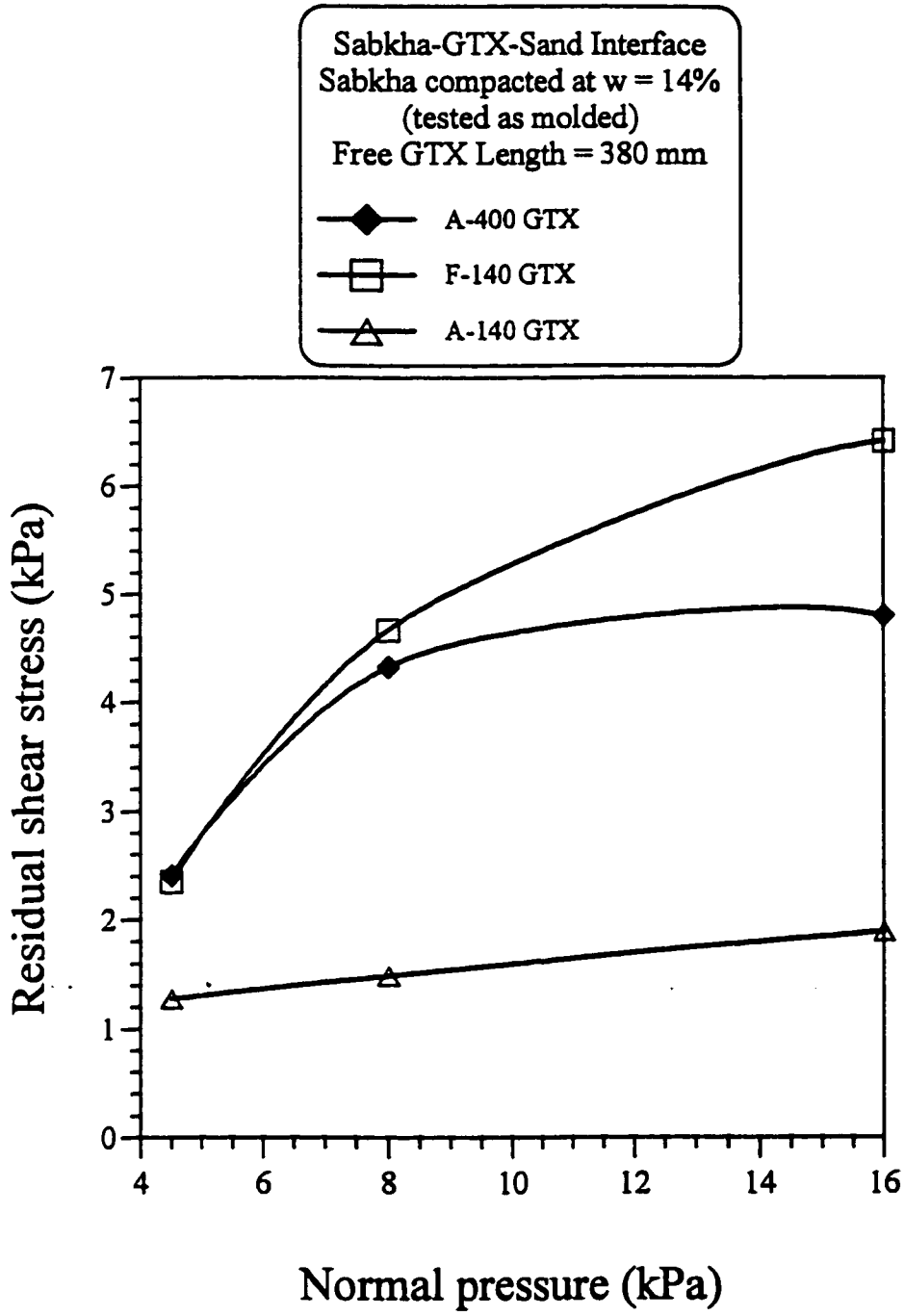

Fig. 4.44: Variation of the shear stress at residual state with the applied normal pressure for sabkha-GTX-sand interface, 380 mm long free geotextile, and 14% moisture content of sabkha (as-molded)

out resistance. The pull-out tests performed on the plate alone (with 120 mm geotextile glued to it) show that as the normal pressure increases the difference between the pull-out resistance of the plates glued with F-140 and A-400 geotextiles increases. This shows the importance of geotextile texture, because the effect of geotextile extensibility has been eliminated when performing the pull-out tests on the plate alone. This effect is also observed in Fig. 4.44. This means that the effect of the texture of the F-140 geotextile becomes more pronounced at higher normal pressure values. Therefore, the geotextile texture plays an important role in increasing the shear stresses mobilized on the F-140 geotextile in the case of sabkha–GTX–sand interface as compared with the A-400 geotextile.

Fig. 4.45 shows the variation of the overall average strain with the normal pressure. It is clearly seen, in the figure, that at the peak stress level, the overall strain increases with the increase in normal pressure except for A-140 and A-400 geotextile under low pressures. The results in the figure indicate also that the peak and residual states are very close for the A-400 geotextile. This figure also indicates that for A-140 geotextile, the geotextile continues to strain upto the 120 mm capacity of the system without reaching the residual condition. For such tests, the end of the test results are labeled as the residual condition.

Fig. 4.46, 4.47 and 4.48 presents the average axial strain variation along the geotextile for different normal pressures. The general trend is that the strain increases with the increase in the normal pressure and the strain decreases along the geotextile showing the progressive development of shear stresses. It seems that the strains shown in Fig. 4.48

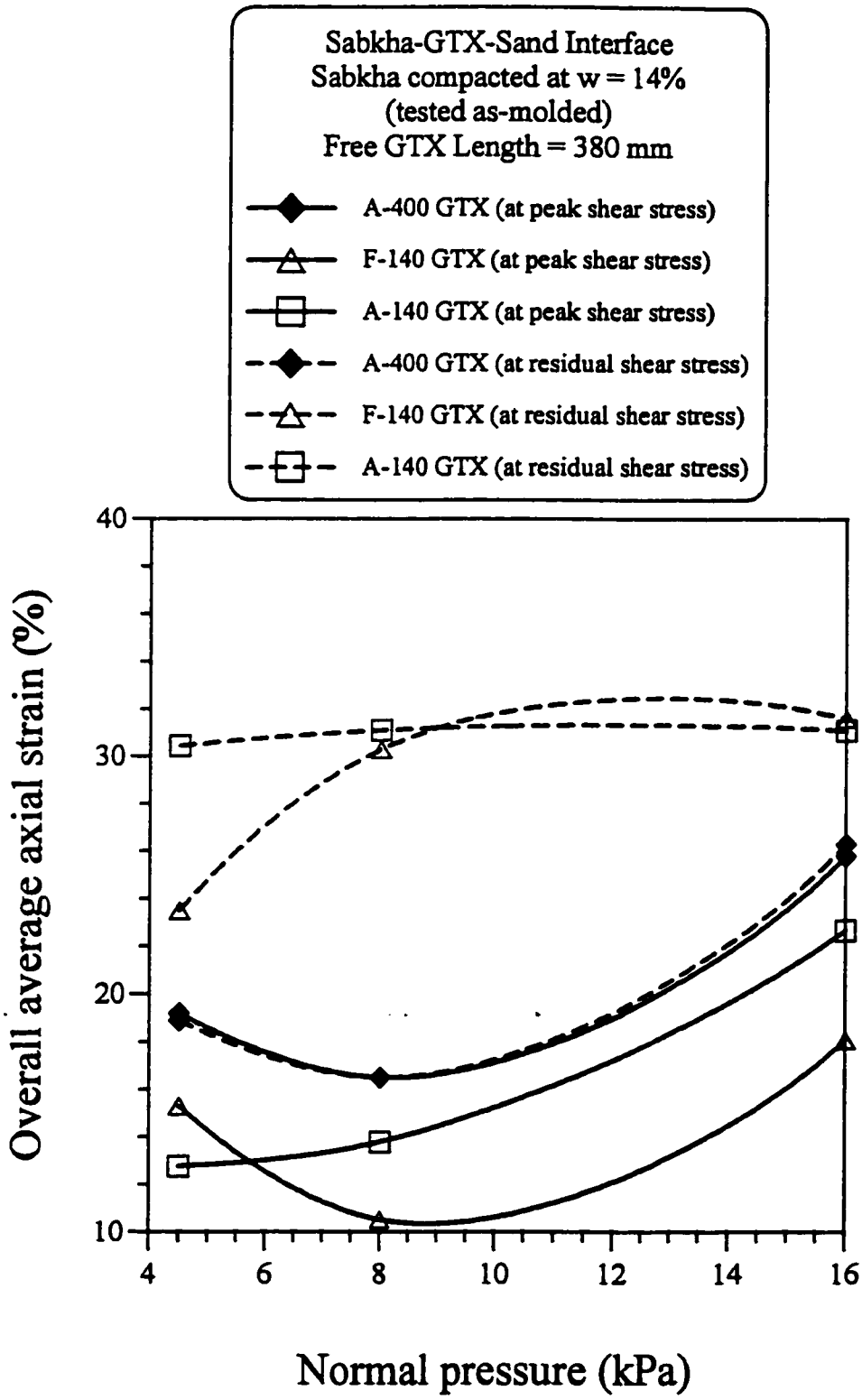

Fig. 4.45: Variation of the overall average axial strain with the applied normal pressure for sabkha-GTX-sand interface, 380 mm long free geotextile, and 14% moisture content of sabkha (as-molded)

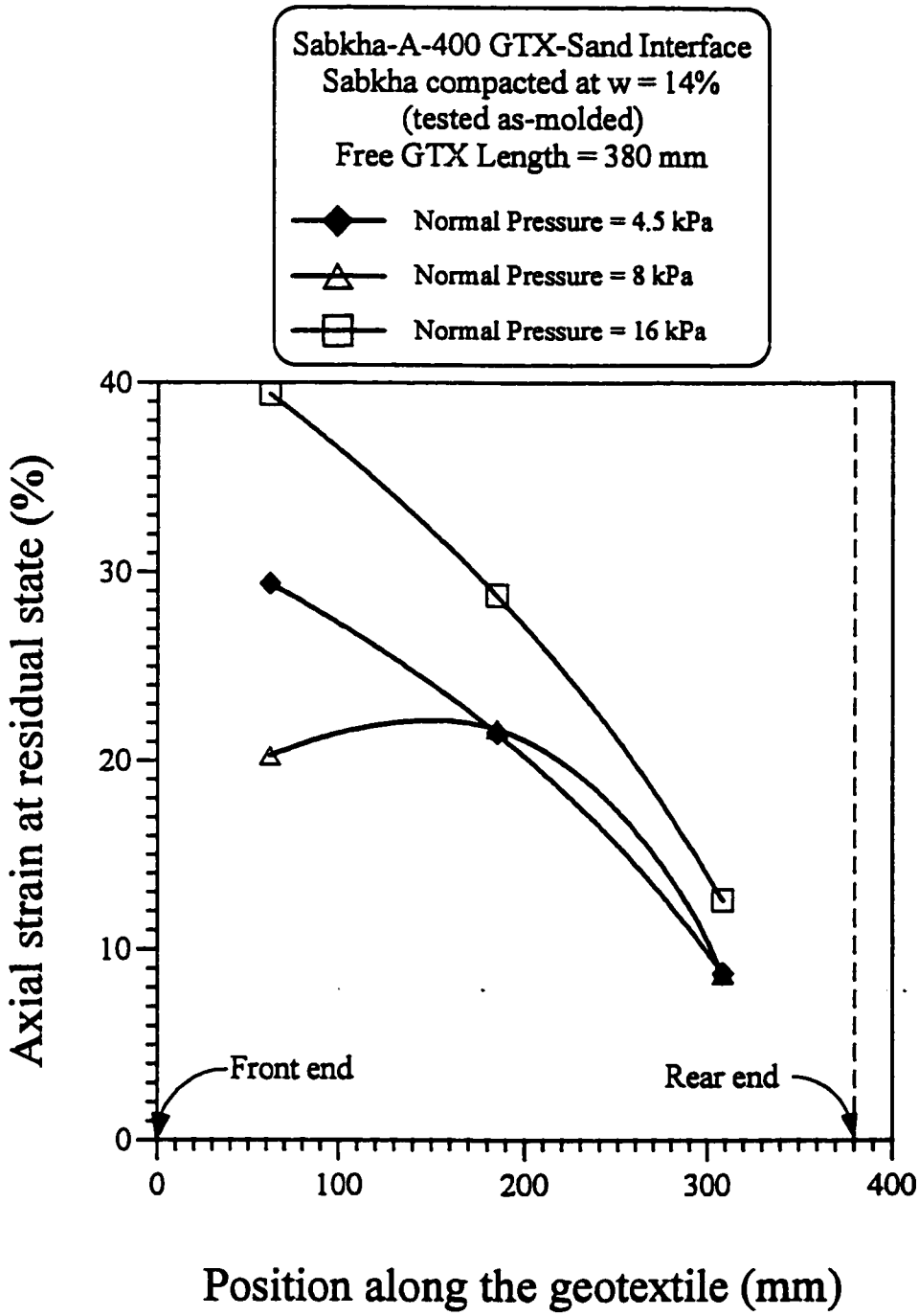

Fig. 4.46: Variation of the average axial strain at the residual state with the postion along geotextile for sabkha-A-400 GTX-sand interface, 380 mm long free geotextile, and 14% moisture content of sabkha (as-molded)

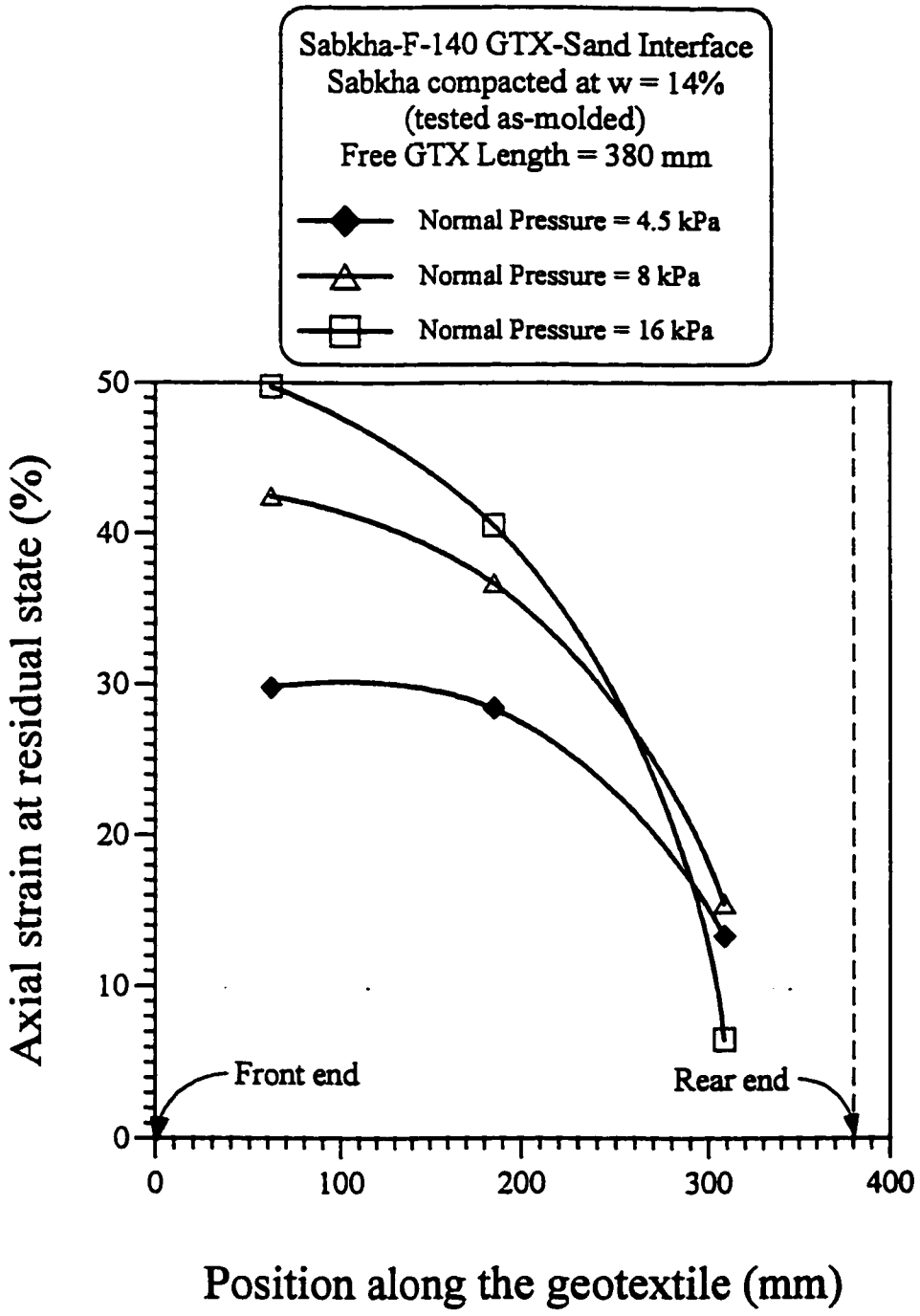

Fig. 4.47: Variation of the average axial strain at the residual state with the postion along geotextile for sabkha-F-140 GTX-sand interface, 380 mm long free geotextile, and 14% moisture content of sabkha (as-molded)

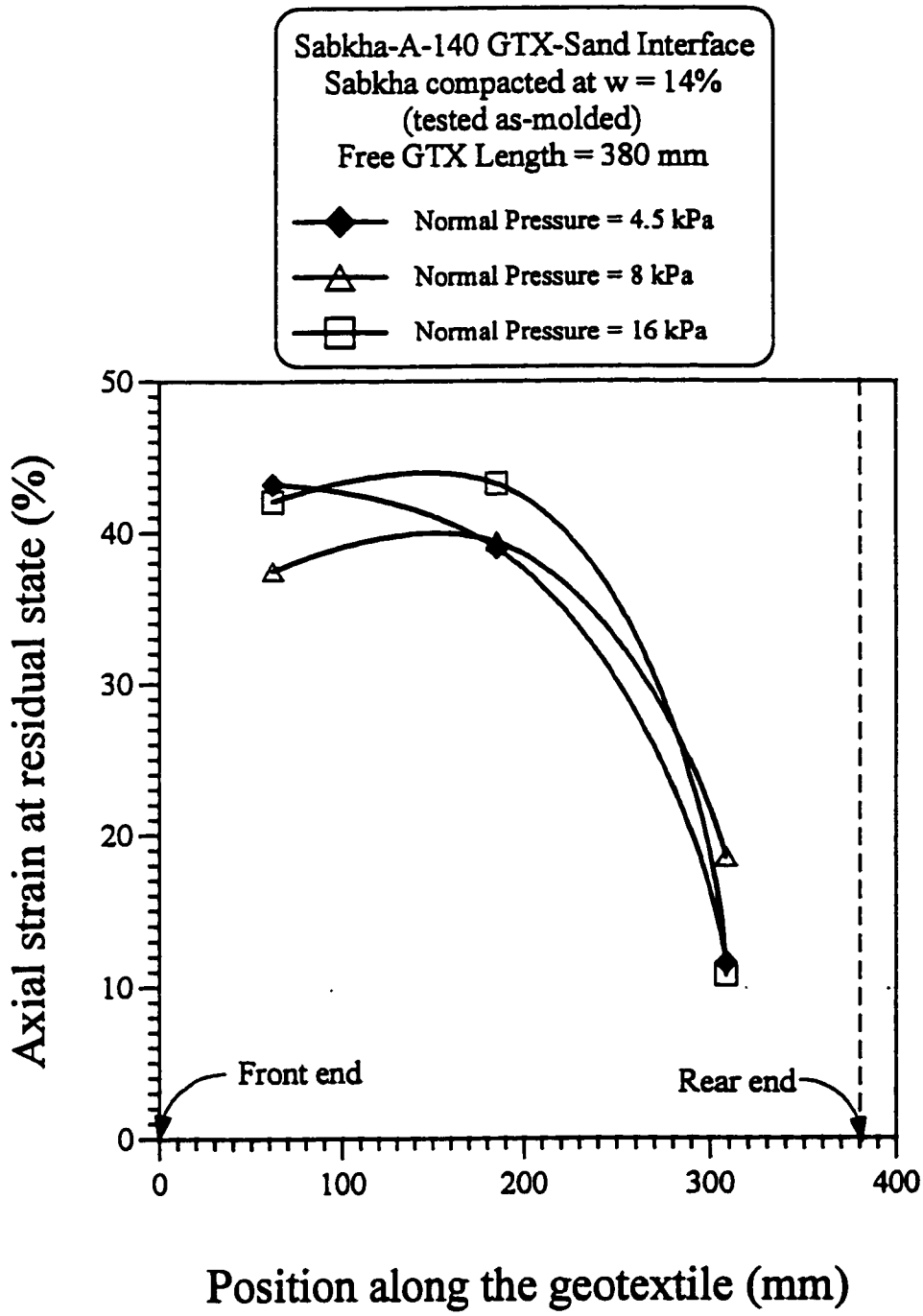

Fig. 4.48: Variation of the average axial strain at the residual state with the postion along geotextile for sabkha-A-140 GTX-sand interface, 380 mm long free geotextile, and 14% moisture content of sabkha (as-molded)

(A-140 geotextile) are concentrated in the front one-third and it has reached a uniform value in that portion; it decreases thereafter, for the remaining parts of the geotextile due to the high extensibility and low tensile strength of the A-140 geotextile.

4.7.2 Effect of Geotextile Type

The results of the pull-out tests for sabkha–GTX–sand interface using different geotextiles are summarized in Tables 4.13 and 4.14. These results are presented in Figs. 4.49, 4.50, 4.51 and 4.52. It is seen that for all values of normal pressure, the F-140 geotextile produced higher pull-out resistance, compared to A-400 and A-140 geotextiles. This is mainly, because the F-140 geotextile has lower extensibility compared to the other two geotextiles and the sabkha soil is highly compressible. Therefore, the reinforcement effect of the F-140 geotextile becomes pronounced. These figures also show that A-400 gives higher pull-out force compared to the A-140 geotextile irrespective of the moisture content of the sabkha layer.

Fig. 4.53 shows the shear stress developed in the geotextile during the pull-out test. It is clear that higher shear stresses were developed in the F-140 geotextile, compared to both A-400 and A-140 geotextiles, especially for normal pressure other than 4.5 kPa. It is also observed, from this figure, that as the normal pressure increases, the effect of geotextile extensibility and surface texture becomes more pronounced. For a normal pressure of 16 kPa the difference between shear stress mobilized for both F-140 and A-400 geotextile is higher as compared to that at 8 kPa normal pressure. Fig. 4.54 presents the overall average strain for the three geotextiles. It clearly shows that the A-140

Table 4.13: Interface characteristics for sabkha-GTX-sand interface, 8 kPa normal pressure, 380 mm long free geotextile and 14% moisture content of sabkha with different geotextiles

At peak pull-out state				
Type of geotextile	Pull-out force (N)	Shear stress (kPa)	Overall average strain (%)	Front end displacement (mm)
A-400	418.89	4.73	16.50	65.00
F-140	574.87	6.84	10.53	40.00
A-140	152.06	1.76	13.80	52.50
At residual pull-out state				
Type of geotextile	Pull-out force (N)	Shear stress (kPa)	Overall average strain (%)	Front end displacement (mm)
A-400	383.57	4.33	16.50	76.00
F-140	462.44	4.67	30.30	112.98
A-140	148.13	1.49	31.11	118.24
At the end of the test				
Type of geotextile	Pull-out force (N)	Shear stress (kPa)	Overall average strain (%)	Front end displacement (mm)
A-400	334.62	3.78	16.50	104.00
F-140	462.44	4.67	30.30	112.98
A-140	148.13	1.49	31.11	118.24
Axial strain in the geotextile at the residual state				
Type of geotextile	Average strain in the front one third (%)	Average strain in the middle one-third (%)	Average strain in the rear one-third (%)	Overall average strain (%)
A-400	20.27	21.70	8.72	16.50
F-140	42.50	36.70	15.45	30.30
A-140	37.50	39.40	18.50	31.11
Axial strain in the geotextile at the end of the test				
Type of geotextile	Average strain in the front one third (%)	Average strain in the middle one-third (%)	Average strain in the rear one-third (%)	Overall average strain (%)
A-400	18.85	21.70	9.73	16.57
F-140	42.50	36.70	15.45	30.30
A-140	37.50	39.40	18.50	31.11

Table 4.14: Interface characteristics for sabkha-GTX-sand interface, 8 kPa normal pressure, 380 mm long free geotextile and 10% moisture content of sabkha with different geotextiles

At peak pull-out state				
Type of geotextile	Pull-out force (N)	Shear stress (kPa)	Overall average strain (%)	Front end displacement (mm)
A-400	506.49	5.80	14.95	56.80
A-140	239.36	2.64	19.11	72.63
At residual pull-out state				
Type of geotextile	Pull-out force (N)	Shear stress (kPa)	Overall average strain (%)	Front end displacement (mm)
A-400	382.59	4.26	18.13	78.60
A-140	192.67	1.94	31.02	117.89
At the end of the test				
Type of geotextile	Pull-out force (N)	Shear stress (kPa)	Overall average strain (%)	Front end displacement (mm)
A-400	400.25	4.44	18.56	114.00
A-140	192.67	1.94	31.02	117.89
Axial strain in the geotextile at the residual state				
Type of geotextile	Average strain in the front one-third (%)	Average strain in the middle one-third (%)	Average strain in the rear one-third (%)	Overall average strain (%)
A-400	26.10	20.82	9.42	18.13
A-140	38.20	36.80	20.10	31.02
Axial strain in the geotextile at the end of the test				
Type of geotextile	Average strain in the front one-third (%)	Average strain in the middle one-third (%)	Average strain in the rear one-third (%)	Overall average strain (%)
A-400	26.10	20.82	9.42	18.56
A-140	38.20	36.80	20.10	31.02

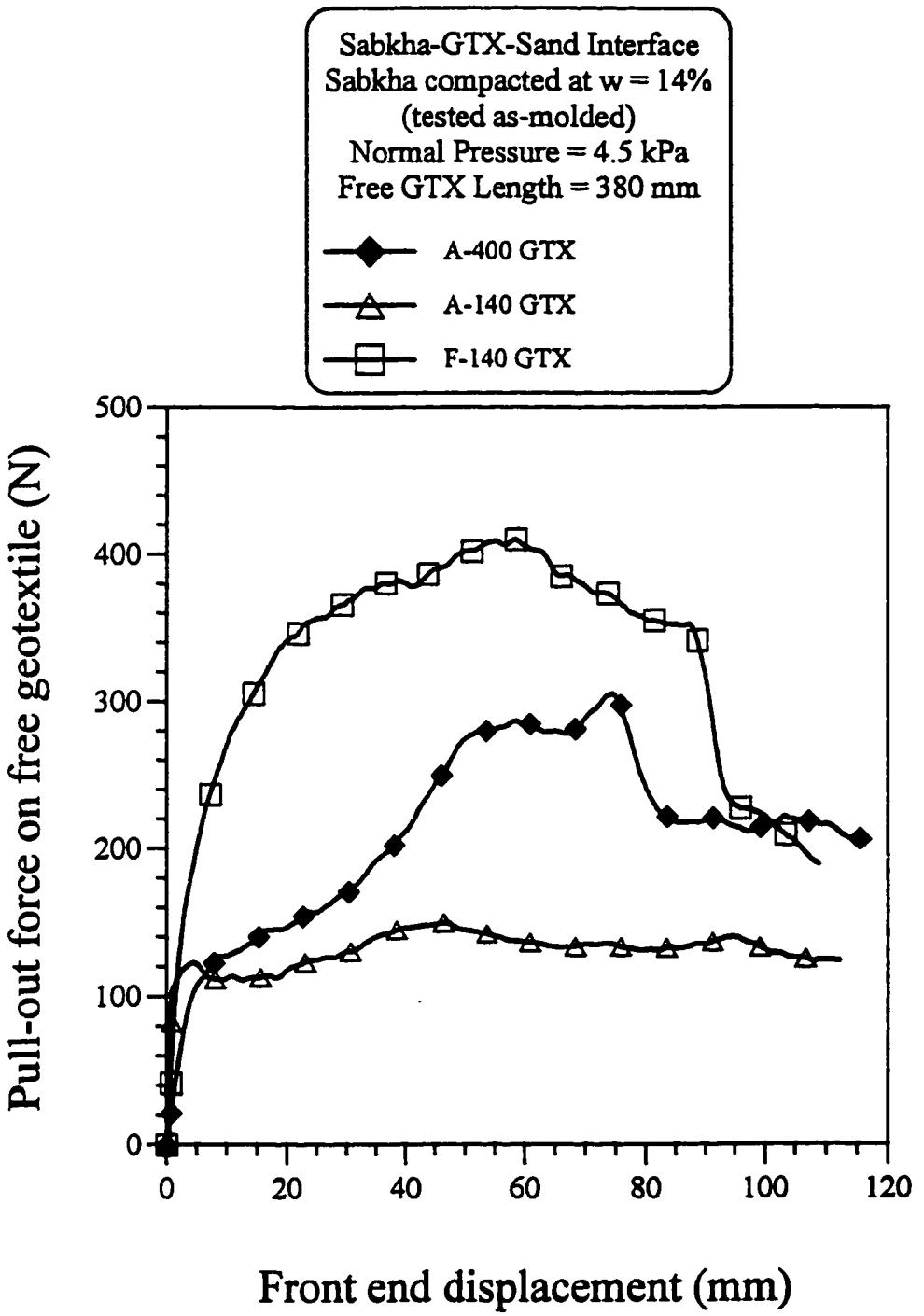

Fig. 4.49: Variation of the pull-out force on geotextile with the front end displacement for sabkha-GTX-sand interface at 4.5 kPa normal pressure, 380 mm long free geotextile and 14% moisture content of sabkha (as-molded)

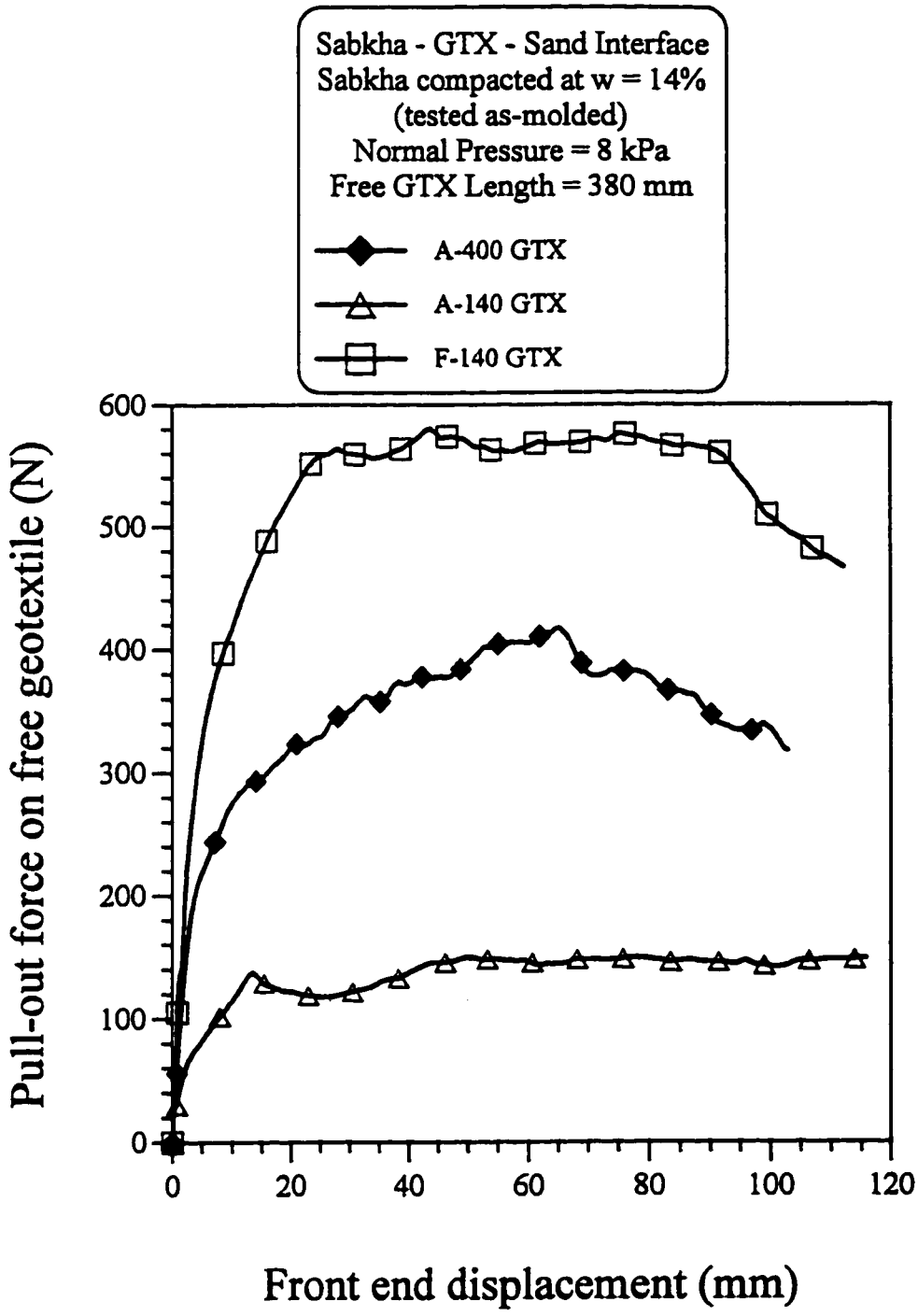

Fig. 4.50: Variation of the pull-out force on geotextile with the front end displacement for sabkha-GTX-sand interface at 8 kPa normal pressure, 380 mm long free geotextile and 14% moisture content of sabkha (as-molded)

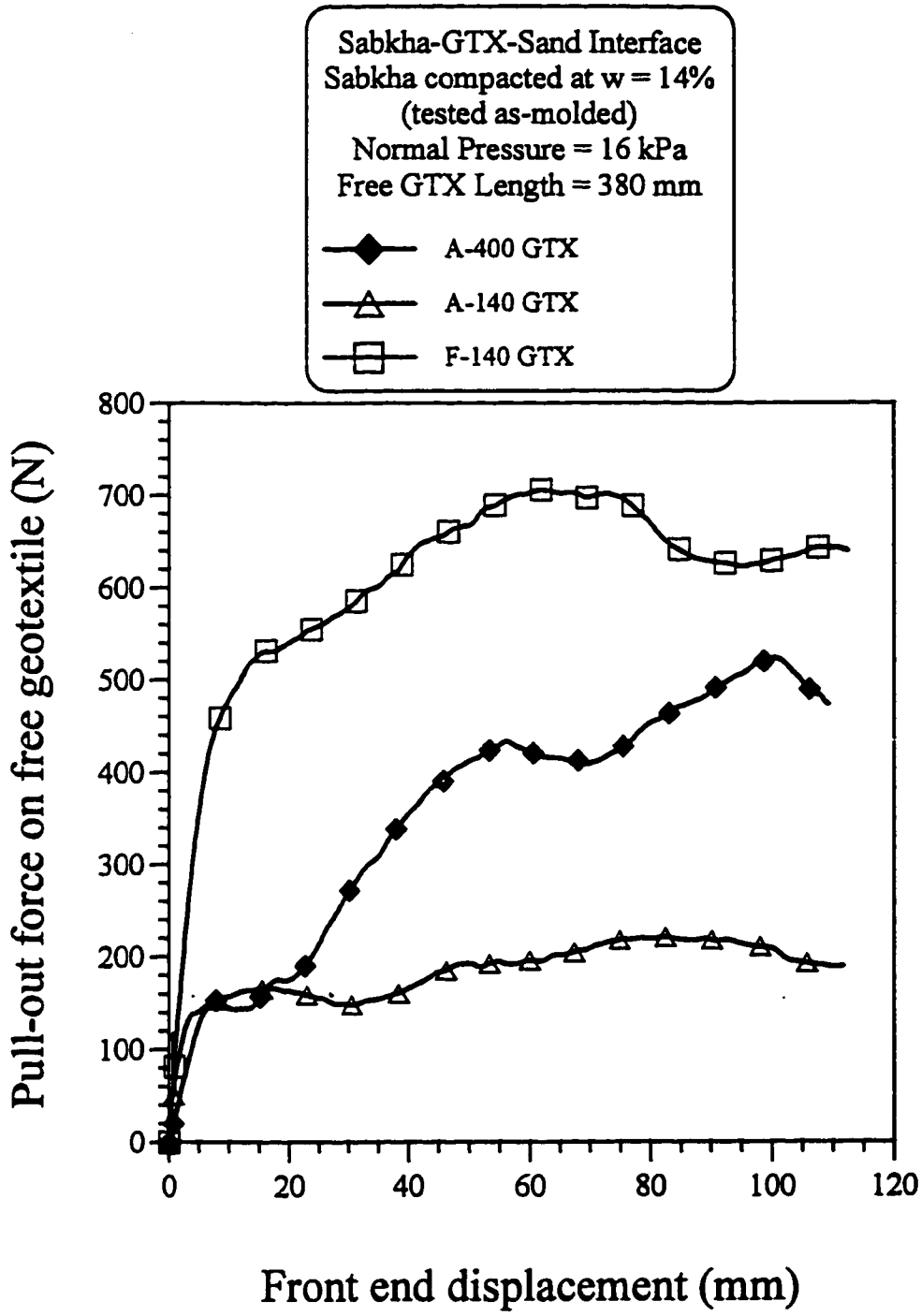

Fig. 4.51: Variation of the Pull-out force on geotextile with the front end displacement for sabkha-GTX-sand interface at 16 kPa normal pressure, 380 mm long free geotextile and 14% moisture content of sabkha (as-molded)

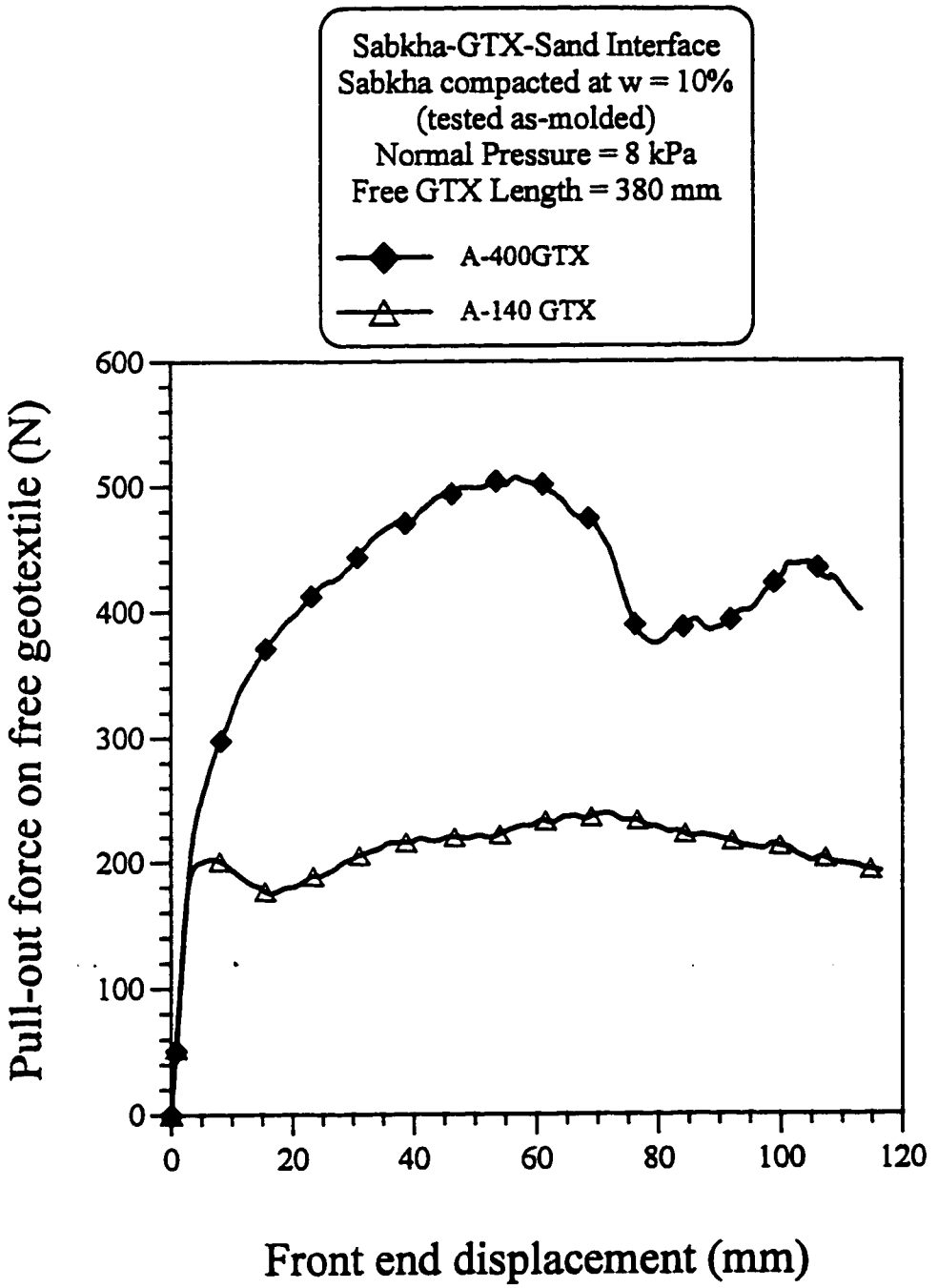

Fig. 4.52: Variation of the pull-out force on the geotextile with the front end displacement for sabkha-GTX-sand interface at 8 kPa normal pressure, 380 mm long free geotextile and 10% moisture content of sabkha (as-molded)

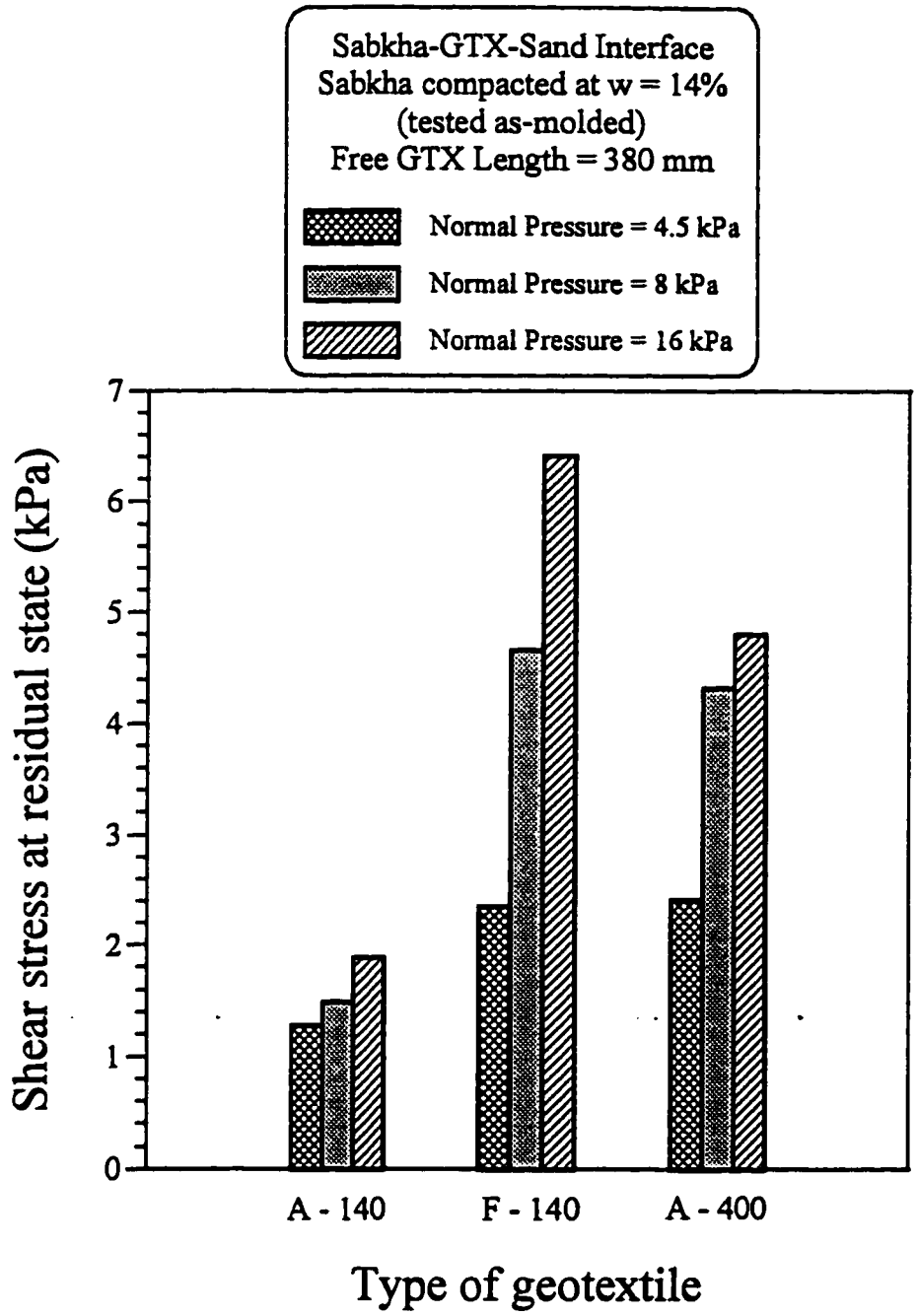

Fig. 4.53: Variation of the shear stress at the residual state with geotextile type for sabkha-GTX-sand interface, 380 mm long free geotextile, and 14% moisture content of sabkha (as-molded)

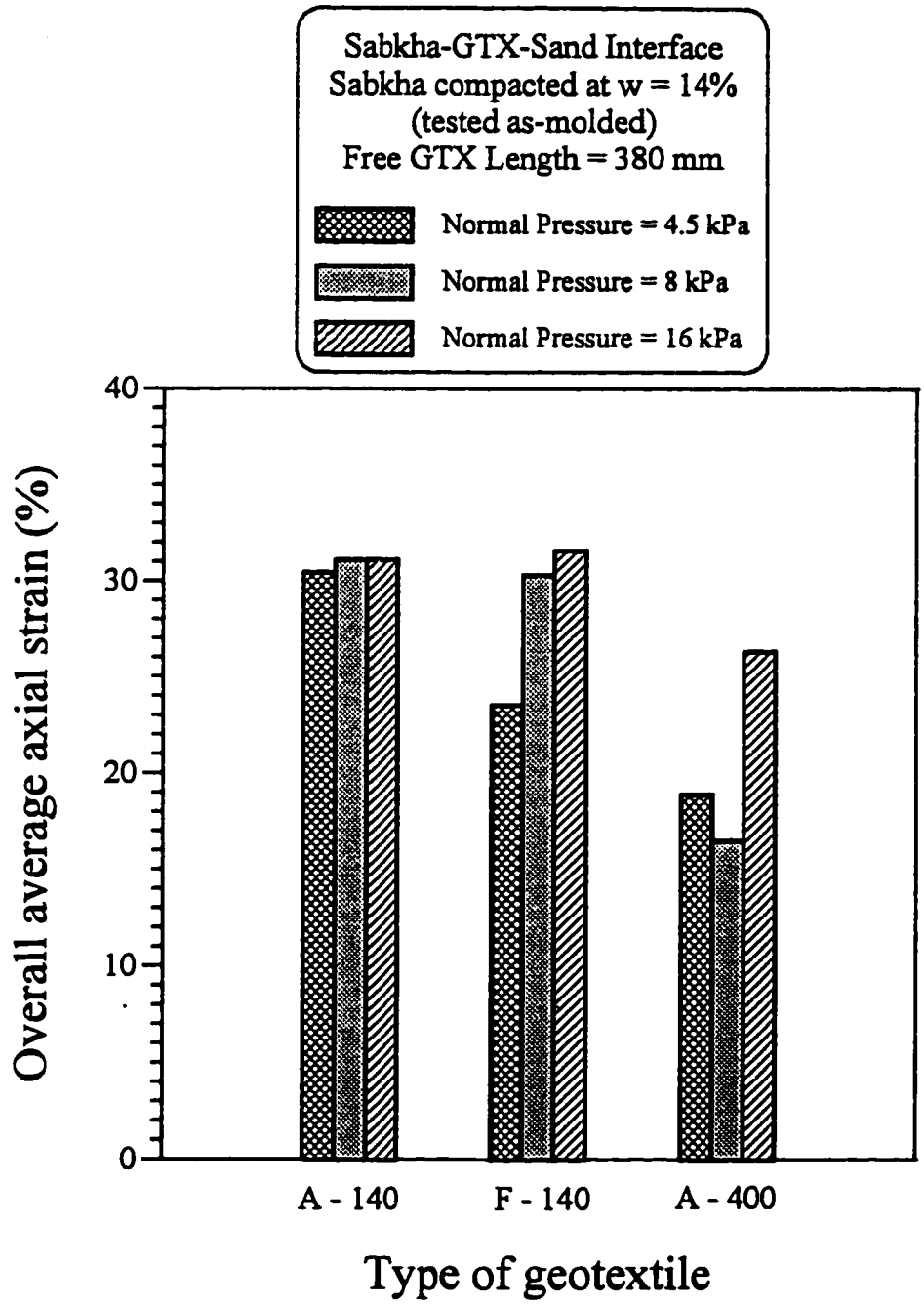

Fig. 4.54: Variation of the overall average axial strain at the residual state with geotextile type for sabkha-GTX-sand interface, 380 mm long free geotextile, and 14% moisture content of sabkha (as-molded)

geotextile is strained upto the maximum experimental limit for all normal pressure values, whereas for the A-400 geotextile, the strain is lower than the maximum possible strain value even at 16 kPa normal pressure. This indicates that low tensile strength geotextile (A-140) requires higher percentage of strain to reach the residual state as compared to high tensile strength geotextile (A-400). In addition the strain is concentrated in the front part of the geotextile due to its high extensibility, as shown in Fig. 4.48. However, the shear stresses developed in the geotextile with low tensile strength are less than those developed in geotextile with high tensile strength, as shown in Fig. 4.53.

Figs. 4.55, 4.56, and 4.57 present the variations of the axial strain at the residual state with position along the geotextile for different normal pressure values. For a normal pressure of 4.5 kPa, it is clear that A-140 geotextile has the highest strain and the strain decreases with the increase in the distance from the plate. Figs. 4.56 and 4.57 show that at normal pressure values of 8 and 16 kPa, the difference between the strains in A-140 and F-140 geotextile reduces throughout the geotextile length except in the front part where the strains in F-140 geotextile are little higher than the strains in the A-140 geotextile. The reason for this behavior is that at higher normal pressures (8 and 16 kPa) the strains in the A-140 geotextile become uniform in the front part of geotextile and reduces in the rear part due to the high necking observed after the test.

Figs. 4.58 and 4.59 show the variation of the shear stress and axial strain with the type of geotextile, respectively, for 10% moisture content of sabkha. The A-400 geotextile carried more shear stress and strained less, compared with the A-140 geotextile. This is mainly due to the higher tensile strength of A-400 geotextile. Fig. 4.60 shows the variation

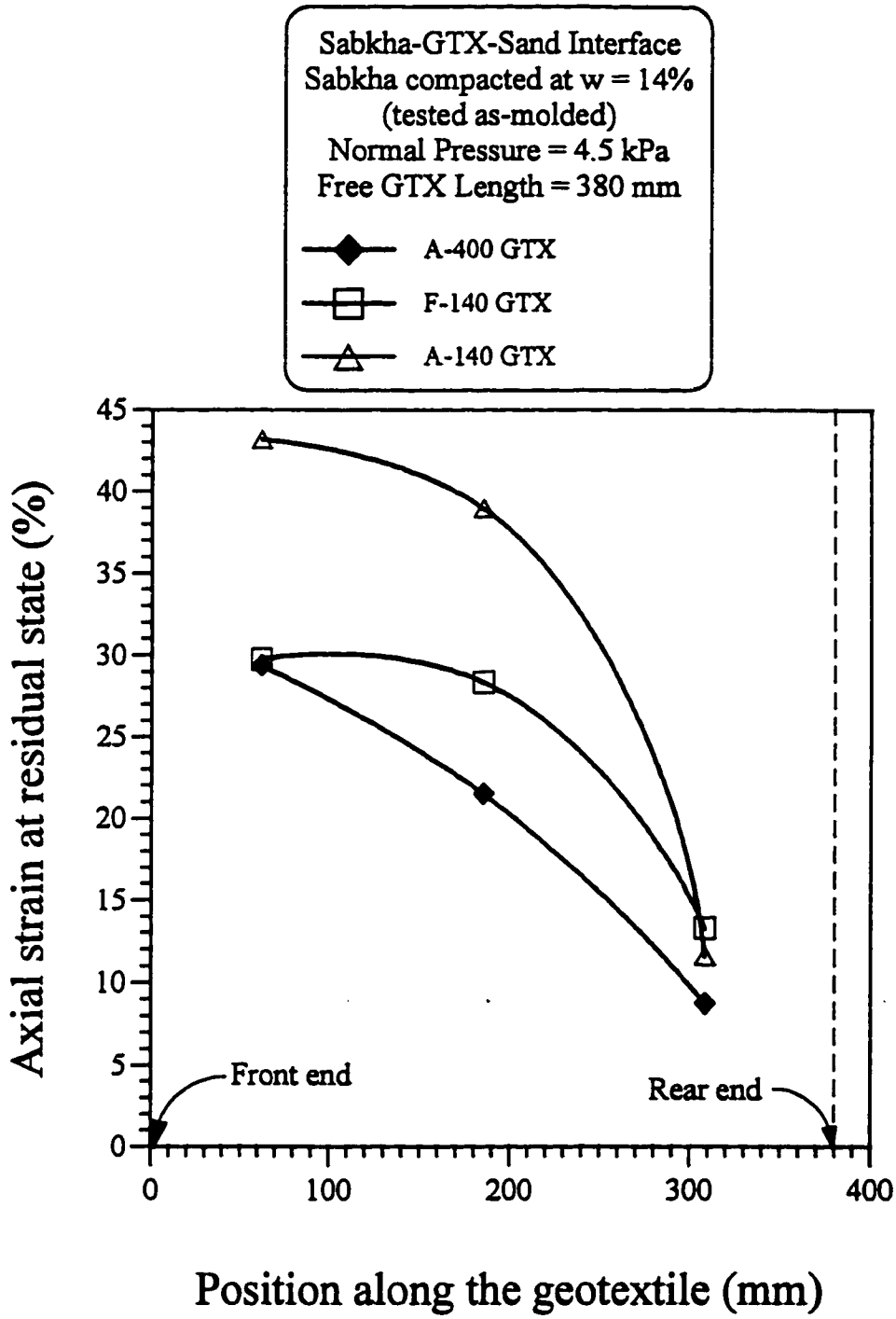

Fig. 4.55:Variation of the average axial strain at the residual state with the position along the geotextile for sabkha-GTX-sand interface at 4.5 kPa normal pressure, 380 mm long free geotextile, and 14% moisture content of sabkha (as-molded)

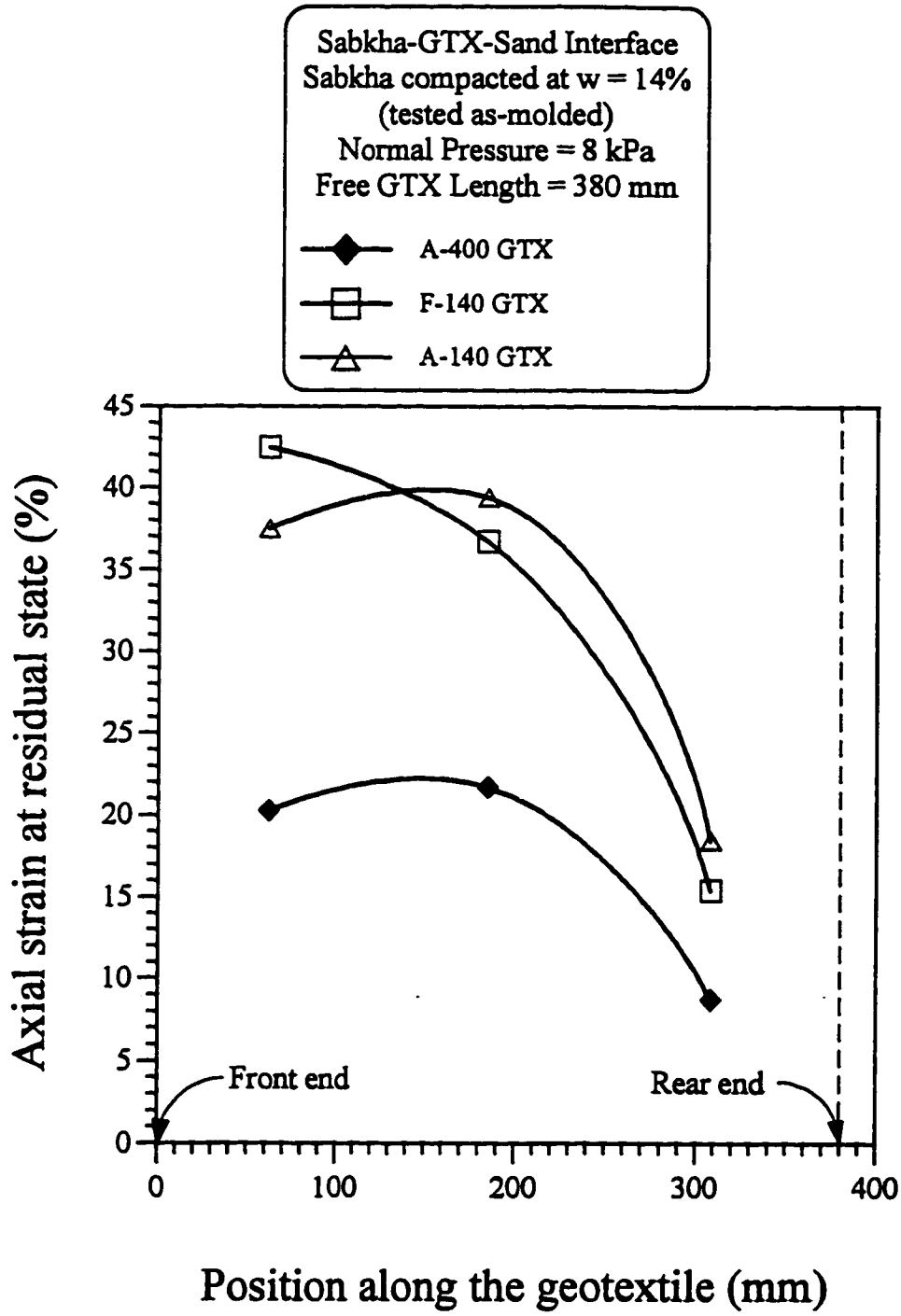

Fig. 4.56: Variation of the average axial strain at the residual state with the position along the geotextile for sabkha-GTX-sand interface at 8 kPa normal pressure, 380 mm long free geotextile, and 14% moisture content of sabkha (as-molded)

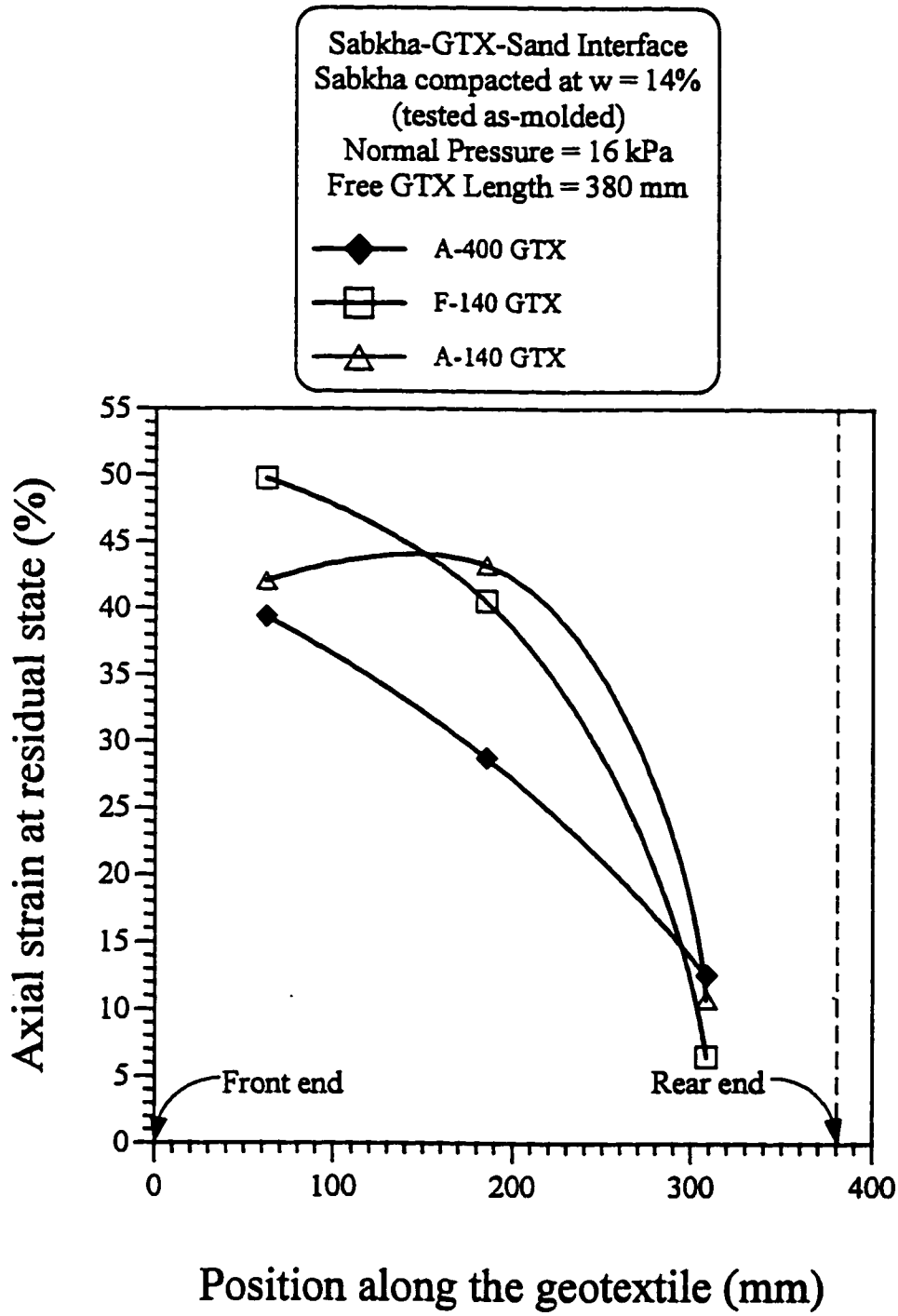

Fig. 4.57: Variation of the average axial strain at the residual state with the position along the geotextile for sabkha-GTX-sand interface at 16 kPa normal pressure, 380 mm long free geotextile, and 14% moisture content of sabkha (as-molded)

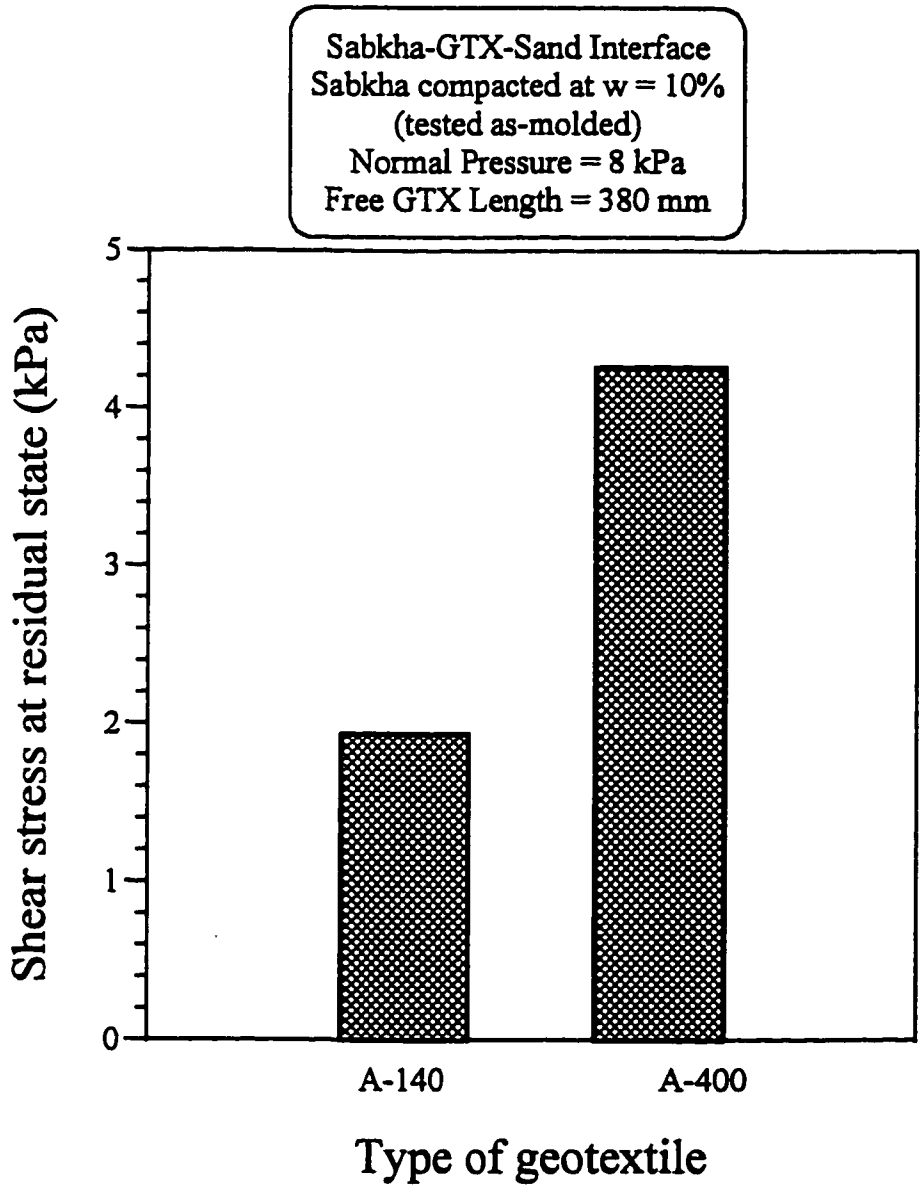

Fig. 4.58: Variation of the shear stress at the residual state with the geotextile type for sabkha-GTX-sand interface under 8 kPa normal pressure, 380 mm long free geotextile, and 10% moisture content of sabkha (as-molded)

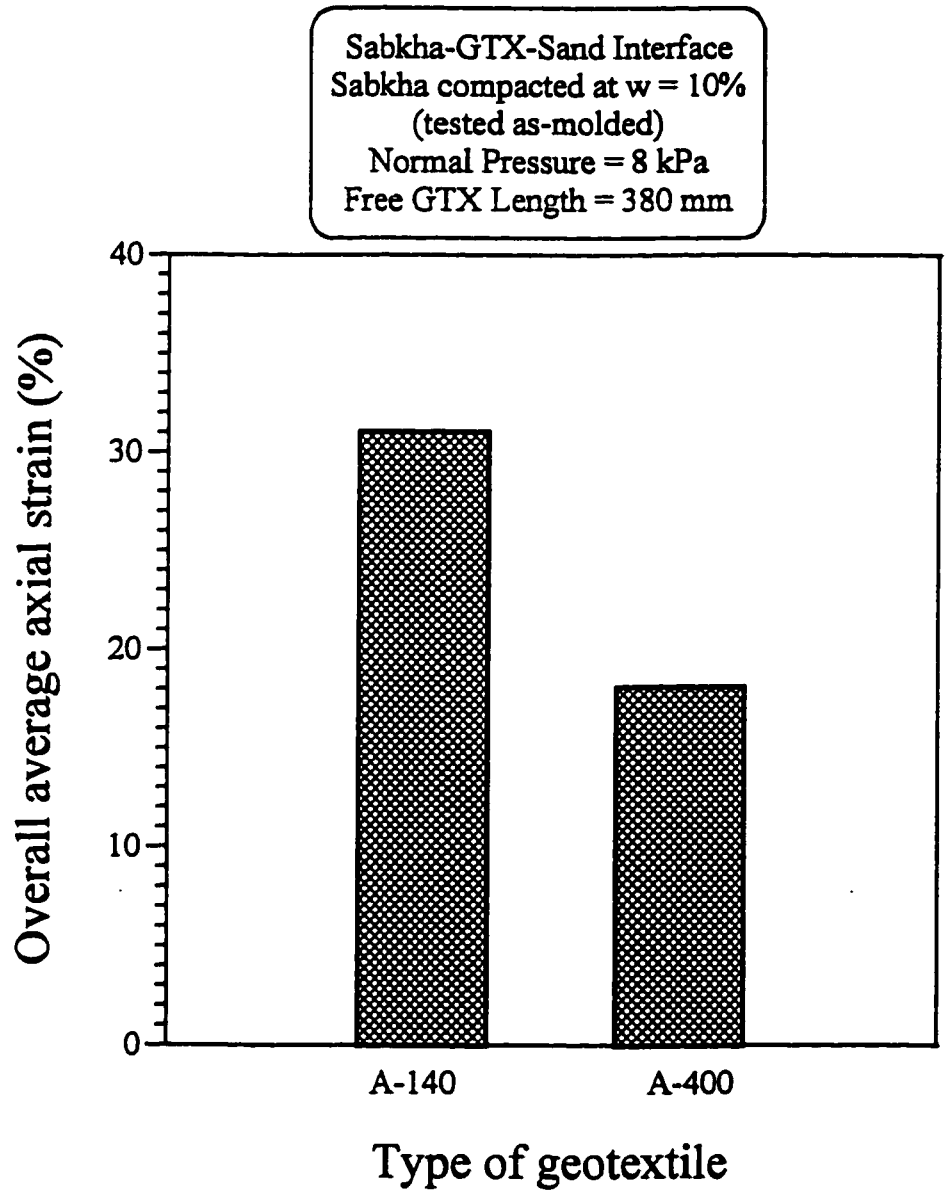

Fig. 4.59: Variation of the overall average axial strain at the residual state with the geotextile type for sabkha-GTX-sand interface under 8 kPa normal pressure, 380 mm long free geotextile, and 10% moisture content of sabkha (as-molded)

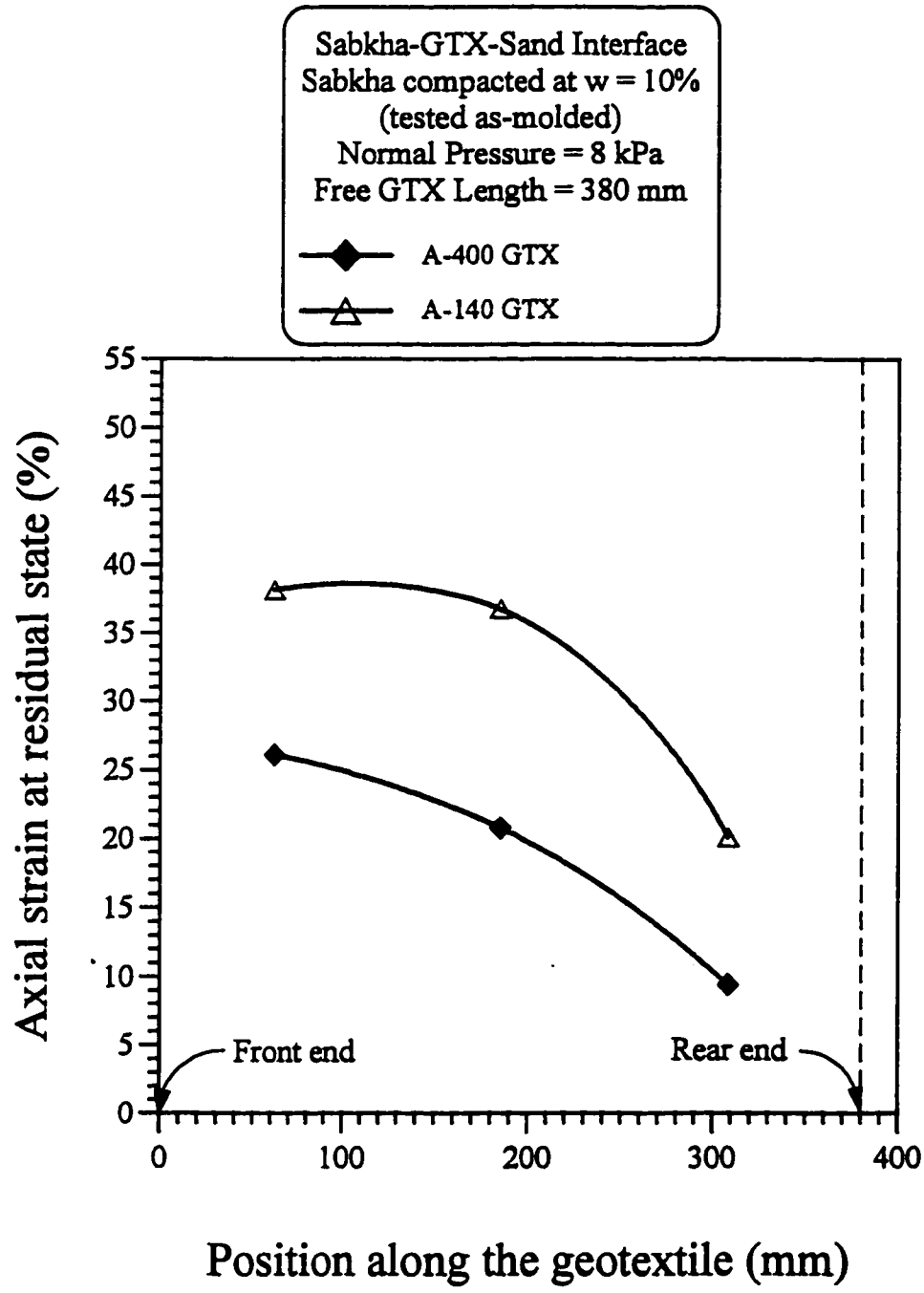

Fig. 4.60: Variation of the average axial strain at the residual state with the position along the geotextile for sabkha-GTX-sand interface at 8 kPa normal pressure, 380 mm long free geotextile, and 10% moisture content of sabkha (as-molded)

of the axial strain along the geotextile for A-140 and A-400 geotextiles when 10% moisture content of sabkha was used. It clearly shows that in the A-400 geotextile, the strains are less throughout the geotextile length, compared to that in A-140 geotextile.

4.7.3 Effect of Geotextile length

Pull-out tests on sabkha-GTX-sand interface were performed on three different geotextile length, i.e., 380 mm, 257 mm, and 133 mm. The results are summarized in Table 4.15 and Fig. 4.61. It is clear from the figure that the short geotextile length behaves like glued steel plate without undergoing large strain. Samples came into residual state at low value of axial strain and therefore the shear stress is not fully mobilized as shown in Fig. 4.62. This figure presents the variation of the shear stress and axial strain with length of geotextile. As the length of geotextile increases, the overall average strain increases. Fig. 4.63 presents the variations of the axial strain versus position along the geotextile for different lengths. For short specimens the strain drops quickly within the middle-third portion and then it increases at the rear end of the geotextile. This behavior is similar to that observed for sand–GTX–sand interface.

4.7.4 Effect of Moisture Content of Sabkha

Sabkha, being water sensitive soil, was compacted to the same density at different moisture contents. The results of the pull-out tests using different moisture contents of sabkha layer are summarized in Table 4.16. The test results are shown in Figs. 4.64 and 4.65 which indicate that as the moisture content increases from 10% to 14%, the pull-out resistance drop for A-400 and A-140 geotextiles. Farrag (1995) performed pull-out tests

Table 4.15: Interface characteristics for sabkha-A-400 GTX-sand interface, 8 kPa normal pressure and 14% moisture content of sabkha with different geotextile length

At peak pull-out state				
Length of free geotextile	Pull-out force (N)	Shear stress (kPa)	Overall average strain (%)	Front end displacement (mm)
380	418.89	4.73	16.50	65.00
257	404.37	6.84	15.20	40.00
133	268.79	9.26	8.80	11.93
At residual pull-out state				
Length of free geotextile	Pull-out force (N)	Shear stress (kPa)	Overall average strain (%)	Front end displacement (mm)
380	383.57	4.33	16.50	76.00
257	326.67	5.51	15.60	54.03
133	72.89	2.47	10.50	120.00
At the end of the test				
Length of free geotextile	Pull-out force (N)	Shear stress (kPa)	Overall average strain (%)	Front end displacement (mm)
380	334.62	3.78	16.50	104.00
257	182.47	3.05	16.50	117.50
133	72.89	2.47	10.50	120.00
Axial strain in the geotextile at the residual state				
Length of free geotextile (mm)	Average strain in the front one-third (%)	Average strain in the middle one-third (%)	Average strain in the rear one-third (%)	Overall average strain (%)
380	20.27	21.70	8.72	16.50
257	21.77	19.70	7.00	15.60
133	27.40	0.80	5.90	10.50
Axial strain in the geotextile at the end of the test				
Length of free geotextile (mm)	Average strain in the front one-third (%)	Average strain in the middle one-third (%)	Average strain in the rear one-third (%)	Overall average strain (%)
380	18.85	21.70	9.73	16.57
257	21.40	24.14	6.08	16.50
133	27.40	0.80	5.90	10.50

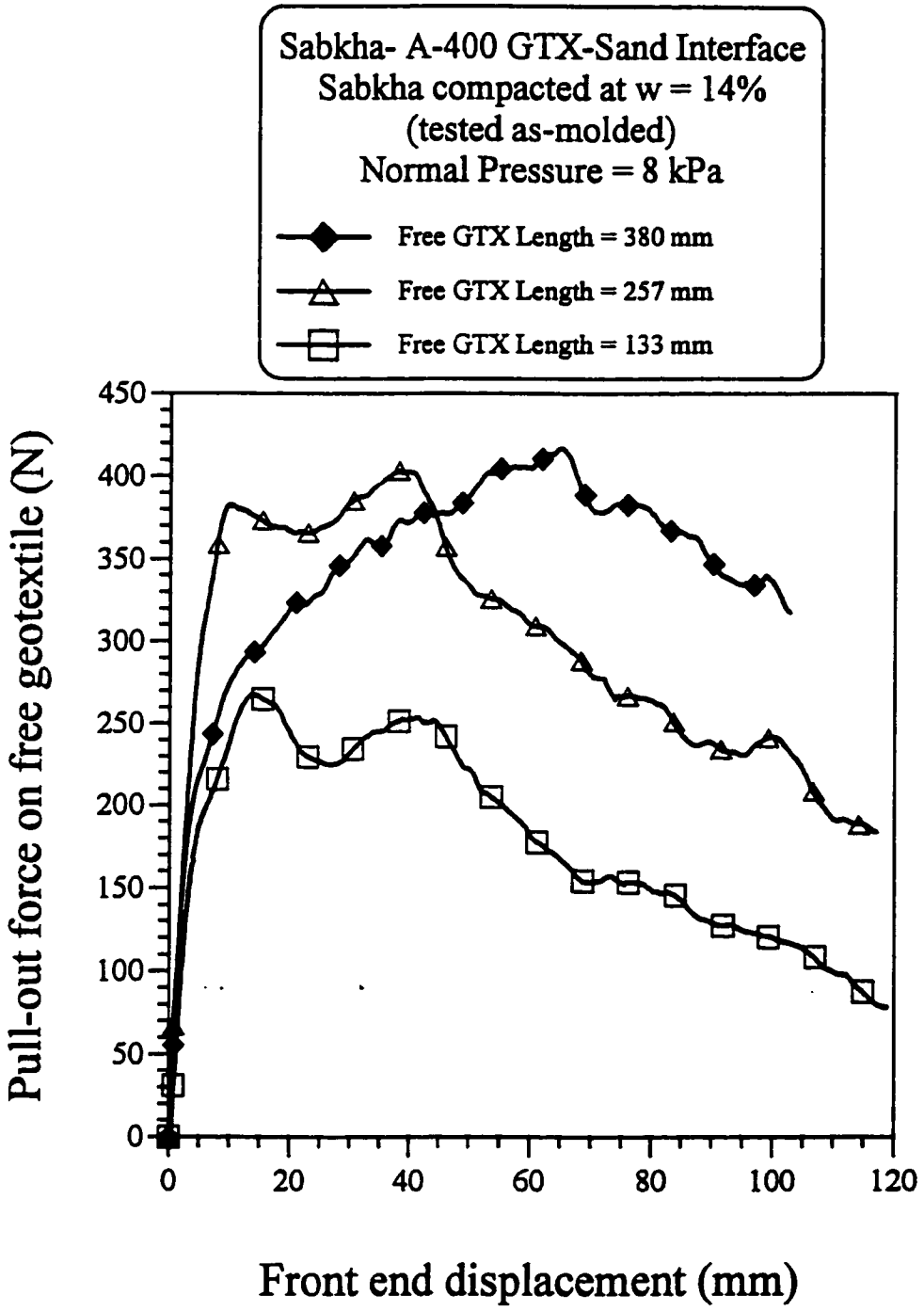

Fig. 4.61: Variation of the pull-out force on A-400 geotextile with the front end displacement for sabkha-GTX-sand interface, at 8 kPa normal pressure, and 14% moisture content of sabkha (as-molded)

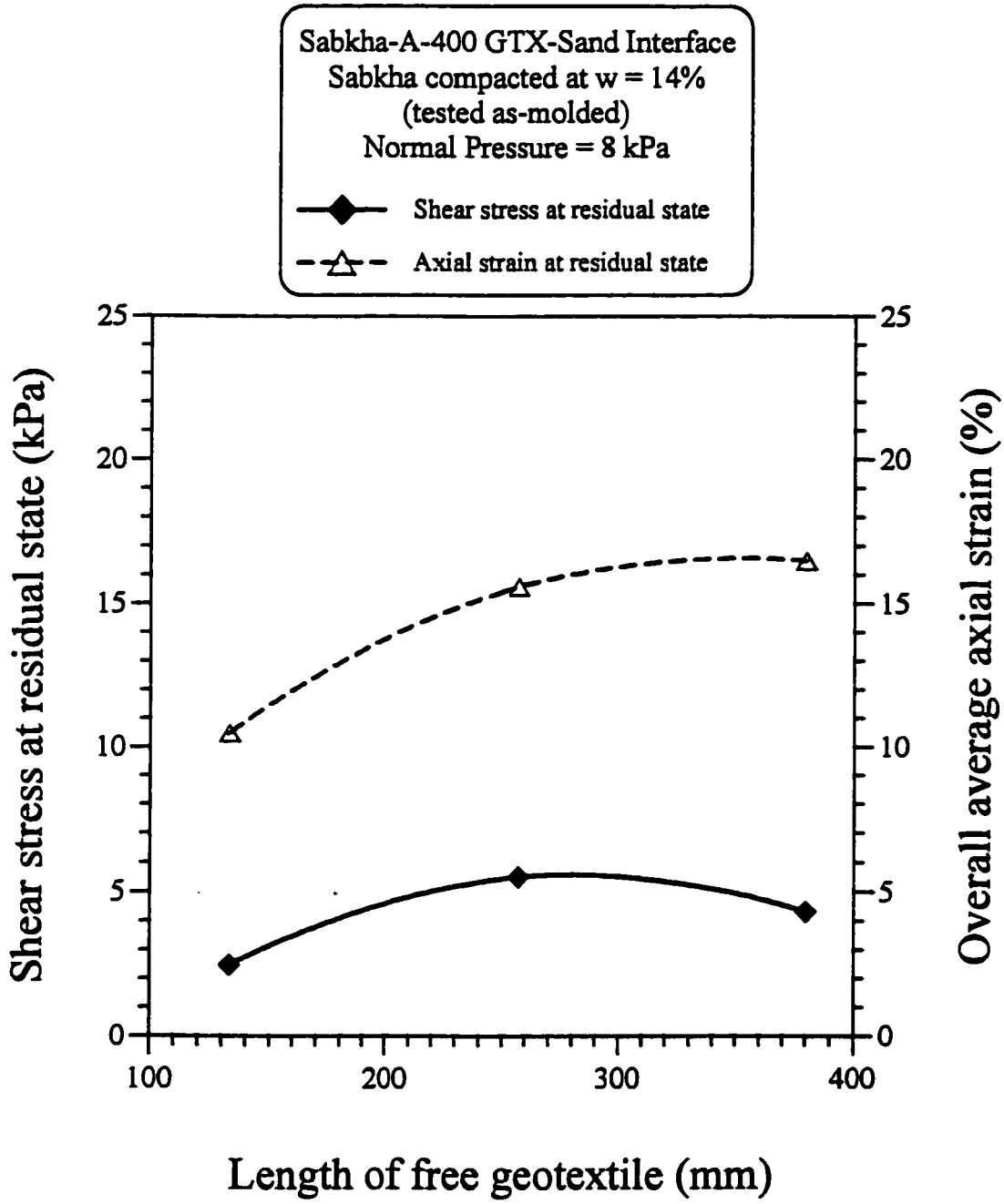

Fig. 4.62: Variation of the shear stress at the residual state and the overall average axial strain at the residual state with length of free geotextile for sabkha -A-400 GTX-sand interface at 8 kPa normal pressure, and 14% moisture content of sabkha (as-molded)

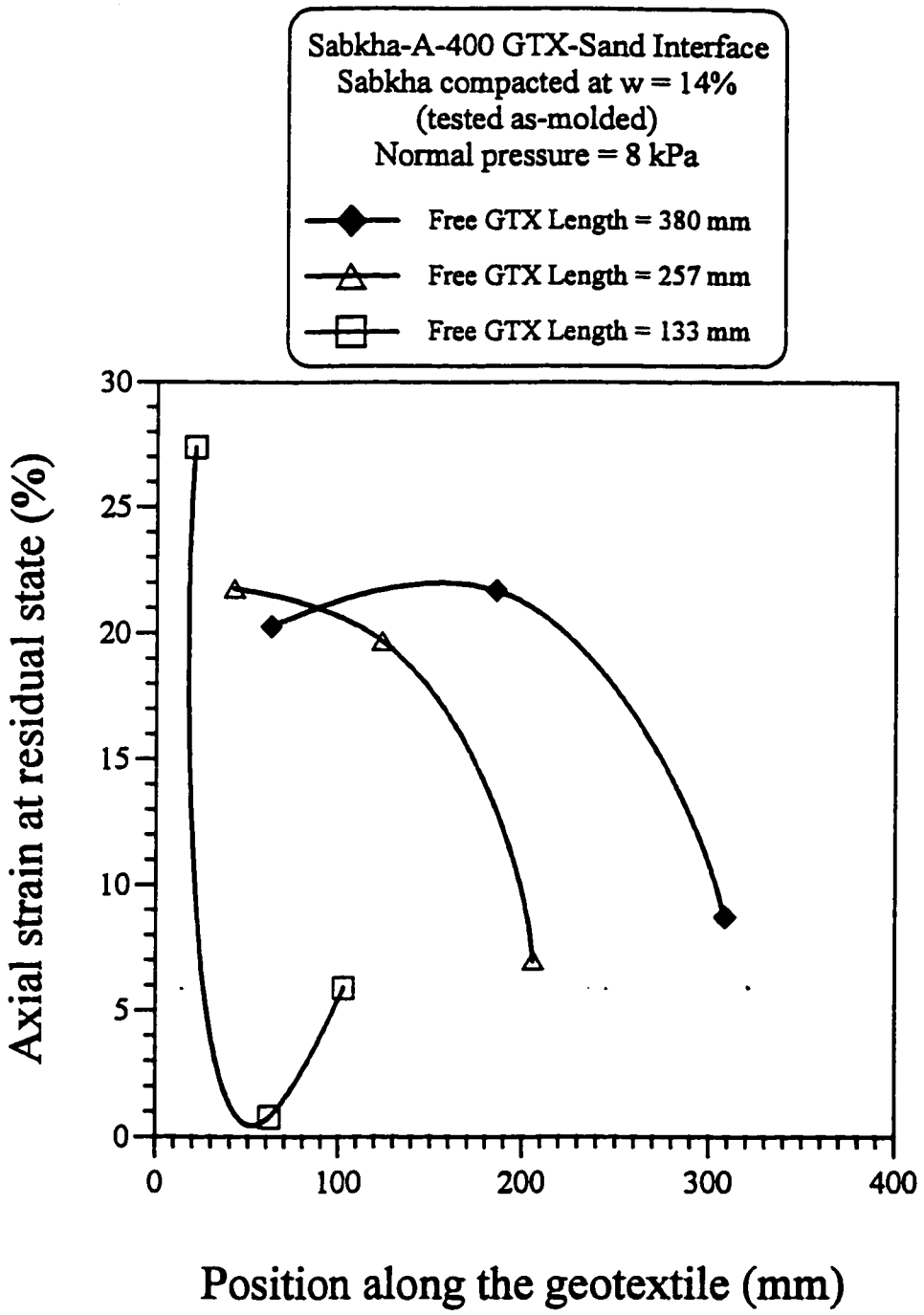

Fig. 4.63: Variation of the average axial strain at the residual state with the position along the geotextile for sabkha-A-400 GTX-sand interface at 8 kPa normal pressure, and 14% moisture content of sabkha (as-molded)

Table 4.16: Interface characteristics for sabkha-A-400 GTX-sand interface, 8 kPa normal pressure and 380 mm long free geotextile, at different moisture contents of sabkha

At peak pull-out state				
Moisture content of sabkha (%)	Pull-out force (N)	Shear stress (kPa)	Overall average strain (%)	Front end displacement (mm)
10	506.49	5.80	14.95	56.80
14	418.89	4.73	16.50	65.00
16	606.26	6.66	19.70	76.80
soaked*	790.98	8.50	21.60	102.15
At residual pull-out state				
Moisture content of sabkha (%)	Pull-out force (N)	Shear stress (kPa)	Overall average strain (%)	Front end displacement (mm)
10	382.59	4.26	18.13	78.60
14	383.57	4.33	16.50	76.00
16	564.08	6.14	20.89	84.00
soaked*	790.98	8.50	21.60	102.15
At the end of the test				
Moisture content of sabkha (%)	Pull-out force (N)	Shear stress (kPa)	Overall average strain (%)	Front end displacement (mm)
10	400.25	4.44	18.56	114.00
14	334.62	3.78	16.50	104.00
16	459.11	4.99	21.05	111.02
soaked*	790.98	8.50	22.50	109.55
Axial strain in the geotextile at the residual state				
Moisture content of sabkha (%)	Average strain in the front one-third (%)	Average strain in the middle one-third (%)	Average strain in the rear one-third (%)	Overall average strain (%)
10	26.10	20.82	9.42	18.13
14	20.27	21.70	8.72	16.50
16	26.10	26.10	10.65	20.89
soaked*	36.30	22.40	8.10	21.60
Axial strain in the geotextile at the end of the test				
Moisture content of sabkha (%)	Average strain in the front one-third (%)	Average strain in the middle one-third (%)	Average strain in the rear one-third (%)	Overall average strain (%)
10	26.10	20.82	9.42	18.56
14	18.50	21.70	9.73	16.57
16	26.10	26.10	10.65	20.89
soaked*	36.90	23.30	8.80	22.50

* Only the bottom sabkha layer was soaked

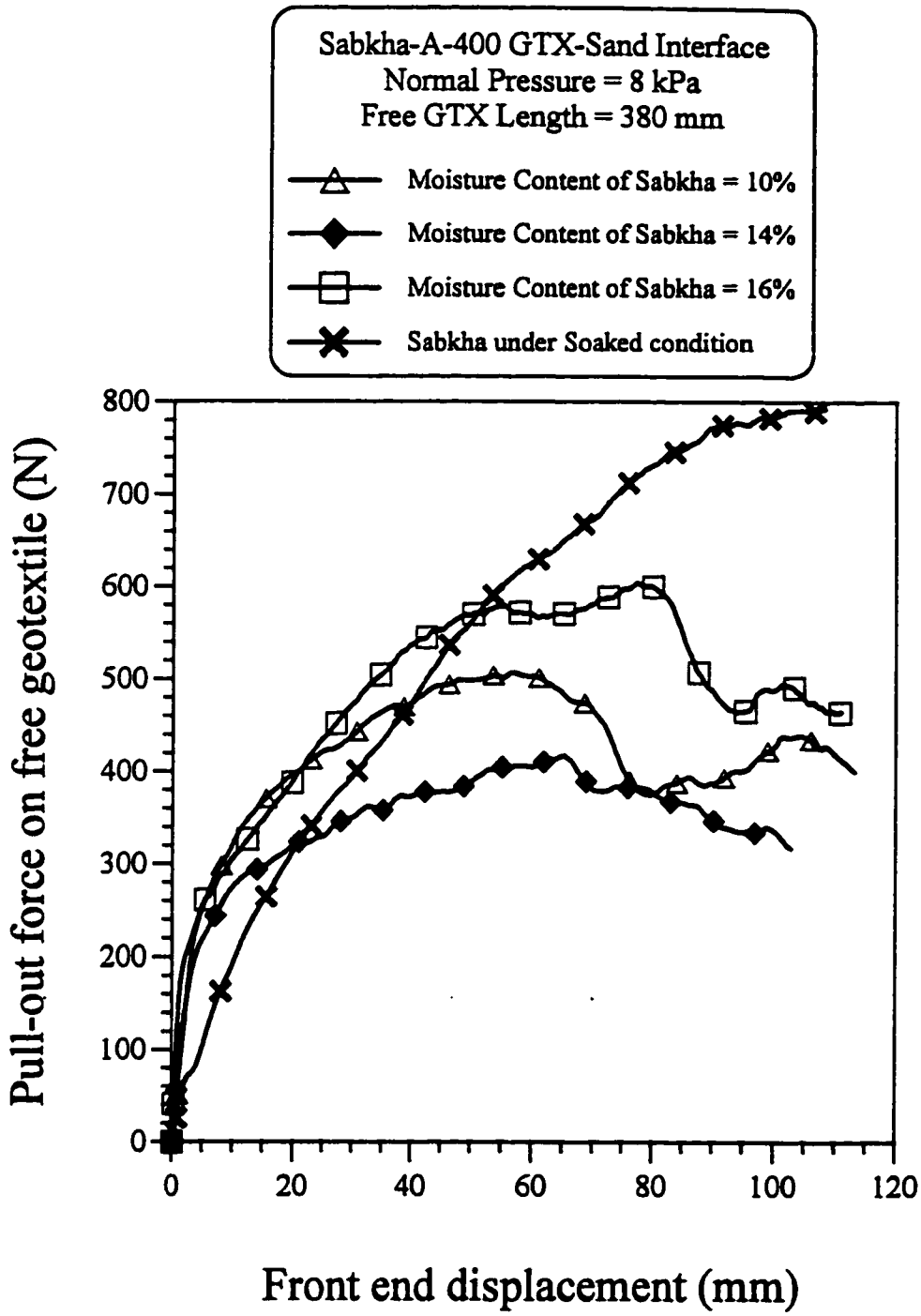

Fig. 4.64: Variation of the pull-out force on A-400 geotextile with the front end displacement for sabkha-GTX-sand interface at 8 kPa normal pressure, and 380 mm long free geotextile

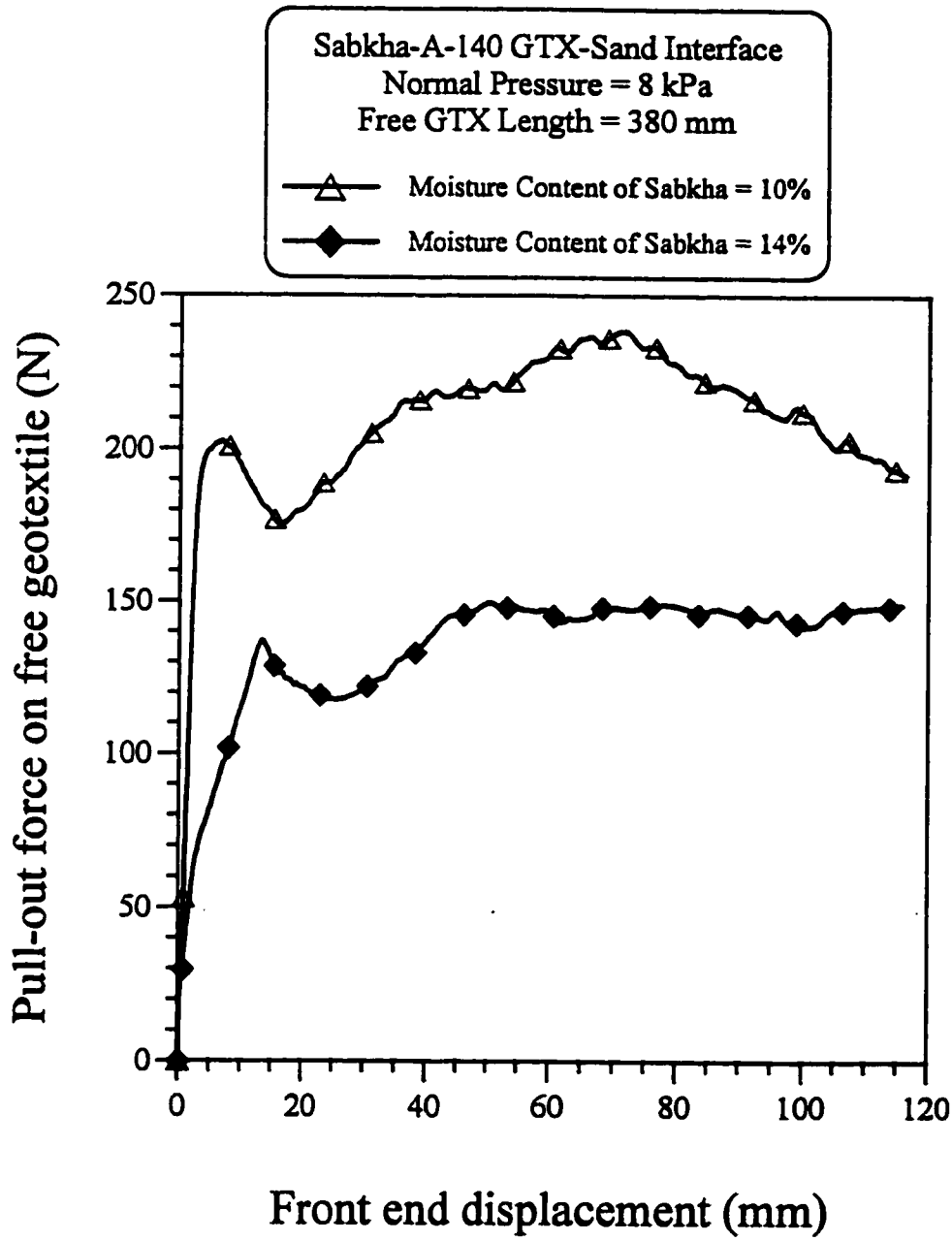

Fig. 4.65: Variation of the pull-out force on A-140 geotextile with the front end displacement for sabkha-GTX-sand interface, at 8 kPa normal pressure, and 380 mm long free geotextile

on clayey soil and obtained similar results. However, when the moisture content was increased from the optimum (14%) to 16%, the pull-out resistance increased due to the presence of a water film at the interface that developed some adhesion between the geotextile and sabkha. Pull-out test was also performed with the bottom sabkha layer being soaked, in distilled water, while the upper sand layer was not soaked. The data shows higher value of pull-out resistance for this test when compared with the other tests performed at different moisture contents. The comparison is shown in Fig. 4-66. The increase of the pull-out resistance with increase in moisture content after the optimum value can be due to the development of strong adhesion between sabkha and the geotextile due to presence of enough water at the interface. This water causes sabkha soil to be compressed into the geotextile due to its softness. Thus the shear strength and moisture content of the soil itself are playing a role in the pull-out resistance. It is also observed, during the soaked test, that the water rose up into the upper sand layer due to the capillary action. Hence another reason for the increase in the shear stress upon soaking is the suction or capillary action in the sand layer above the geotextile. This increases the normal effective stress and that results in higher pull-out resistance. This is supported by the results presented in Fig. 4.39, which shows that the pull-out resistance is higher for the soaked test as compared to the dry test even for sand–GTX–sand interface. Suction and the adhesion phenomena, in the case of sabkha-GTX-sand interface, are developed due to the partial soaking i.e., the soaking of the bottom sabkha layer alone.

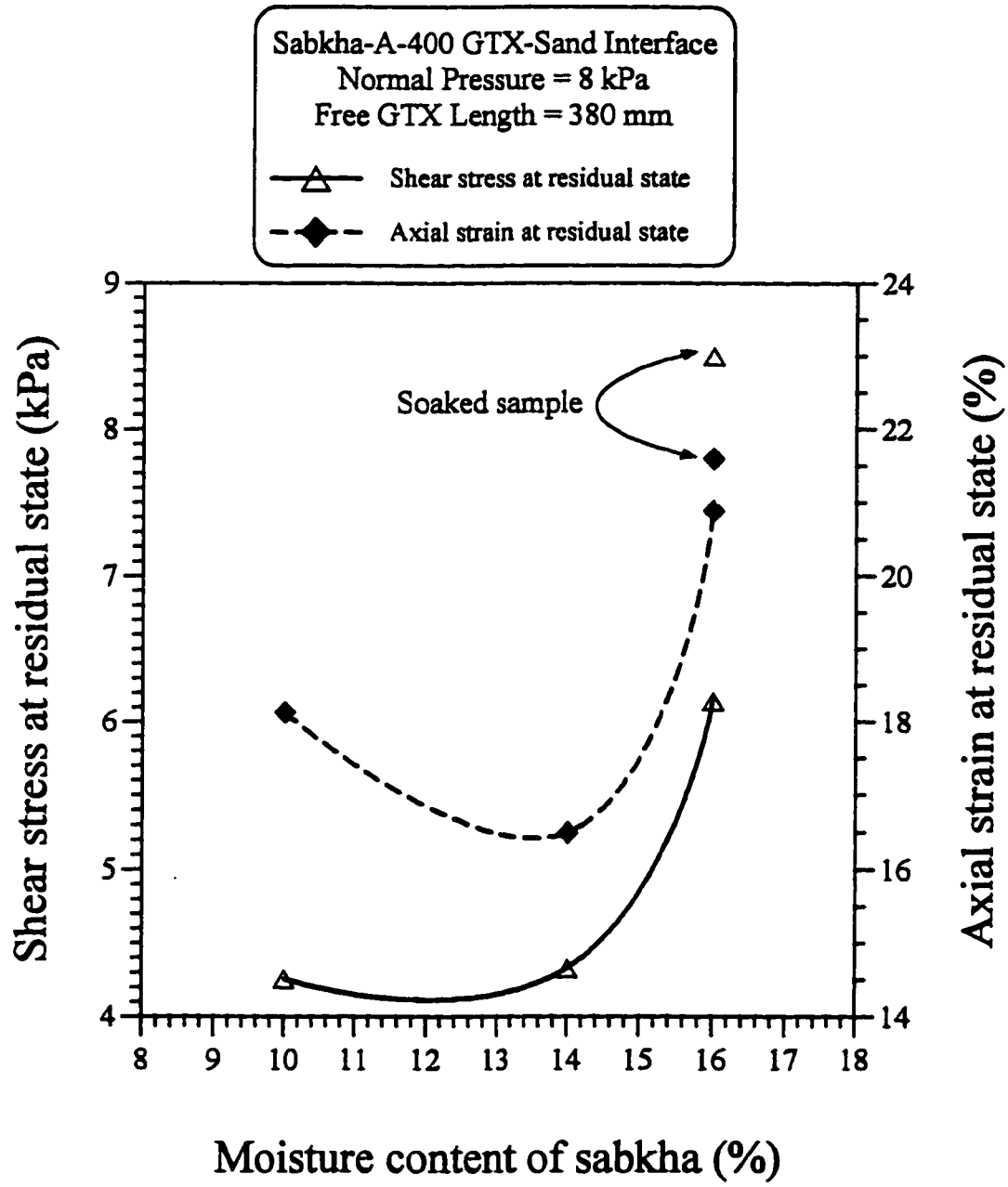

Fig. 4.66: Variation of the shear stress at the residual state and the overall average axial strain at the residual state with moisture content of sabkha for sabkha-A-400 GTX-Sand interface at 8 kPa normal pressure, and 380 mm long free geotextile

4.7.5 Interface Interaction Factor (c_i) for Sabkha–GTX–Sand interface

Interface interaction factor (c_i) for sabkha–GTX–sand interface is presented in Table 4.17. The c_i values for sabkha–GTX–sand interface are much less than the corresponding values for sand–GTX–sand interface, shown in Table 4.6. Results clearly indicate that the shear stresses mobilized on the sabkha–GTX–sand interface are smaller than those for sand–GTX–sand interface or the average shear strength of the two soils (sand and sabkha) at the interface. The average of the shear strength is considered because there are two different types of soil (sand and sabkha) at the interface. This decrease in the c_i values is due to the absence of interlock between the soil particles and the geotextile openings. The interlock does not exist because of the fineness of sabkha (92% is passing ASTM sieve No. 200).

The variation of Interface interaction factor (c_i) with the moisture content of sabkha soil is presented in Table 4.18 and plotted in Fig. 4.67. This figure shows that the Interface interaction factor increases with the increase in moisture content of the sabkha soil. The reason for the increase in the c_i values with the increase in moisture content of sabkha soil is the increase in the value of the shear stresses mobilized at the interface with the increase in moisture content as shown in Fig. 4.66.

Table 4.17: Interface interaction factor c_i for sabkha-GTX-sand interface, 380 mm long free geotextile, and 14% moisture content of sabkha

Normal Pressure (kPa)	Geotextile Type		
	A-400	F-140	A-140
4.50	0.07	0.07	0.04
8.00	0.12	0.13	0.04
16.00	0.12	0.15	0.05

Table 4.18: Interface interaction factor c_i for sabkha-A-400 GTX-sand interface, and 380 mm long free geotextile

Moisture content of sabkha (%)	Interaction Factor (c_i)
10	0.08
14	0.12
16	0.17
soaked	0.27

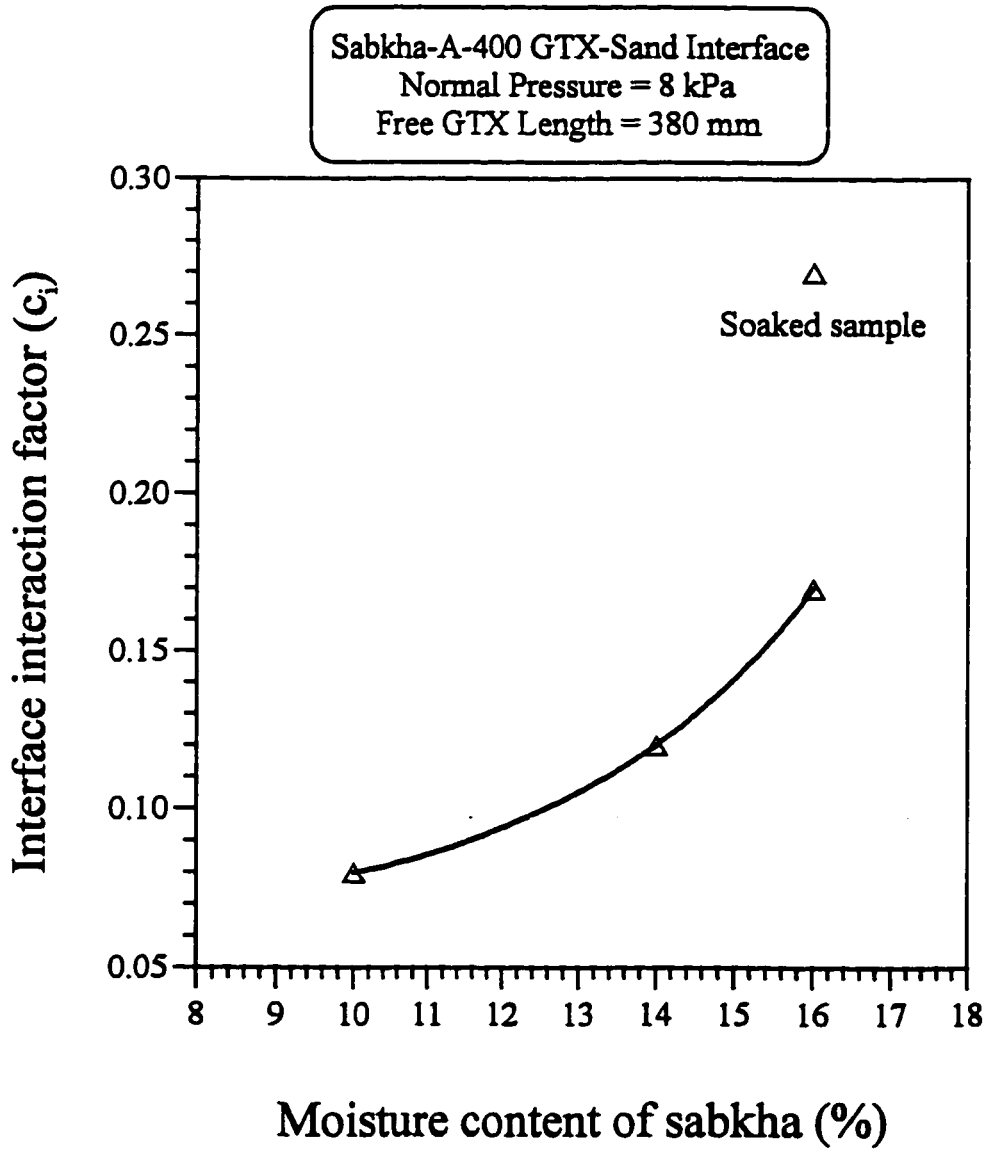

Fig. 4.67: Variation of the Interface interaction factor (c_i) with moisture content of sabkha for sabkha-A-400 GTX-sand interface at 8 kPa normal pressure, and 380 mm long free geotextile

4.8 Comparison between Sand–GTX–Sand and Sabkha–GTX–Sand Interfaces

This section present a comparison between the pull-out tests performed on sand–GTX–sand and sabkha–GTX–sand interfaces. Figs. 4.68, 4.69 and 4.70 present a comparison between the residual shear stress on the two interfaces at different normal stress levels for A-400, F-140 and A-140 geotextile, respectively. Fig. 4.68 shows that in the case of A-400 geotextile, higher values of shear stresses are mobilized on sand–GTX–sand interface as compared with that on sabkha–GTX–sand interface. This means that the A-400 geotextile is more efficient in the case of sand–GTX–sand interface and, this has the implication that thin sand layer should be placed on the sabkha surface before placing the A-400 geotextile. The figure also shows that the contribution of sabkha soil in mobilizing shear stress on the A-400 geotextile is less than that of sand if the contribution of sand-geotextile interface is assumed to be same in sand-GTX-sand and sabkha-GTX-sand interfaces. The contribution of sand-geotextile interface is assumed to be the one-half of the shear stress developed on sand-A-400 GTX-sand interface. This assumption is reasonable in the case of the A-400 geotextile because both faces of geotextile are needle-punched and have same texture. The reason for the higher contribution of sand as compared to that of sabkha is the surface roughness and texture of the geotextile as well as the roughness of sand particles compared to the sabkha soil. The granular sand particles can easily indent into the openings of the geotextile, thus increasing the shear strength.

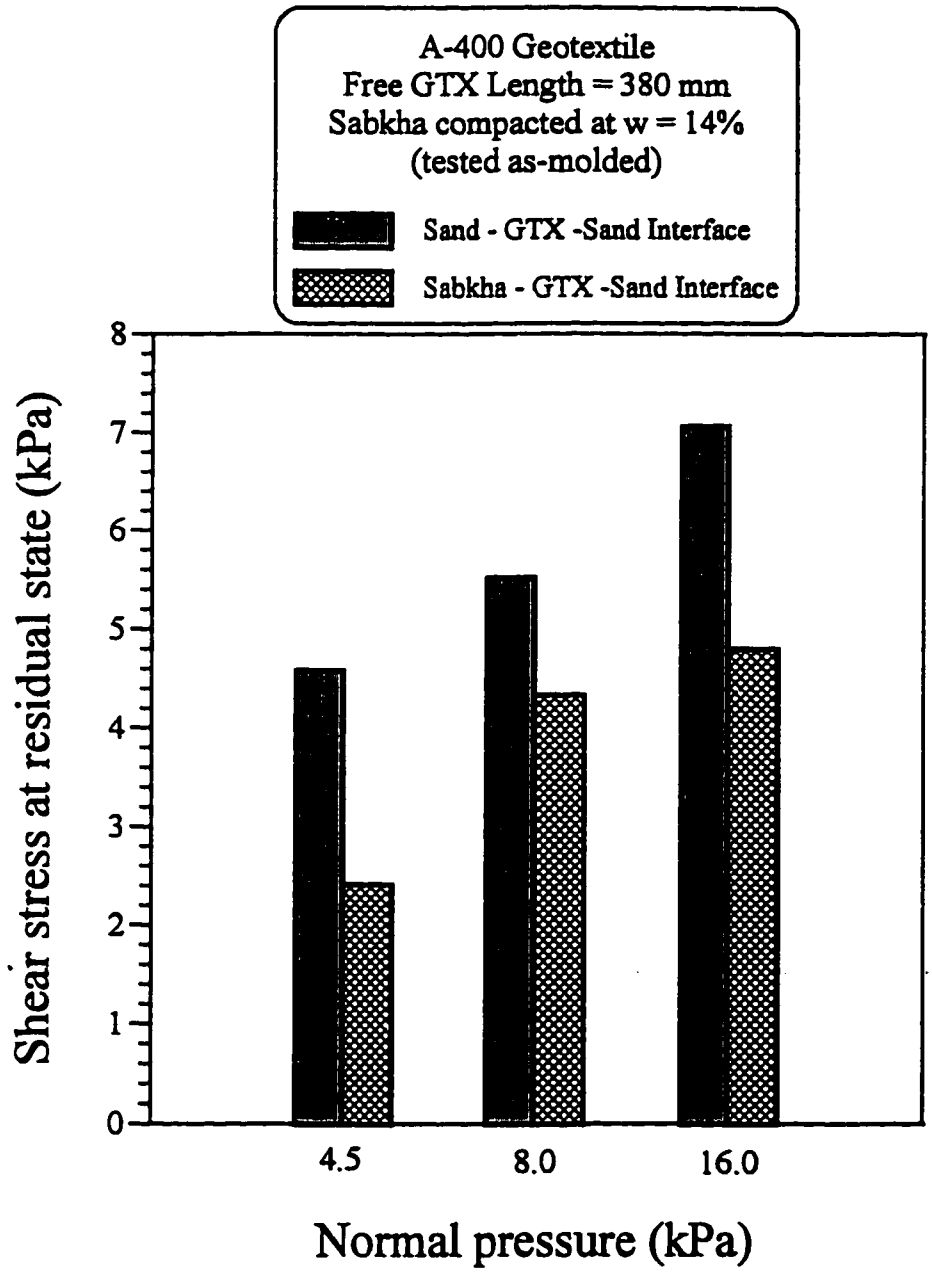

Fig. 4.68: Variation of the shear stress at the residual state with the normal pressure for the A-400 geotextile and for different soil-geotextile interfaces

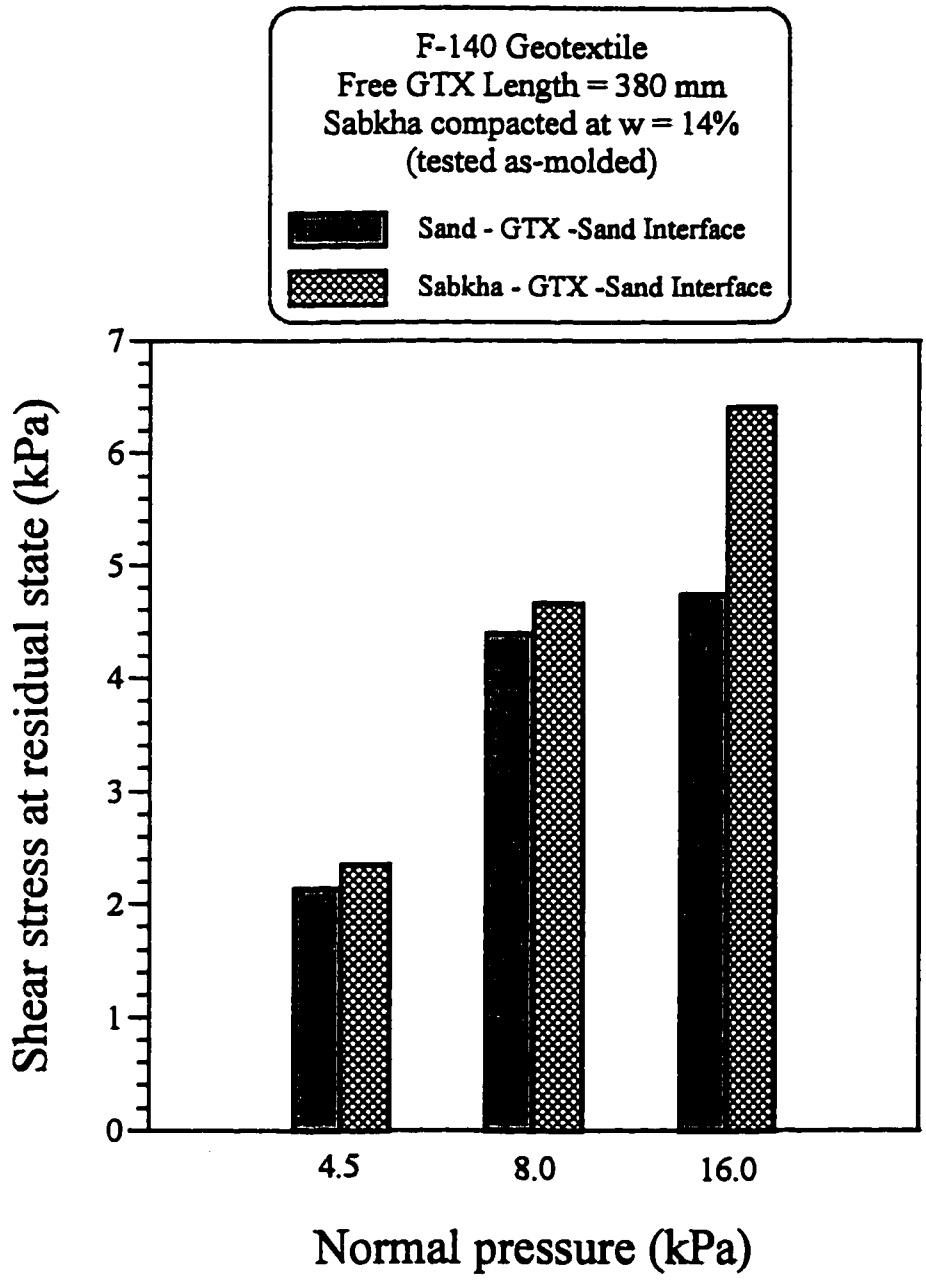

Fig. 4.69: Variation of the shear stress at the residual state with the normal pressure for the F-140 geotextile and for different soil-geotextile interfaces

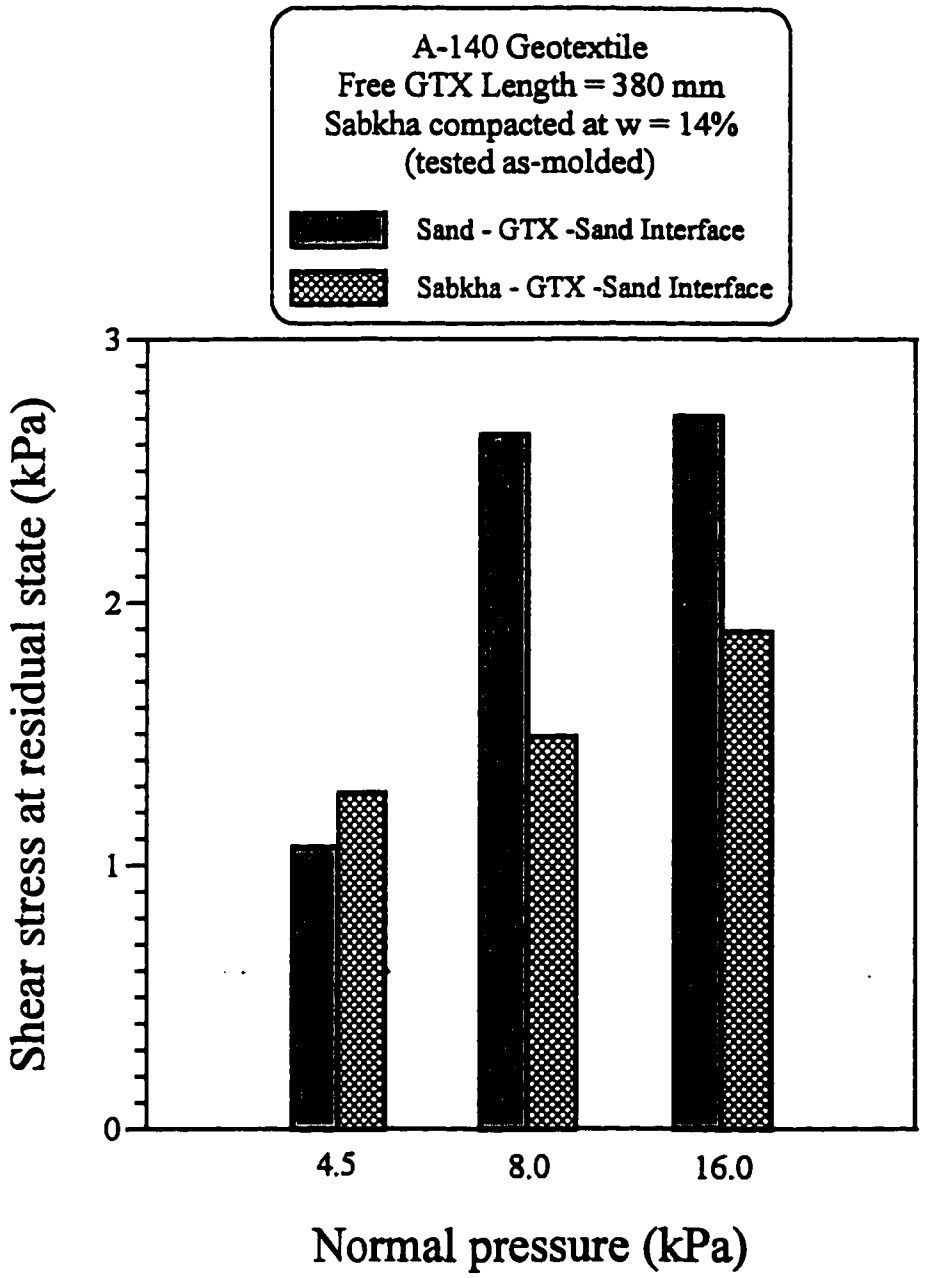

Fig. 4.70: Variation of the shear stress at the residual state with the normal pressure for the A-140 geotextile and for different soil-geotextile interfaces

An opposite behavior is observed in the case of F-140 geotextile, which has lower tensile strength and lower extensibility compared with the A-400 geotextile, as shown in Fig. 4.69. This figure shows that in the case of the F-140 geotextile, higher shear stresses are mobilized on sabkha–GTX–sand interface as compared to that on sand–GTX–sand interface. Moreover, in this case, the contribution of sabkha soil in mobilizing shear stress is higher than that of sand if the same assumptions are applied as that in the case of the A-400 geotextile. However the F-140 geotextile is needle punched on one side and thermally bonded on the other side. Therefore, the two sides of geotextile have different surface texture and roughness even in the case of sand-GTX-sand interface. The pull-out tests on the F-140 geotextile were performed with the needle-punched side of geotextile facing the sand while the thermally bonded side facing the sabkha. The permeability of the F-140 geotextile is very low as compared to that of the A-400 or the A-140 geotextile and this increases the suction developed during the movement of F-140 geotextile over the sabkha soil and thus, increases the adhesion between the geotextile and the sabkha soil.

From the above discussion, it is clearly seen that the surface texture and the permeability of the geotextile play an important role in the mobilization of higher shear stresses on sabkha–geotextile interface as compared with sand–geotextile interface. Fig. 4.70 presents a comparison between the residual shear stress on the two interfaces at the different normal stress levels for the A-140 geotextile. This figure shows that higher shear stresses are mobilized in sand-GTX–sand interface for a normal pressure of 8 kPa and higher. The reason for such behavior is that A-400 and A-140 geotextiles have similar surface texture (needle punched on both sides) and, therefore, the contribution of sabkha

is less in this case. Furthermore these geotextiles have higher extensibility when compared to the F-140 geotextile. However, at 4.5 kPa normal pressure, little higher shear stress value is mobilized on sabkha-GTX-sand interface, compared to that on sand-GTX-sand interface.

The comparison of the three geotextiles in the case of sand–GTX–sand interface shows that the A-400 geotextile is the most efficient geotextile due to its high tensile strength. However, if the three geotextiles are compared in the case of sabkha–GTX–sand interface, one will find that F-140 geotextile is better than the other two geotextiles at higher normal pressure due to its low extensibility, low permeability and surface texture.

Figs. 4.71, 4.72, and 4.73 present a comparison of the axial strain developed along the geotextile in the sand–GTX–sand and the sabkha–GTX–sand interfaces. Fig 4.71 shows that higher tensile strains are developed in the case of sabkha–GTX–sand interface, compared with that in sand–GTX–sand interface for the A-400 geotextile. Similar results are obtained for the F-140 geotextile, except at the front end. The reason for such behavior is that in the case of sand–GTX–sand interface, the particles of sand intrude into the geotextile opening and increases its modulus thus the strains are reduced in sand–GTX–sand interface. It is clear from Fig. 4.71 that the strains are somewhat linearly distributed in the case of A-400 geotextile at the residual state at a normal pressure of 4.5 kPa. Whereas, the strains become almost uniform in the front portion of the F-140 geotextile as shown in Fig. 4.72. This is mainly due to the low extensibility of the F-140 geotextile when the strains become uniform in the front end and the geotextile reached at the slippage condition. This type of behavior is observed for sabkha–GTX–sand interface

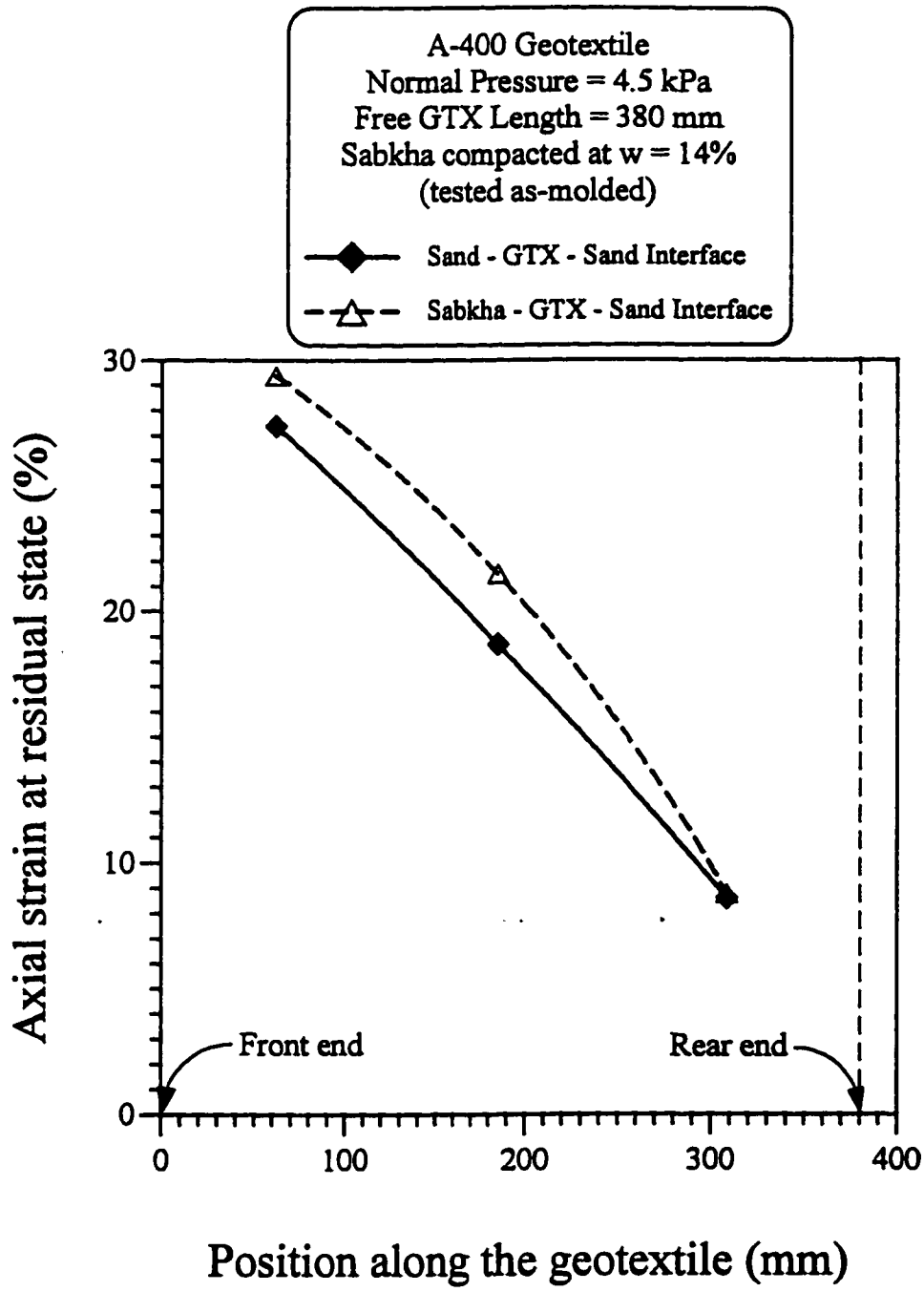

Fig. 4.71: Variation of the average axial strain at the residual state with the position along the geotextile for A-400 Geotextile, 380 mm long free geotextile, at a normal pressure of 4.5 kPa with different soil-geotextile interfaces

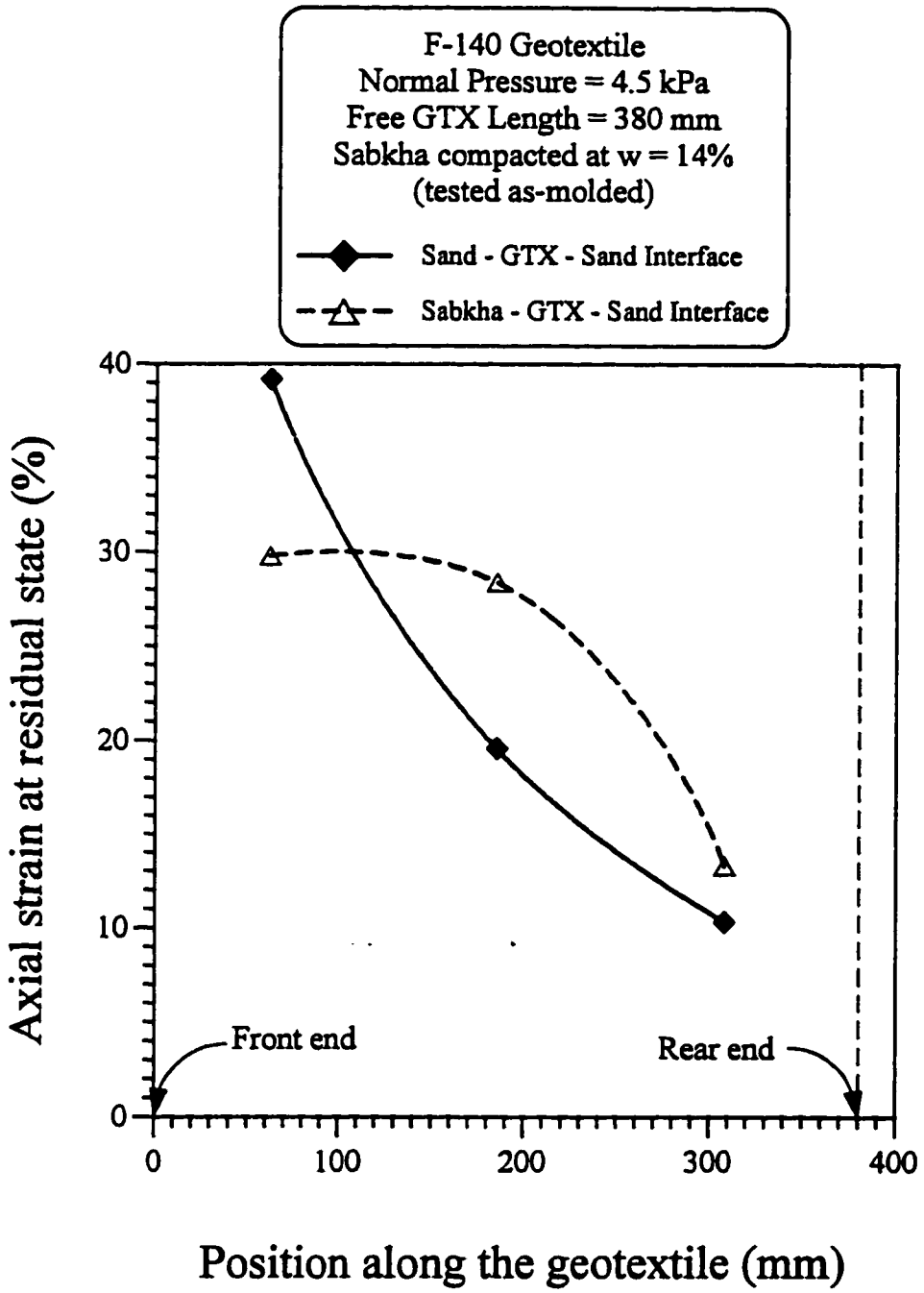

Fig. 4.72: Variation of the average axial strain at the residual state with the position along the geotextile for F-140 Geotextile, 380 mm long free geotextile, at a normal pressure of 4.5 kPa with different soil-geotextile interfaces

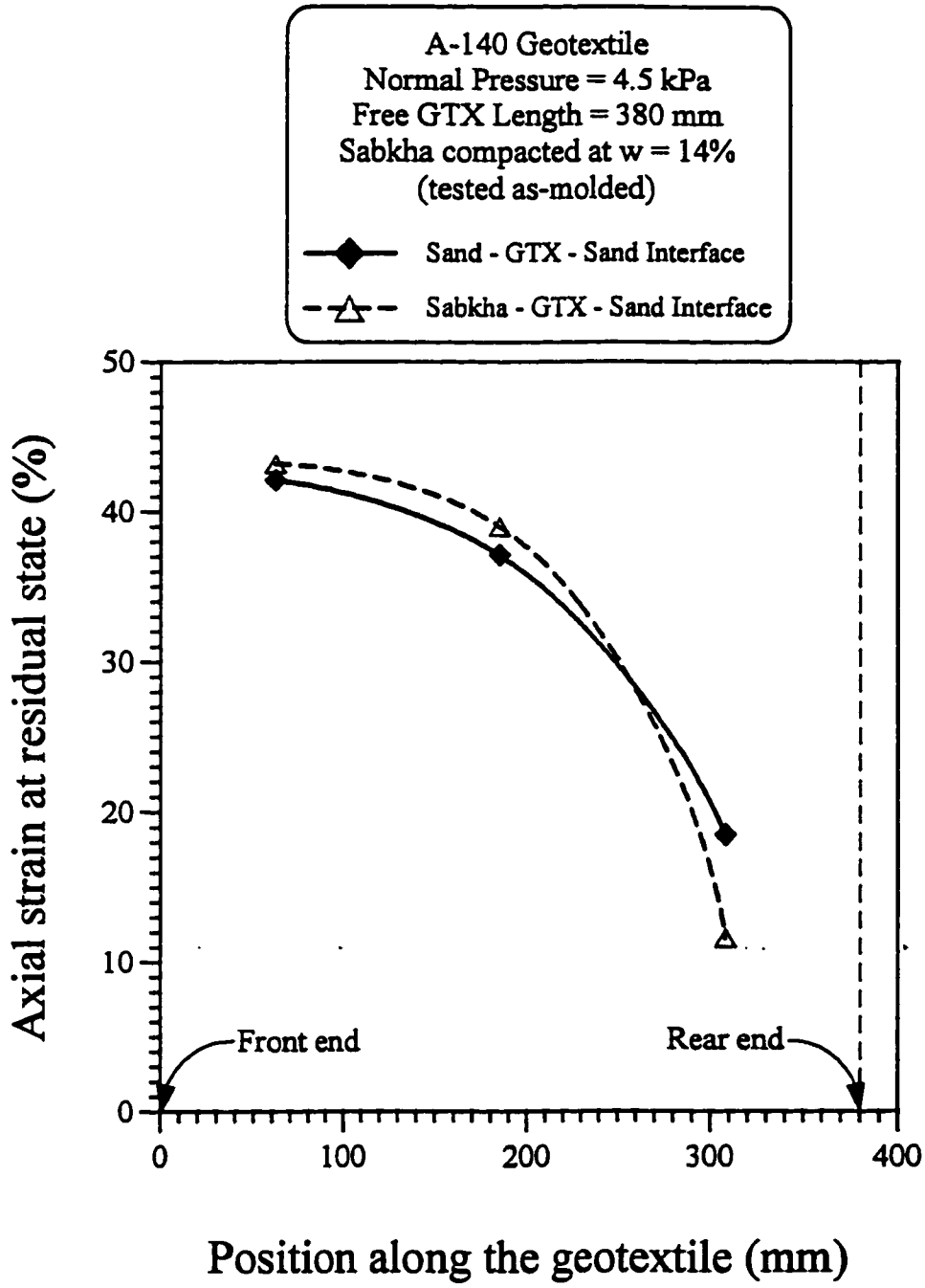

Fig. 4.73: Variation of the average axial strain at the residual state with the postion along the geotextile for A-140 Geotextile, 380 mm long free geotextile, at a normal pressure of 4.5 kPa with different soil-geotextile interfaces

only. Fig. 4.73 shows that the variation of strain is approximately similar for both interfaces. This is mainly due to the fact that the normal pressure is low and geotextile has high extensibility due to which it extends by 43% in the front portion while the strain in the rear portion is only 11%. It is observed, from Figs. 4.71, 4.72 and 4.73, that A-400 geotextile has only 27.4% strain in the front portion while the F-140 and A-140 geotextiles have strains greater than 35% in their front portion, when used in sand-GTX-sand interface.

Fig. 4.74 presents the variation of the shear stress at the residual state with the geotextile length for sand–A-400 GTX–sand and sabkha–A-400 GTX-sand interfaces. This figure shows that smaller values of shear stress are mobilized for sabkha–GTX–sand interfaces even for short geotextile lengths. However the shear stress mobilized in the 133 mm long geotextile sample in sabkha–A-400 GTX–sand interface was exceptionally low. The reason for this low value can be predicted from Fig. 4.61 which shows that the 133 mm long geotextile sample in sabkha–GTX–sand interface behaves like plate alone and very small value of shear stress was mobilized when the geotextile slipped out. This is mainly due to the lack of proper anchorage. This figure also shows that the sand has friction even for the short geotextiles whereas, the sabkha has very little friction and adhesion for A-400 geotextile. As discussed earlier, the 133 mm long geotextile sample is effected by the front wall roughness and confinement therefore, this particular size or length of geotextile sample did not produce any reliable results.

Fig. 4.75 presents a comparison of the overall average axial strain for sabkha–A-400 GTX–sand and sand–A-400 GTX–sand interfaces for different lengths. It is clear

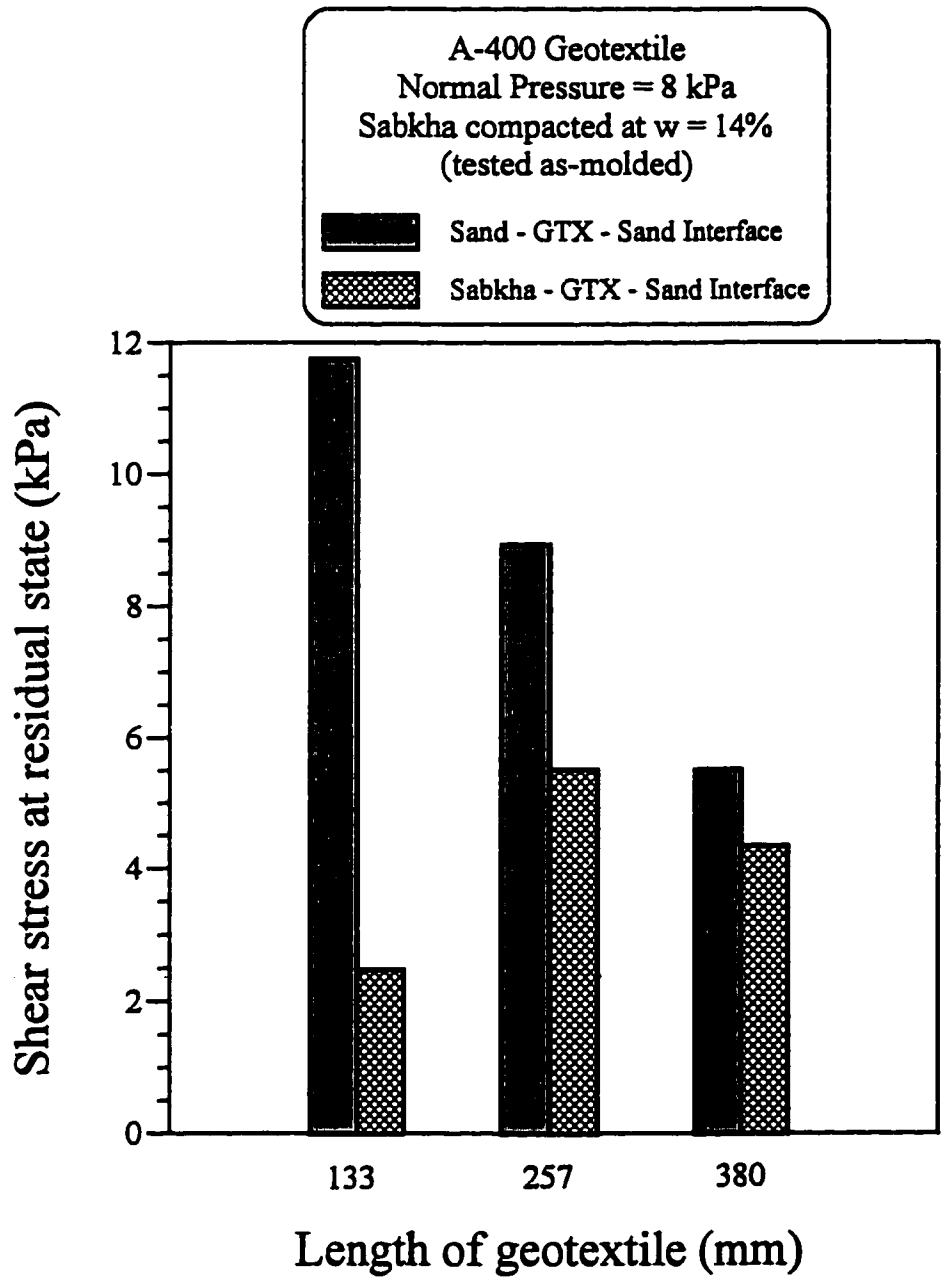

Fig. 4.74: Variation of the shear stress at the residual state with the geotextile length, at a normal pressure of 8 kPa for different soil-geotextile interfaces

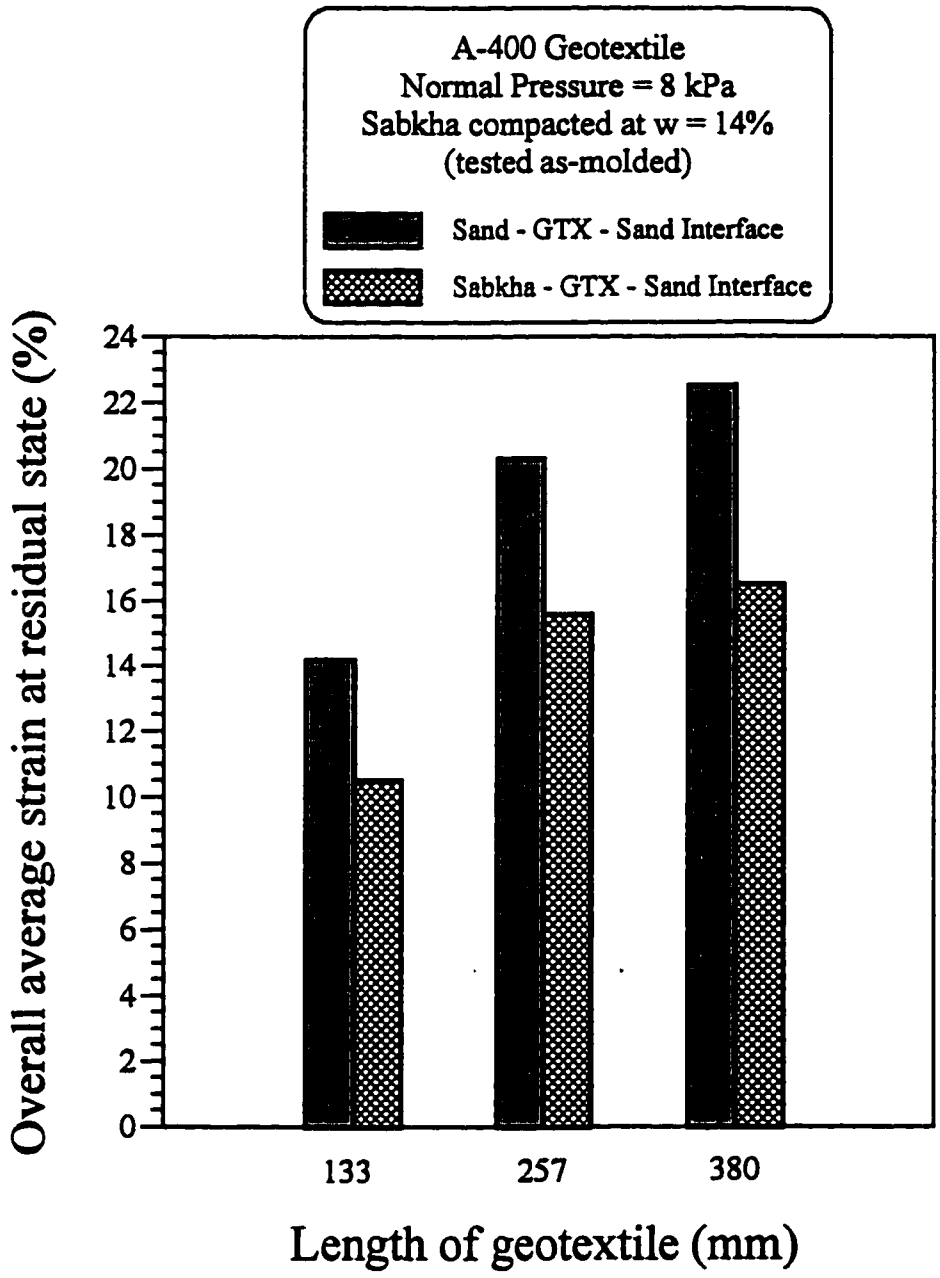

Fig. 4.75: Variation of the overall average axial strain at the residual state with the geotextile length, at normal pressure of 8 kPa for different soil-geotextile interfaces

from the figure that the A-400 geotextile is strained higher in the case of sand–GTX–sand interface, compared to that in sabkha–GTX–sand interface for all lengths. This is due to the fact that shear stresses are higher in the case of sand–GTX–sand interface, compared to that in sabkha–GTX–sand interface. This figure also shows that as the geotextile length increases the strain increases in the geotextile, which could be attributed to the fact that the geotextile gets properly anchored as the length increases.

Fig. 4.76 presents a comparison of the shear stress at residual state for dry and soaked condition for the two interfaces. In the case of dry or "as-molded" tests, higher values of shear stress are mobilized on sand–GTX–sand interface compared to sabkha-GTX-sand interface. Whereas, in the case of soaked test, higher values of shear stress are mobilized in sabkha–GTX–sand interface compared to sand-GTX-sand interface. The contribution of sabkha in the development of shear stresses on sabkha–GTX–sand interface has increased due to soaking. This could be attributed to the increase of the adhesion between the geotextile and the sabkha upon soaking. This increase resulted because when water becomes available to sabkha, the sabkha becomes very soft and sticky. In the case of sand–GTX–sand interface, the main cause of the increase in the shear stress is the capillary action in the sand layer above the geotextile. The effect of capillary action is also present in the case of sabkha–GTX–sand interface, but the adhesion from the sabkha is an additional contribution.

Fig. 4.77 presents the overall average axial strain at the residual state for both types of interfaces. The figure shows that as the sample is soaked the overall strain is

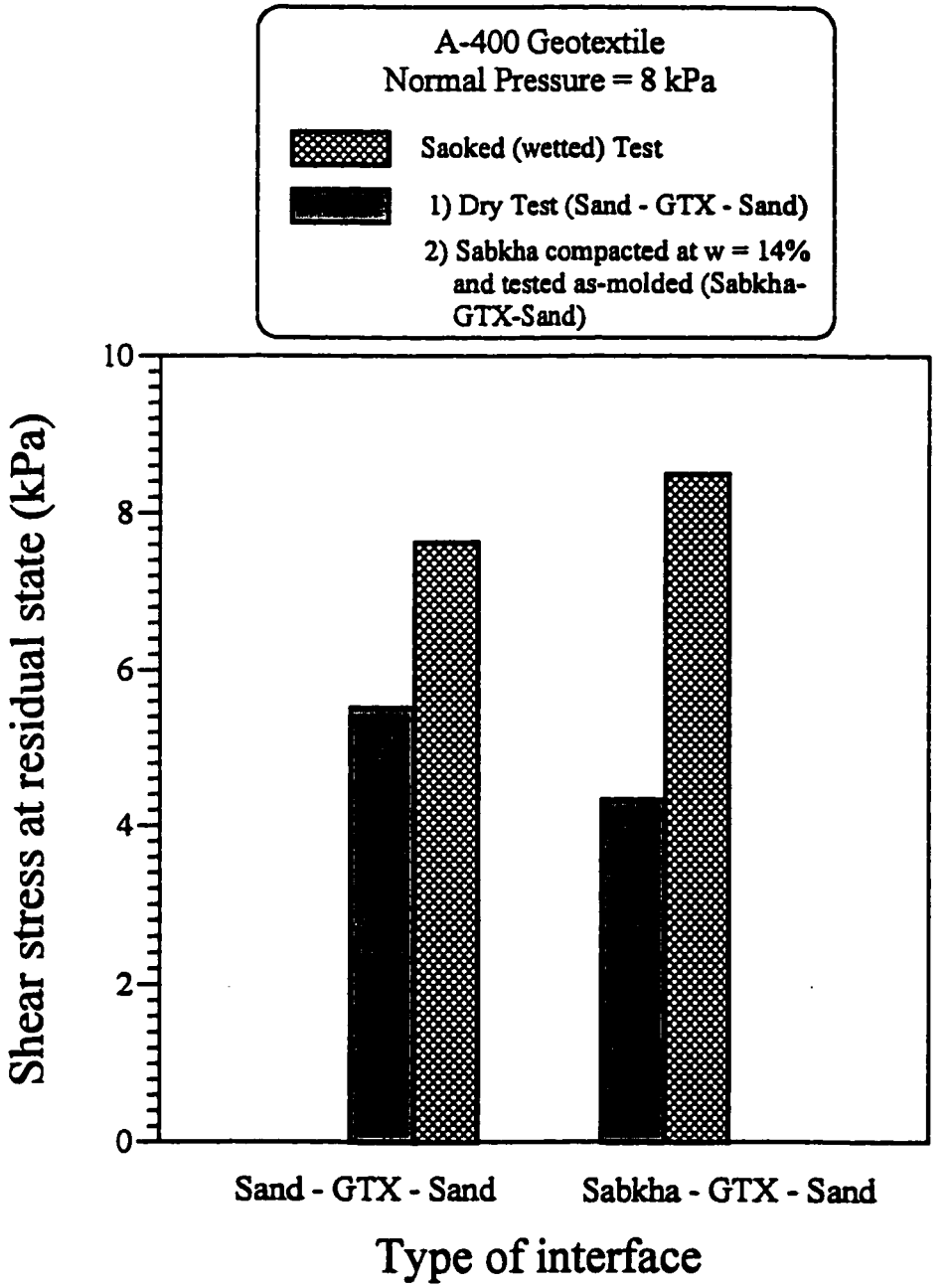

Fig. 4.76: Variation of the shear stress at the residual state with the type of interface for the A-400 geotextile under dry and soaked condition

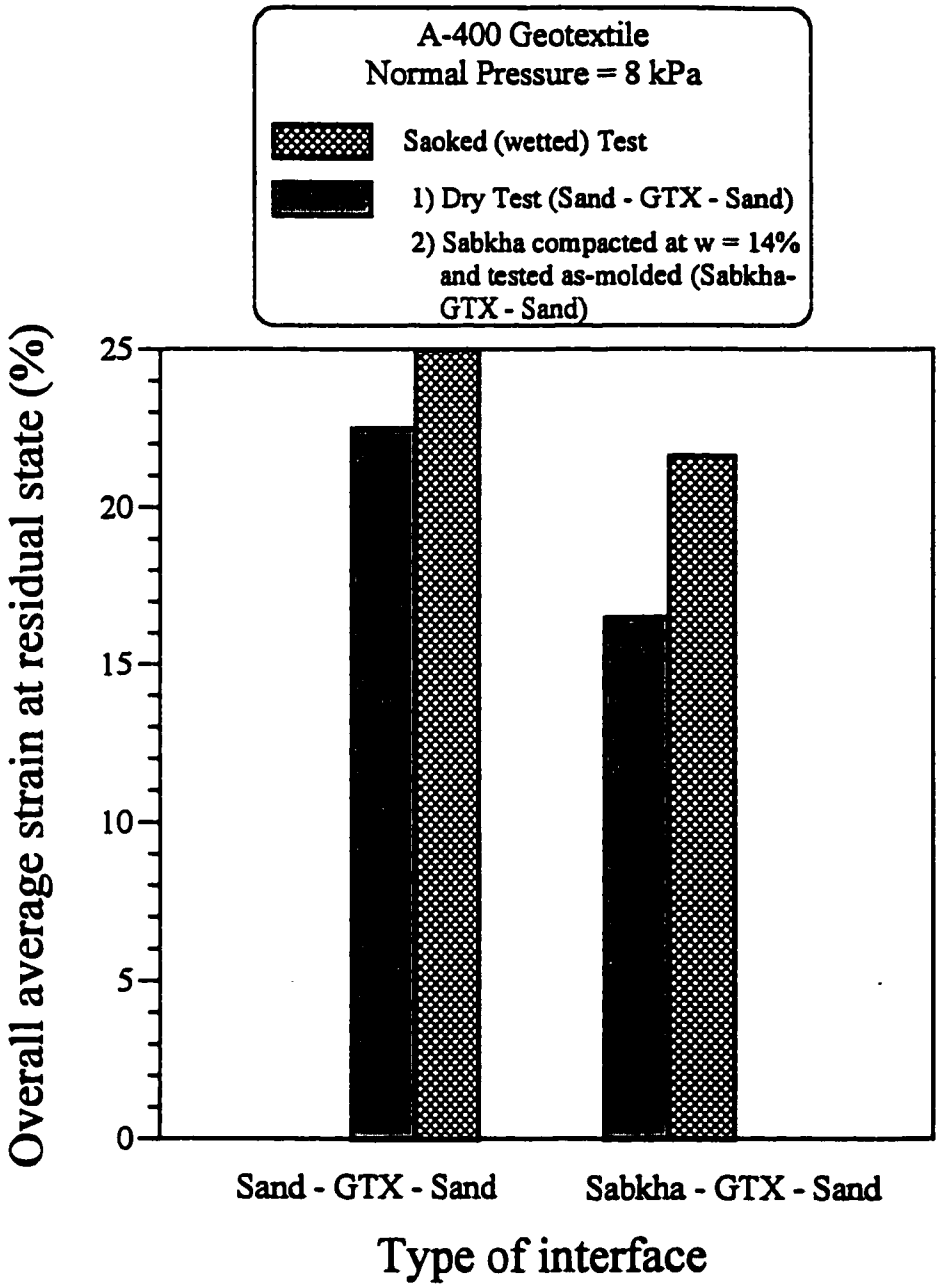

Fig. 4.77: Variation of the overall average strain at residual state with the type of interface for the A-400 geotextile under dry and soaked condition

increased. This is due to increase in the pull-out resistance upon soaking which is caused by the adhesion/suction developed between geotextile and soil.

4.9 Practical Application of Pull-out Test Data

One of the primary input parameters required in the design of soil structures reinforced with geosynthetics is the Interface Interaction Factor (c_i) of the geosynthetic material interacting with the soil. There are two design concepts in the reinforced earth structures:

1) Limiting Strain Concept
2) Allowable Design Load Concept

In the first case the movement of structure (for example reinforced retaining wall) is limited by a certain value. Using the pull-out test data it is possible to find the pull-out load corresponding to that strain percentage and then comparing that load with the tensile strength of the geotextile, to find out the factor of safety. If this factor of safety satisfies the design requirements then the design is considered adequate. In the allowable design load method the factor of safety is fixed and the corresponding allowable design pull-out load is determined. Using the data of the pull-out test one can find the percentage of strain for that pull-out load and if this strain value can be allowed in the field, the design would be considered adequate.

For the design of reinforced slopes, c_i value from pull-out test data is used to calculate the bond length behind the critical failure surface using the following equation:

$$\text{Bond length (L)} = \frac{P}{2 \times c_i \times \sigma_n \times \tan\phi} \qquad (4.7)$$

Where:

L = Bond or development length (m)

P = Pull-out load (kN/m)

σ_n = Normal pressure (kPa)

For the comparison of residual pull-out resistance with ultimate tensile strength of geotextile, a factor of safety has been calculated at the residual state in Table 4.19. This factor of safety corresponds to the residual state and is defined as follows:

$$F.S = \frac{\text{pull - out force at residual state}}{\text{Tensile strength of geotextile}} \qquad (4.8)$$

Table 4.19: Factor of safety available at residual state

Sand - GTX -Sand Interface			
Normal Pressure (kPa)	F.S.		
	A-400	A-140	F-140
4.5	6.8	9.0	4.0
8.0	5.5	3.7	1.9
16.0	4.2	3.6	1.7
Sabkha - GTX -Sand Interface			
Normal Pressure (kPa)	F.S.		
	A-400	A-140	F-140
4.5	12.9	7.6	3.6
8.0	7.3	6.5	1.7
16.0	6.1	5.1	1.2

CHAPTER 5

SUMMARY, CONCLUSIONS AND RECOMMENDATIONS

5.1 Summary

Sabkha soil is widely spread along the Arabian Gulf and Red Sea coasts and is known to be a problematic soil due to its acute water sensitivity. In many situations, there is a need to improve the load carrying capacity of sabkha and the use of geotextile for such purpose was found appropriate. The lack of information regarding pull-out resistance of locally available geotextile embedded within local soils, including sand and sabkha led to this experimental research program. The objectives of this research were to compare the pull-out resistance of non-woven geotextiles and to study the frictional characteristics of sand–geotextile–sand and sabkha–geotextile–sand interfaces, taking into account different parameters. An experimental setup was developed in the soil laboratory at KFUPM to carry out the pull-out tests. The experimental research involved characterization and

strength testing of Baggah sand and Ar-Riyas sabkha and the pull-out testing on geotextiles embedded in sand and sabkha soils. Normal applied pressure, geotextile type, geotextile length, water content and soil type were the five parameters that were investigated. Pull-out test results have indicated the existence of three stages of deformation in the geotextile under pull-out testing, which ultimately leads to the slippage of the entire length of the geotextile. This condition was labeled the residual state. The Interface characteristics were determined for this state, which is considered a limit for the pull-out resistance at failure.

5.2 Conclusions

In light of experimental work done on pull-out resistance of geotextile embedded in sand and sabkha soils, the following conclusions are drawn:

1- The undrained triaxial tests on sabkha soil show that cohesion decreases with the increase in moisture content for sample compacted on the Dry side of optimum, whereas the Angle of internal friction remains approximately constant. Soaking of the sabkha soil results in decrease in the angle of internal friction, however the cohesion value does not change very much.

2- It has been found that the stresses mobilized at the interface at any point on the geotextile, during the pull-out test, depend on the strain produced at that point. Therefore, as shown by the strain versus front end displacement curves, the strains are produced progressively and so are the stresses. This is the case for stresses lower than the residual value.

3- The A-400 geotextile produces the maximum pull-out resistance in the case of sand–GTX–sand interface while the F-140 geotextile produces the maximum pull-out resistance in the case of sabkha–GTX–sand interface. Accordingly, for sabkha soils it is recommended to use geotextiles with low extensibility such as the F-140 geotextile. This produces higher shear stresses at lower strain values.

4- The surface texture and permeability of the geotextile are two important properties that should be considered alongwith the tensile strength and elongation at rupture for the selection of a geotextile for reinforcement purposes.

5- For the A-140 geotextile, the strains are concentrated mostly in the front part and extensive necking was observed after the test. Therefore, it is recommended not to use geotextiles with low tensile strength and high extensibility such as the A-140 geotextile for reinforcement application due to the large deformations occurring in the soil mass.

6- The shear stress versus normal stress graphs show that the interfaces do not obey Mohr-Coulombs law even though the angle of interface friction depends on applied normal pressure. This means that the effect of dilatancy is pronounced more at the relatively "low" normal pressure values.

7- The results of the pull-out tests on the 133 mm long geotextiles are very much affected by the lateral earth pressure developed on the front wall of the pull-out box. Whereas in the 380 mm long geotextile, this effect is not very much pronounced. Therefore, short lengths of geotextile should be avoided in predicting the pull-out behavior.

8- The shear strength of soil–geotextile interface depends on the geotextile length. The longer the sample, the lower would be the shear strength due to the progressive failure

along the interface. This is mainly because some parts of the geotextile (front portions) are extending while the rare portions have lower elongation and therefore, such portions are not yet activated.

9- The angle of interface friction at peak stress state is affected by the assumption that the pull-out force is equally distributed over the length of the geotextile. Therefore, as this assumption becomes less accurate, at peak stress, the corresponding interface friction will be also less accurate.

10- As the length of the geotextile decreases, necking in the sample is reduced even at the end of test. This is due to the lack of enough anchorage, which reduces the magnitude of strain in the geotextile due to slippage.

11- Under the same normal pressure values, low tensile strength geotextiles are subjected to higher necking as compared to geotextiles with high tensile strength. As the normal pressure increases, more necking is observed in the samples and strains are concentrated in the front portion of geotextile.

12- Soaking of the sabkha soil improved the shear stresses mobilized on the sabkha-geotextile interface due to the development of adhesion between the geotextile and the sabkha soil.

13- The Interface Interaction Factor is not a constant value. For a given dimension of geotextile specimen, it is dependent on the confining pressure, geotextile type, soil type, and the magnitude of relative displacement at the interface.

5.3 Recommendations for Future Study

Following are the recommendations based on the experimental findings:

1- Pull-out test should be performed on F-140 geotextile in the case of soaked condition of sabkha to check the effect of soaking using this geotextile.

2- The size of the pull-out box should be increased to accommodate longer geotextile and larger normal stresses.

3- In order to study the effect of dilitancy the pull-out test should be performed at wide range of normal stress (high and low).

4- The front end of the geotextile should be positioned far from the front wall as practical as possible.

5- Pull-out resistance of geotextile should be studied for other soil types like marl and steel slag aggregates.

6- Pull-out tests should be performed by soaking the upper and lower soil layers in sand-GTX-sand and sabkha-GTX-sand interface (full soaking) to study the effect of flooding.

References

Abduljauwad, S. N., Fouad Bayomy, Abdul-Karim Al-sheikh, and Omar S. Baghabra Al-Amoudi (1994). "Influence of geotextile on performance of saline sebkha soil", *ASCE Journal of Geotechnical Engineering*, Vol. 120, No. 11, Nov. 1994, pp. 1939-1960.

Aiban, S. A., Al-Abdul Wahhab H. I., Al-Amoudi, O. S. B. (1994). "Identification, evaluation and reinforcement of eastern Saudi soils for constructional purposes", *Progress report no. 1, KACST*, Oct. 6, 1994, pp. 11-37.

Aiban, S. A., Al-Abdul Wahhab H. I., Al-Amoudi, O. S. B. (1999). "Identification, evaluation and reinforcement of eastern Saudi soils for constructional purposes", *Final report, KACST*, Vol. 5, 1999

Aiban, S. A., Al-Amoudi, O. S. B., Ahmed H. R., Al-Abdul Wahhab H. I., (1998). "Characterization and stabilization of eastern Saudi calcareous soils", *Proceedings of Fourteenth International Conference on Soil Mechanics and Foundation Engineering*, Atlanta, Vol. 1, pp. 13-16.

Akili, W. and Fletcher, E. H. (1978). "Ground condition for housing in Dhahran region, Eastern province, Saudi Arabia", *Proceedings, 1st International Conference on Housing Problems in Developing Countries*, Dhahran, Vol. 2, pp. 533-546.

Al-Amoudi, O. S. B, Abdul jauwad, S. N., El- Naggar, Z. R. and Rasheeduzafar (1992b). "Response of sabkha to laboratory tests: A case study", *Engineering Geology*, Vol. 33, No. 2, pp. 111-125.

Al-Amoudi, O. S. B. (1994) "A State-of-the-art report on the geotechnical problems in sabkha soils and methods of treatment", *Proc., ASCE-SAS First Regional Conference and Exhibition, Bahrain*, pp. 53-77.

Al-Amoudi, O. S. B. and Abdul jauwad S. N. (1995). "Compressibility and collapse characteristics of arid saline sabkha soils", *Engineering Geology*, Vol. 39, pp. 185-202.

Al-Amoudi, O. S. B., Abdul Jauwad, S. N., Rasheeduzzafar and Maslehuddin, M (1992a). "Effect of chloride and sulfate contamination in soils on corrosion of steel and Concrete", *Transportation Research Record*, No 1345, pp. 67-73.

Alfaro, M. C. and Miura, N. (1995). "Soil-geogrid reinforcement interaction by pull-out and direct shear test", ASTM, *Geotechnical Testing Journal*, Vol. 18, pp. 157-167.

Alobaidi, I. M., Hoare, D. J., and Ghataora, G. S. (1997). "Load transfer mechanism in pull-out tests" *Geosynthetics International*, Vol. 4, No. 5, pp.509-521.

Al-Sheikh, Abdul Karim. (1998). Personal Communication with the material engineer, Isaam Kabani and Partners, Khobar - Dammam Highway, Al-Khobar, Saudi Arabia.

Amoco Fabrics and Fibers Company (1993). "Technical note No. 1: Geosynthetic functions", *Amoco Company Brochure*, pp. 1-6.

Bergado, D. T., Hardiyatino, H.C., Cisneros, c. b., Chun, C. J., Alfaro, M. C., Balasubramanium, A. S., and Anderson, L. R., (1992). "Pull out resistance of steel geogrid with weathered clay as backfill material", ASTM *Geotechnical Testing Journal*, Vol. 15, No. 1, pp. 33-46.

Bourdeau, Y., Ogunro, T., Lareal, P., Riondy, G. (1994). "Use of strain gages to predict soil-geotextile interaction in pull-out tests", *Fifth Int. Conf. on Geotextiles, Geomembranes and related products*, Singapore, Sep. 1994, pp. 451-456.

Boyle, S. R., Gallagher M. and Holtz, R. D. (1996). "Influence of strain rate, specimen length and confinement on measured geotextile properties", *Geosynthetics International*, Vol. 3, No. 2, pp. 205-225.

Chang, D. T. T. and Wey, W. T. (1993). "Study on geotextile behaviors of tensile strength and pull-out capacity", *Geosynthetic 93 proceedings*, Vancouver, Canada, pp. 607.

Collios, A., Delmas, P., Gourc, J. P. and Giroud, J. P. (1980). "Experiments on soil reinforcement with Geotextile", *The use of geotextile for soil improvement*, ASCE National Convention, Portland, Oregon, U.S.A, April 1980, pp. 53-73.

Cowell, M. J. and Sprague, C. J., "Comparison of pull-out performance of geogrids and geotextiles", *Proceedings Geosynthetics 93*, Vancouver, Canada, pp. 579-592.

Ellis, G. I. (1973). "Arabian salt-bearing soil (sabkha) as an engineering material", *TRRL Report, LR 523*, Crowthrone, Bershire, England.

Espinoza, R. D. and David (1994). "Soil–geotextile interaction: evaluation of membrane support", *Geotextiles and Geomembranes*, Vol. 13, No. 5, pp. 281-293.

Fannin, R. J. and Raju, D. M. (1993). "On the pull-out resistance of geosynthetics", *Canadian Geotechnical Journal*, Vol. 30, pp. 409-417.

Fannin, R. J. and Raju, D. M. (1991). "Pull-out resistance of geosynthetics", *Proceedings of 44th Canadian Geotechnical Conf.*, Vol. 2, pp. 81/1-81/8.

Farrag, K. (1995). "Evaluation of the effect of moisture content on the interface properties

of geosynthetics", *Geosynthetics 95 Proceedings*, Vol. 3, pp. 1031-1041.

Fibertex non-wovens, (1995). "Fibertex non-wovens, hydraulic works – coastal protection construction sheet", Fibertex Company Brochure, Sheet 611, pp. 1-3 and Sheet 619, pp. 1-3.

Forsman, J. and Slunga, E. (1994), "The interface friction and anchor capacity of synthetic georeinforcements, *Fifth Int. Conf. on Geotextiles, Geomembranes and related products*, Singapore, Sep. 1994, pp. 405-410.

Fourie, A. B. and Fabian K. J. (1987). "Laboratory determination of clay-geotextile interaction", *Geotextiles and Geomembranes*, Vol. 6 , pp. 275-294.

Hari, D. Sharma, Donald E. Hullings (1997). "Interface strength tests and application to landfill design", *Geosynthetic 97 Proceedings*, Vol. 2, pp. 913-926.

Imaizumi, S., Nishigata, T and Limura, K. (1994) "Effect of variation in sample sizes on soil-polymer interface strength", *Fifth Intl. Conference on Geotextile, Geomembranes and related products*, Singapore, pp. 423-426.

Imtiaz Ahmed (1997). Improvement of eastern Saudi sabkha soils for road construction, *M.S. Thesis, Department of Civil Engineering, King Fahd University of Petroleum and Minerals*, Dhahran, Saudi Arabia.

Ingold, T. S. (1982). "Some observations on the laboratory measurements of soil-geotextile Bond", *Geotechnical Testing Journal*, GTJODJ, Vol. 5, No. 3/4, Sept./Dec. 1982, pp. 57-67.

Ingold, T. S. (1984). " A laboratory investigation of soil-geotextile friction", *Ground Engineering*, Vol. 17, No. 18, pp. 21-28.

John, N. W. M. (1986). Geotextiles, First edition by Blackie 1986 by Chapman and Hall, NewYork, pp. 1-34.

Johnson, H., Kamal, M. R., Pierson, G. O and Ramsay, J. B. (1978). "Sabkhas of eastern Saudi Arabia", in Al-Sayari, S. S and Zotl, J. G (Ed) *Quaternary Period in Saudi Arabia*, Springer-Verlag, Austria, pp. 84-93.

Juran, I. and Christopher, B. R. (1989). "Laboratory model study on geosynthetic reinforced soil retaining wall", *Journal of Geotechnical Engineering*", ACSE, Vol. 115, No. 7, pp. 905-926.

Kabeya, H., Karmorkar, A. K., Kamata, Y. (1993), "Influence of surface roughness of woven geotextiles on interfacial frictional behavior - Evaluation through model experiments", *Textile Research Journal*, Vol. 63, No. 10. pp. 604-610.

Karmokar, K. A. and Kabeya, H. (1998). "An approach to analyze the pull-out resistance of woven geotextile", *Sixth International Conference on Geosynthetics*, Vol. 1, pp. 725-728.

Kharchafi, M., and Dysli, M. (1993). "Study of soil-geotextile interaction by an x-ray method", *Geotextiles and Geomembranes*, Vol. 12, pp. 307-325.

Khera, Raj. P., Ram, M. R., M. Khair ul alam, Issa, S. Oweis (1997). "Depth and width effect on pull out resistance of woven geotextiles in sand", *Geosynthetic 97 Proceedings*, Vol. 2, pp. 851-862.

Koerner, R. M. (1997). Designing with geosynthetics, Fifth Edition 1997 by Prentice–Hall Inc., pp. 67-203.

Koutsourais, M., Sandri, D. and Swan R. (1998). "Soil interaction characteristics of geotextiles and geogrid", *Proc., Sixth International Conference On Geosynthetics,* Vol. 1, pp. 739-744.

Lo, S. C. R. (1998). "Pull-out resistance of polyester strap at low overburden stress", *Geosynthetic International,* Vol. 5, No. 4 1998, pp. 361-382.

Long, P. V., Bergado, D. T., Balasubramanium, A. S., and Delmas, P. (1997). "Interaction between soil and geotextile reinforcement", *Proceedings, Ist national Conference ASCE Geo-Institute, Geotechnical Special Publication,* Vol. 69, pp. 560-578.

Lopes, M. L. and Ladeira, M. (1996) " Role of specimen geometry, soil height and sleeve length on the pull out behavior of gogrids", *Geosynthetics International,* Vol. 3, No. 6, pp. 701-719.

Madhav, M. R.; Gurrung. N. and Iwao, Y. (1998). "A theoretical model for the pull-out response of geosynthetic reinforcement", *Geosynthetics International,* Vol. 5, No. 4, pp. 399-424.

Mallick, S. B. and Zhai, H. (1995). "A laboratory study on pull out performance of woven Geotextile", *Geosynthetic 95 Proceedings,* Vol. 3, pp. 1169-1178.

Mallick, S. B. and Zhai, H. (1996). "Pull-out and direct shear testing of geosynthetic reinforcement state-of-the art report", *Transportation Research Record,* No. 1534, Nov. 1996, pp. 80-90.

Mallick, S. B., Elton, D. J. (1997). "An experimental characterization of soil–woven geotextile interface in large box pull out test", *Geosynthetic 97 Proceedings*, Vol. 2, pp. 927-939.

Martin, J. P., Koerner, R. M. and Whitty, J. E. (1984). "Experimental friction evaluation of slippage between geomembranes, geotextiles and soils", *Proceedings of International Conference On Geomembranes*, Denver, U.S.A, pp. 191-196.

Miyamori, T.; Iwai, S. and Makiuchi, K. (1986). "Frictional characteristics of non-woven fabrics", *Third International Conference on Geotextiles*, Vienna, Austria, pp. 701-715.

Murthy, B. R. S., Sridharan, A., Bindumadhava, (1993). "Evaluation of interfacial frictional resistance", *Geotextiles and Geomembranes*, Vol. 12 , pp. 235-253.

Palmeira, E. M., and Milligan, G. W. E. (1989). "Scale and other factors affecting the results of pull out test of grid burried in sand", *Geotechnique*, Vol. 39, No. 3, pp. 511-524.

Rao, G. V. and Pandey, S. K. (1988). "Evaluation of geotextile–soil friction", *Indian Geotechnical Journal*, Vol. 18, No.1, pp.77-105.

Richards, E.A. and Scott, J. D. (1985). "Soil-geotextile frictional properties", *Proceedings, Second Canadian Symposium on Geotextile and Geomembranes*, Edmonton, Alberta, Canada, September 1985, pp. 13-24.

Rowe, R. K., Ho, S. K. and Fisher, D. G. (1985). "Determination of soil-geotextile Interface strength properties" *Proceedings, Second Canadian Symposium on*

Geotextile and Geomembranes, Edmonton, Alberta, Canada, September 1985, pp. 25-34.

Russel, R. B. C. (1974). Chemical and physical properties of sabkha-type materials, *TRRL Supplymentary Report 79 UC*, Crowthrone, Berkshire.

Schlosser, F., and Elias, V. (1978). "Friction in reinforced earth", *Proceedings ASCE Syposium, Earth Reinforcement*, Pittsburg, PA, pp. 735-763.

Shingenori, H. and Marolo, C. (1996). "Dilatancy effects of granular soil on the pull-out resistance of strip reinforcement", *Earth Reinforcement* edited by Hidetoshi Ochiai, Noriyuki Yasufuku ,Vol. 1, pp. 39-44.

Stipho, A. S. (1989). "Some engineering properties of stabilized saline soil", *Engineering Geology*, Vol. 26, pp. 181-197.

Swan, R. H. (1987). "The influence of fabric geometry on soil / geotextile shear strength", *Geotextiles and Geomembranes*, Vol. 6, pp. 81-87.

Tzong, W. H. and Cheng-Kuang, S. (1987). "Soil-geotextile interaction mechanism in pull-out test", *Proceedings Geosynthetics 1987 Conference*, New Orleans, U.S.A, Vol. 1-2, pp. 250-259.

William, N. D. and Houlihan, M. F. (1987). "Evaluation of interface friction properties between geosynthetics and soil" *Proceedings Geosynthetics 1987 Conference*, New Orleans, U.S.A, pp. 616-627.

Wislon-Fahmy, R. F., and Koerner, R. M. (1994). "Long term pull-out behavior of polymeric geogrid", ASCE, *Journal of Geotechnical Engineering*, Vol. 121, No. 10, pp. 723-728.

Yehia, E. El-Mogahzy, Yaser Gowayed and David Elton (1994). "Theory of soil / geotextile interaction", *Textile Research Journal*, Vol. 64, No. 12, pp. 744-755.

Zhai, Honglian, Mallick, S. B., Elton, David and Adanur, Sabit (1996). "Performance evaluation of nonwoven geotextile in soil–fabric interaction", *Textile Research Journal*, Vol. 66, No. 4, pp. 269-276.

Appendix - A

Data for sand-GTX-sand interface

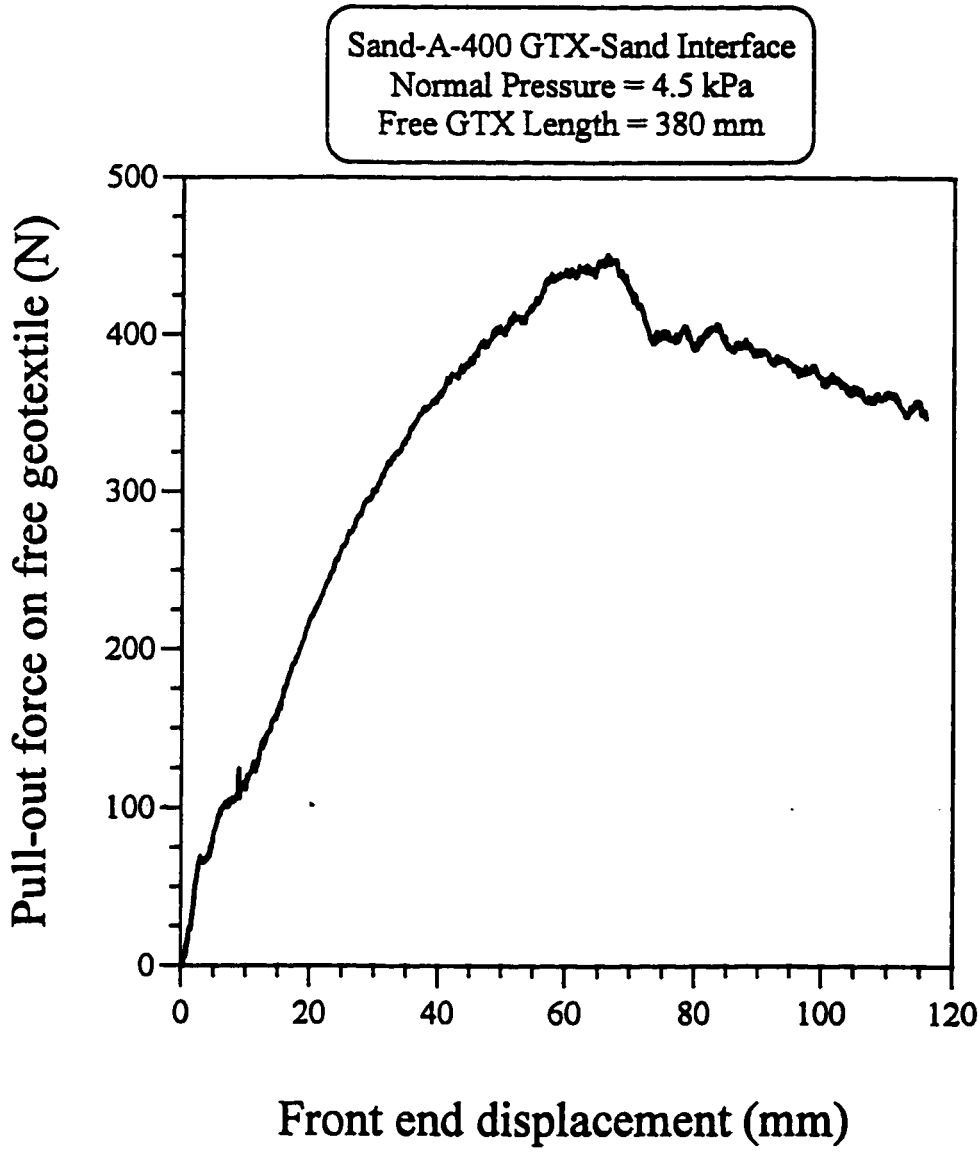

Fig. A1.1: Variation of the pull-out force on A-400 geotextile with the front end displacement for sand-GTX-sand interface, at 4.5 kPa normal pressure, and 380 mm long free geotextile

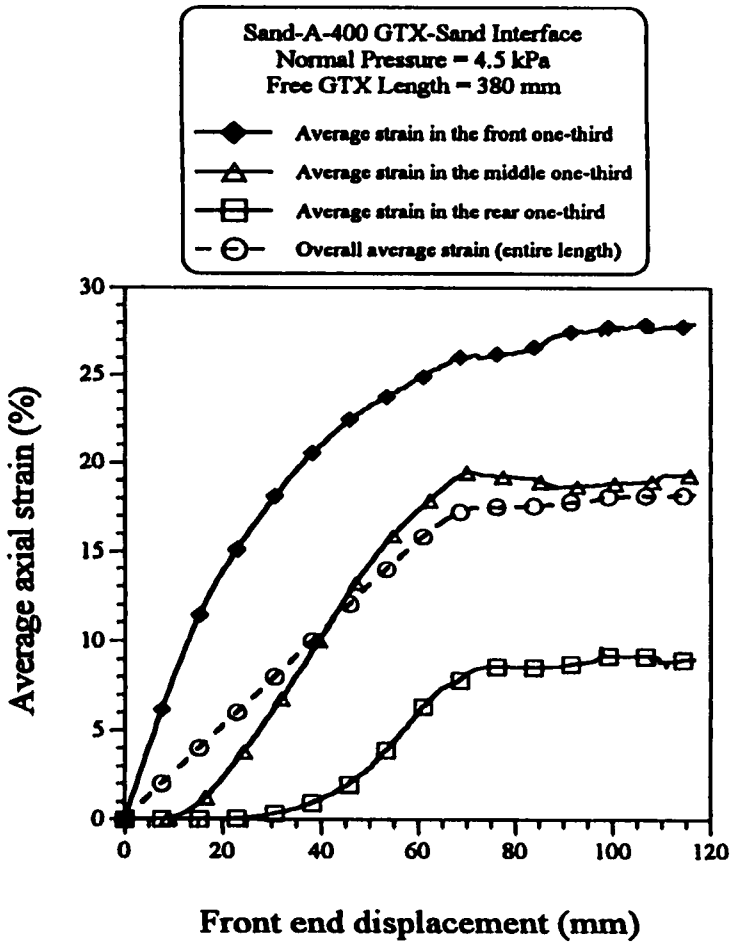

Fig. A1.2: Variation of the average axial strain of A-400 geotextile with the front end displacement for sand-GTX-sand interface, at 4.5 kPa normal pressure, and 380 mm long free geotextile

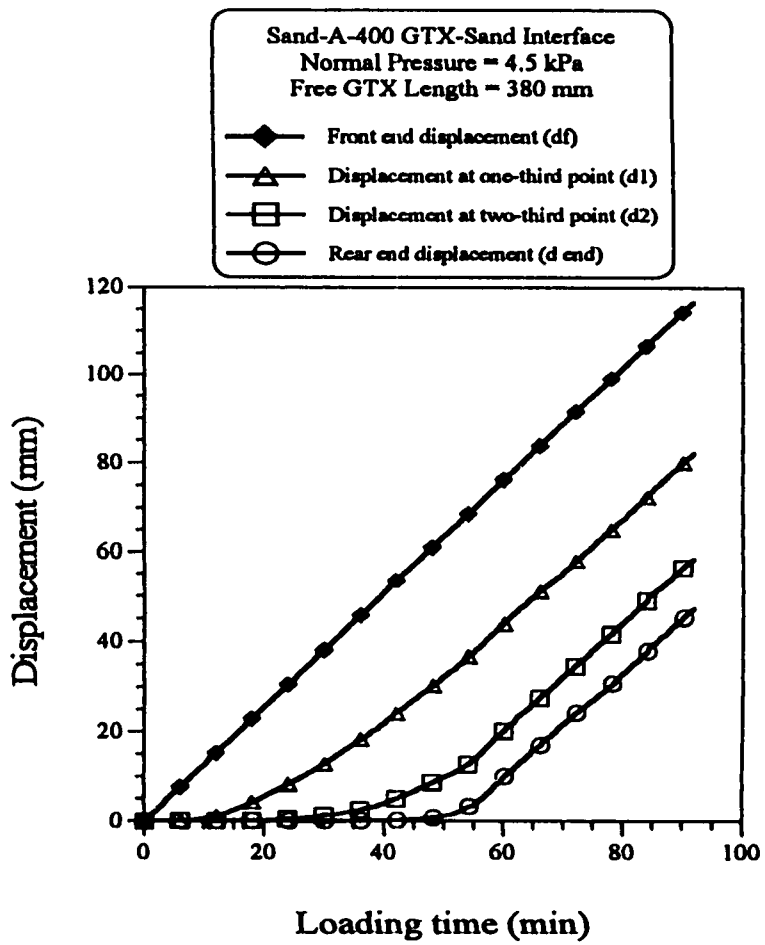

Fig. A1.3: Variation of the displacement of A-400 geotextile with loading time for sand-GTX-sand interface, at 4.5 kPa normal pressure, and 380 mm long free geotextile

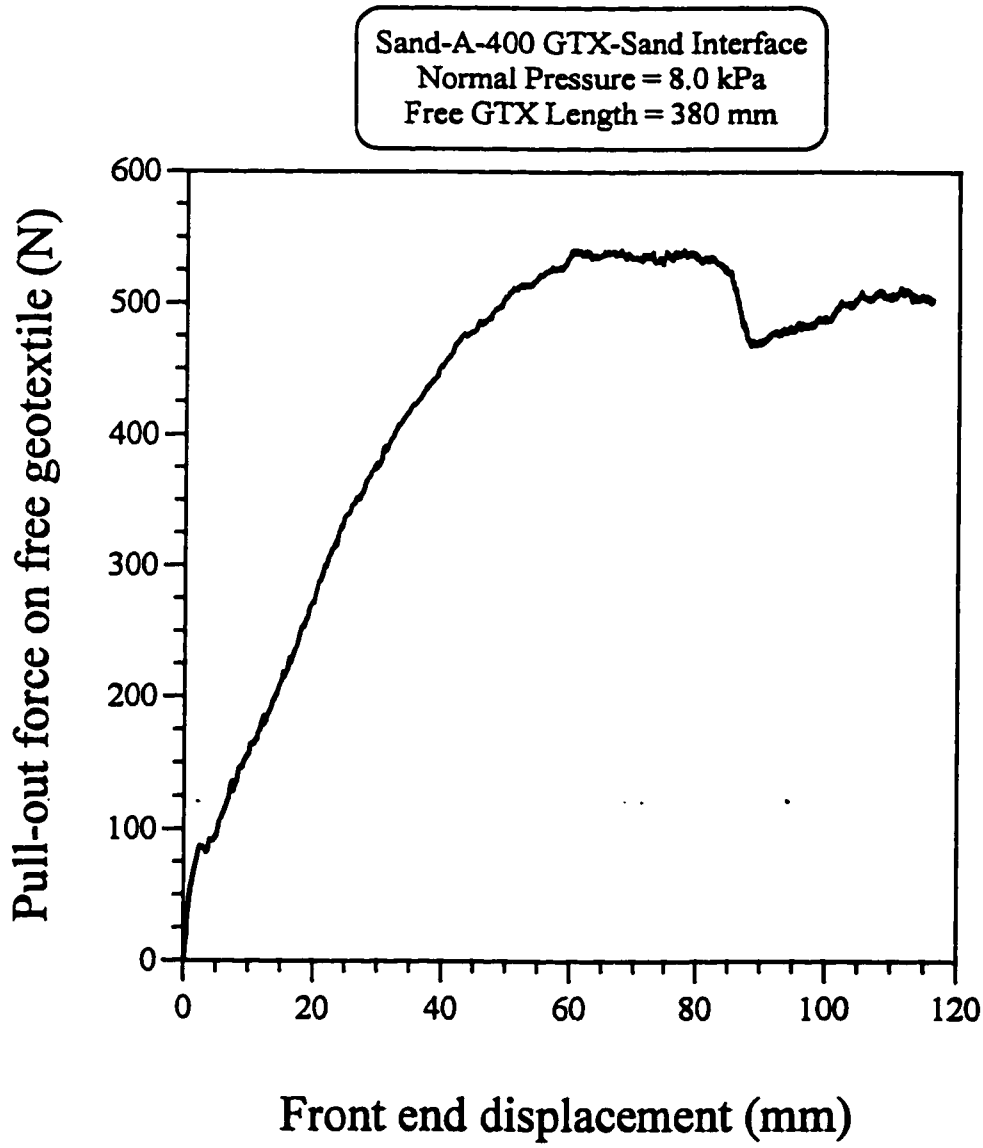

Fig. A1.4: Variation of the pull-out force on A-400 geotextile with front end displacement for sand-GTX-sand interface, under 8.0 kPa normal pressure, and 380 mm long free geotextile

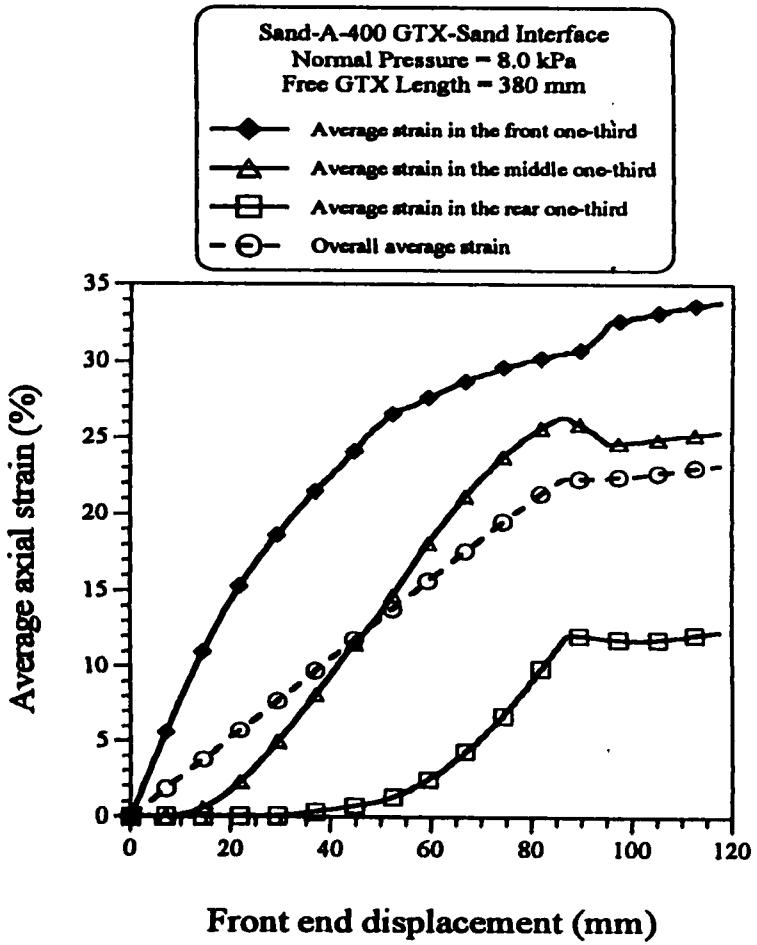

Fig. A1.5: Variation of average axial strain of A-400 geotextile with front end displacement for sand-GTX-sand interface, under 8.0 kPa normal pressure, and 380 mm long free geotextile

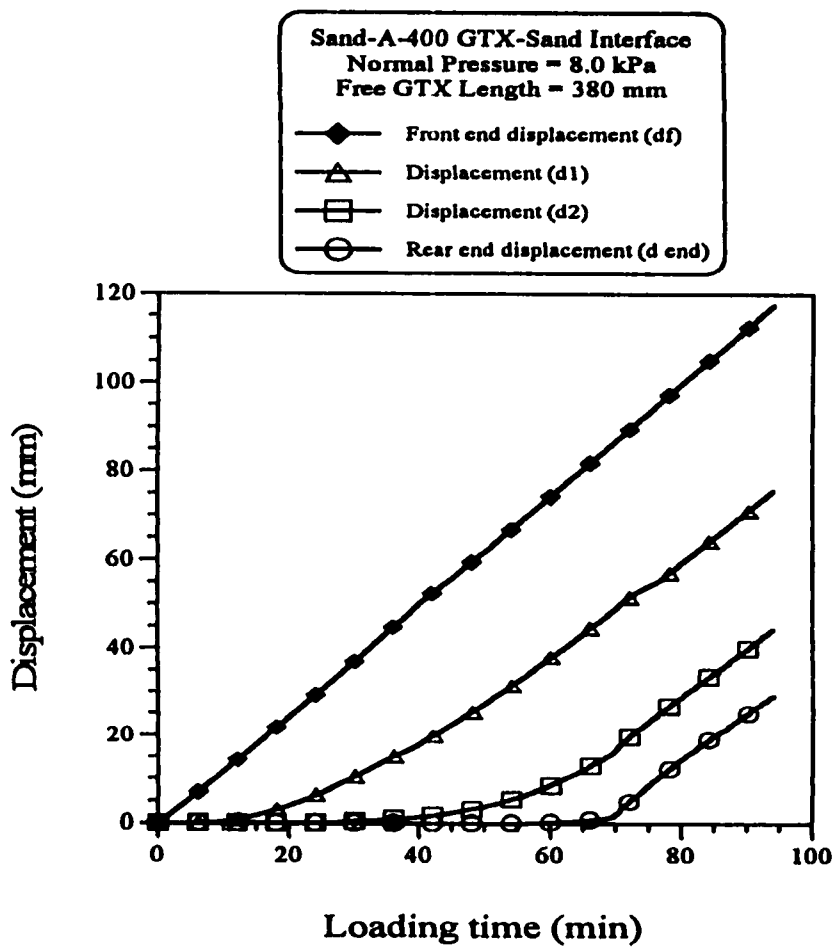

Fig. A1.6: Variation of displacement of A-400 geotextile with loading time for sand-GTX-sand interface, under 8.0 kPa normal pressure, and 380 mm long free geotextile

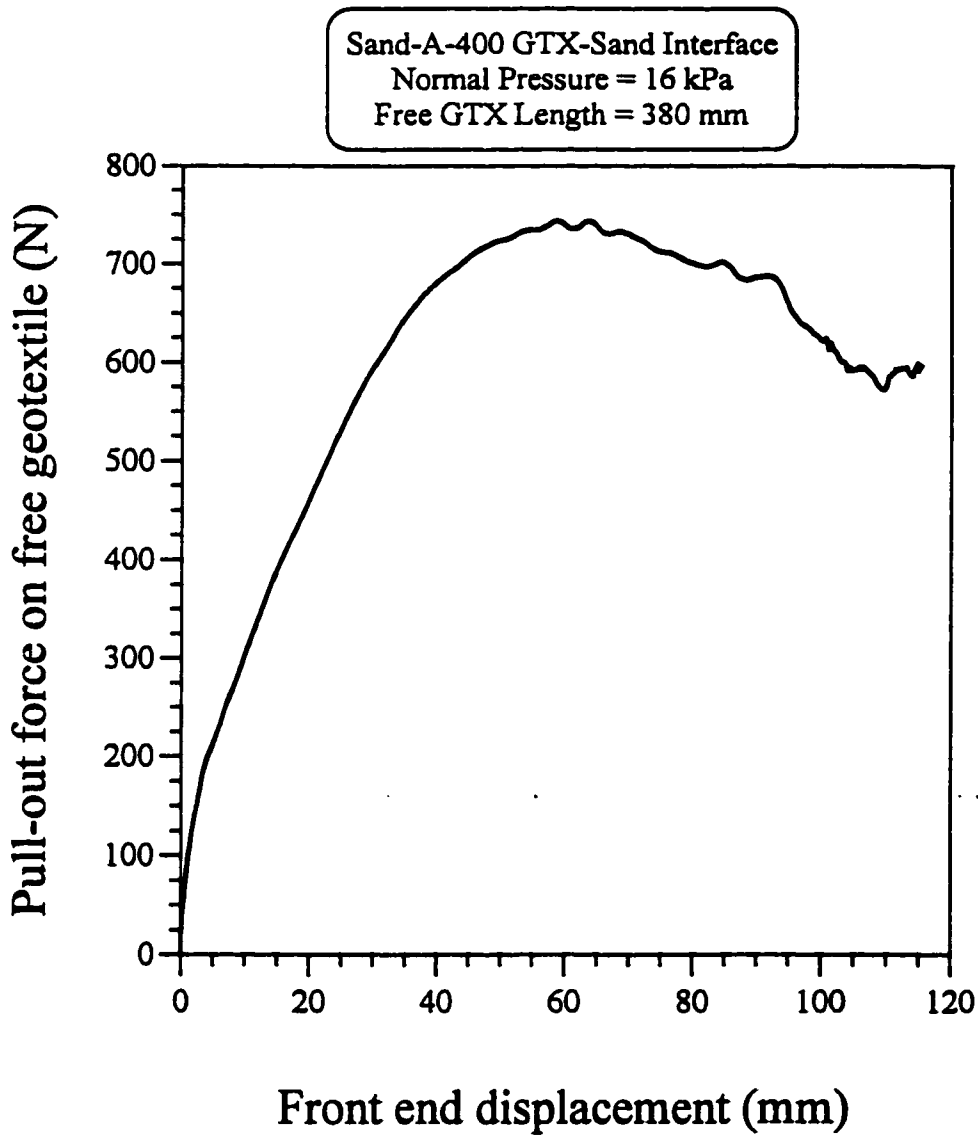

Fig. A1.7: Variation of the pull-out force on A-400 geotextile with front end displacement for sand-GTX-sand interface, under 16 kPa normal pressure, and 380 mm long free geotextile

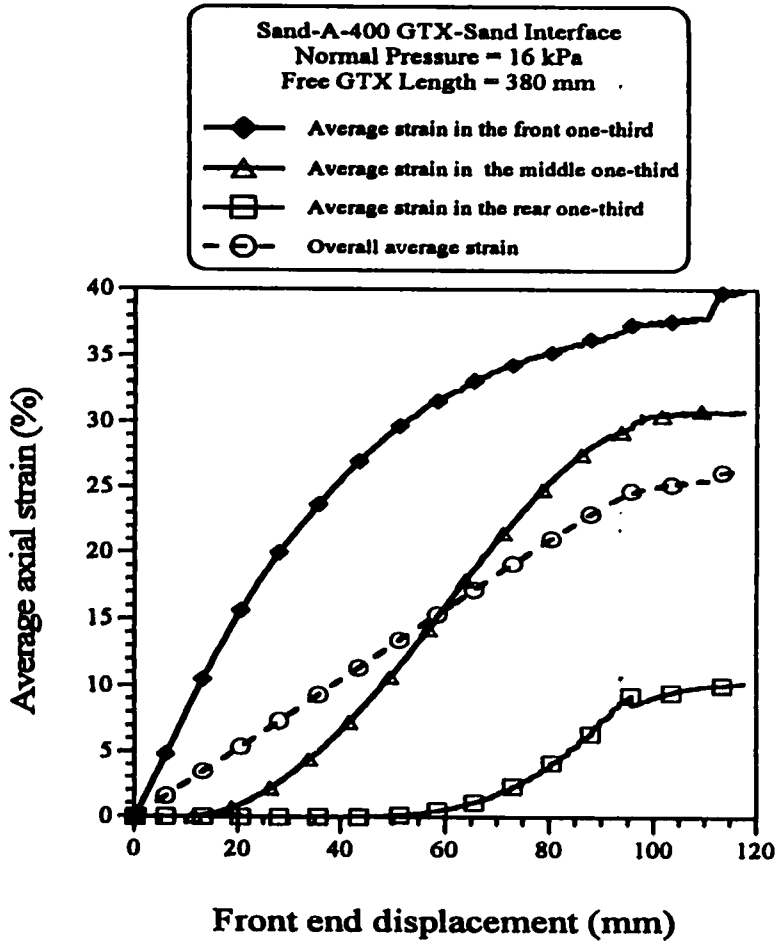

Fig. A1.8: Variation of average axial strain of A-400 geotextile with front end displacement for sand-GTX-sand interface, under 16 kPa normal pressure, and 380 mm long free geotextile

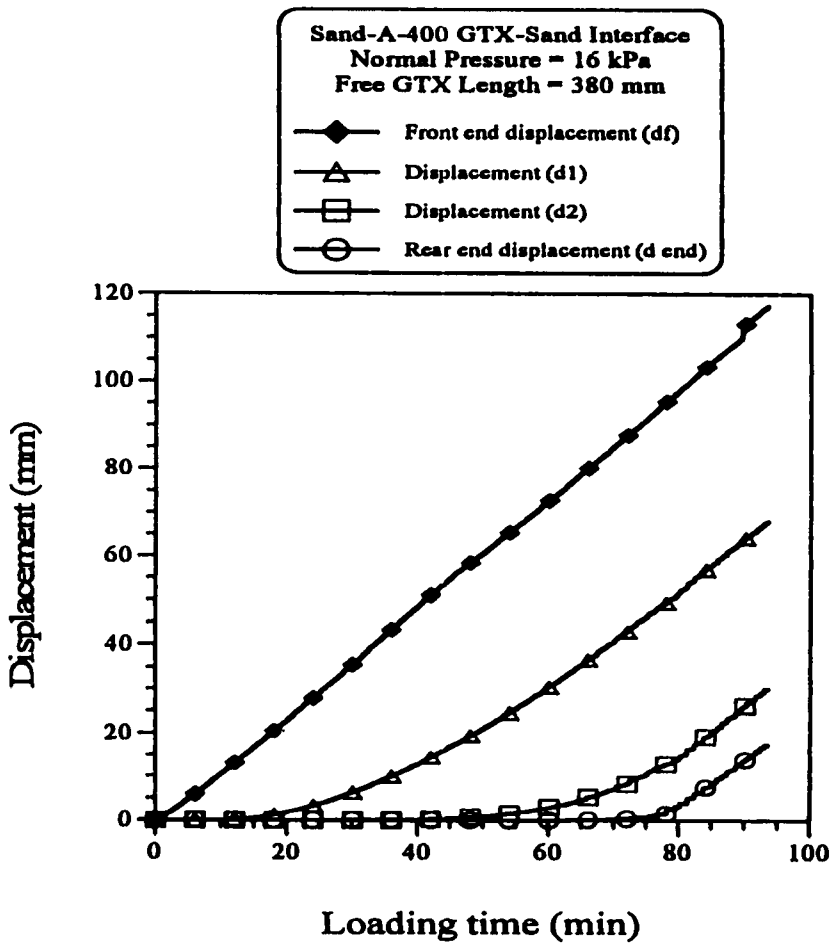

Fig. A1.9: Variation of displacement of A-400 geotextile with loading time for sand-GTX-sand interface, under 16 kPa normal pressure, and 380 mm long free geotextile

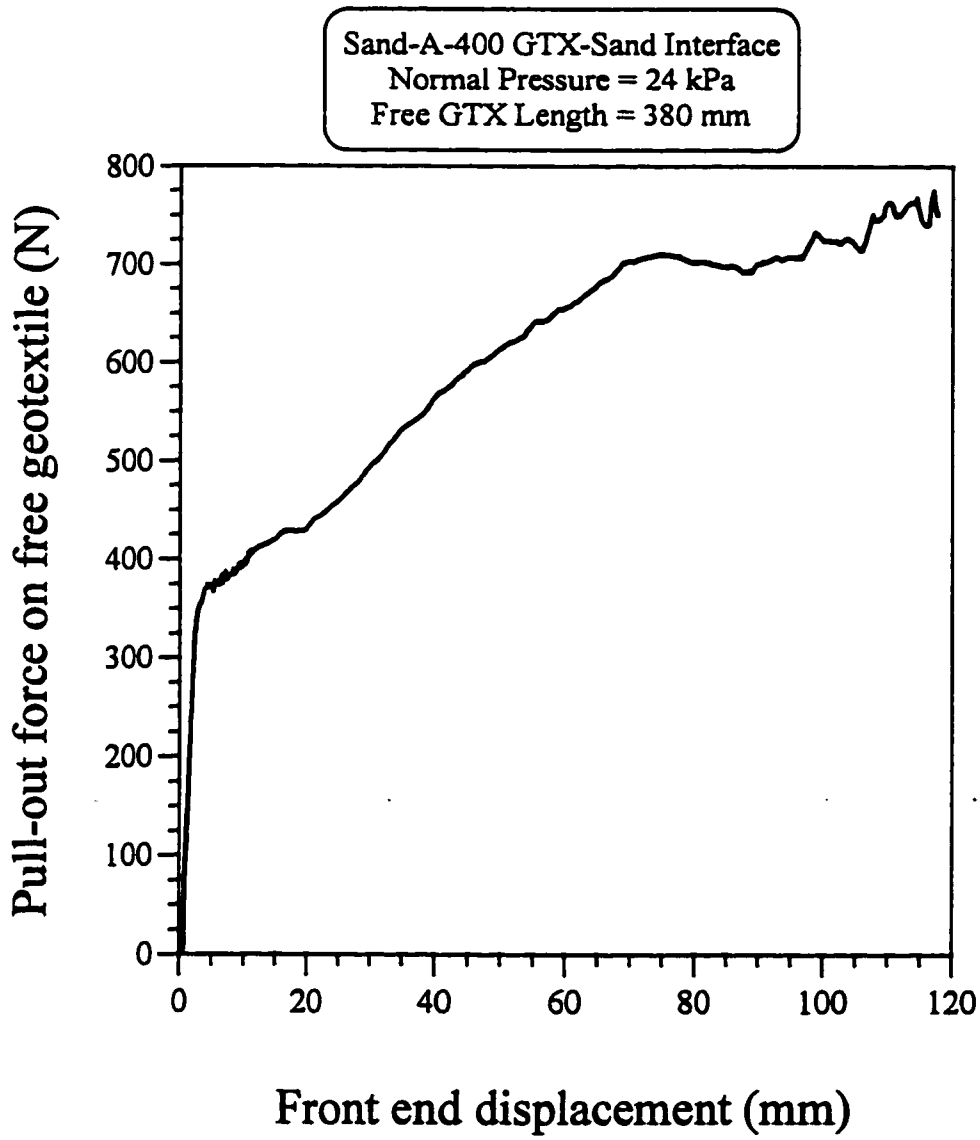

Fig. A1.10: Variation of the pull-out force on A-400 geotextile with front end displacement for sand-GTX-sand interface, under 24 kPa normal pressure, and 380 mm long free geotextile

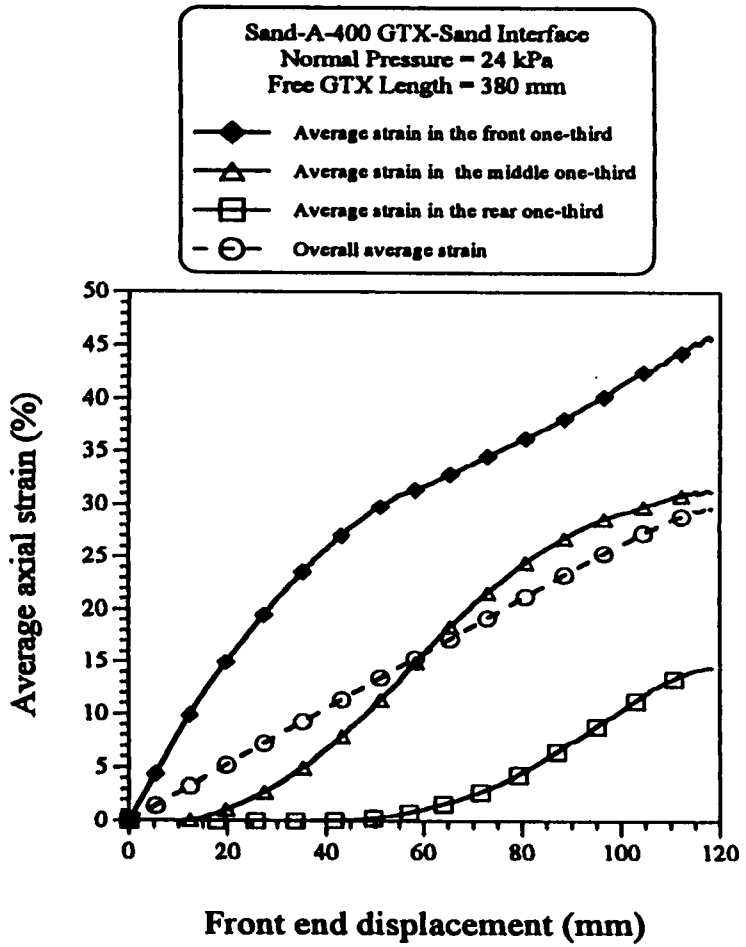

Fig. A1.11: Variation of average axial strain of A-400 geotextile with front end displacement for sand-GTX-sand interface, under 24 kPa normal pressure, and 380 mm long free geotextile

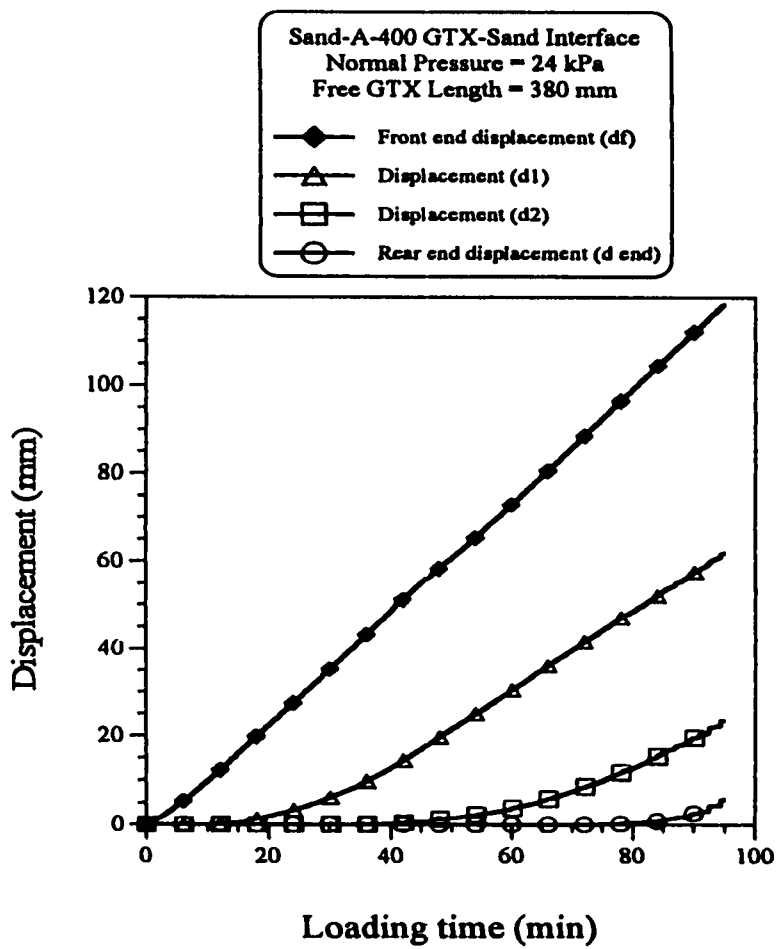

Fig. A1.12: Variation of displacement of A-400 geotextile with loading time for sand-GTX-sand interface, under 24 kPa normal pressure, and 380 mm long free geotextile

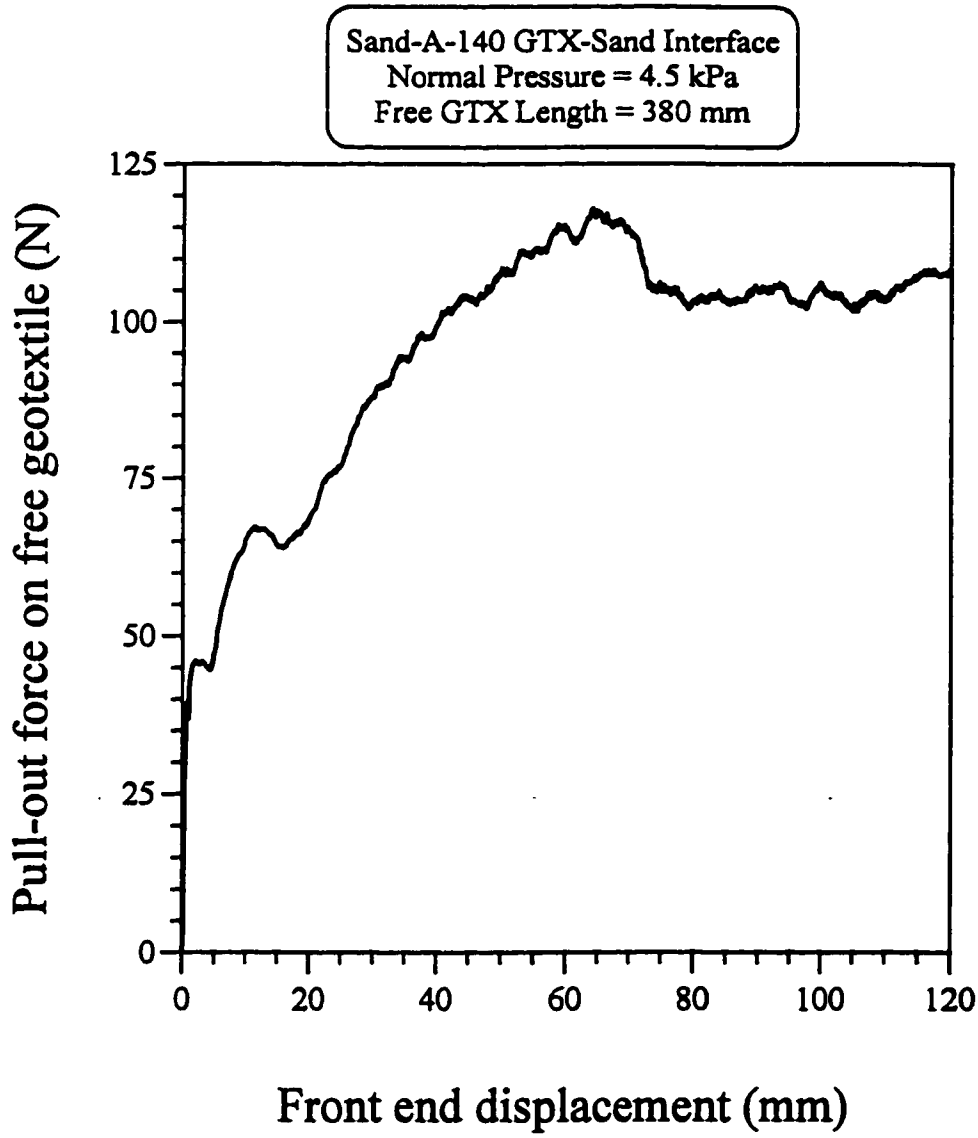

Fig. A1.13: Variation of the pull-out force on A-140 geotextile with front end displacement for sand-GTX-sand interface, under 4.5 kPa normal pressure, and 380 mm long free geotextile

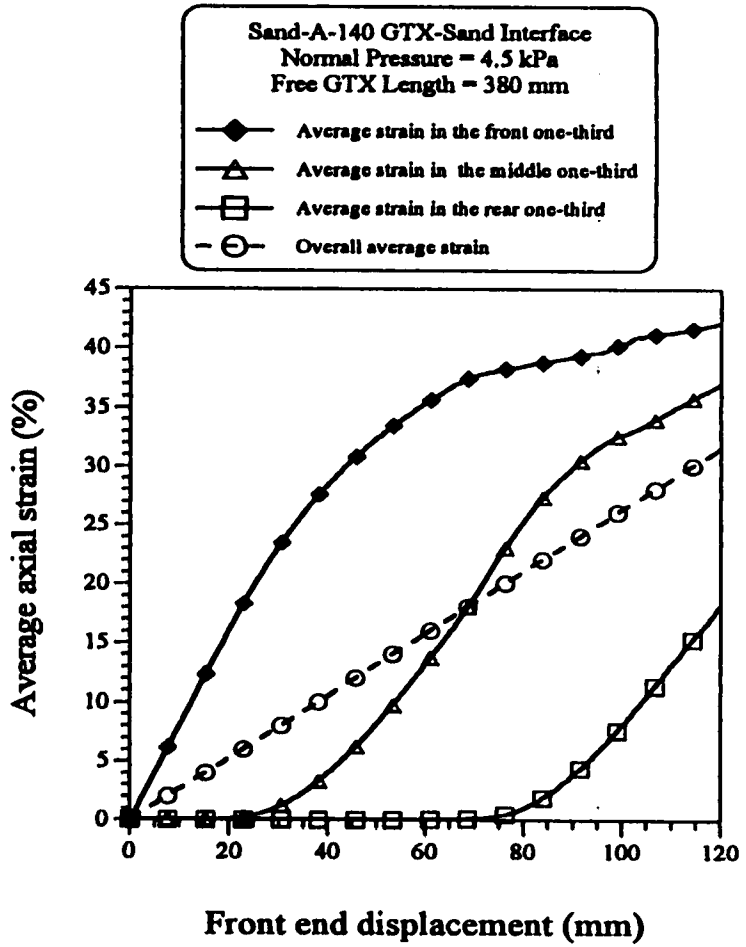

Fig. A1.14: Variation of average axial strain of A-140 geotextile with front end displacement for sand-GTX-sand interface, under 45 kPa normal pressure, and 380 mm long free geotextile

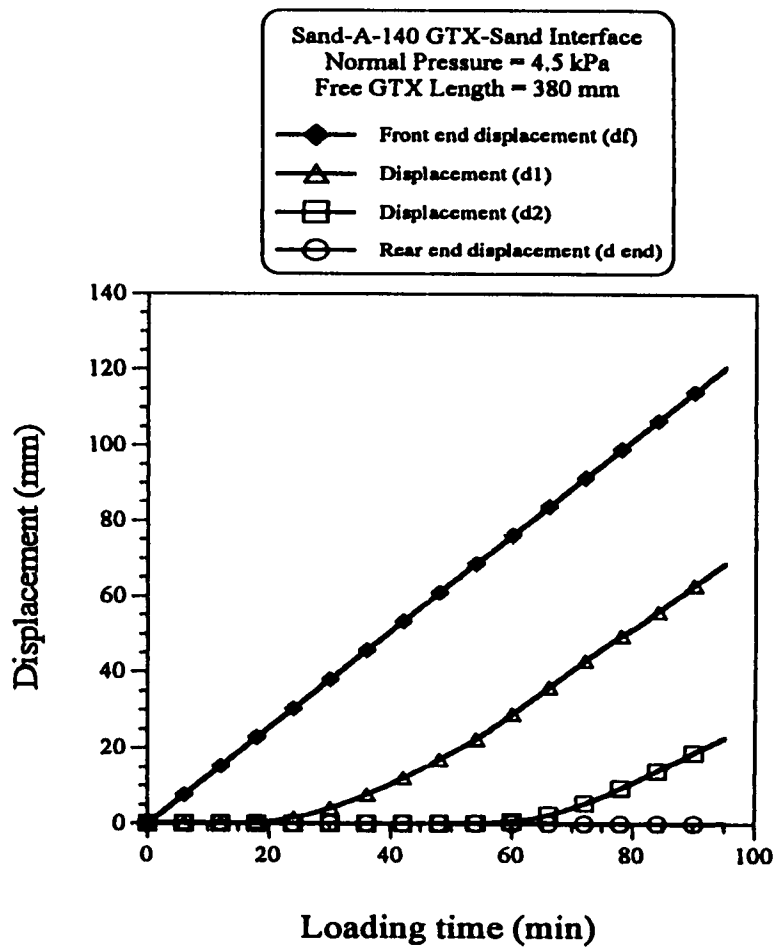

Fig. A1.15: Variation of displacement of A-140 geotextile with loading time for sand-GTX-sand interface, under 4.5 kPa normal pressure, and 380 mm long free geotextile

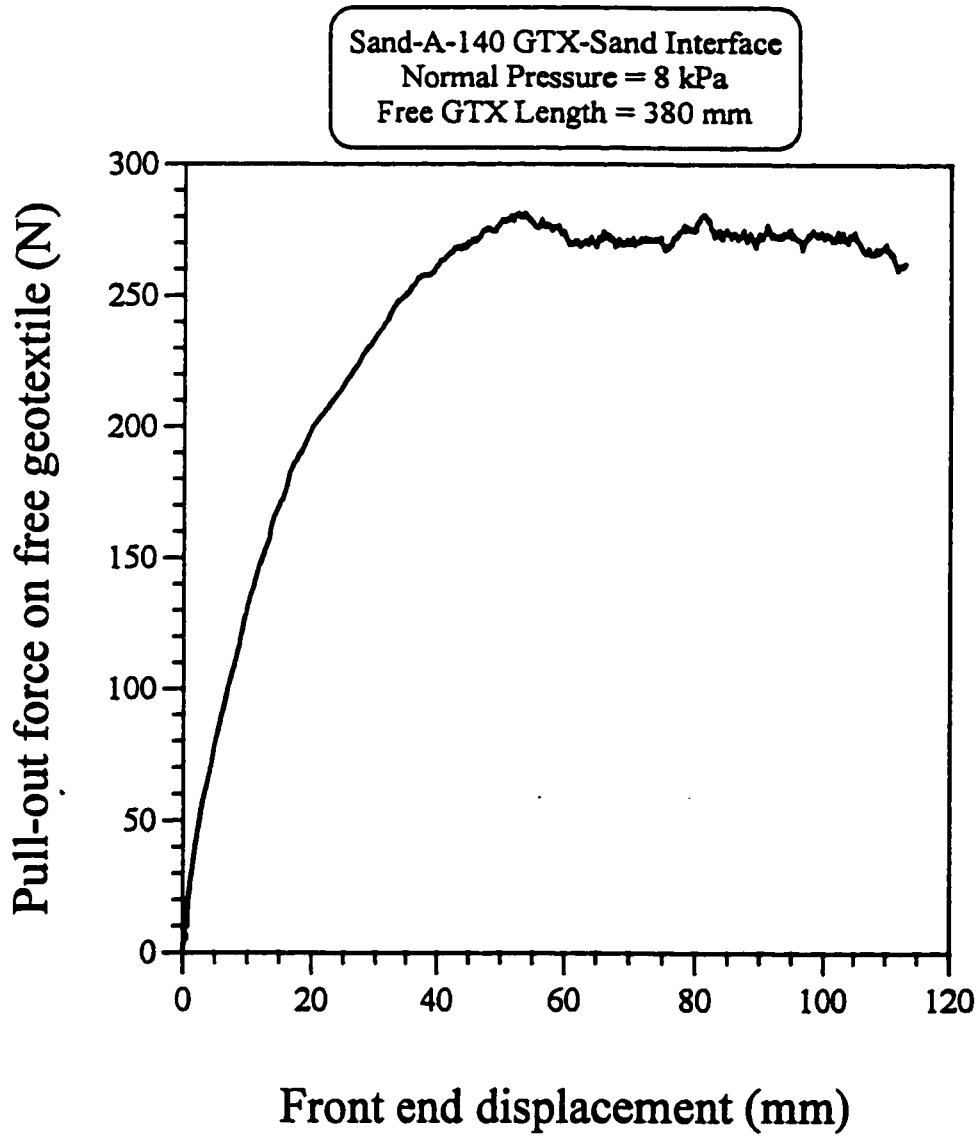

Fig. A1.16: Variation of the pull-out force on A-140 geotextile with front end displacement for sand-GTX-sand interface, under 8 kPa normal pressure, and 380 mm long free geotextile

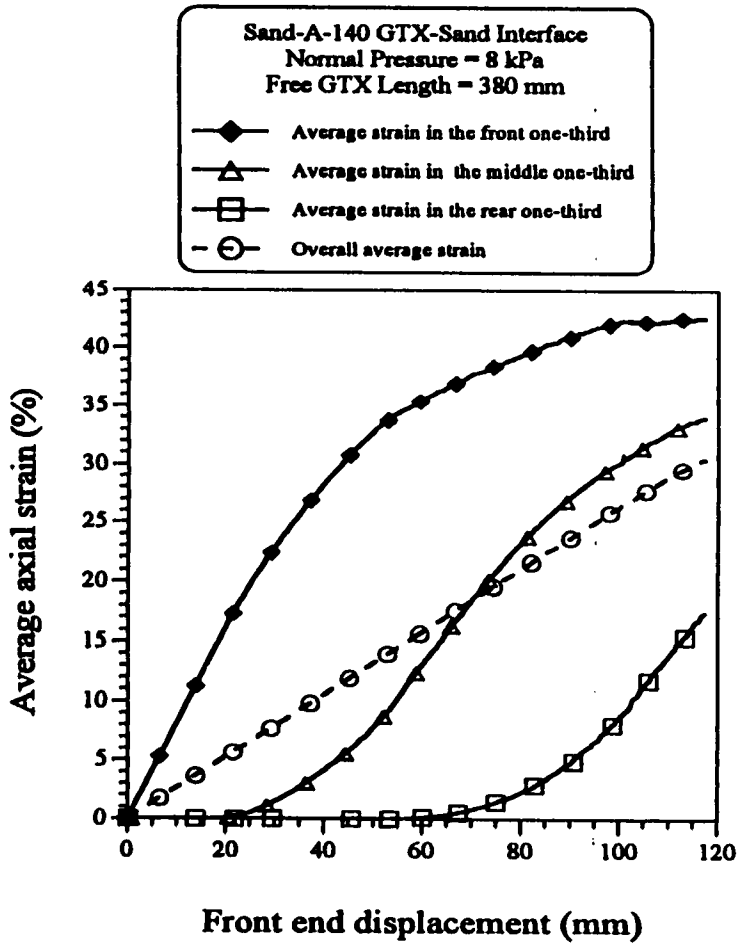

Fig. A1.17: Variation of average axial strain of A-140 geotextile with front end displacement for sand-GTX-sand interface, under 8 kPa normal pressure, and 380 mm long free geotextile

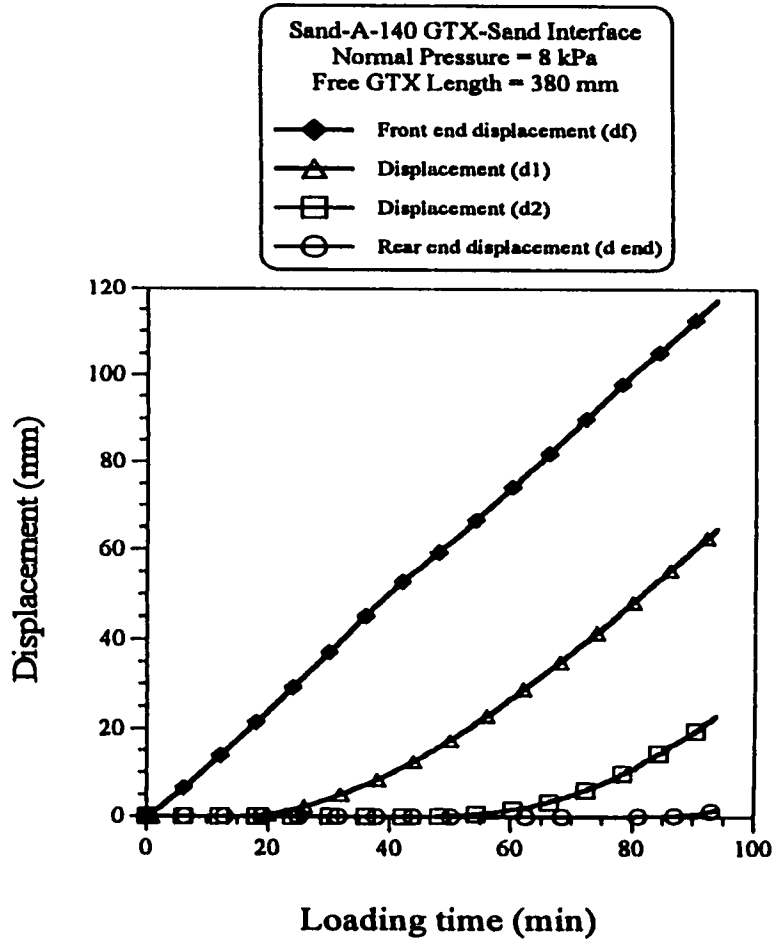

Fig. A1.18: Variation of displacement of A-140 geotextile with loading time for sand-GTX-sand interface, under 8 kPa normal pressure, and 380 mm long free geotextile

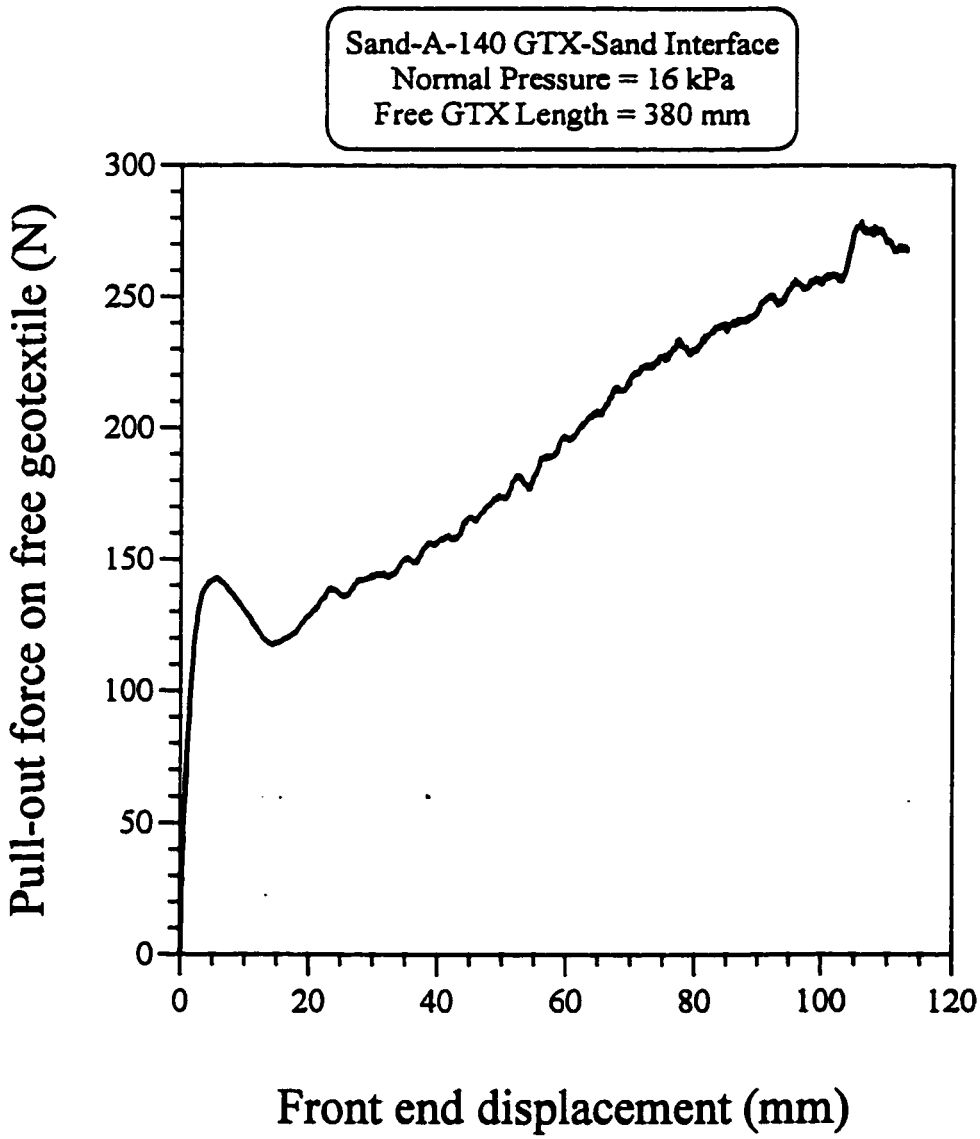

Fig. A1.19: Variation of the pull-out force on A-140 geotextile with front end displacement for sand-GTX-sand interface, under 16 kPa normal pressure, and 380 mm long free geotextile

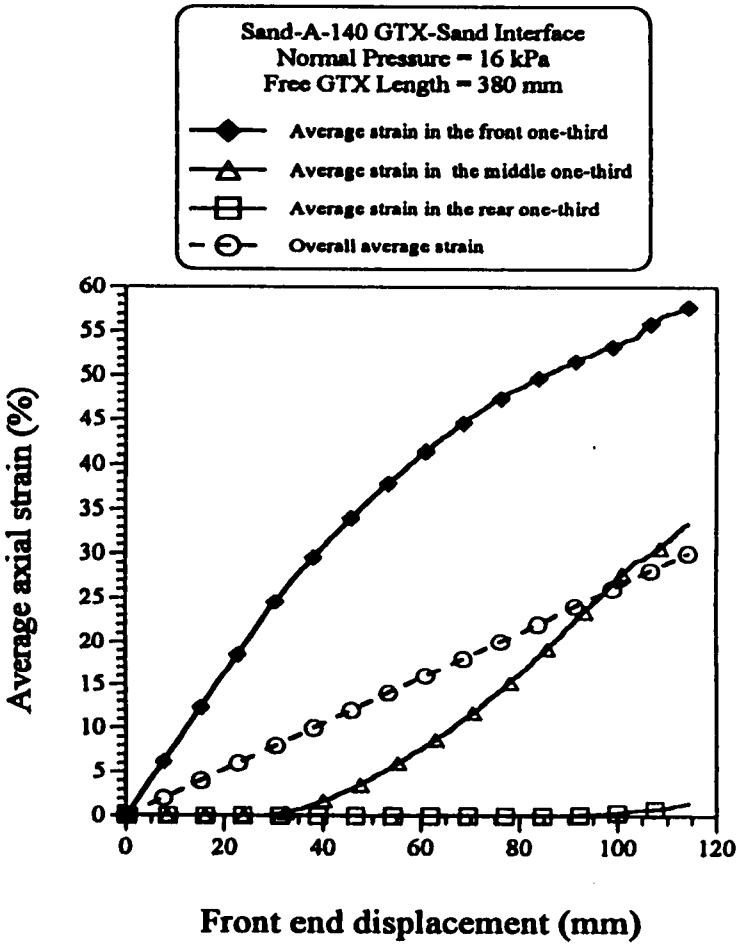

Fig. A1.20: Variation of average axial strain of A-140 geotextile with front end displacement for sand-GTX-sand interface, under 16 kPa normal pressure, and 380 mm long free geotextile

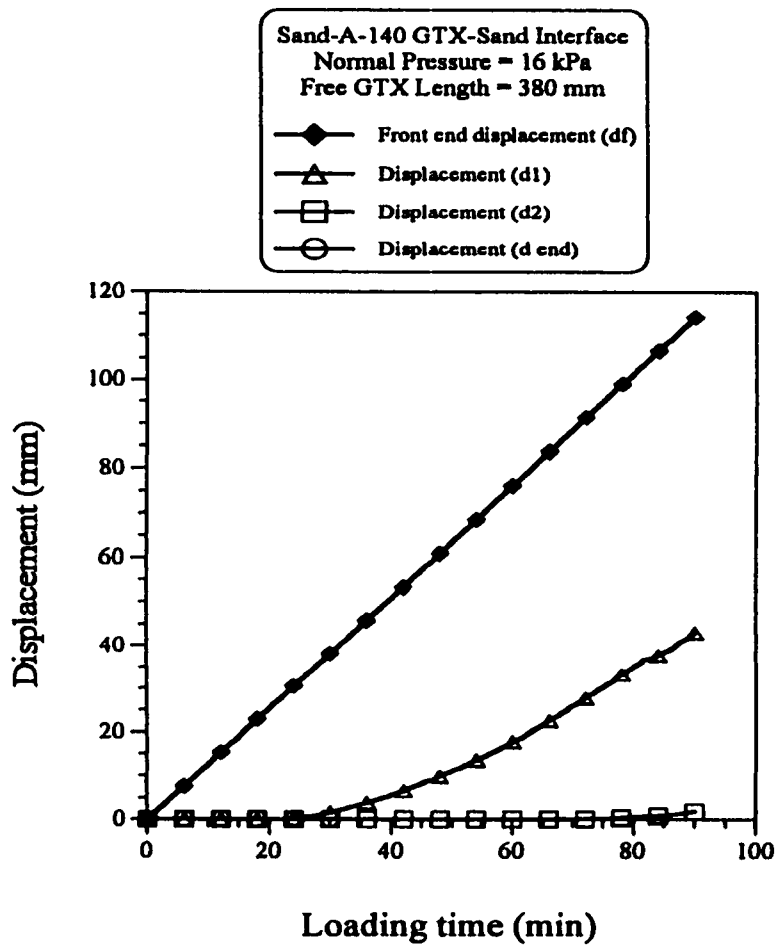

Fig. A1.21: Variation of displacement of A-140 geotextile with loading time for sand-GTX-sand interface, under 16 kPa normal pressure, and 380 mm long free geotextile

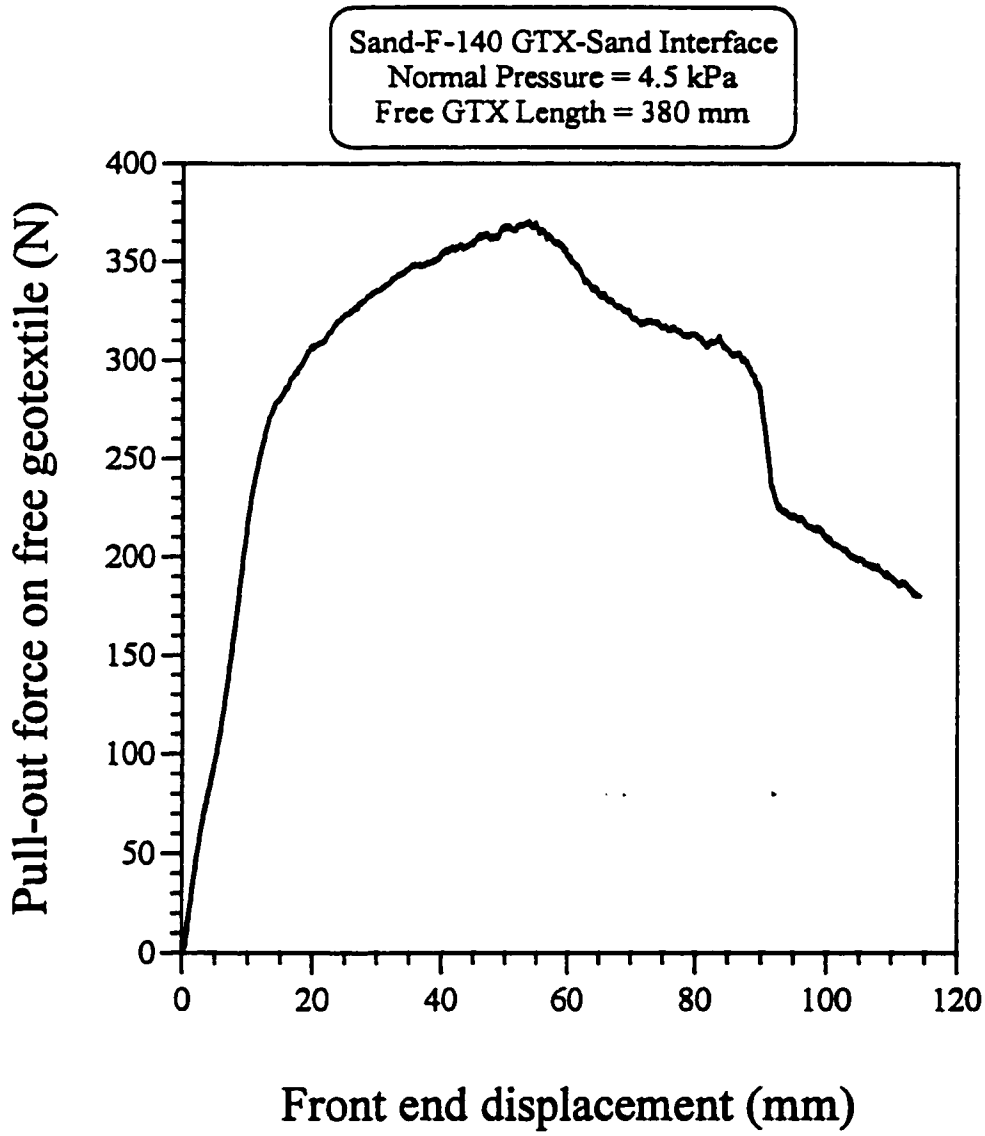

Fig. A1.22: Variation of the pull-out force on F-140 geotextile with front end displacement for sand-GTX-sand interface, under 4.5 kPa normal pressure, and 380 mm long free geotextile

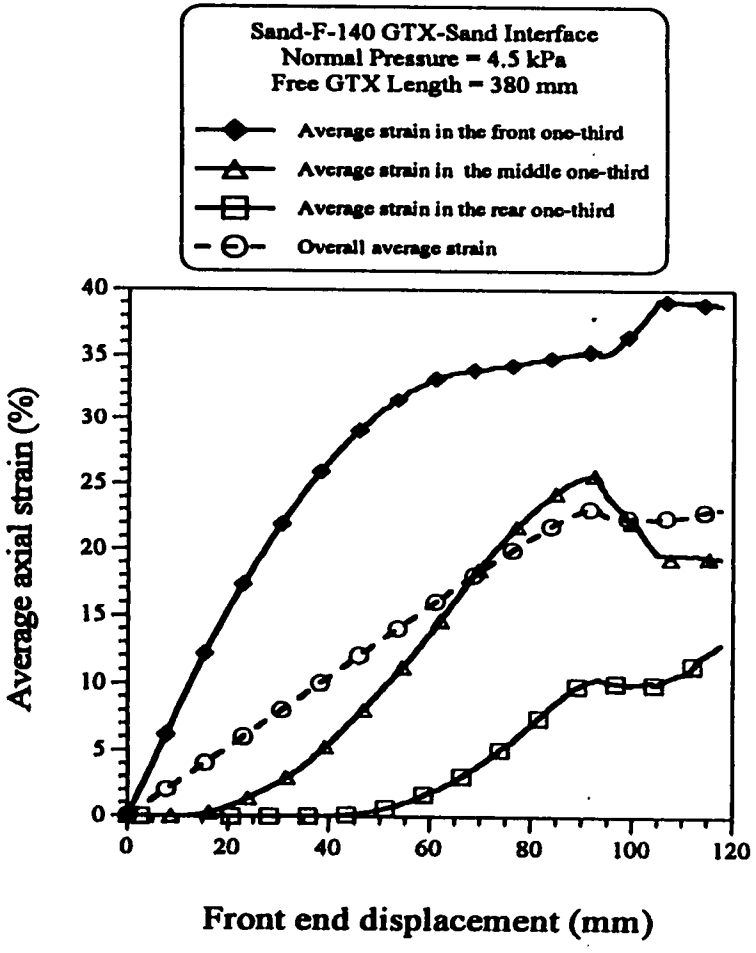

Fig. A1.23: Variation of average axial strain of F-140 geotextile with front end displacement for sand-GTX-sand interface, under 4.5 kPa normal pressure, and 380 mm long free geotextile

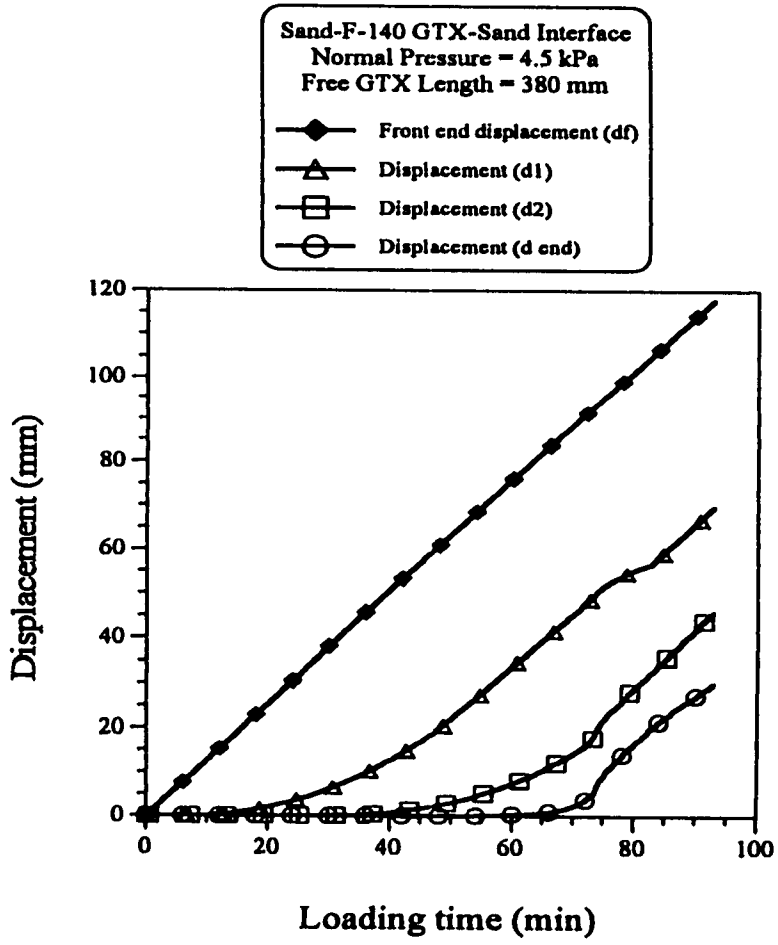

Fig. A1.24: Variation of displacement of F-140 geotextile with loading time for sand-GTX-sand interface, under 4.5 kPa normal pressure, and 380 mm long free geotextile

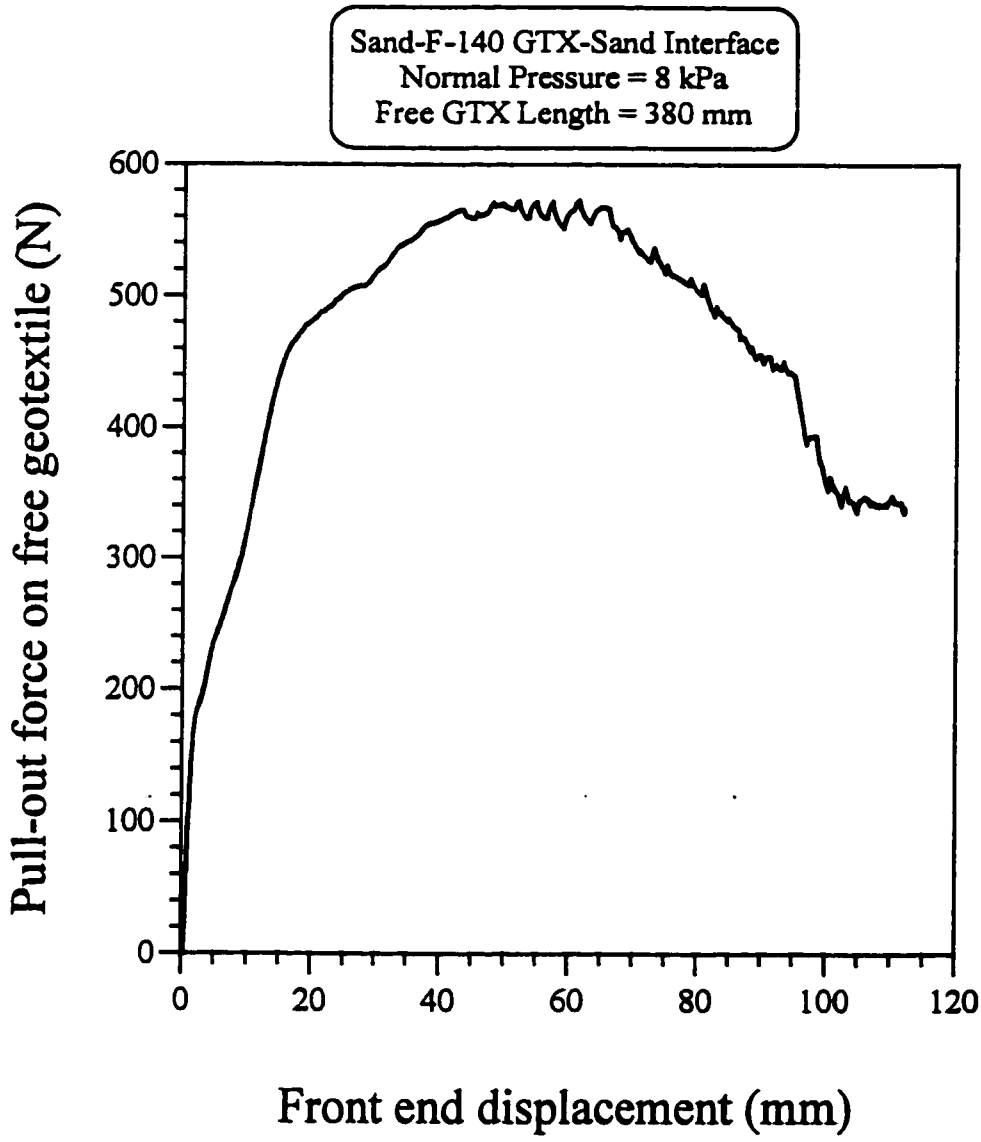

Fig. A1.25: Variation of the pull-out force on F-140 geotextile with front end displacement for sand-GTX-sand interface, under 8 kPa normal pressure, and 380 mm long free geotextile

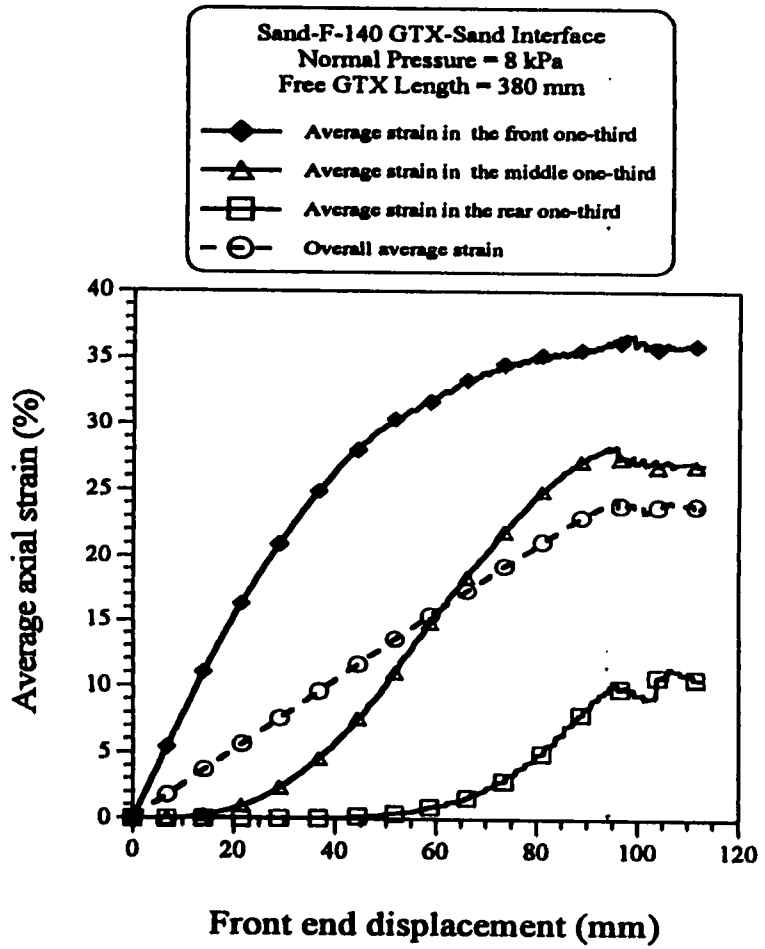

Fig. A1.26: Variation of average axial strain of F-140 geotextile with front end displacement for sand-GTX-sand interface, under 8 kPa normal pressure, and 380 mm long free geotextile

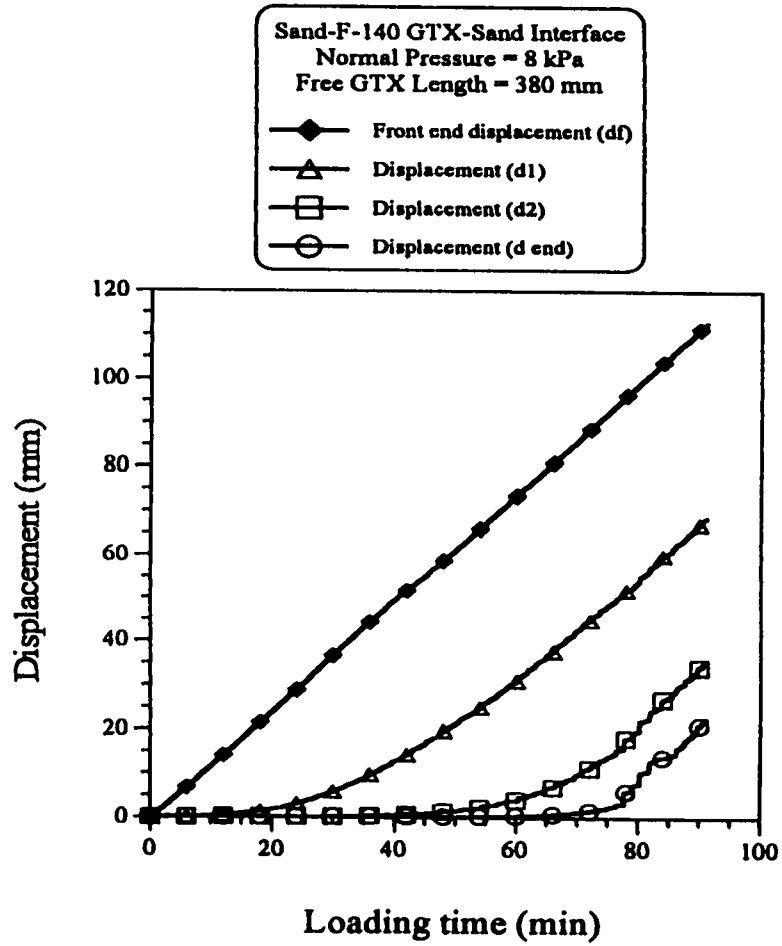

Fig. A1.27: Variation of displacement of F-140 geotextile with loading time for sand-GTX-sand interface, under 8 kPa normal pressure, and 380 mm long free geotextile

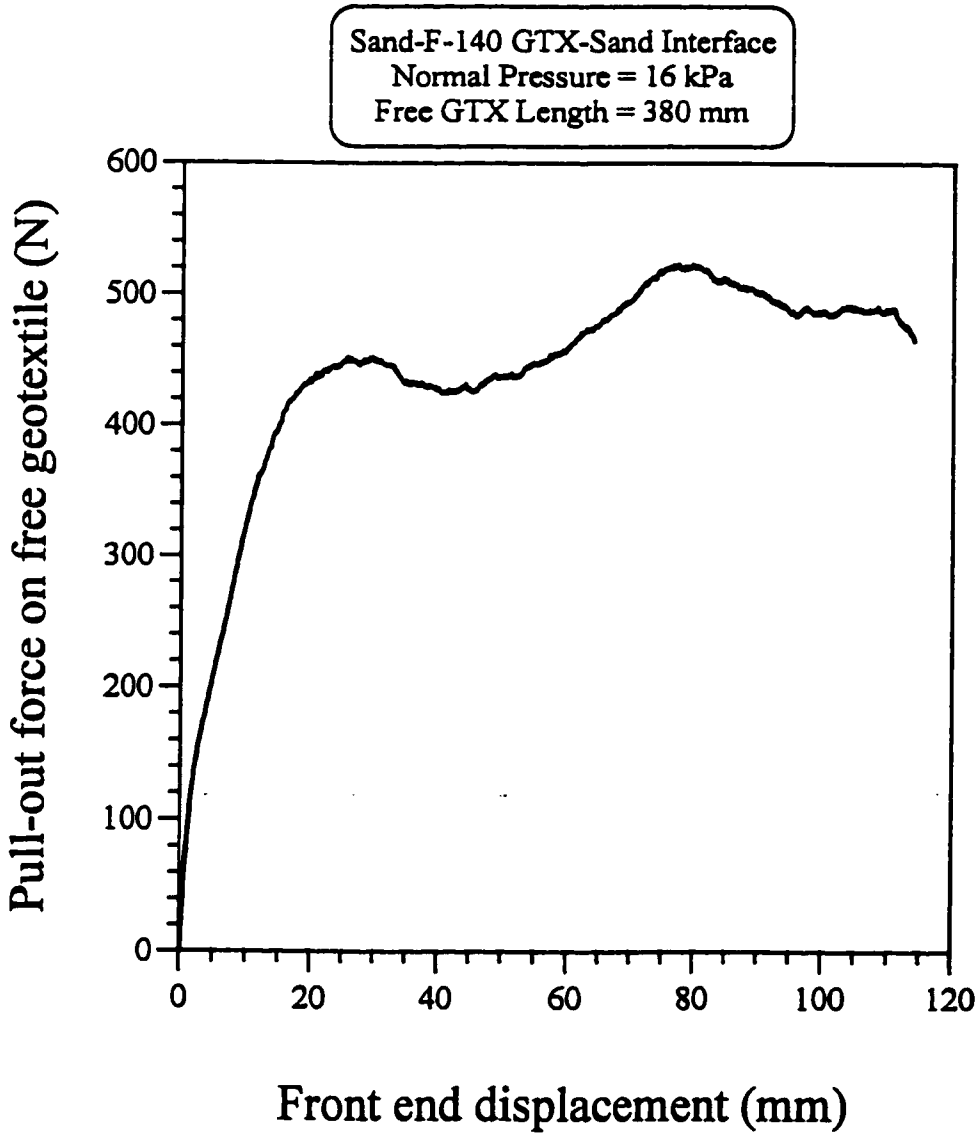

Fig. A1.28: Variation of the pull-out force on F-140 geotextile with front end displacement for sand-GTX-sand interface, under 16 kPa normal pressure, and 380 mm long free geotextile

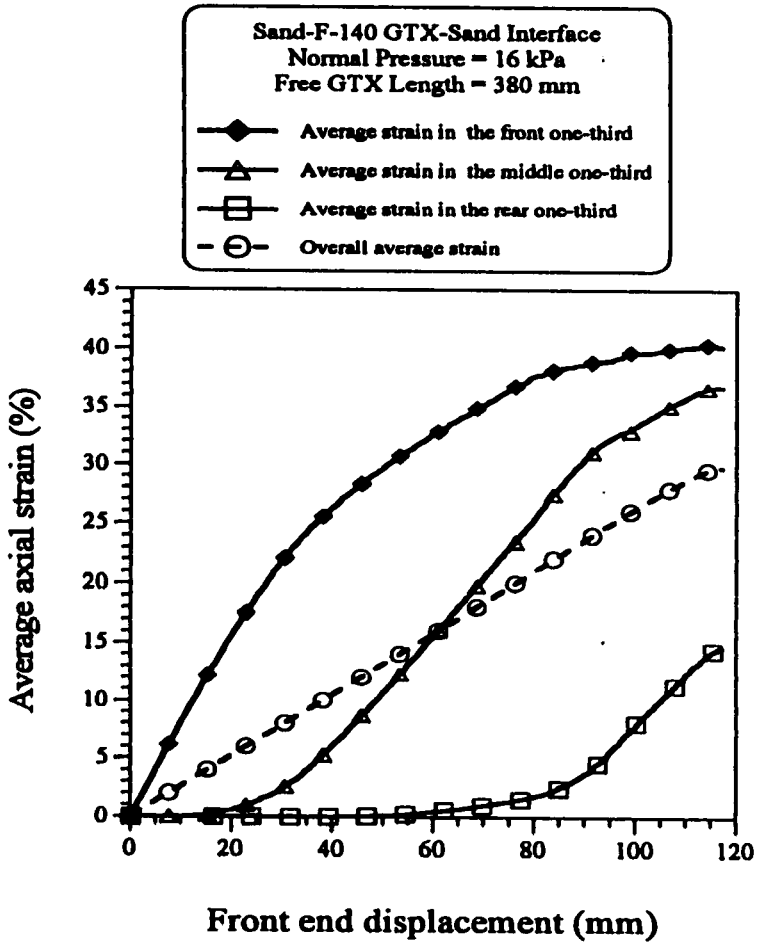

Fig. A1.29: Variation of average axial strain of F-140 geotextile with front end displacement for sand-GTX-sand interface, under 16 kPa normal pressure, and 380 mm long free geotextile

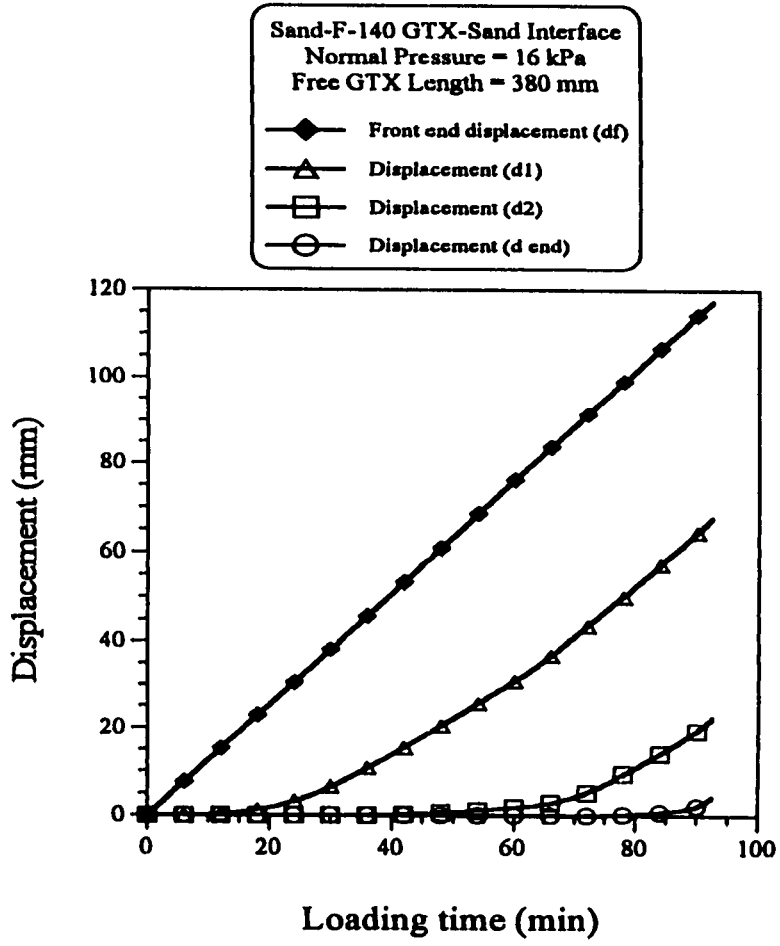

Fig. A1.30: Variation of displacement of F-140 geotextile with loading time for sand-GTX-sand interface, under 16 kPa normal pressure, and 380 mm long free geotextile

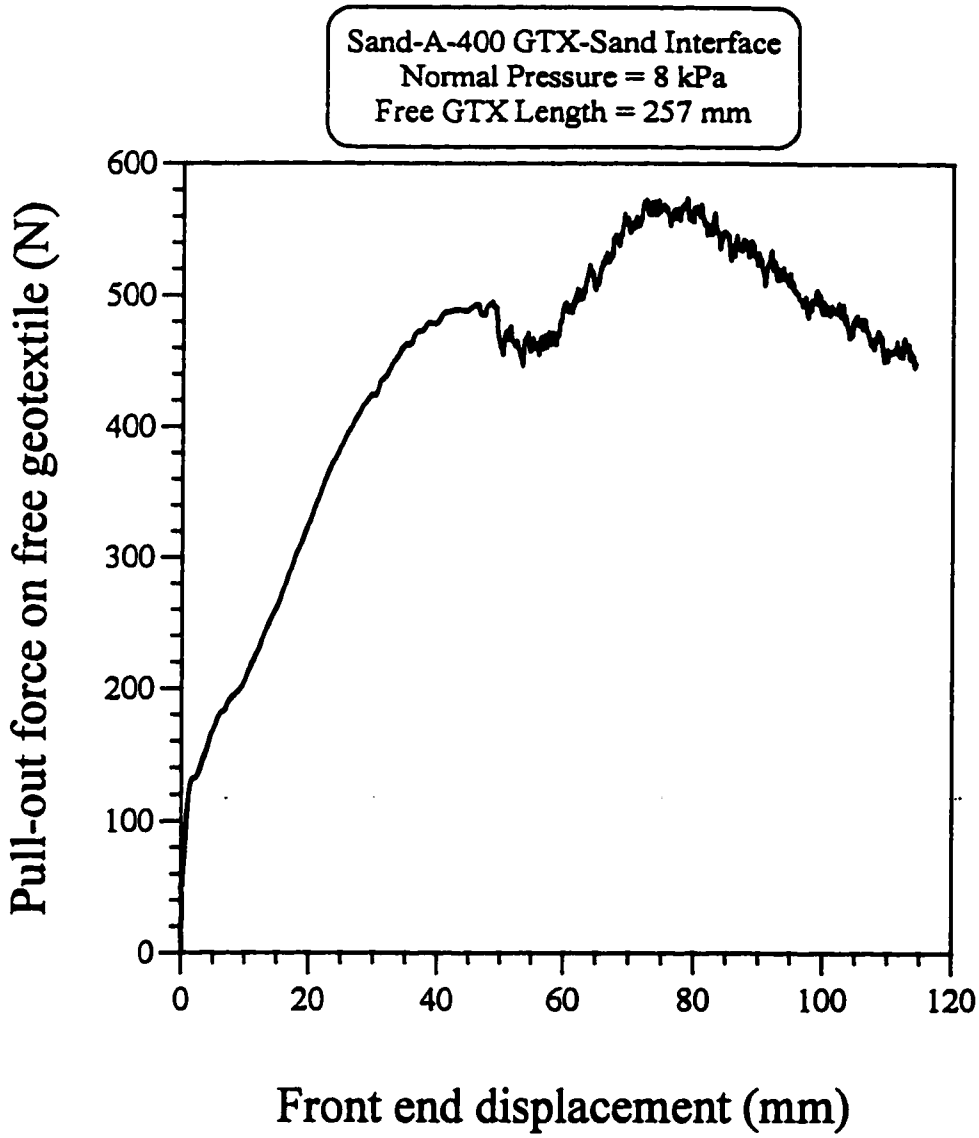

Fig. A1.31: Variation of the pull-out force on A-400 geotextile with front end displacement for sand-GTX-sand interface, under 8 kPa normal pressure, and 257 mm long free geotextile

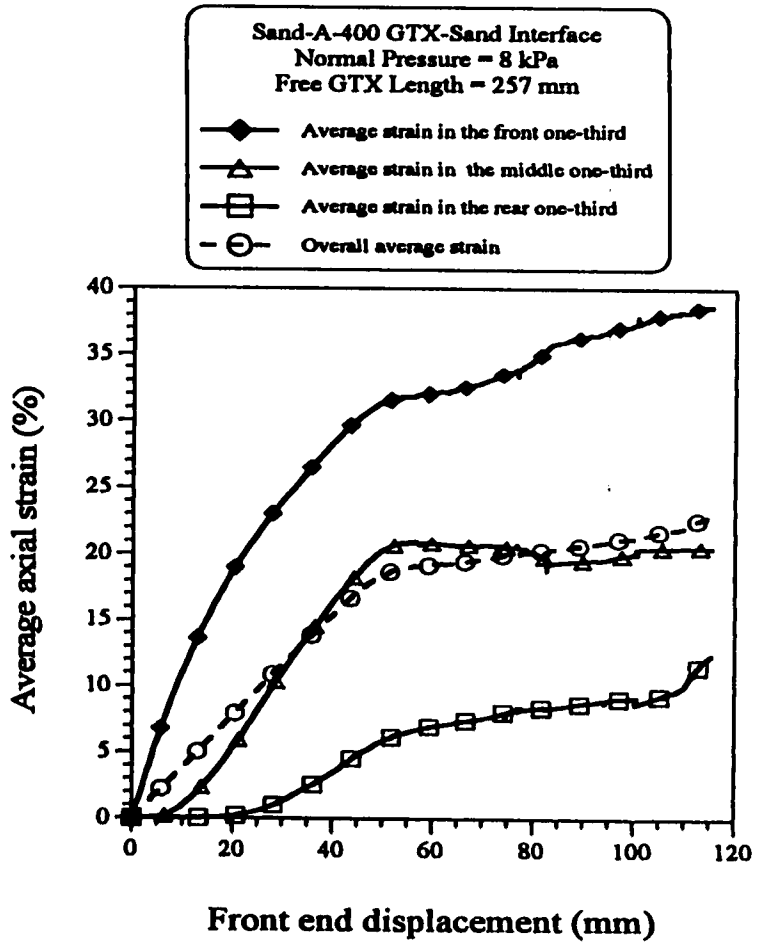

Fig. A1.32: Variation of average axial strain of A-400 geotextile with front end displacement for sand-GTX-sand interface, under 8 kPa normal pressure, and 257 mm long free geotextile

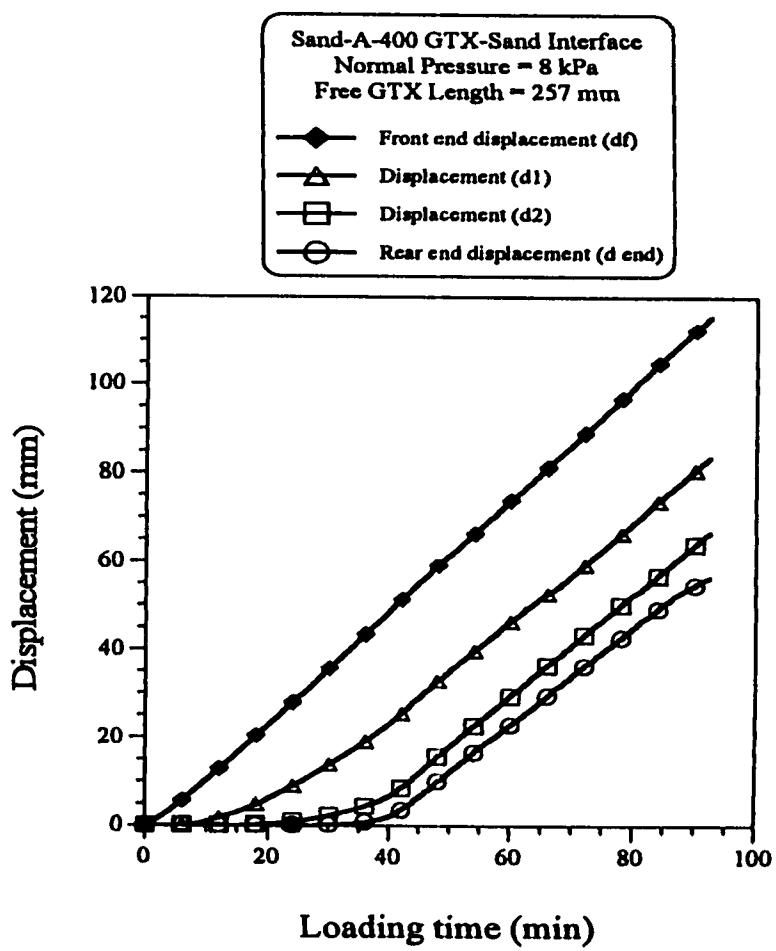

Fig. A1.33: Variation of displacement of A-400 geotextile with loading time for sand-GTX-sand interface, under 8 kPa normal pressure, and 257 mm long free geotextile

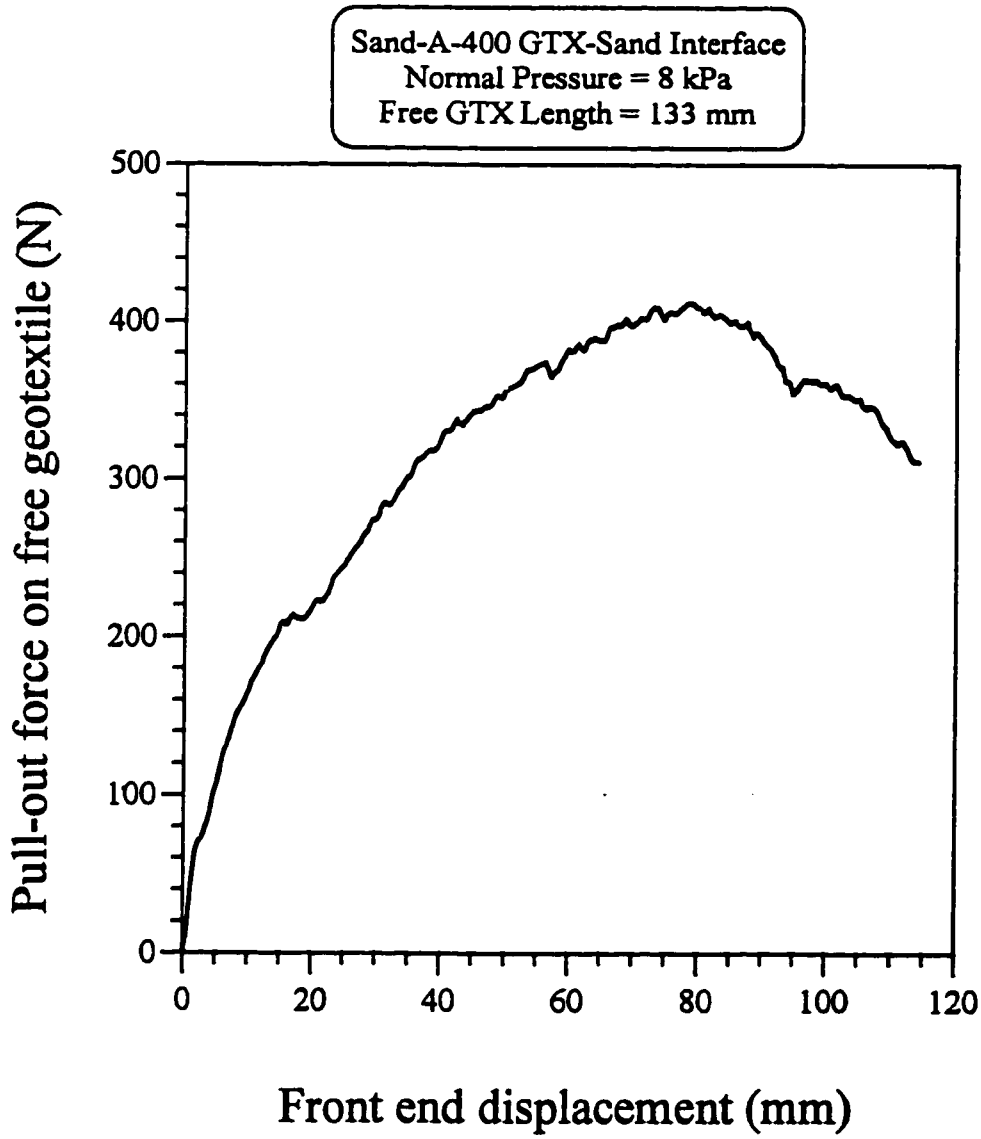

Fig. A1.34: Variation of the pull-out force on A-400 geotextile with front end displacement for sand-GTX-sand interface, under 8 kPa normal pressure, and 133 mm long free geotextile

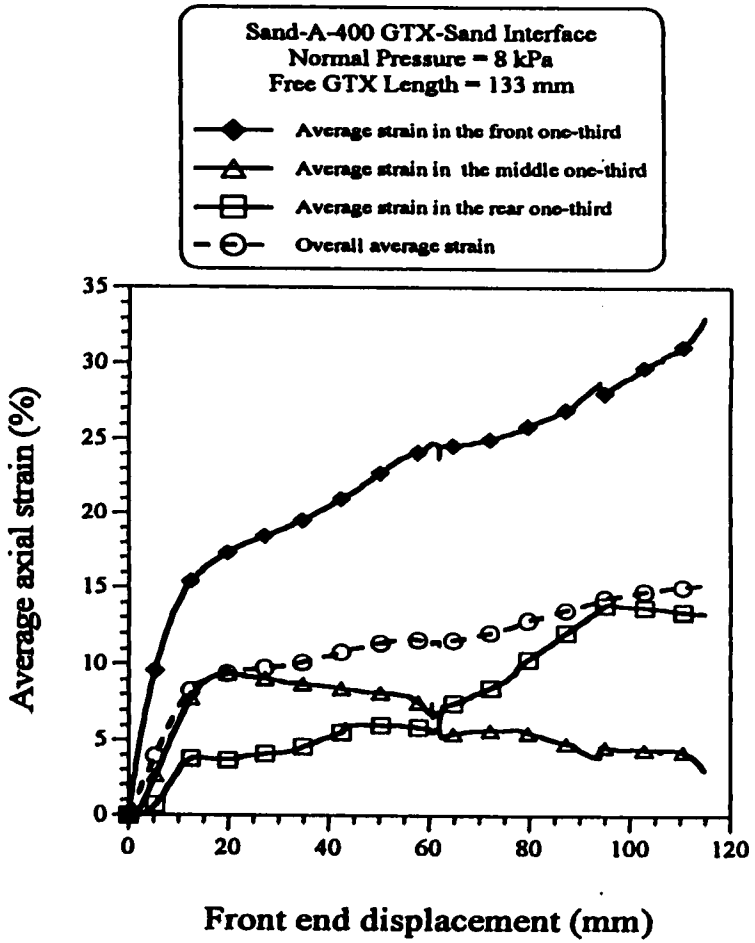

Fig. A1.35: Variation of average axial strain of A-400 geotextile with front end displacement for sand-GTX-sand interface, under 8 kPa normal pressure, and 133 mm long free geotextile

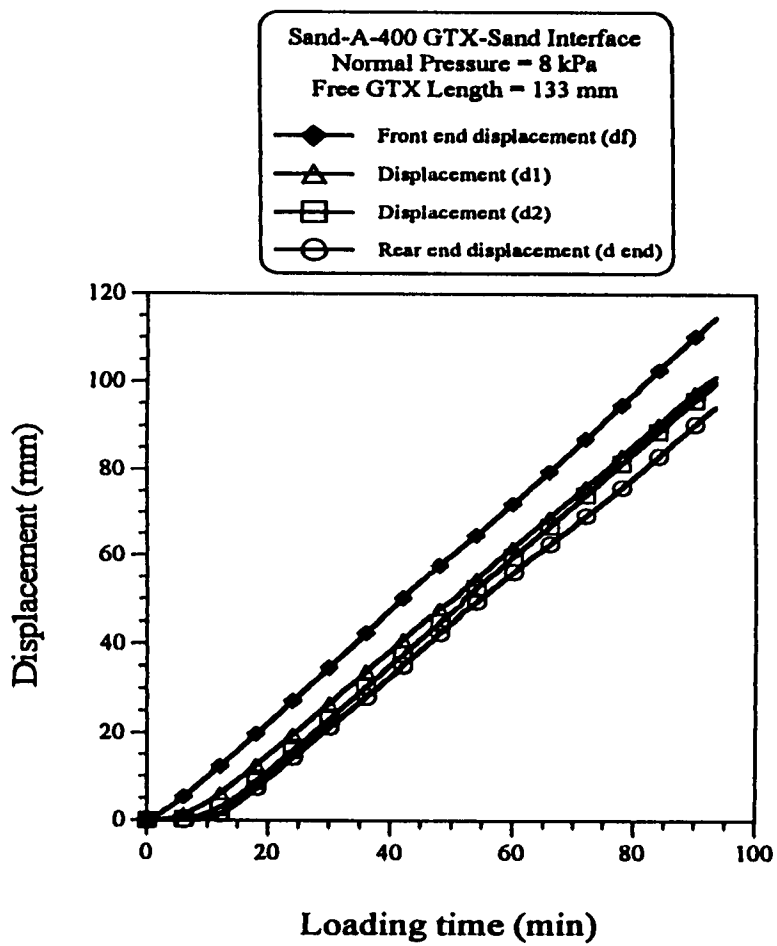

Fig. A1.36: Variation of displacement of A-400 geotextile with loading time for sand-GTX-sand interface, under 8 kPa normal pressure, and 133 mm long free geotextile

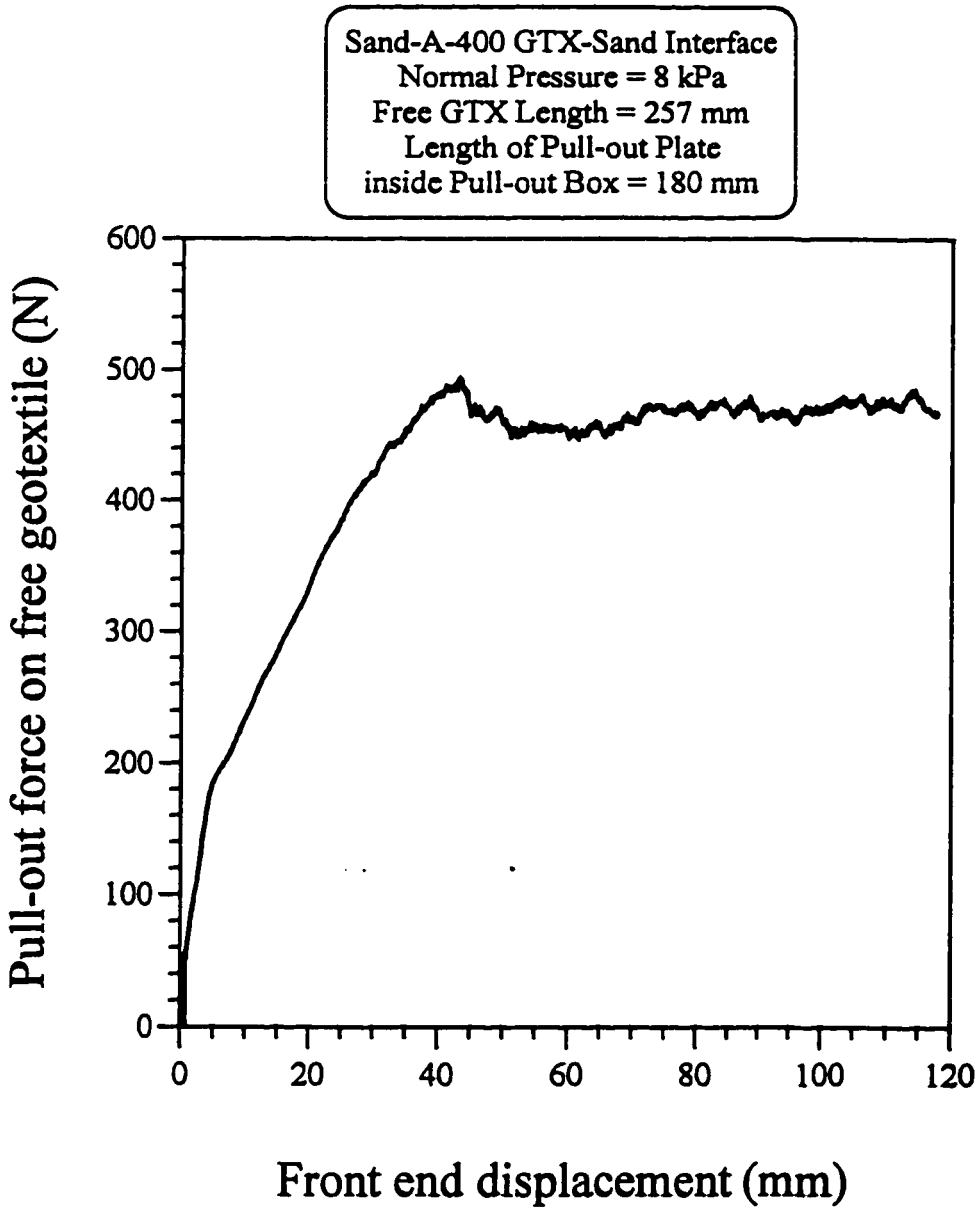

Fig. A1.37: Variation of the pull-out force on A-400 geotextile with front end displacement for sand-GTX-sand interface, under 8 kPa normal pressure, and 257 mm long free geotextile attached to 180 mm long pull-out plate inside pull-out box

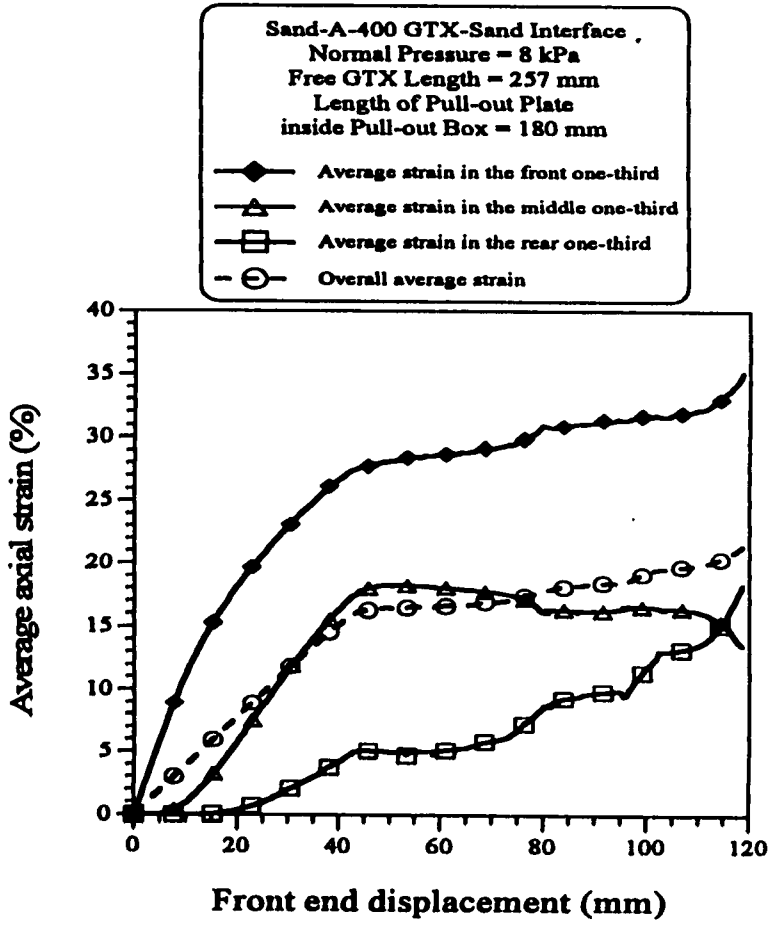

Fig. A1.38: Variation of average axial strain of A-400 geotextile with front end displacement for sand-GTX-sand interface, under 8 kPa normal pressure, and 257 mm long free geotextile attached to 180 mm long pull-out plate inside pull-out box

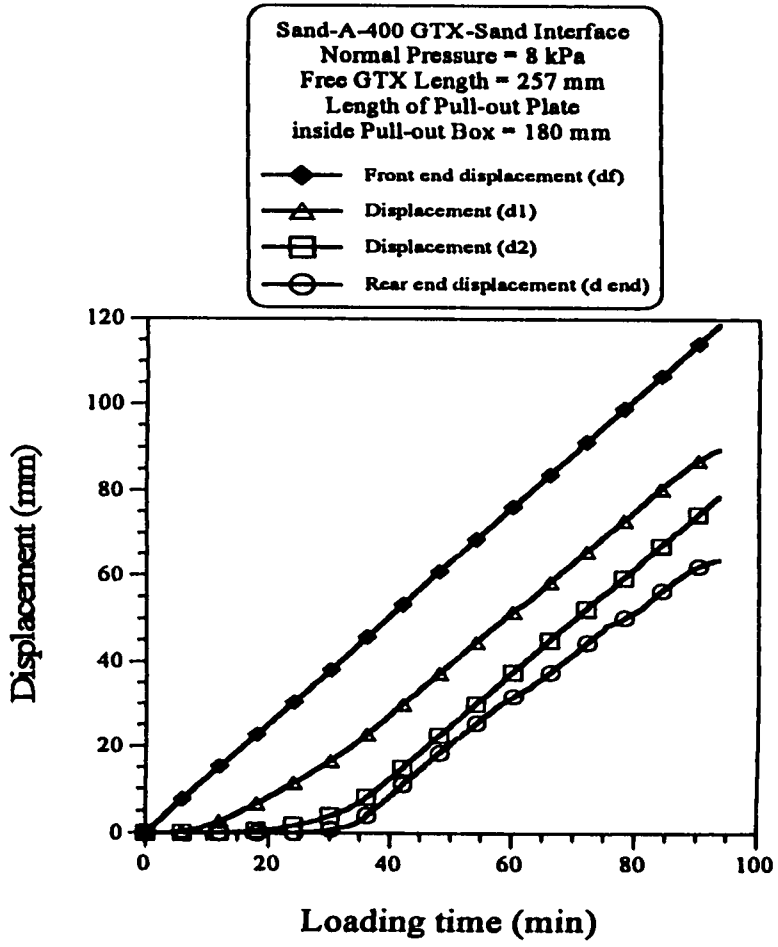

Fig. A1.39: Variation of displacement of A-400 geotextile with loading time for sand-GTX-sand interface, under 8 kPa normal pressure, and 257 mm free long geotextile attached to 180 mm long pull-out plate inside pull-out box

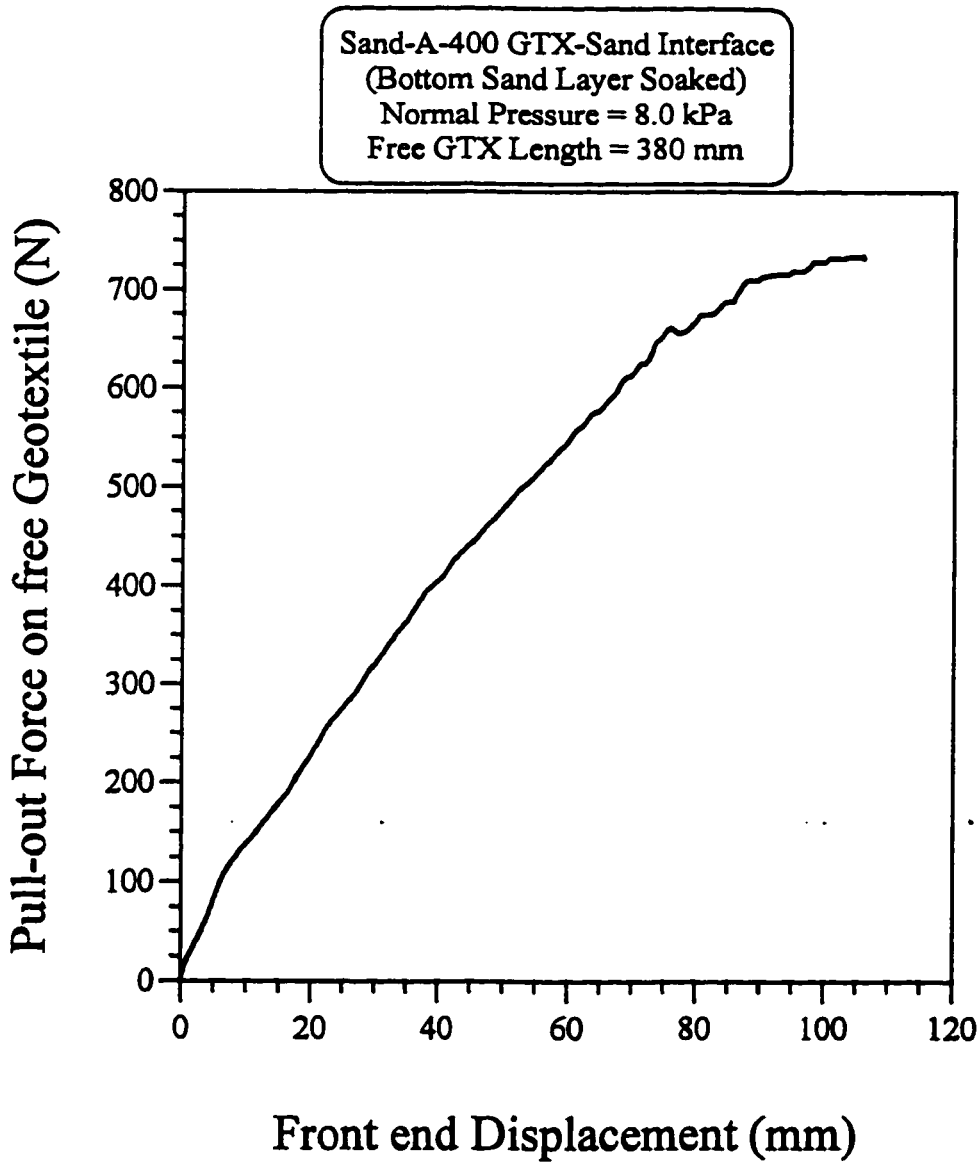

Fig. A1.40: Variation of the pull-out force on A-400 geotextile with front end displacement for sand-GTX-sand interface, under 8.0 kPa normal pressure, 380 mm long free geotextile, with soaked bottom sand layer

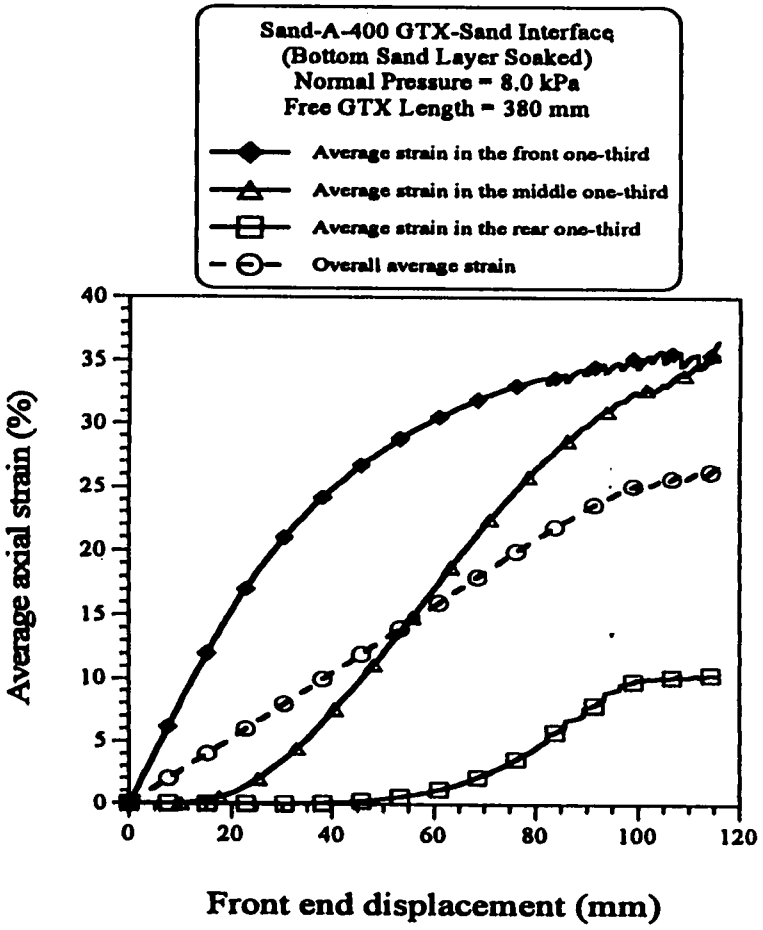

Fig. A1.41: Variation of average axial strain of A-400 geotextile with front end displacement for sand-GTX-sand interface, under 8.0 kPa normal pressure, 380 mm long free geotextile, with soaked bottom sand layer

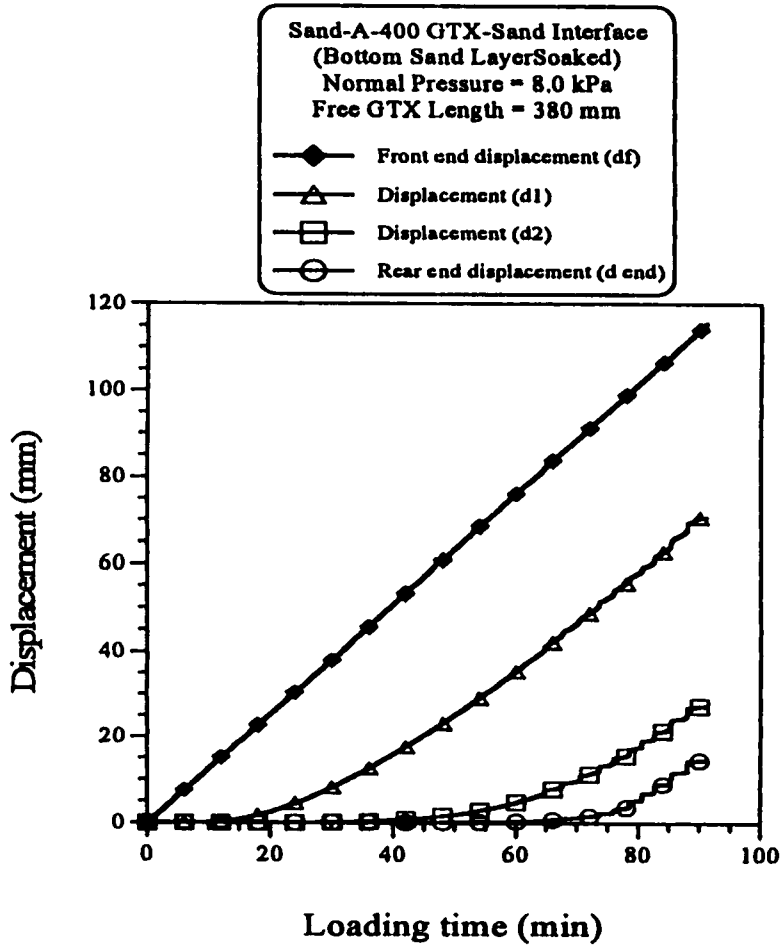

Fig. A1.42: Variation of displacement of A-400 geotextile with loading time for sand-GTX-sand interface, under 8.0 kPa normal pressure, 380 mm long free geotextile, with soaked bottom sand layer

Appendix - B

Data for sabkha-GTX-sand interface

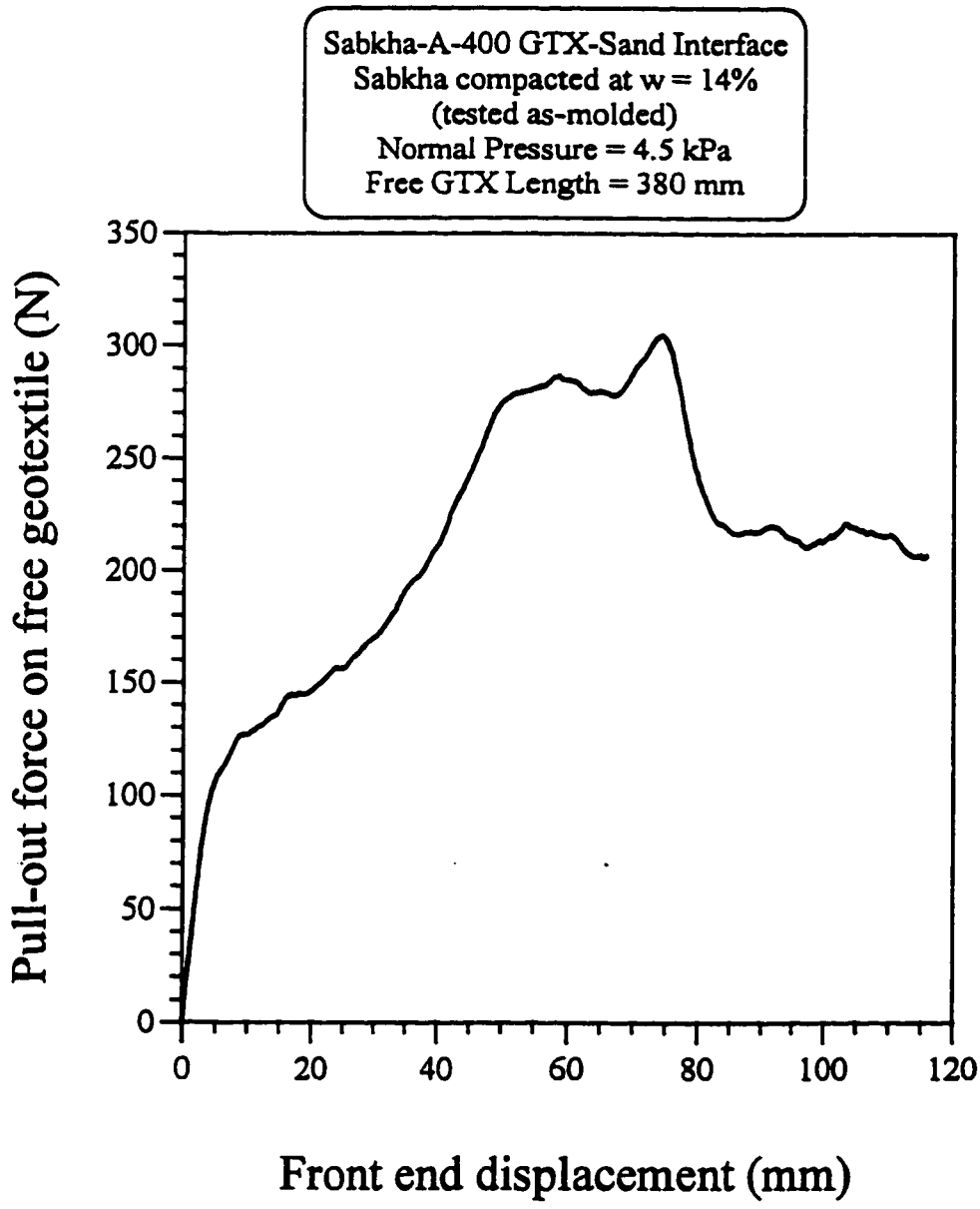

Fig. B1.1: Variation of the pull-out force on A-400 geotextile with the front end displacement for sabkha-GTX-sand interface, at 4.5 kPa normal pressure, and 380 mm long free geotextile

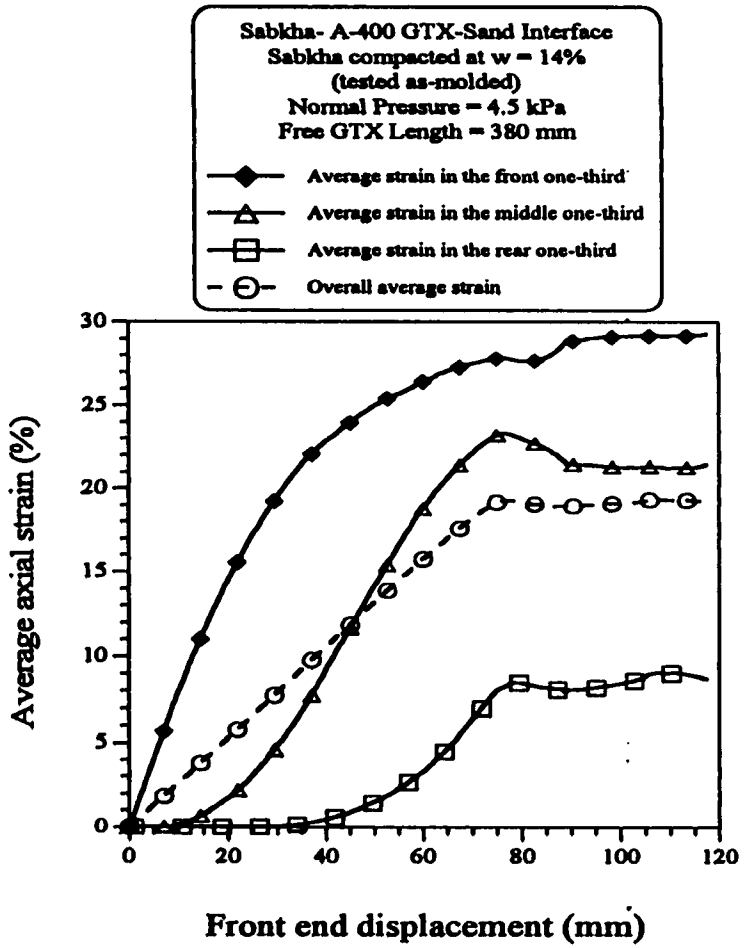

Fig. B1.2: Variation of average axial strain of A-400 geotextile with the front end displacement for sabkha-GTX-sand interface, at 4.5 kPa normal pressure, and 380 mm long free geotextile

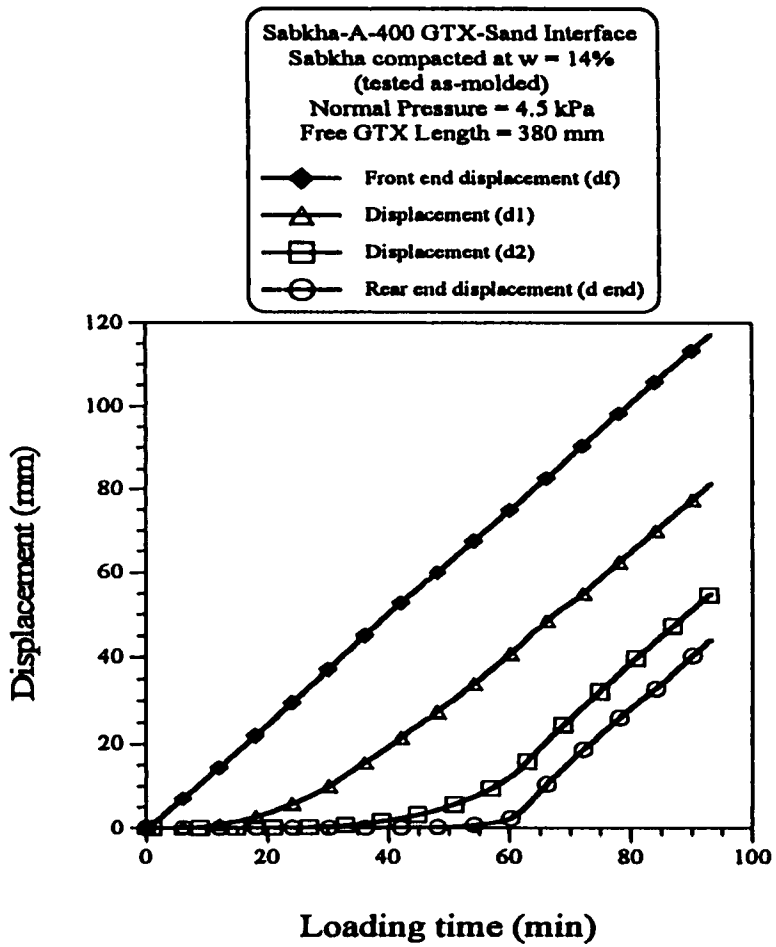

Fig. B1.3: Variation of displacement of A-400 geotextile with loading time for sabkha-GTX-sand interface, at 4.5 kPa normal pressure, and 380 mm long free geotextile

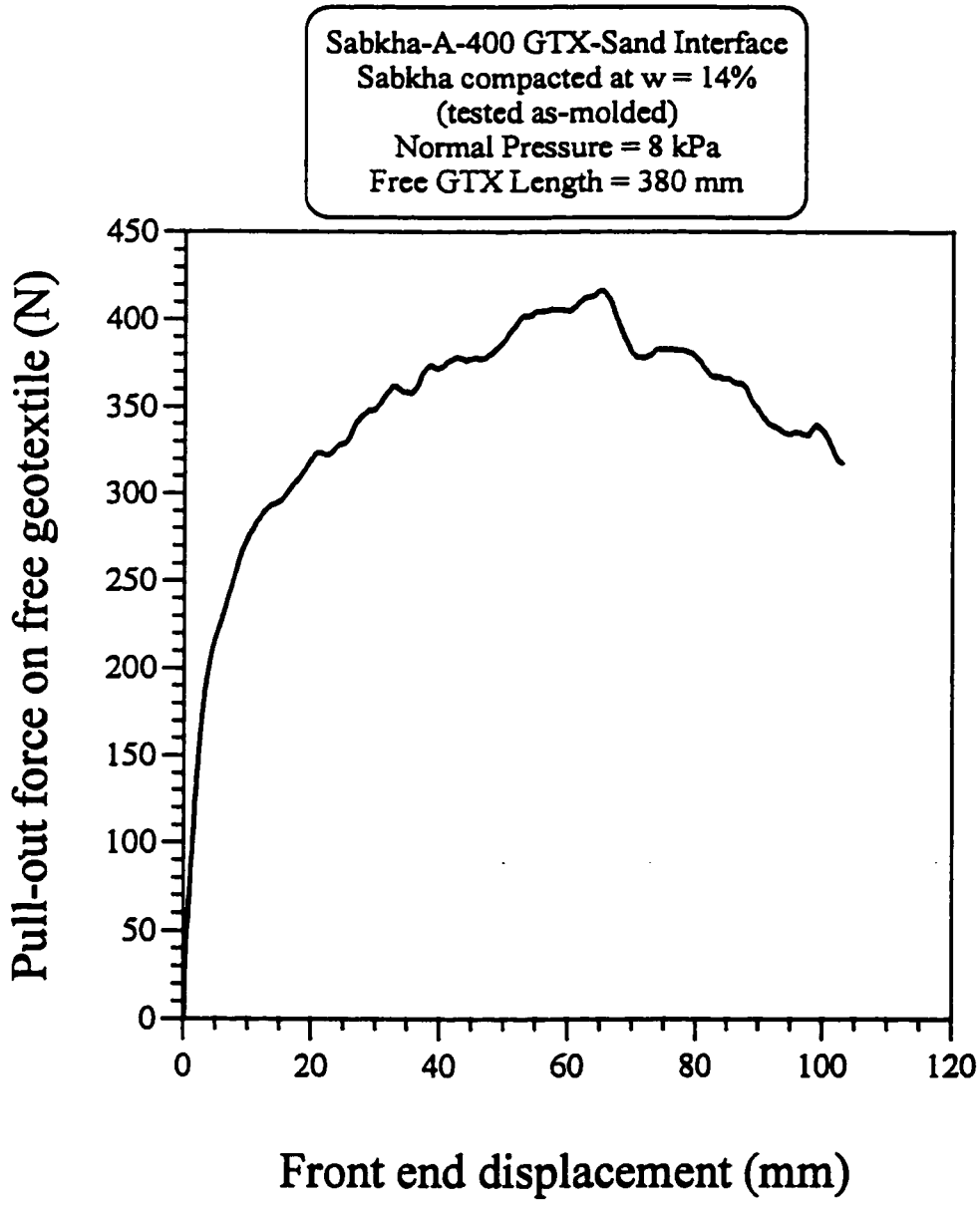

Fig. B1.4: Variation of the pull-out force on A-400 geotextile with the front end displacement for sabkha-GTX-sand interface, at 8 kPa normal pressure, and 380 mm long free geotextile

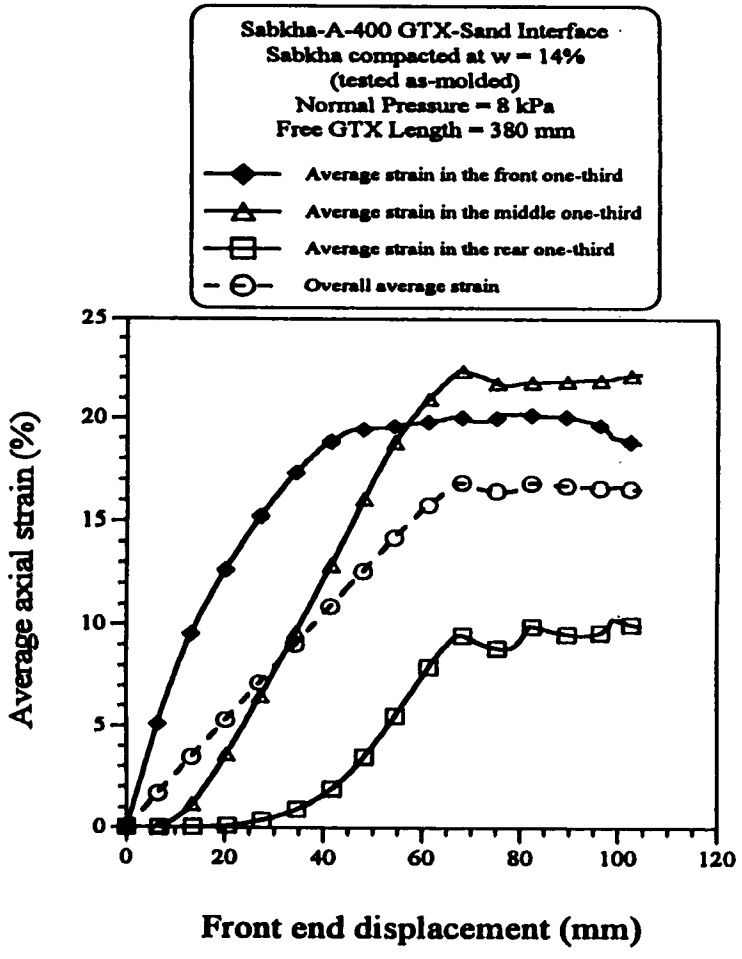

Fig. B1.5: Variation of average axial strain of A-400 geotextile with the front end displacement for sabkha-GTX-sand interface, at 8 kPa normal pressure, and 380 mm long free geotextile

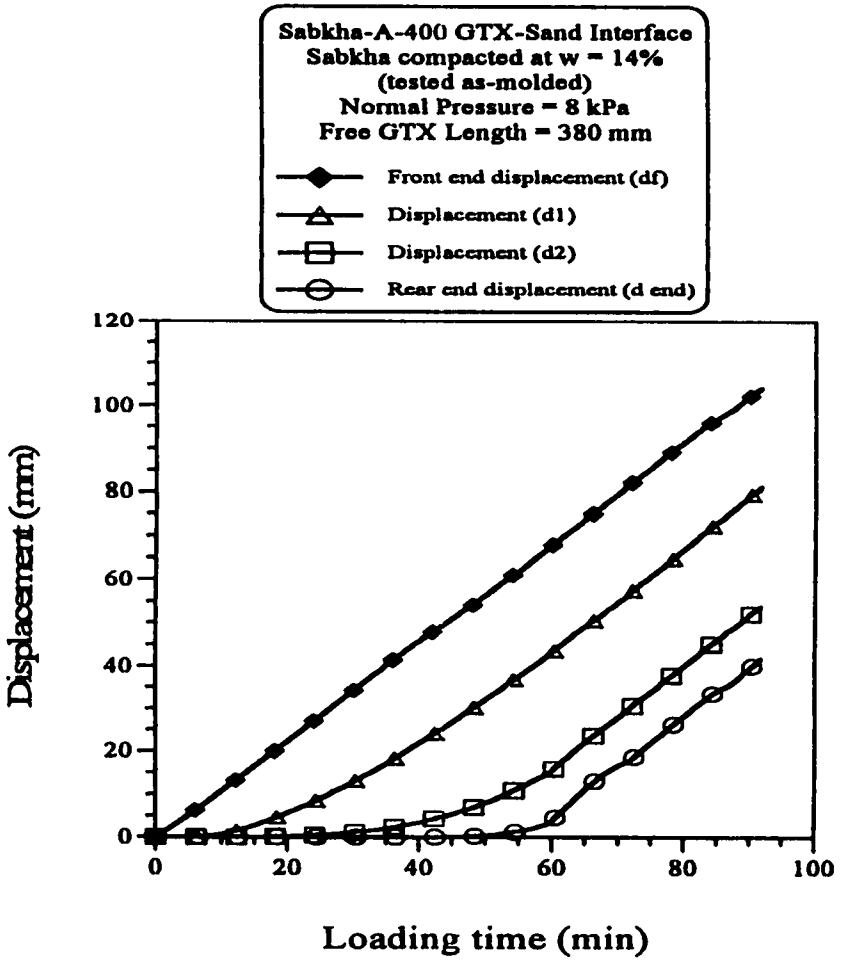

Fig. B1.6: Variation of displacement of A-400 geotextile with loading time for sabkha-GTX-sand interface, at 8 kPa normal pressure, and 380 mm long free geotextile

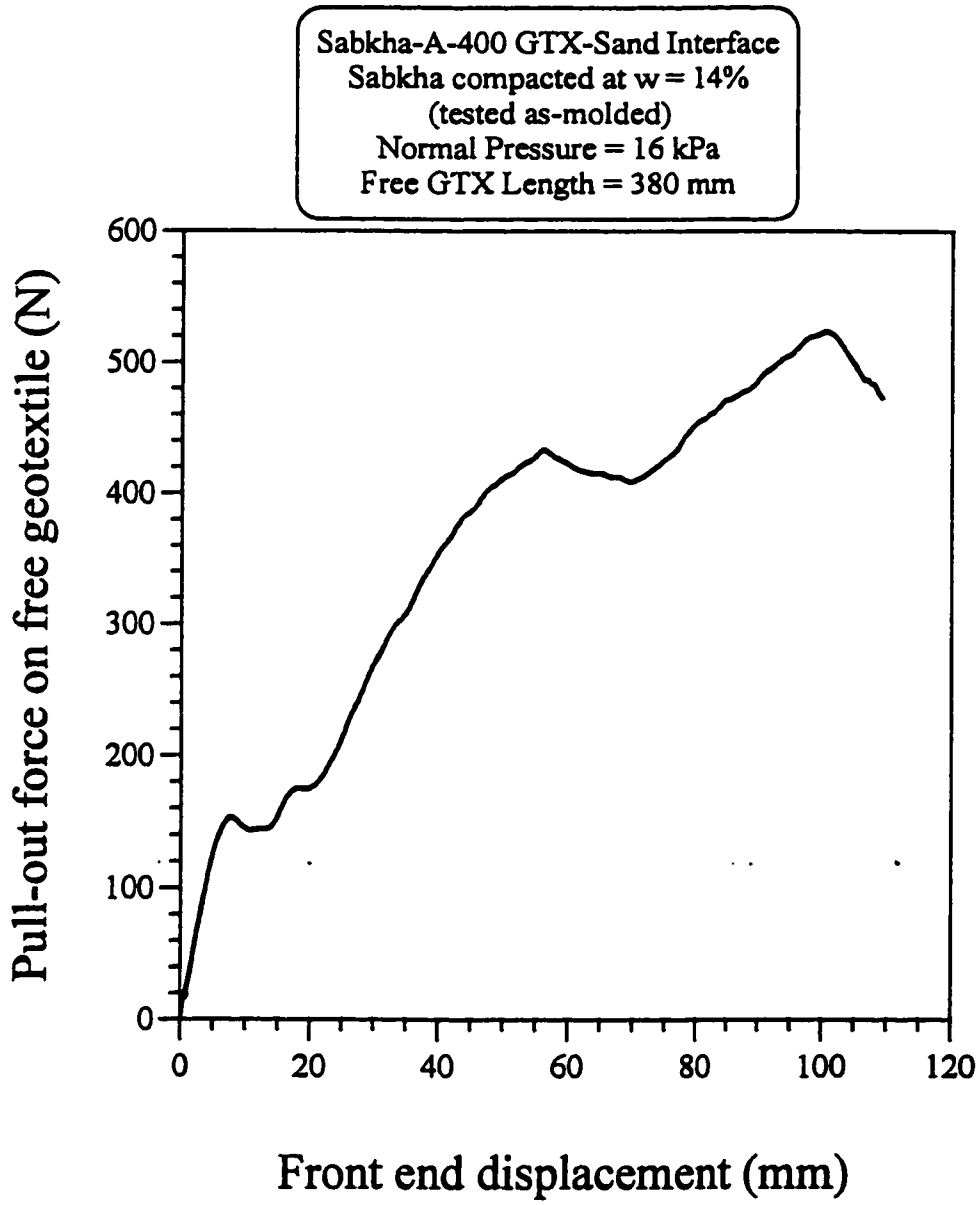

Fig. B1.7: Variation of the pull-out force on A-400 geotextile with the front end displacement for sabkha-GTX-sand interface, at 16 kPa normal pressure, and 380 mm long free geotextile

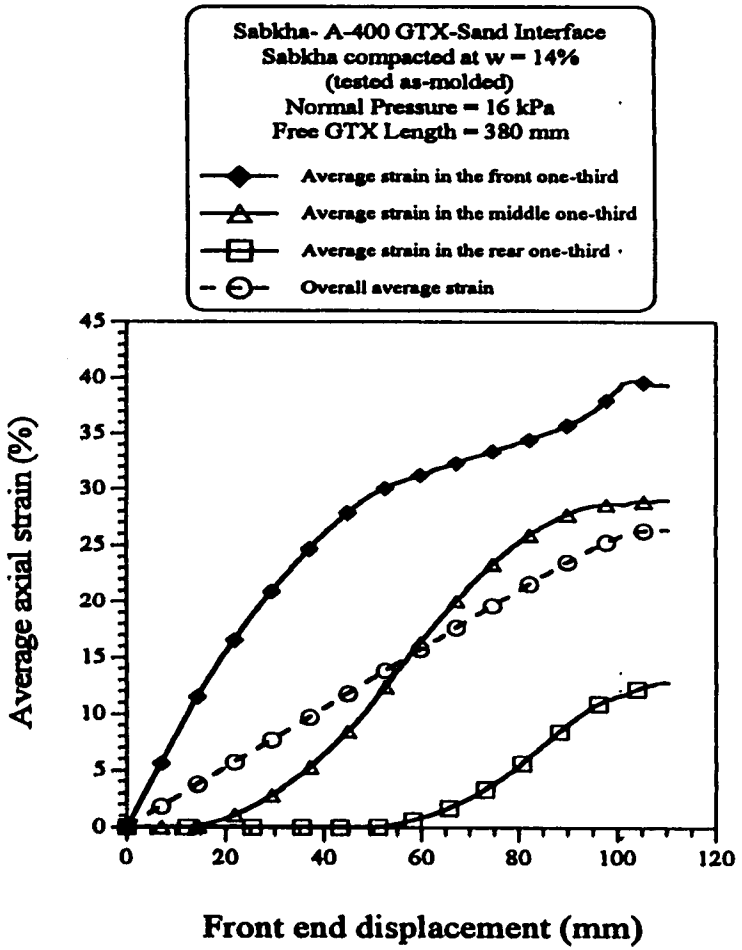

Fig. B1.8: Variation of average axial strain of A-400 geotextile with the front end displacement for sabkha-GTX-sand interface, at 16 kPa normal pressure, and 380 mm long free geotextile

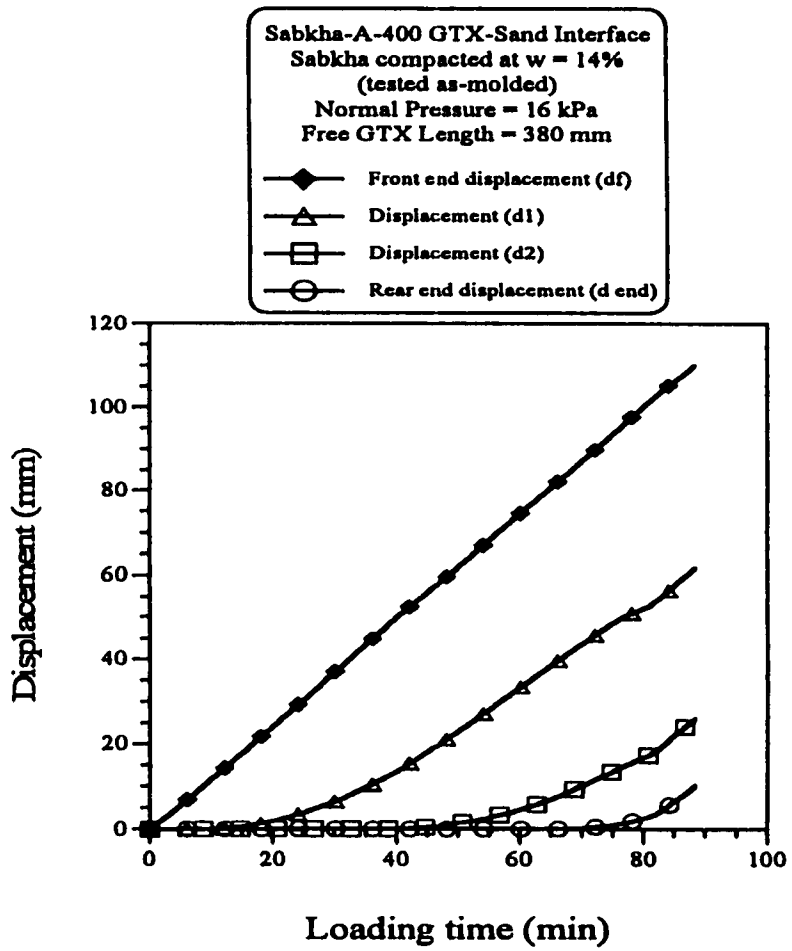

Fig. B1.9: Variation of displacement of A-400 geotextile with loading time for sabkha-GTX-sand interface, at 16 kPa normal pressure, and 380 mm long free geotextile

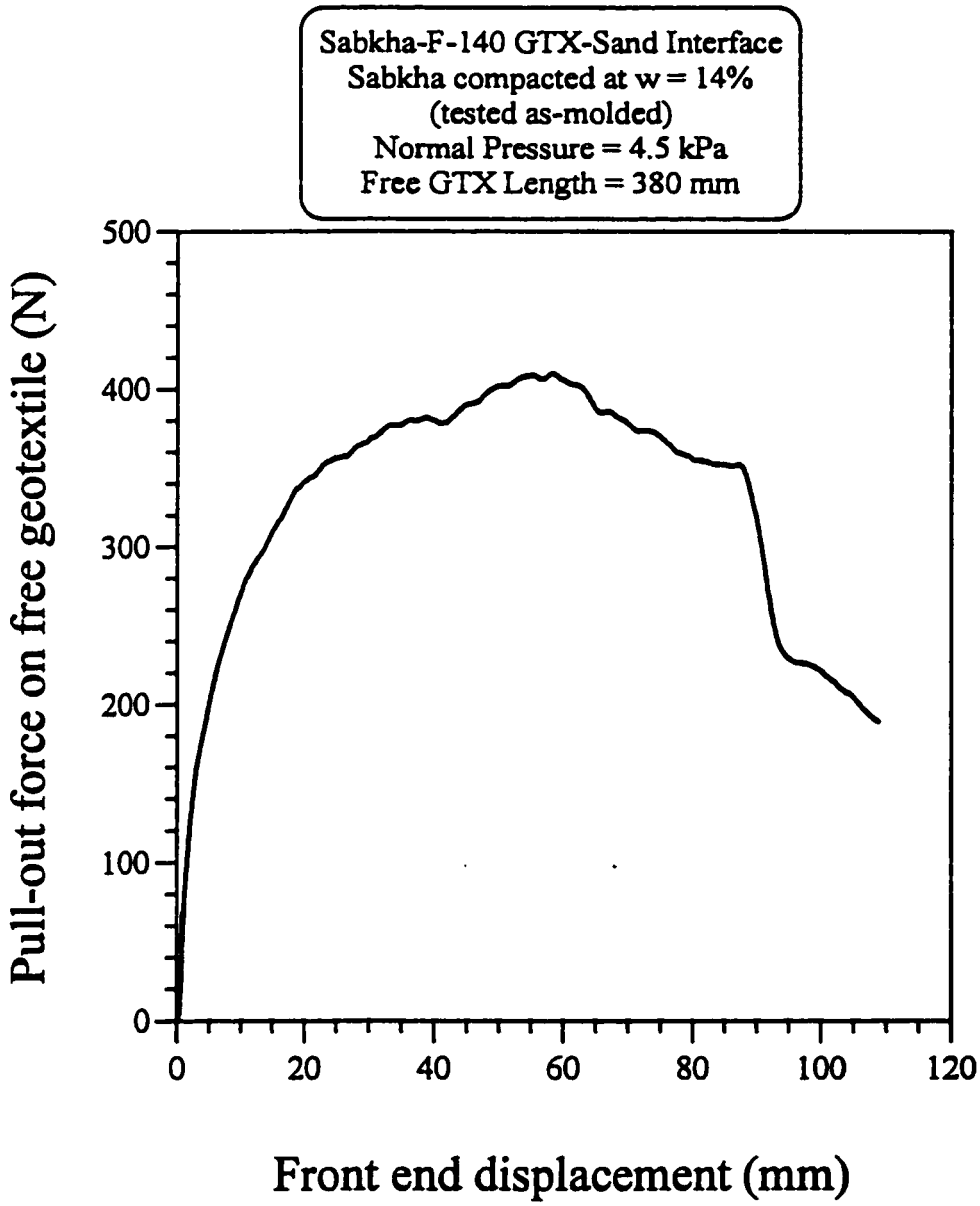

Fig. B1.10: Variation of the pull-out force on F-140 geotextile with the front end displacement for sabkha-GTX-sand interface, at 4.5 kPa normal pressure, and 380 mm long free geotextile

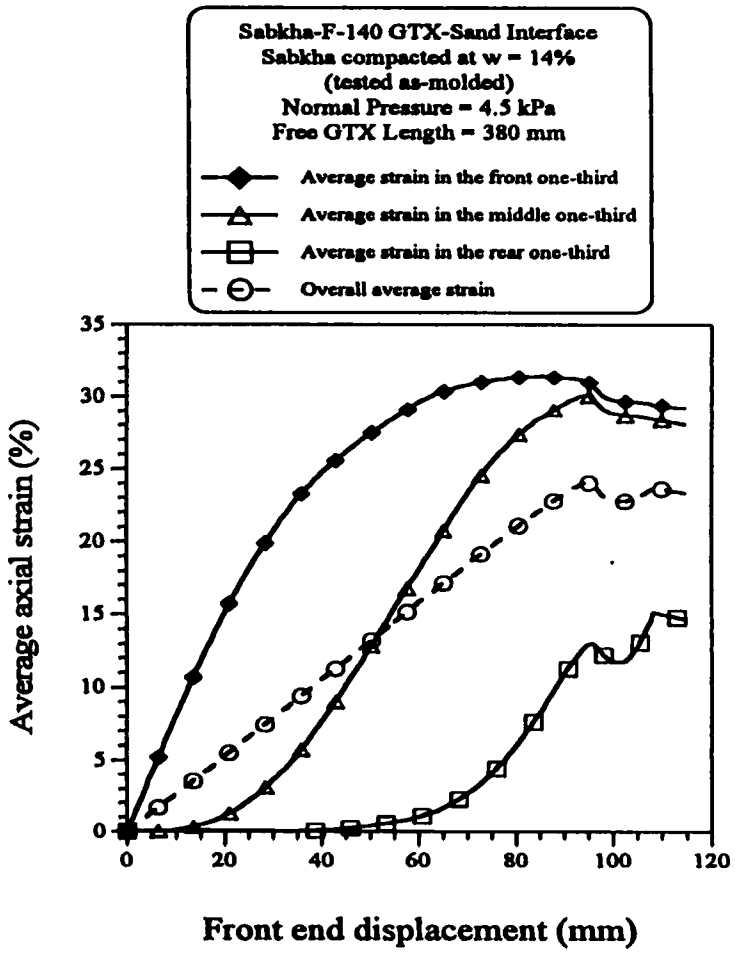

Fig. B1.11: Variation of average axial strain of F-140 geotextile with the front end displacement for sabkha-GTX-sand interface, at 4.5 kPa normal pressure, and 380 mm long free geotextile

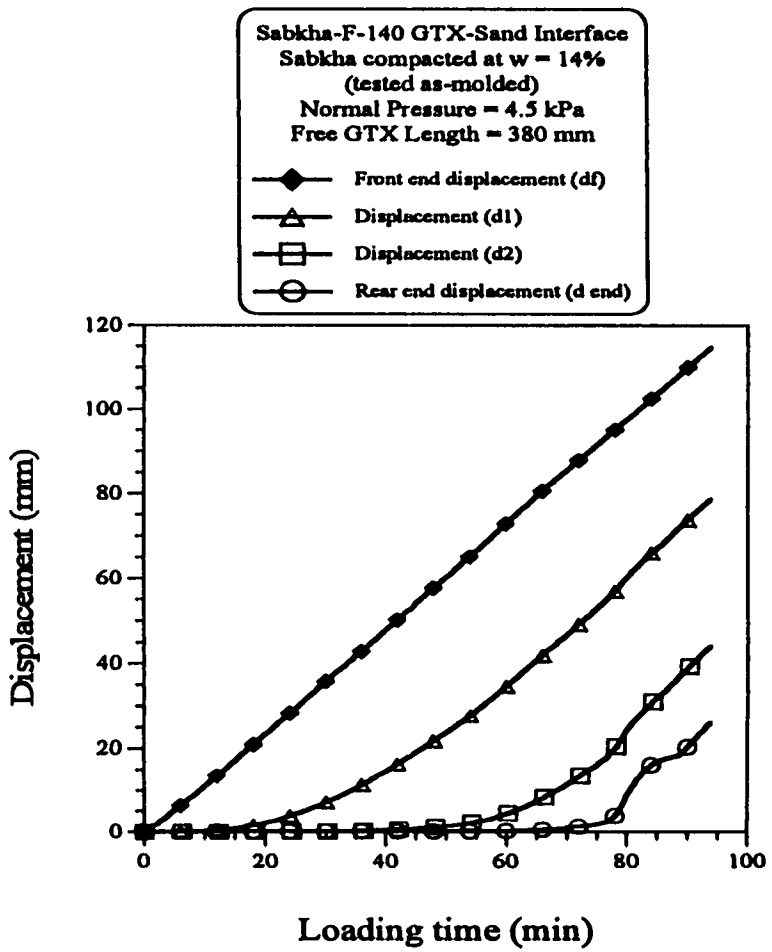

Fig. B1.12: Variation of displacement of F-140 geotextile with loading time for sabkha-GTX-sand interface, at 4.5 kPa normal pressure, and 380 mm long free geotextile

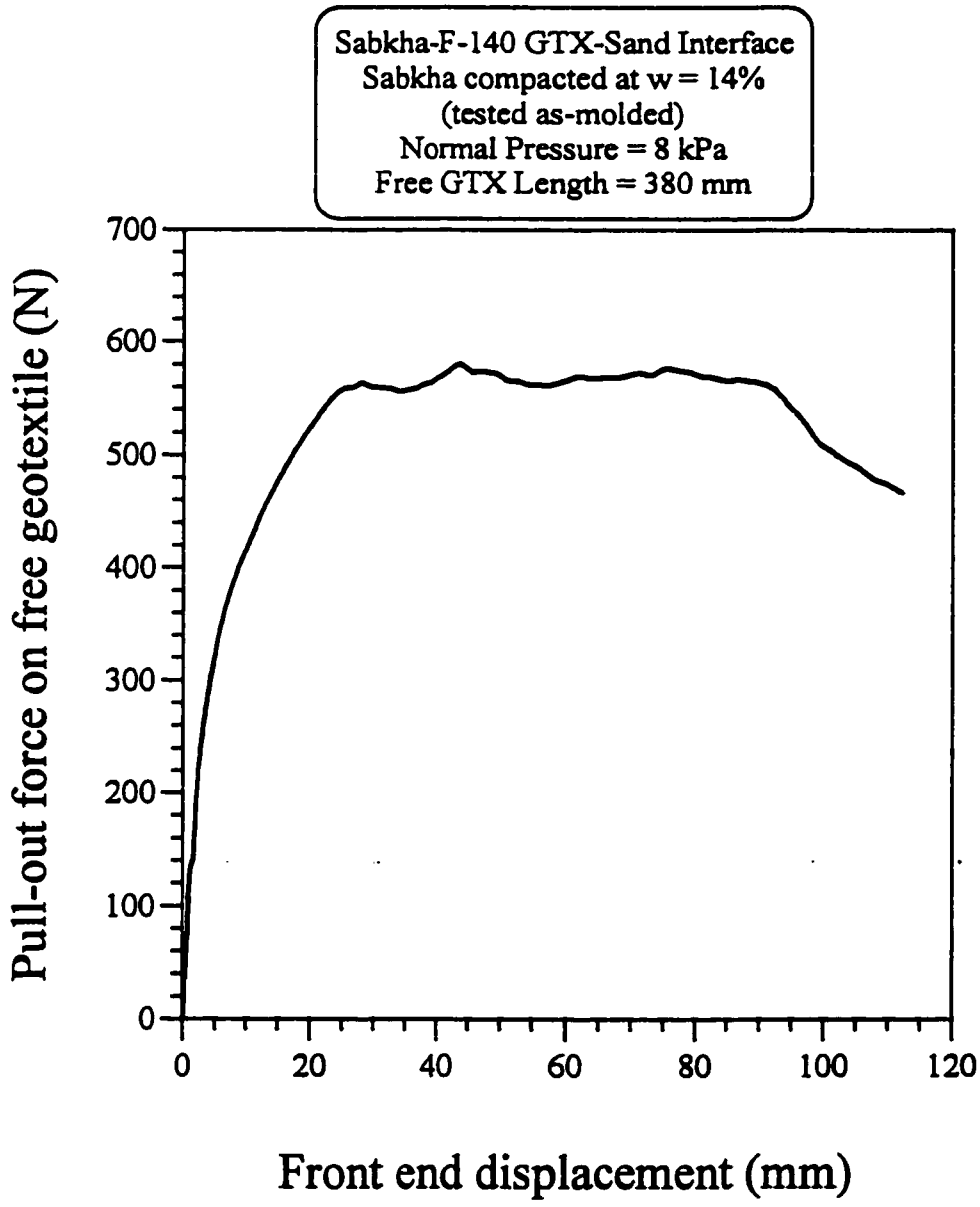

Fig. B1.13: Variation of the pull-out force on F-140 geotextile with the front end displacement for sabkha-GTX-sand interface, at 8 kPa normal pressure, and 380 mm long free geotextile

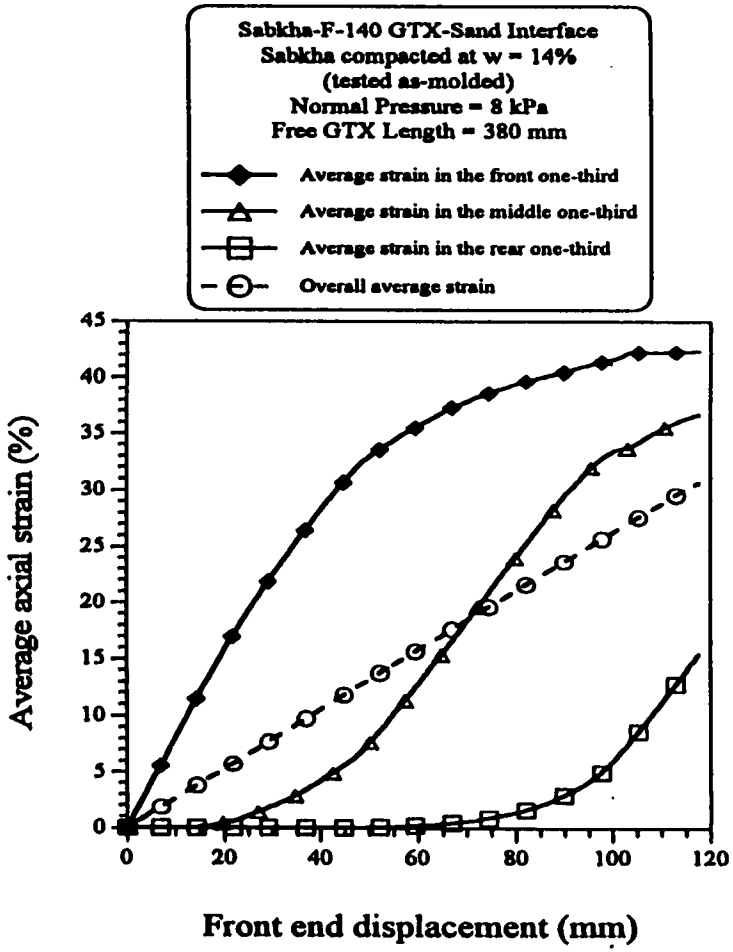

Fig. B1.14: Variation of average axial strain of F-140 geotextile with the front end displacement for sabkha-GTX-sand interface, at 8 kPa normal pressure, and 380 mm long free geotextile

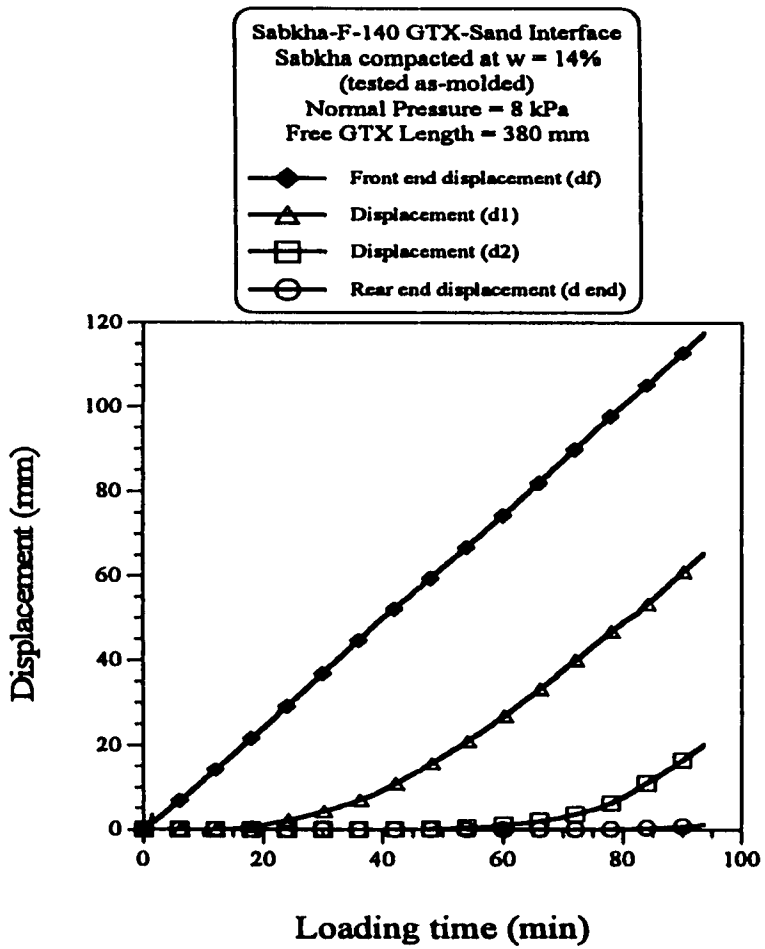

Fig. B1.15: Variation of displacement of F-140 geotextile with loading time for sabkha-GTX-sand interface, at 8 kPa normal pressure, and 380 mm long free geotextile

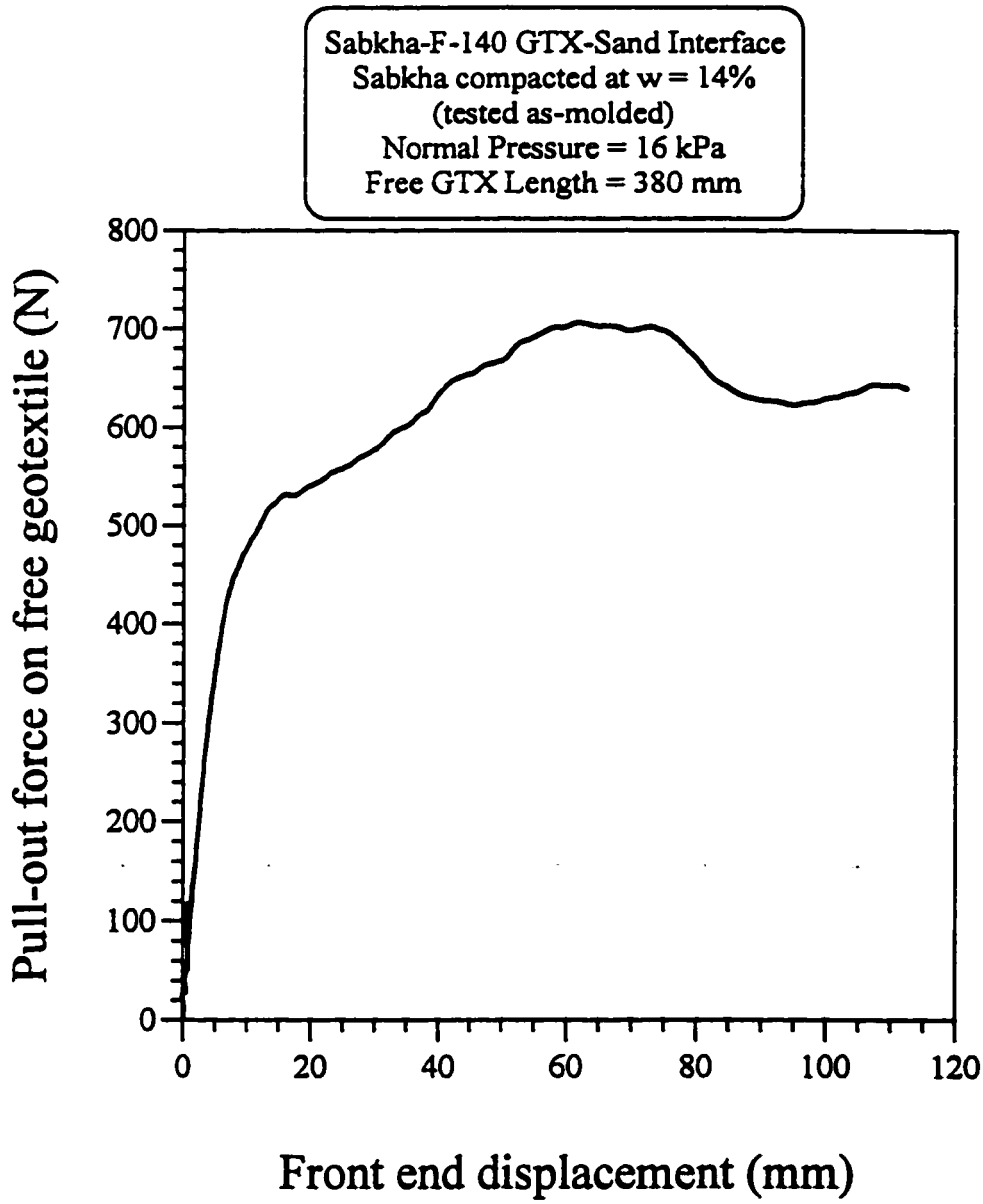

Fig. B1.16: Variation of the pull-out force on F-140 geotextile with the front end displacement for sabkha-GTX-sand interface, at 16 kPa normal pressure, and 380 mm long free geotextile

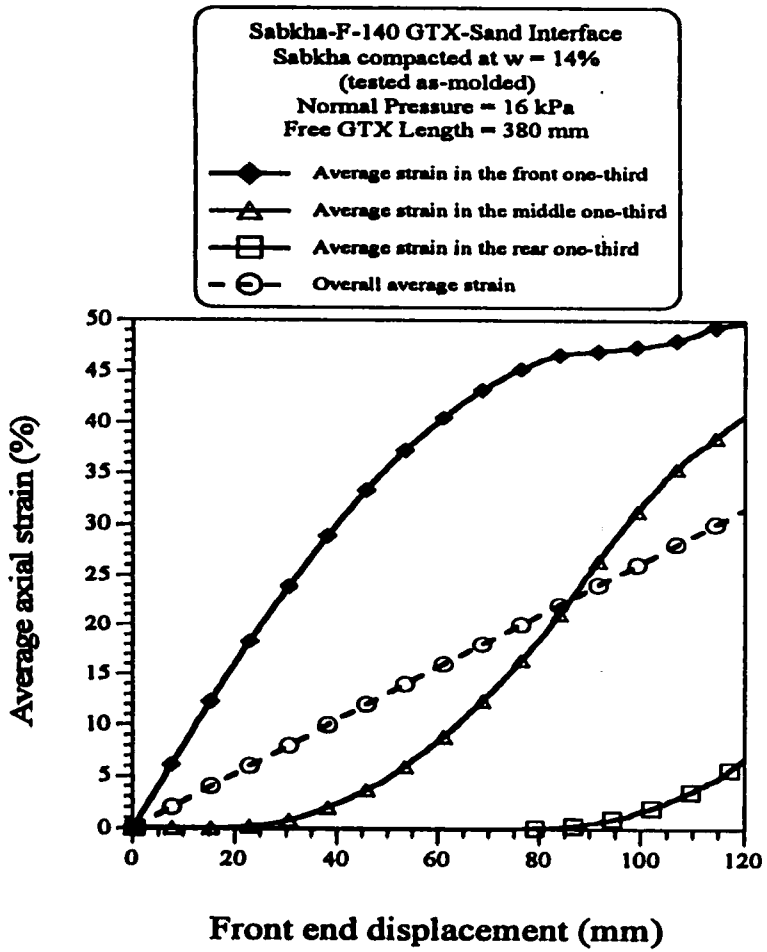

Fig. B1.17: Variation of average axial strain of F-140 geotextile with the front end displacement for sabkha-GTX-sand interface, at 16 kPa normal pressure, and 380 mm long free geotextile

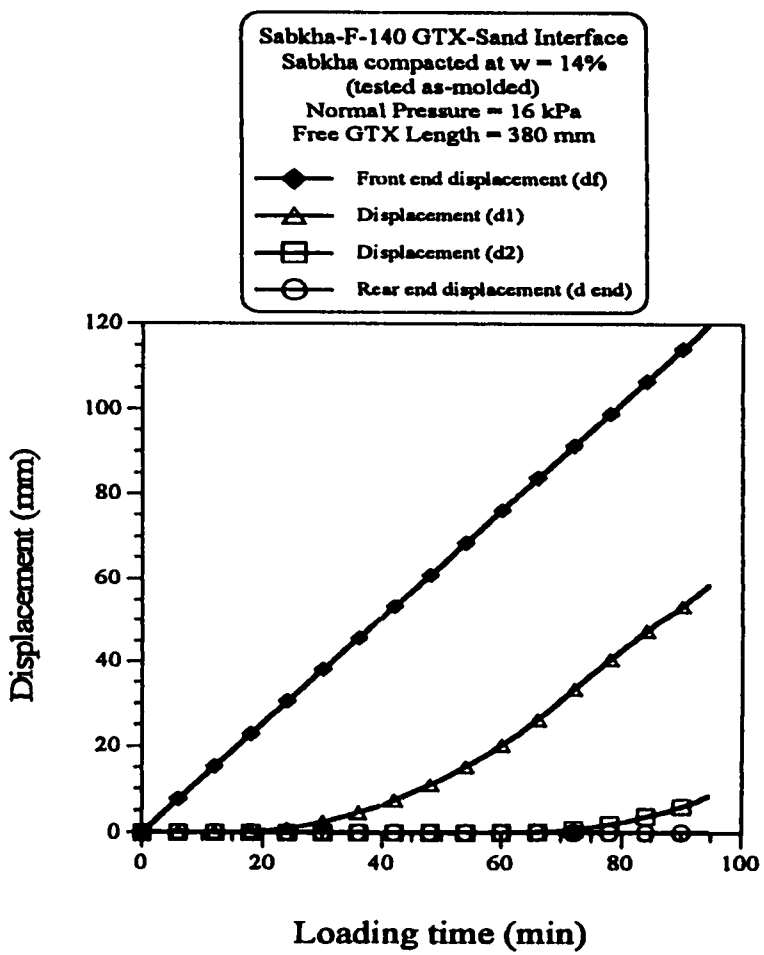

Fig. B1.18: Variation of displacement of F-140 geotextile with loading time for sabkha-GTX-sand interface, at 16 kPa normal pressure, and 380 mm long free geotextile

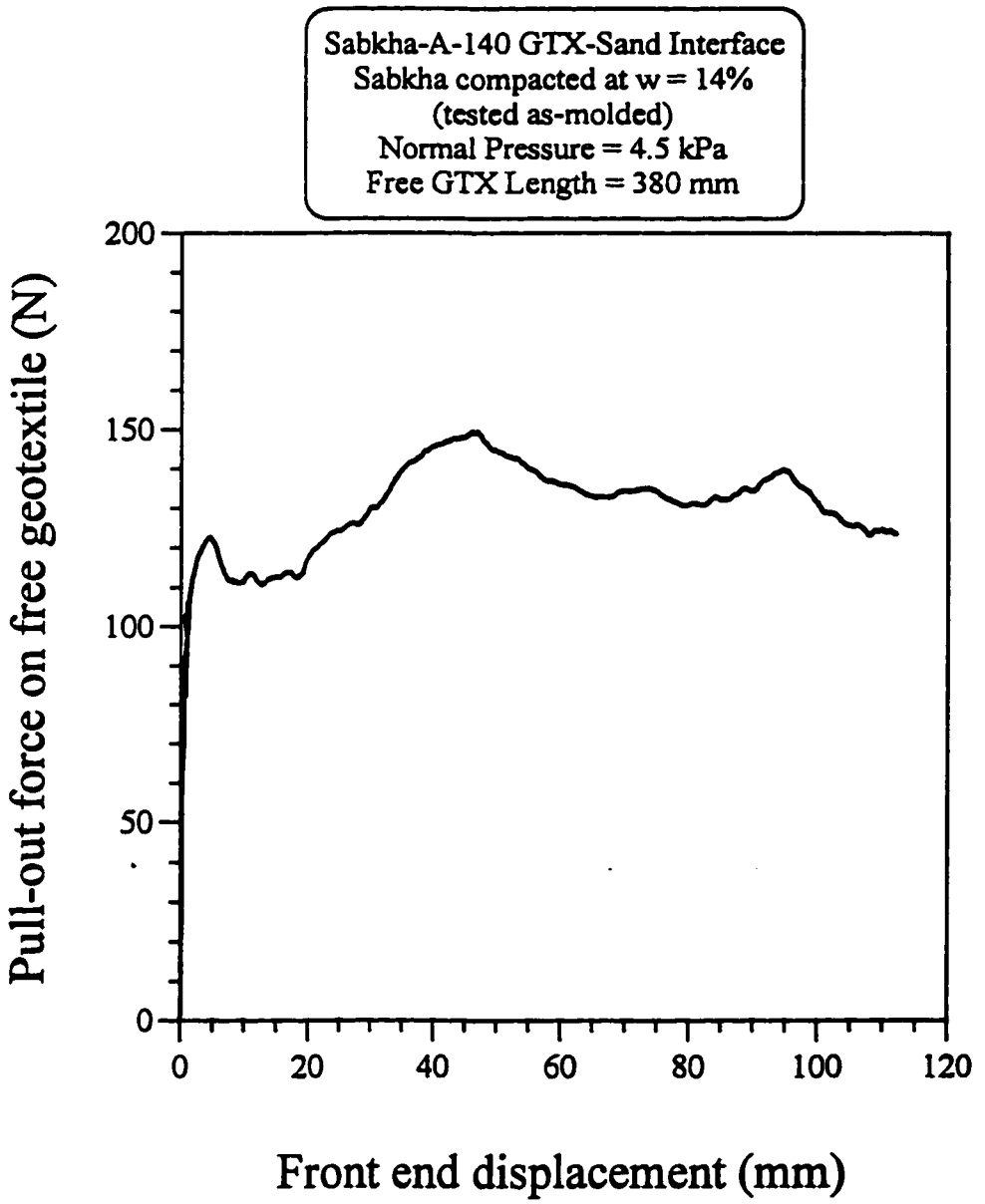

Fig. B1.19: Variation of the pull-out force on A-140 geotextile with the front end displacement for sabkha-GTX-sand interface, at 4.5 kPa normal pressure, and 380 mm long free geotextile

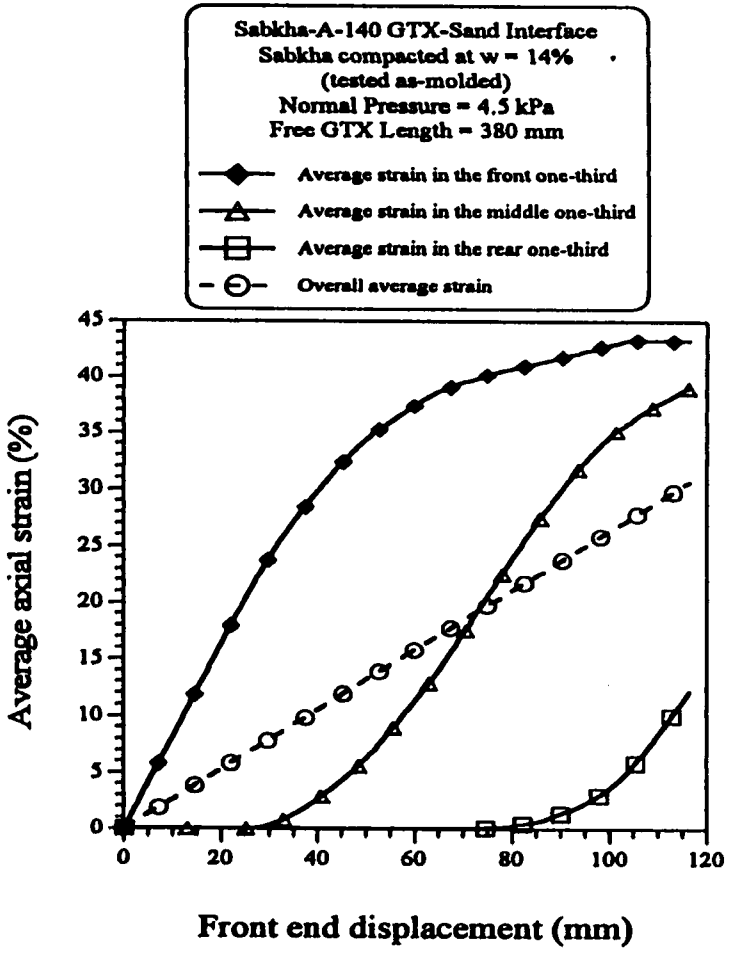

Fig. B1.20: Variation of average axial strain of A-140 geotextile with the front end displacement for sabkha-GTX-sand interface, at 4.5 kPa normal pressure, and 380 mm long free geotextile

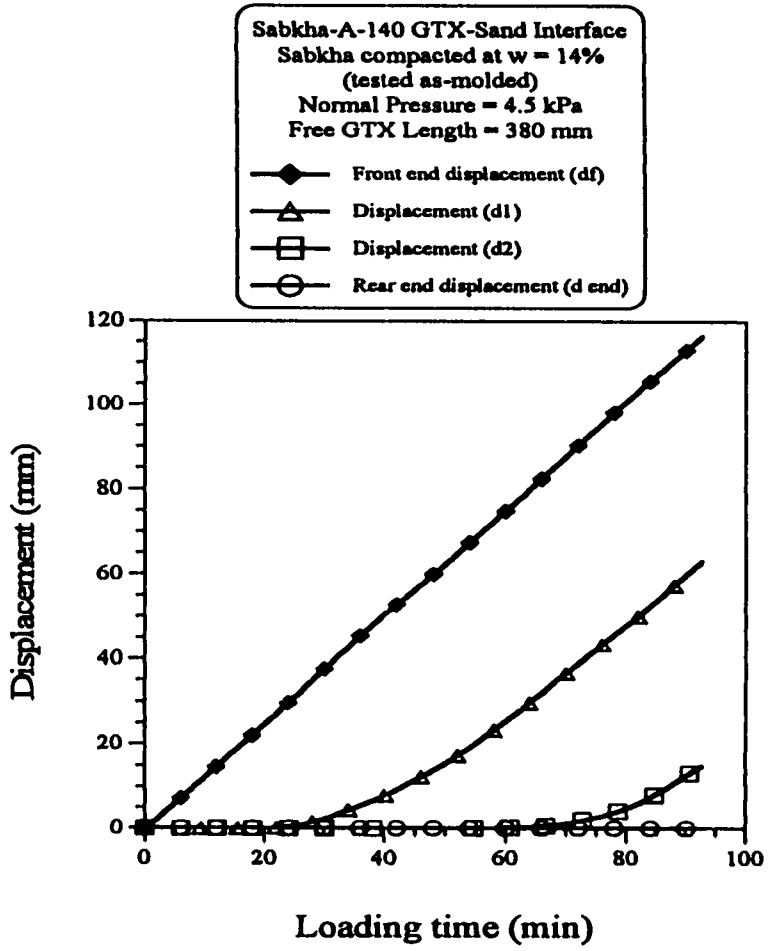

Fig. B1.21: Variation of displacement of A-140 geotextile with loading time for sabkha-GTX-sand interface, at 4.5 kPa normal pressure, and 380 mm long free geotextile

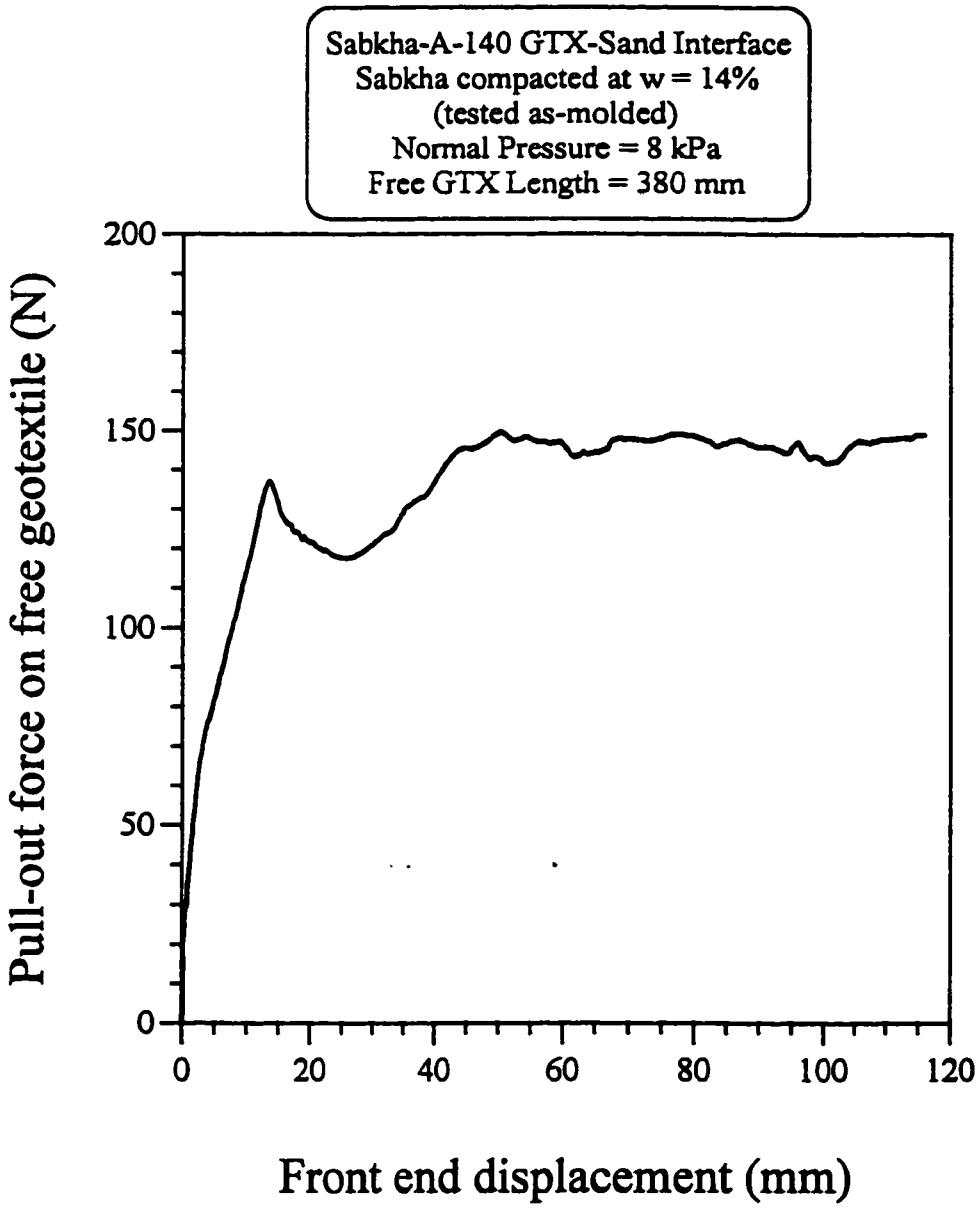

Fig. B1.22: Variation of the pull-out force on A-140 geotextile with the front end displacement for sabkha-GTX-sand interface, at 8 kPa normal pressure, and 380 mm long free geotextile

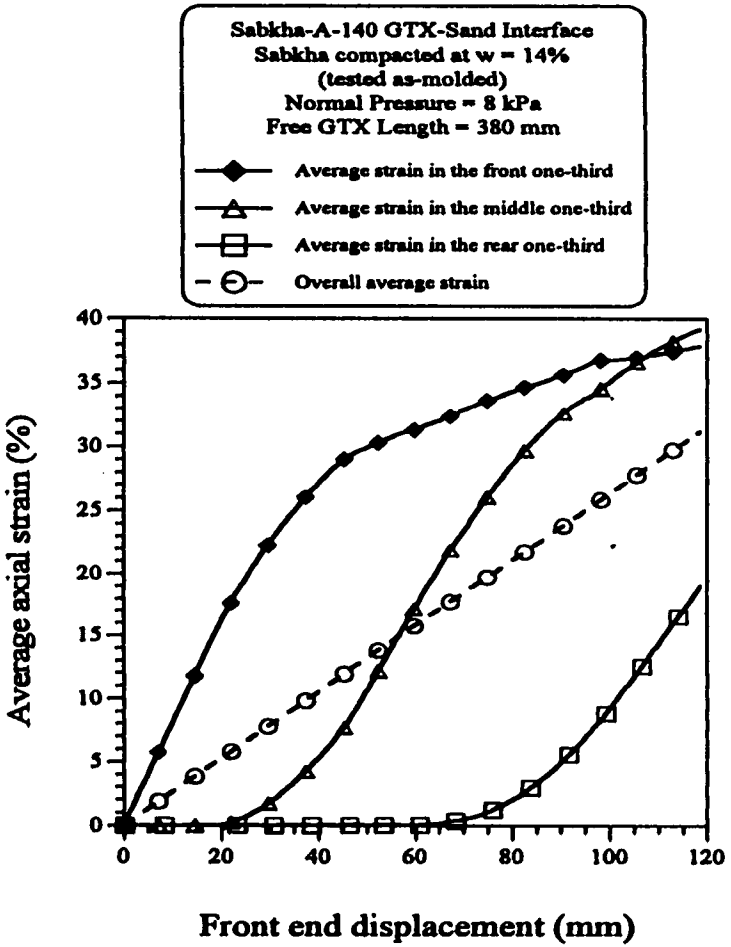

Fig. B1.23: Variation of average axial strain of A-140 geotextile with the front end displacement for sabkha-GTX-sand interface, at 8 kPa normal pressure, and 380 mm long free geotextile

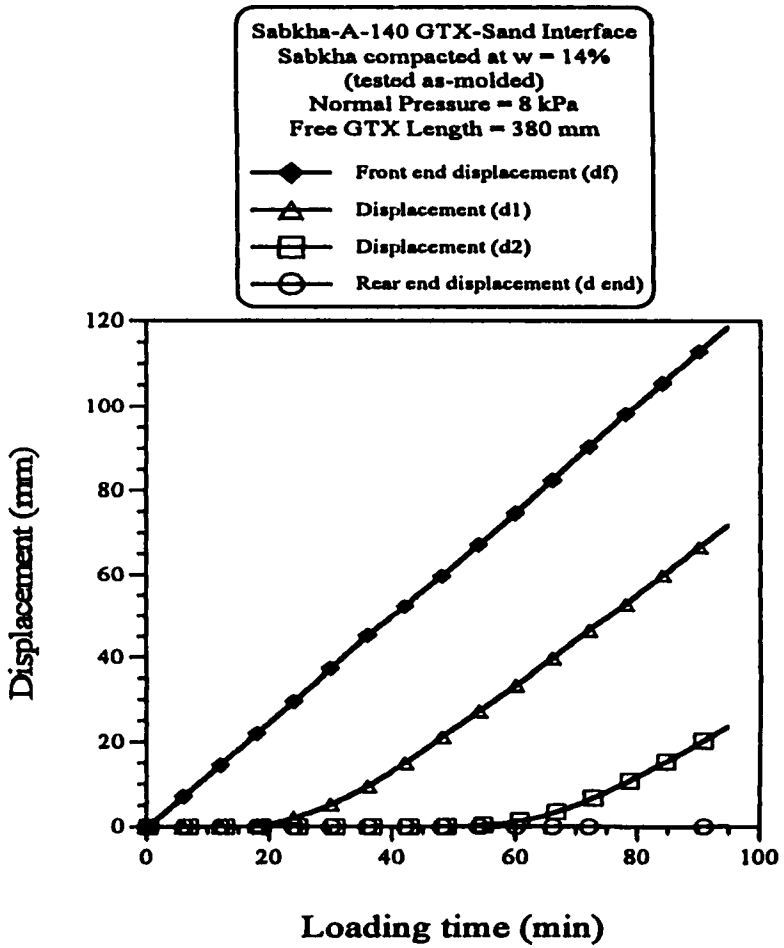

Fig. B1.24: Variation of displacement of A-140 geotextile with loading time for sabkha-GTX-sand interface, at 8 kPa normal pressure, and 380 mm long free geotextile

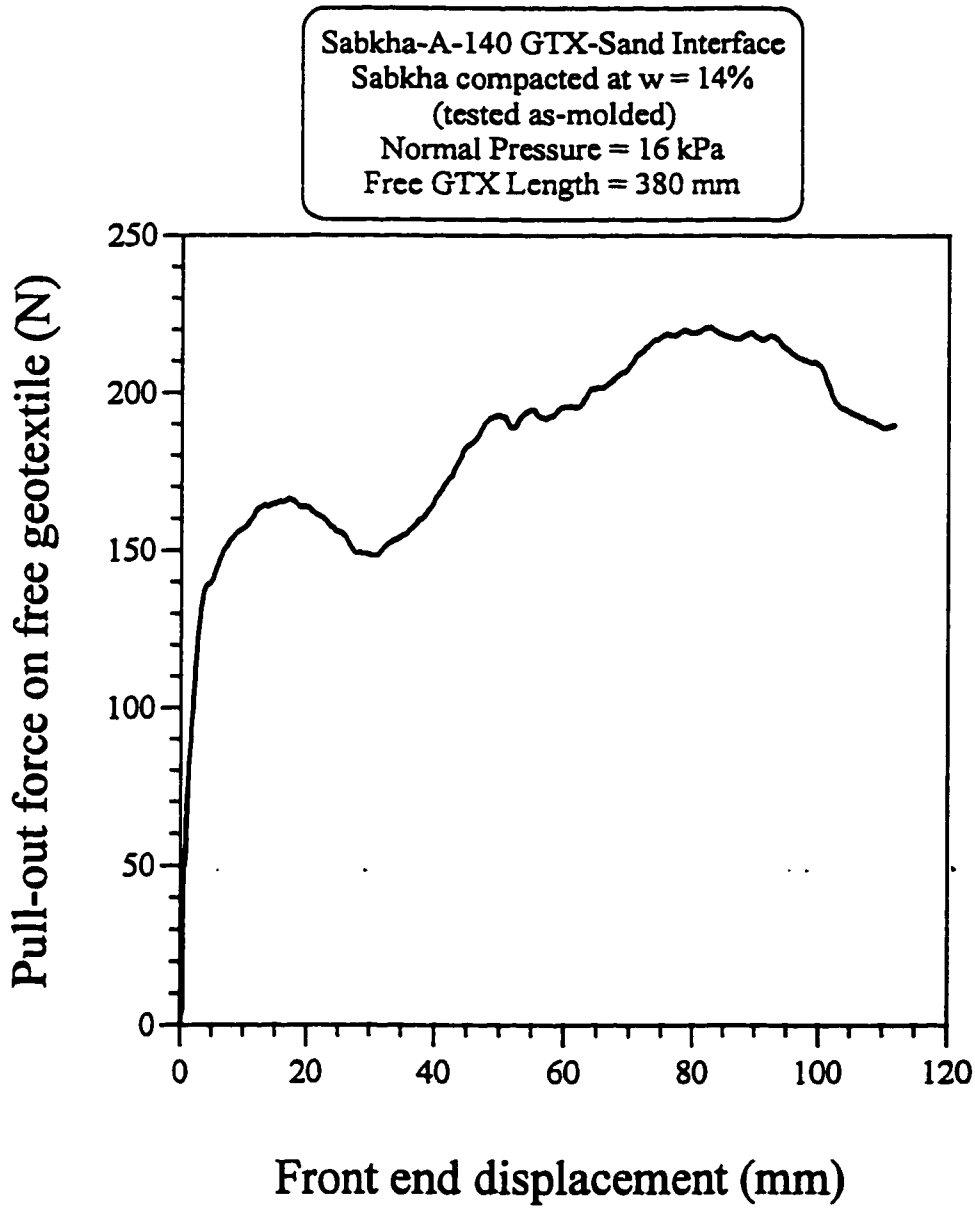

Fig. B1.25: Variation of the pull-out force on A-140 geotextile with the front end displacement for sabkha-GTX-sand interface, at 16 kPa normal pressure, and 380 mm long free geotextile

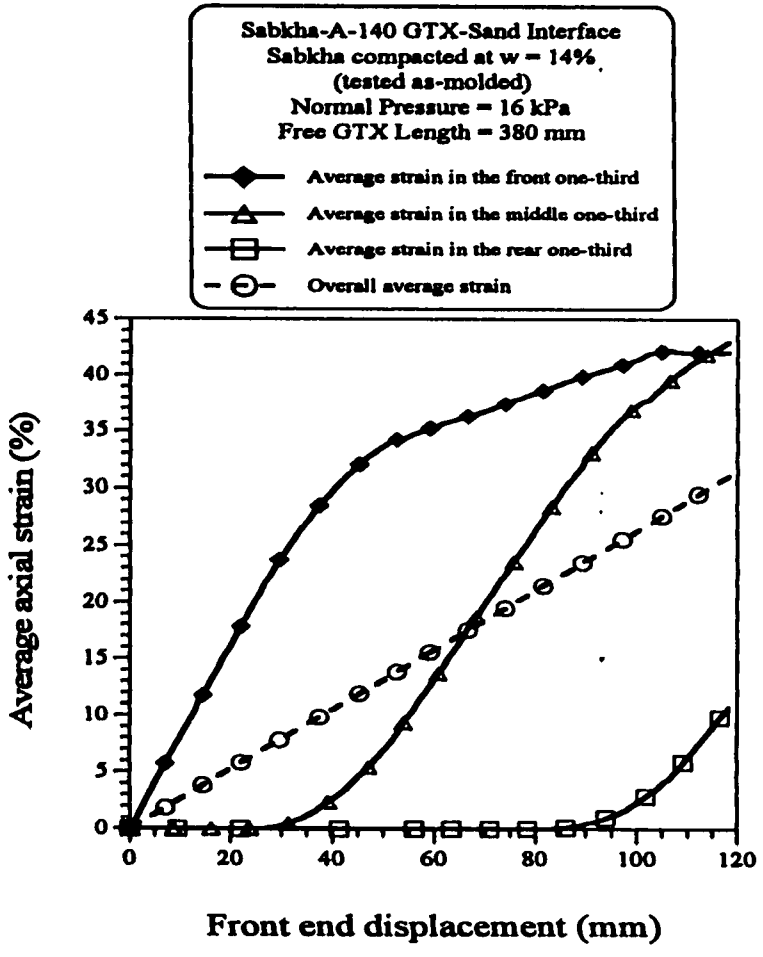

Fig. B1.26: Variation of average axial strain of A-140 geotextile with the front end displacement for sabkha-GTX-sand interface, at 16 kPa normal pressure, and 380 mm long free geotextile

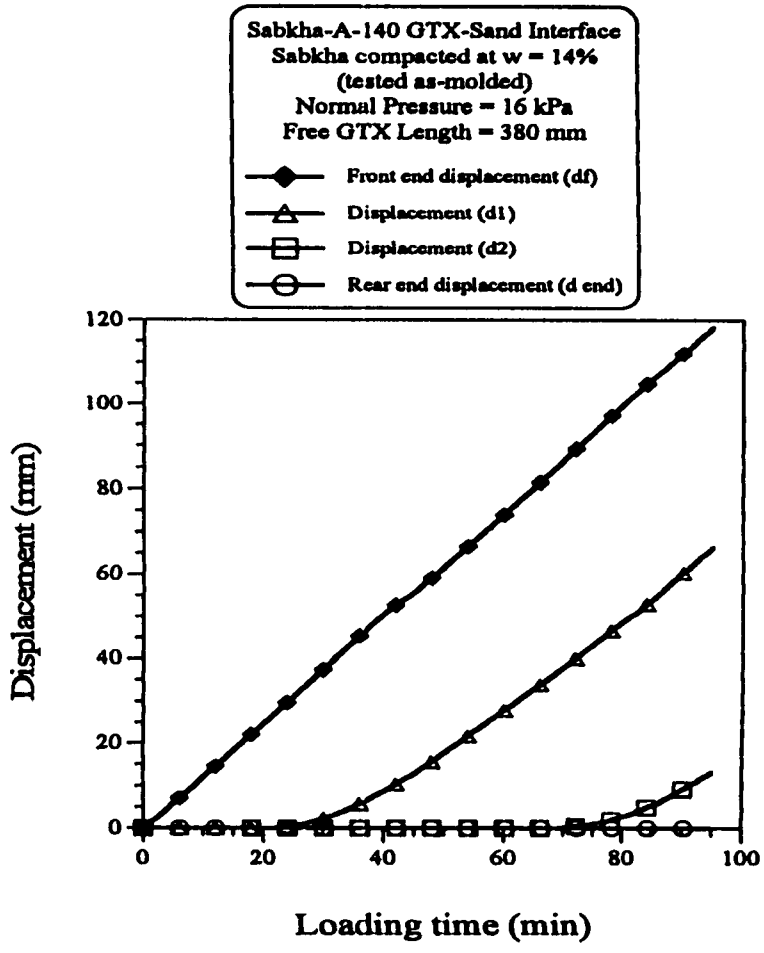

Fig. B1.27: Variation of displacement of A-140 geotextile with loading time for sabkha-GTX-sand interface, at 16 kPa normal pressure, and 380 mm long free geotextile

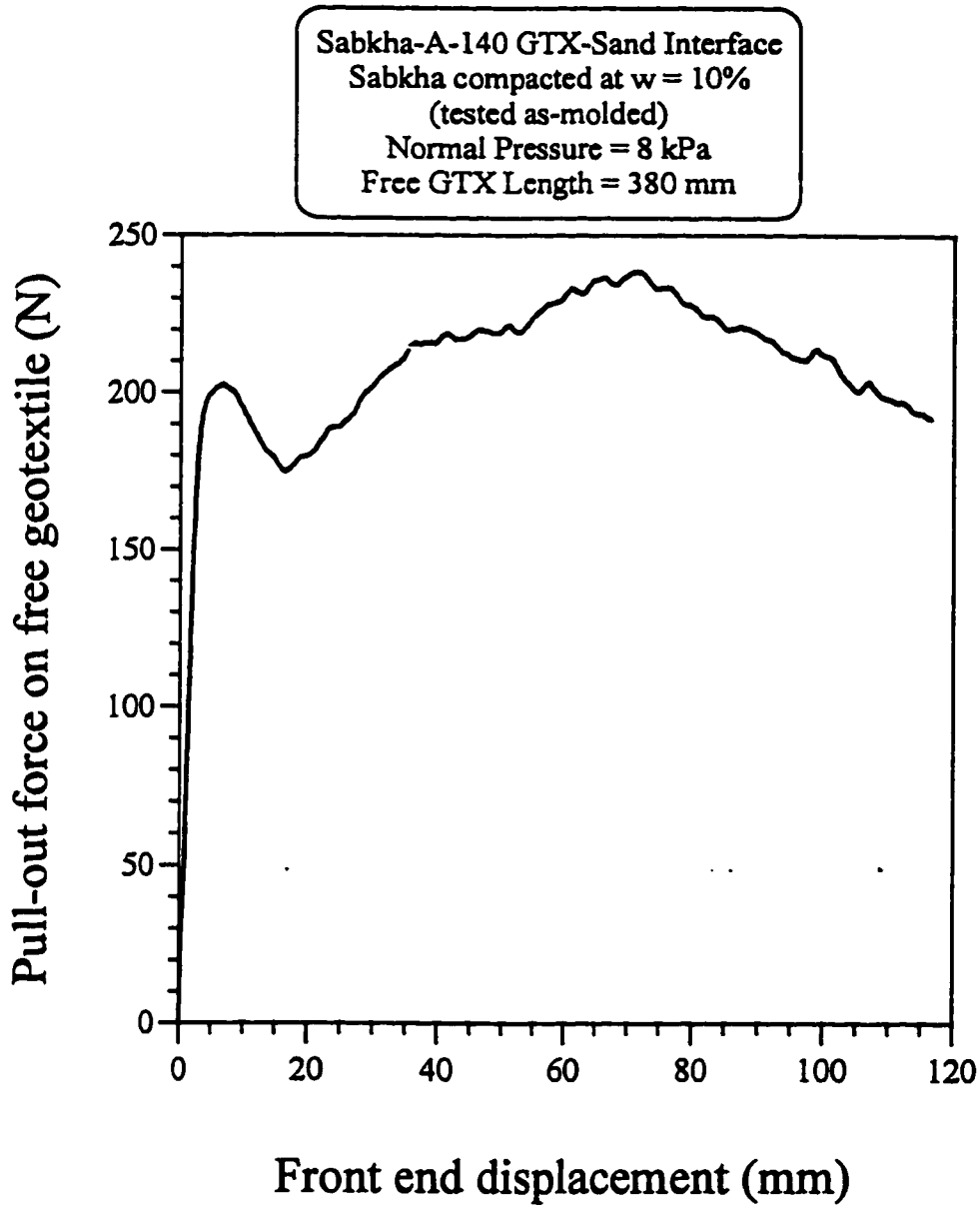

Fig. B1.28: Variation of the pull-out force on A-140 geotextile with the front end displacement for sabkha-GTX-sand interface, at 8 kPa normal pressure, and 380 mm long free geotextile

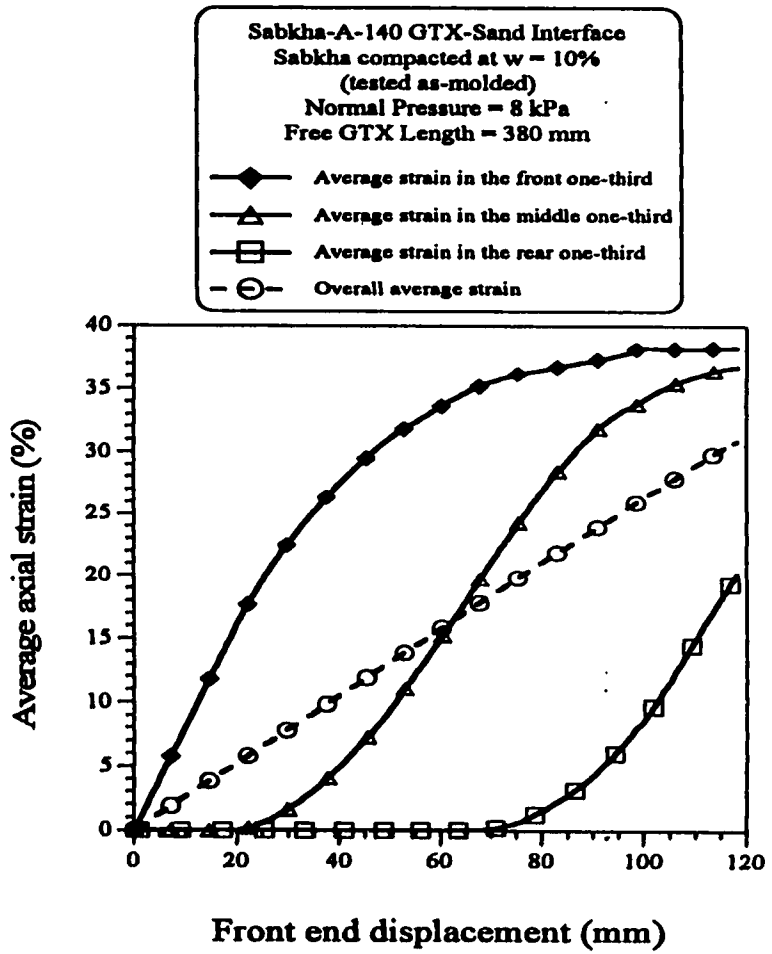

Fig. B1.29: Variation of average axial strain of A-140 geotextile with the front end displacement for sabkha-GTX-sand interface, at 8 kPa normal pressure, and 380 mm long free geotextile

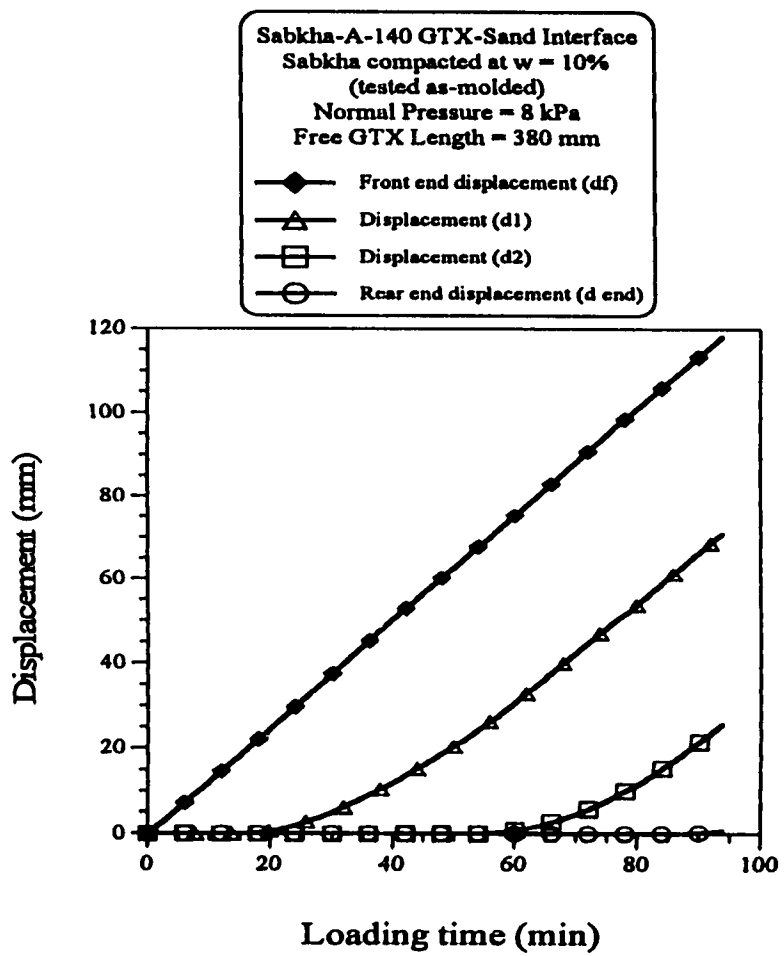

Fig. B1.30: Variation of displacement of A-140 geotextile with loading time for sabkha-GTX-sand interface, at 8 kPa normal pressure, and 380 mm long free geotextile

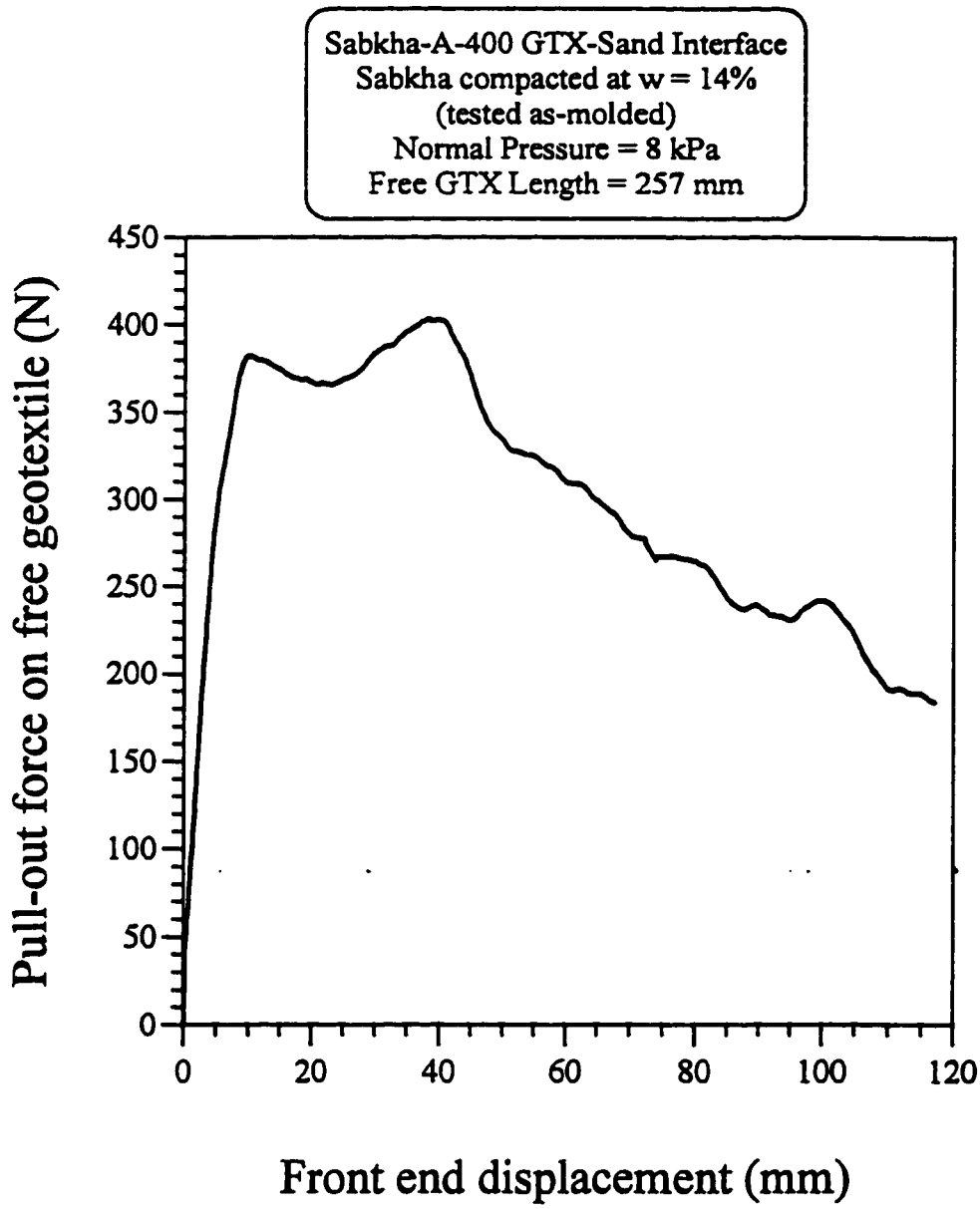

Fig. B1.31: Variation of the pull-out force on A-400 geotextile with the front end displacement for sabkha-GTX-sand interface, at 8 kPa normal pressure, and 257 mm long free geotextile

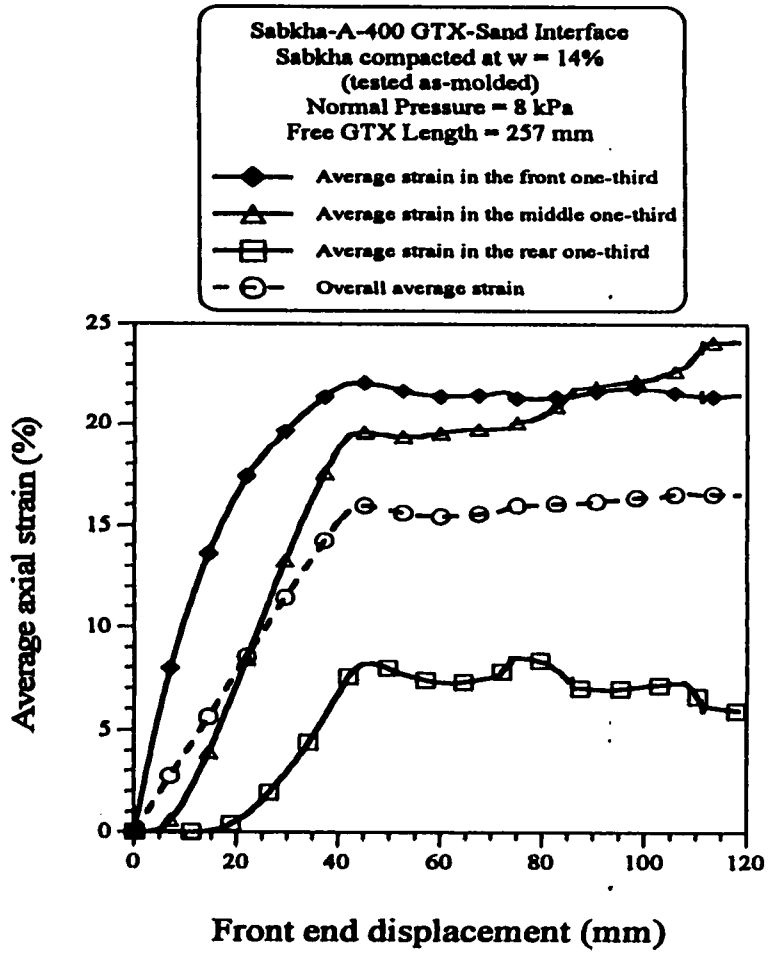

Fig. B1.32: Variation of average axial strain of A-400 geotextile with the front end displacement for sabkha-GTX-sand interface, at 8 kPa normal pressure, and 257 mm long free geotextile

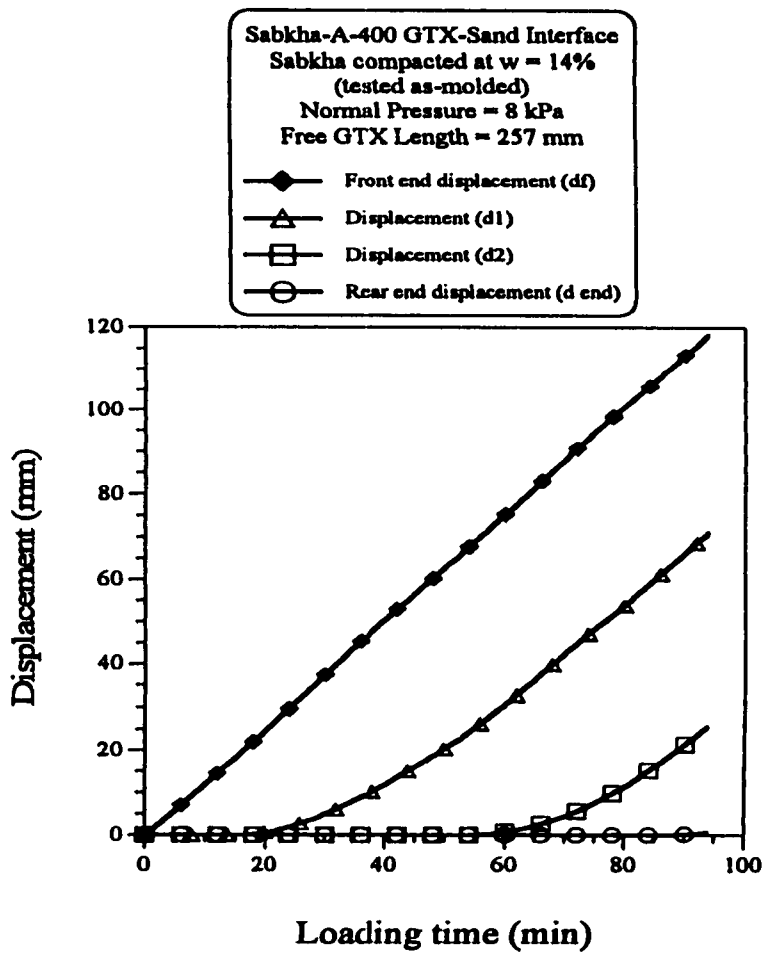

Fig. B1.33: Variation of displacement of A-400 geotextile with loading time for sabkha-GTX-sand interface, at 8 kPa normal pressure, and 257 mm long free geotextile

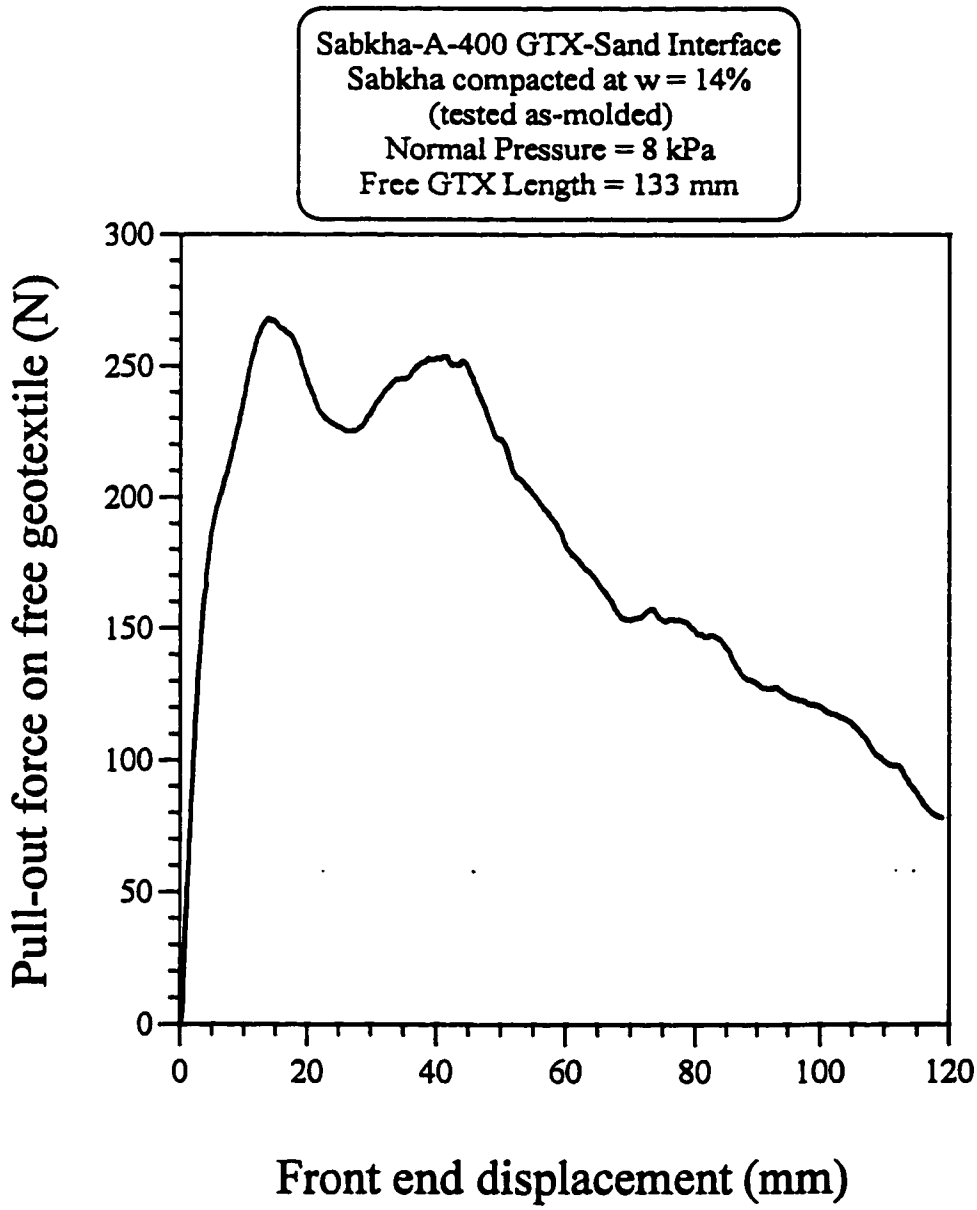

Fig. B1.34: Variation of the pull-out force on A-400 geotextile with the front end displacement for sabkha-GTX-sand interface, at 8 kPa normal pressure, and 133 mm long free geotextile

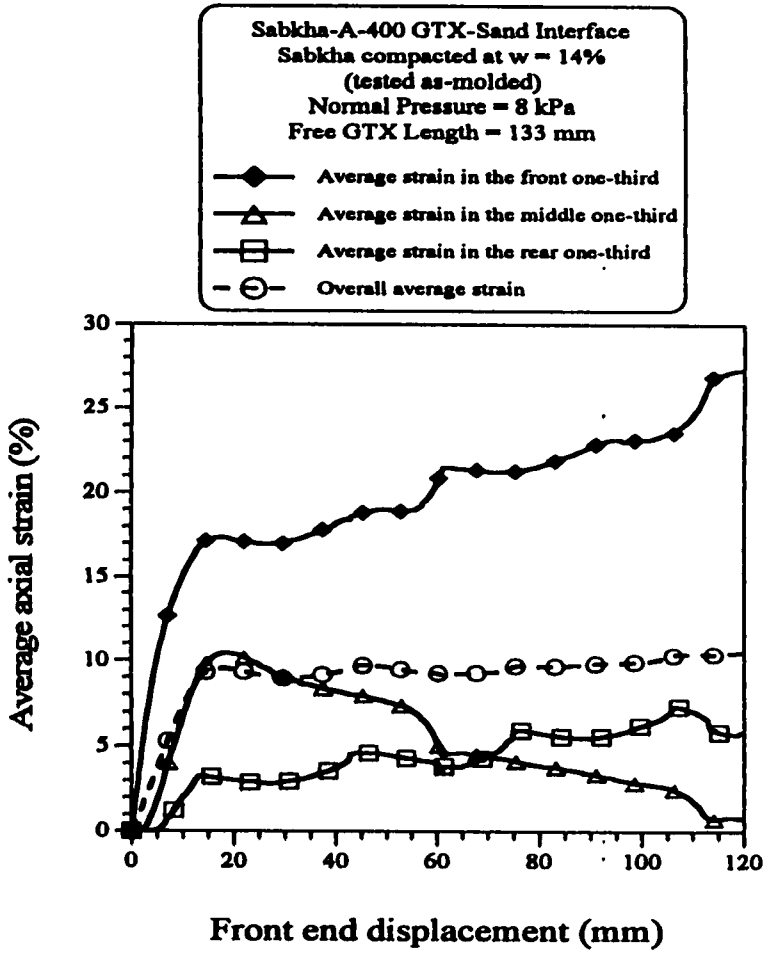

Fig. B1.35: Variation of average axial strain of A-400 geotextile with the front end displacement for sabkha-GTX-sand interface, at 8 kPa normal pressure, and 133 mm long free geotextile

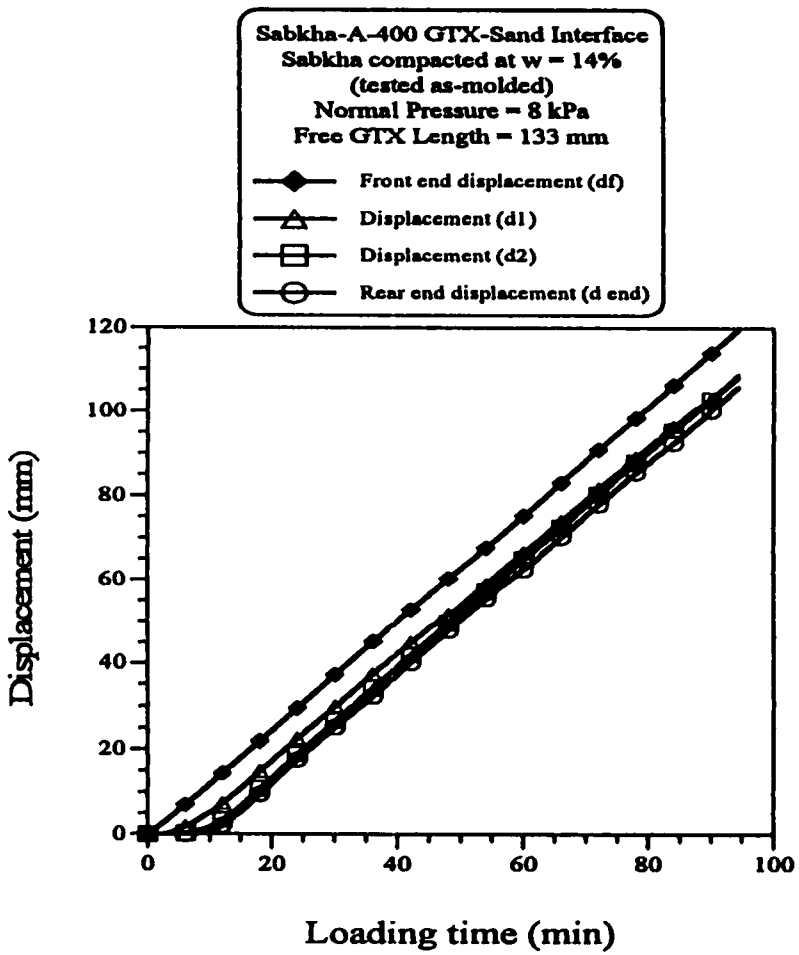

Fig. B1.36: Variation of displacement of A-400 geotextile with loading time for sabkha-GTX-sand interface, at 8 kPa normal pressure, and 133 mm long free geotextile

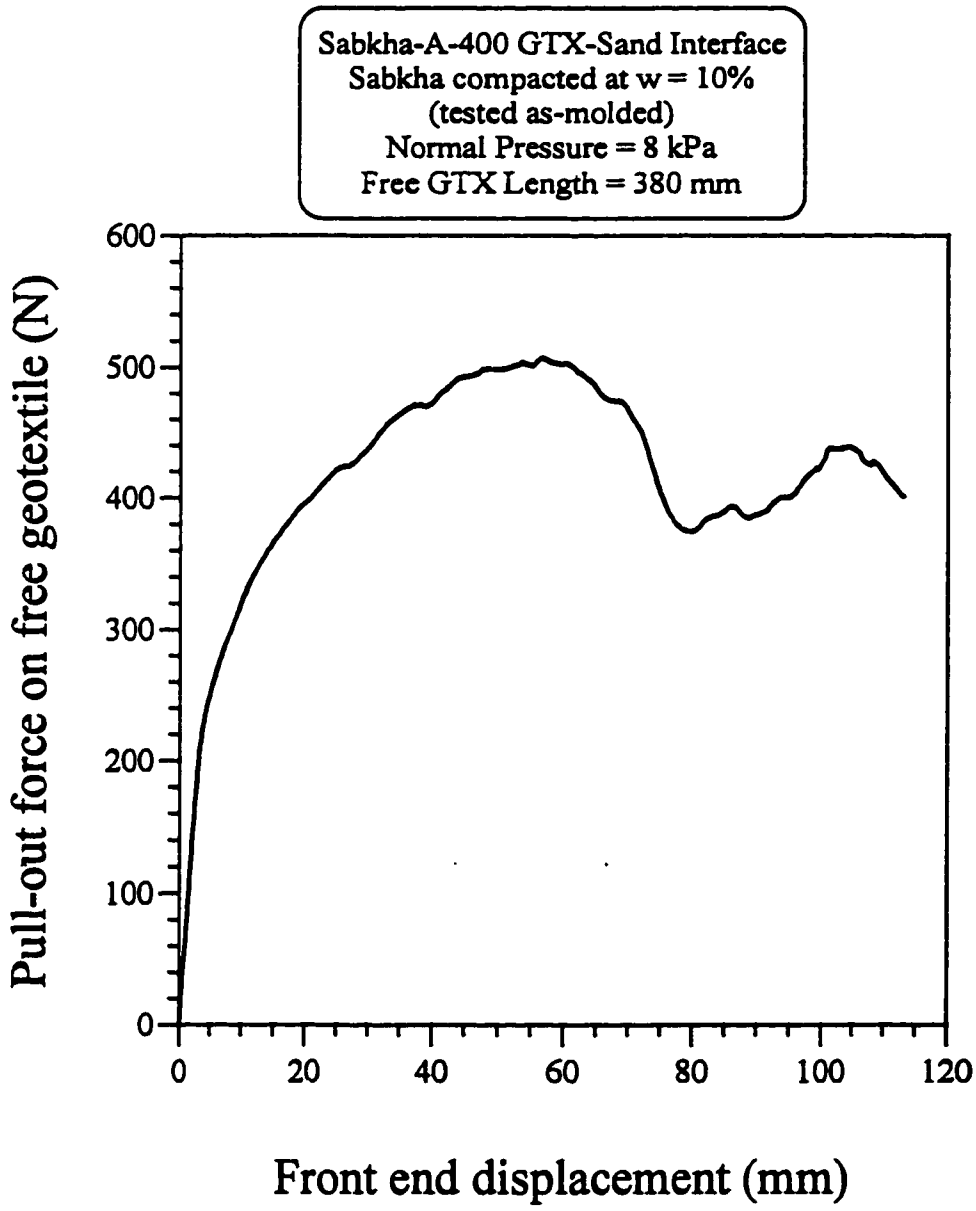

Fig. B1.37: Variation of the pull-out force on A-400 geotextile with the front end displacement for sabkha-GTX-sand interface, at 8 kPa normal pressure, and 380 mm long free geotextile

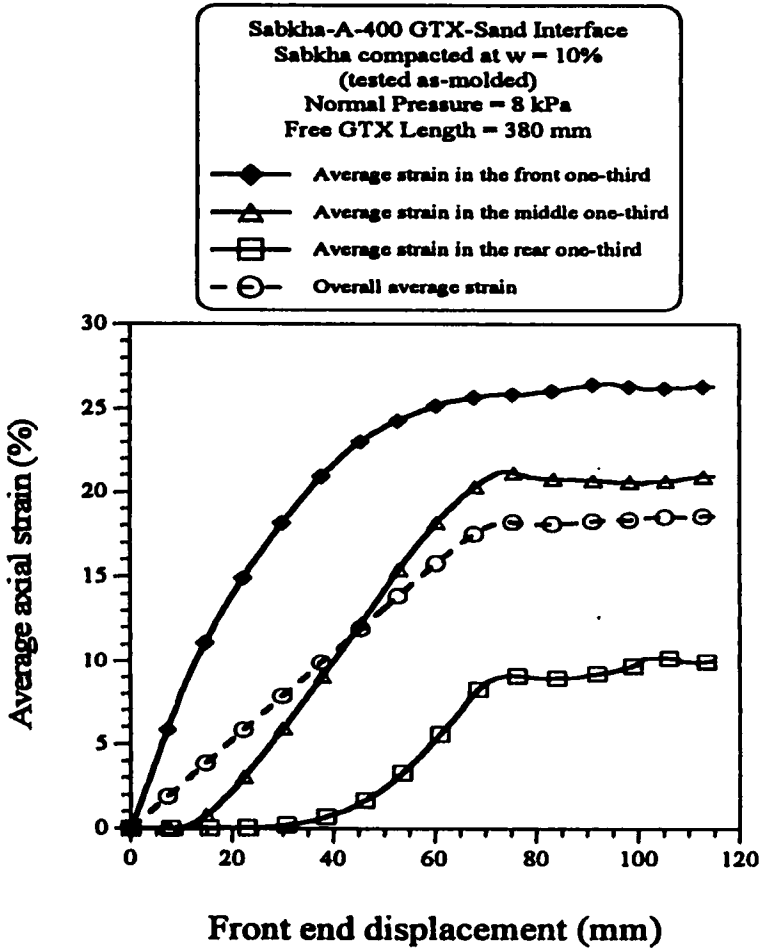

Fig. B1.38: Variation of average axial strain of A-400 geotextile with the front end displacement for sabkha-GTX-sand interface, at 8 kPa normal pressure, and 380 mm long free geotextile

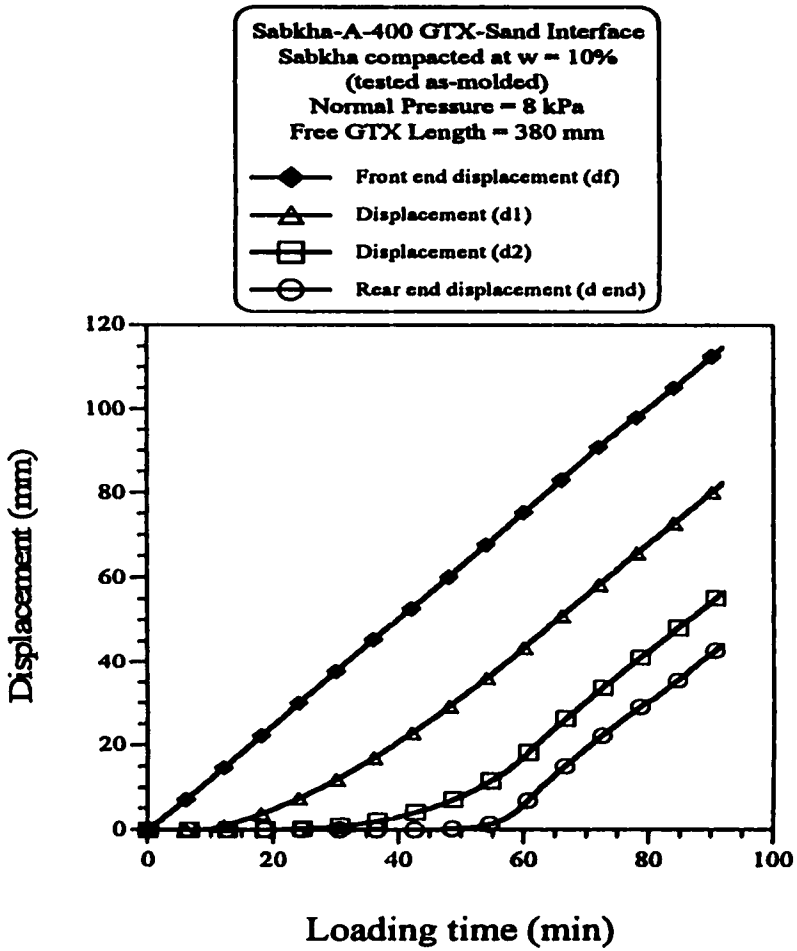

Fig. B1.39: Variation of displacement of A-400 geotextile with loading time for sabkha-GTX-sand interface, at 8 kPa normal pressure, and 380 mm long free geotextile

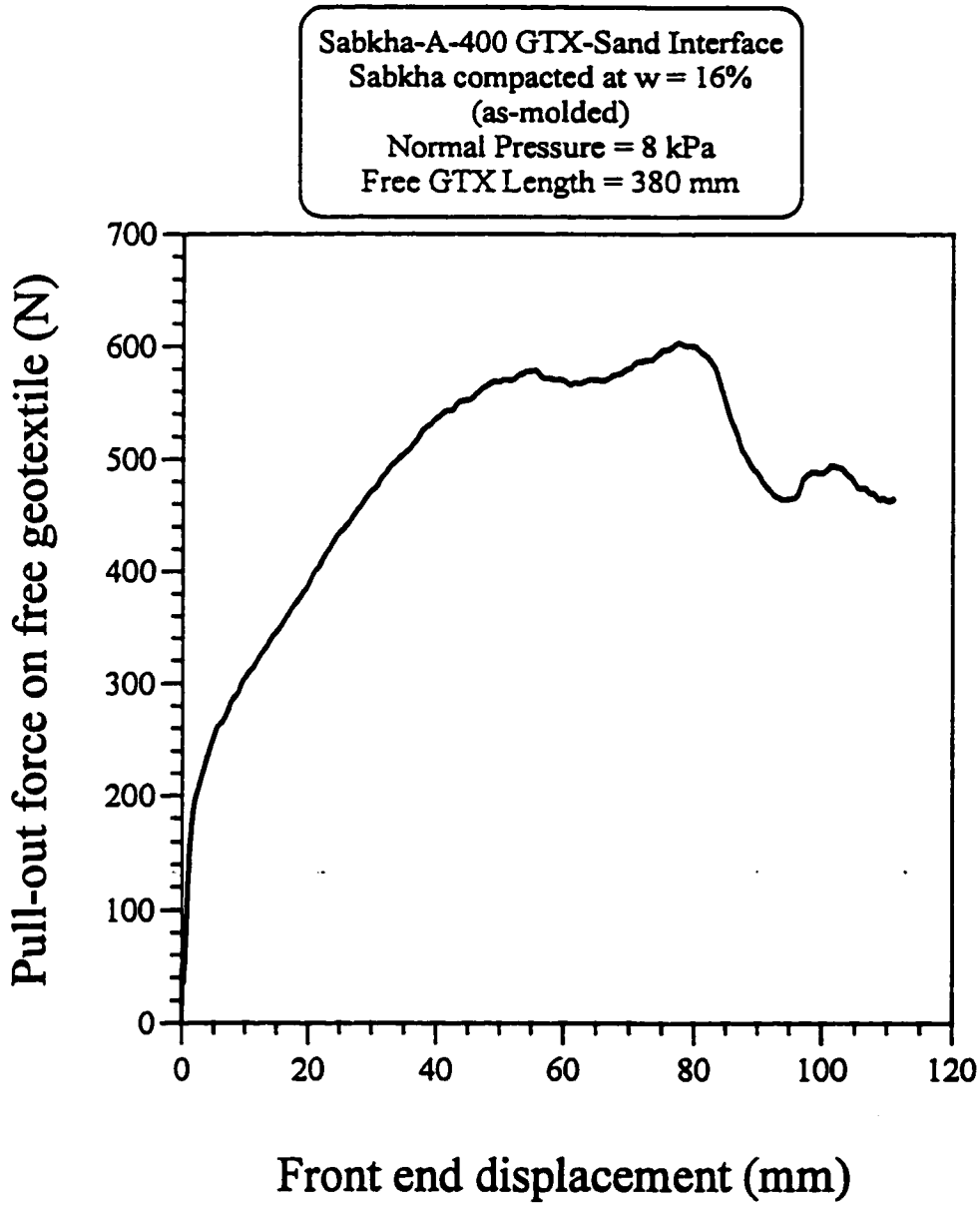

Fig. B1.40: Variation of the pull-out force on A-400 geotextile with the front end displacement for sabkha-GTX-sand interface, at 8 kPa normal pressure, and 380 mm long free geotextile

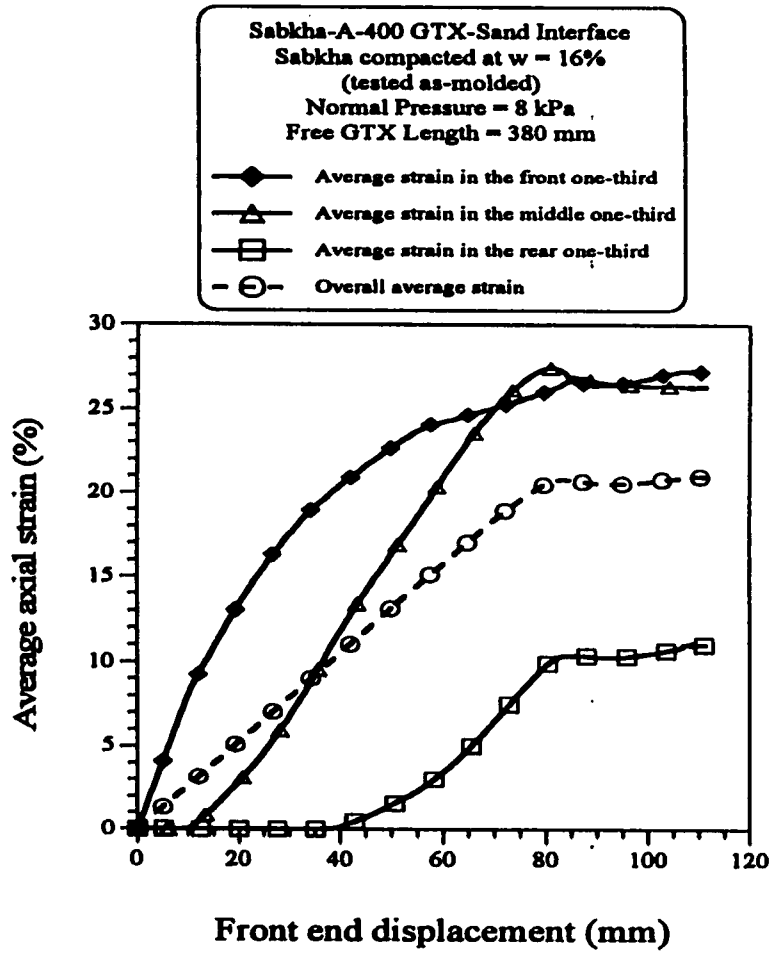

Fig. B1.41: Variation of average axial strain of A-400 geotextile with the front end displacement for sabkha-GTX-sand interface, at 8 kPa normal pressure, and 380 mm long free geotextile

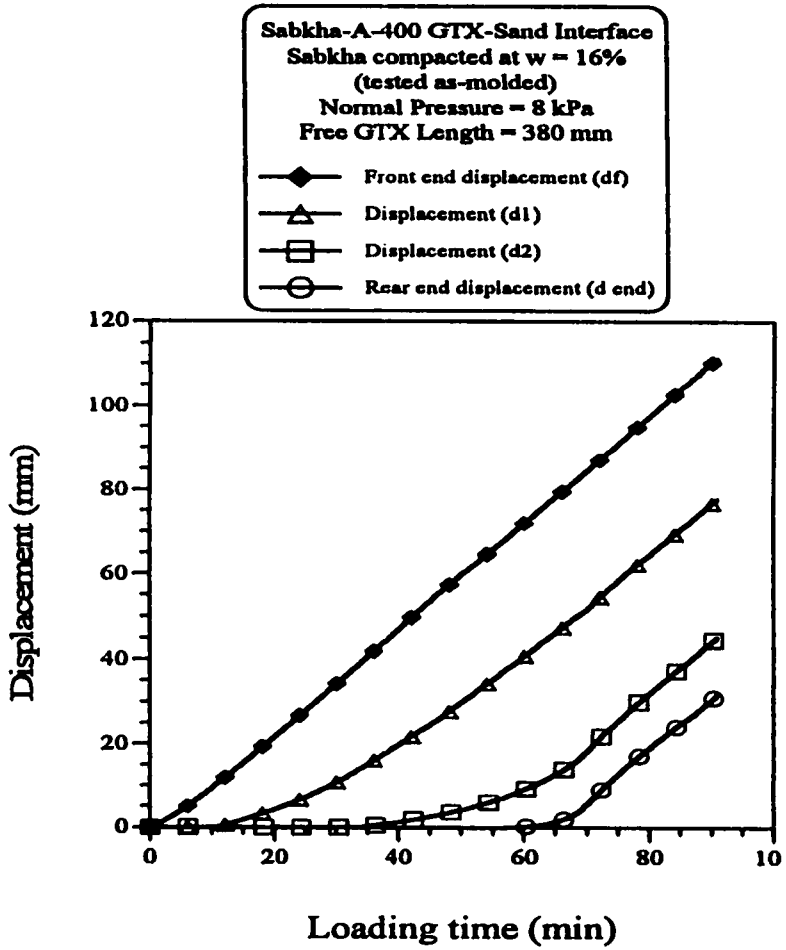

Fig. B1.42: Variation of displacement of A-400 geotextile with loading time for sabkha-GTX-sand interface, at 8 kPa normal pressure, and 380 mm long free geotextile

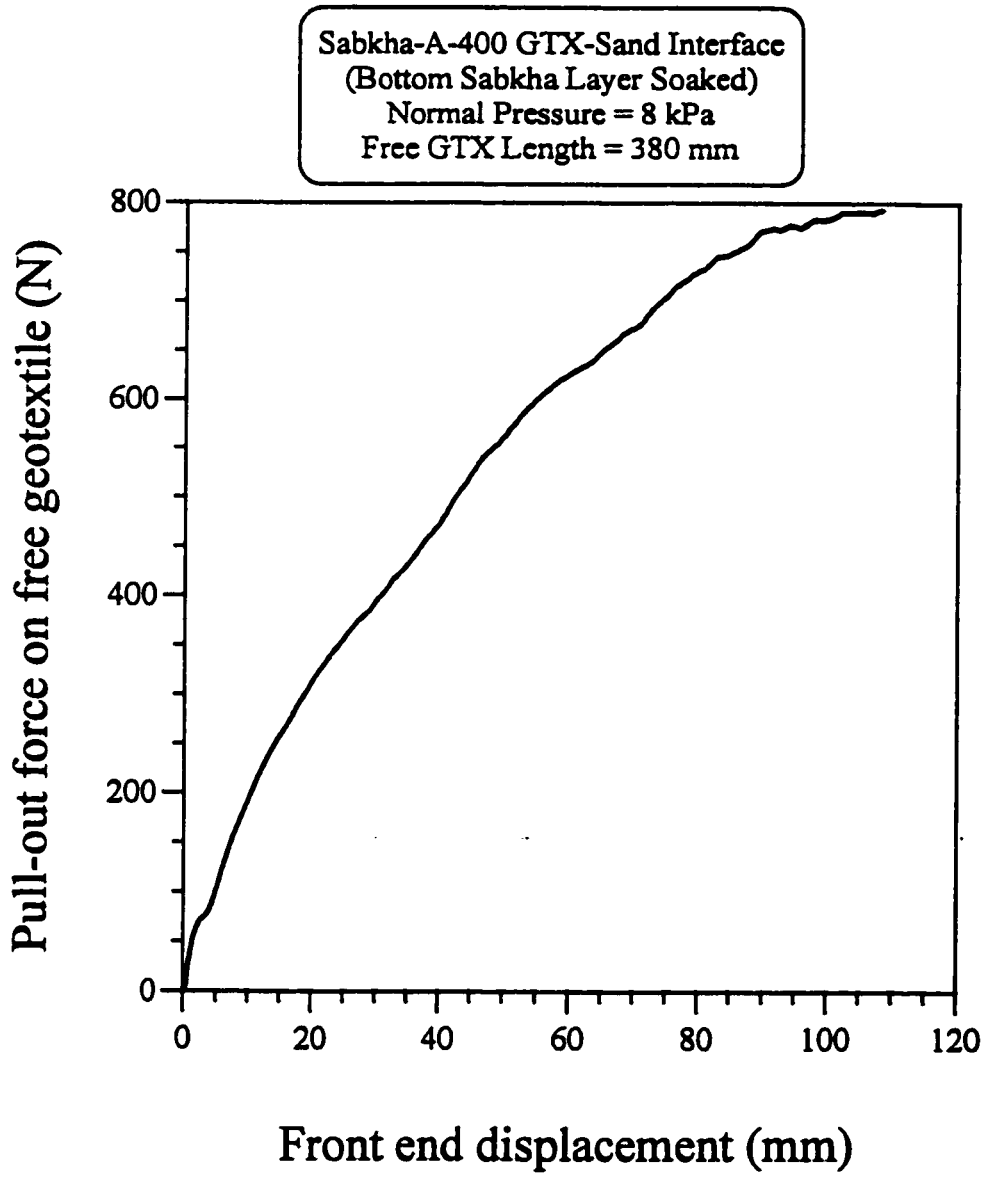

Fig. B1.43: Variation of the pull-out force on A-400 geotextile with the front end displacement for sabkha-GTX-sand interface, at 8 kPa normal pressure, and 380 mm long free geotextile for sabkha layer in the soaked condition

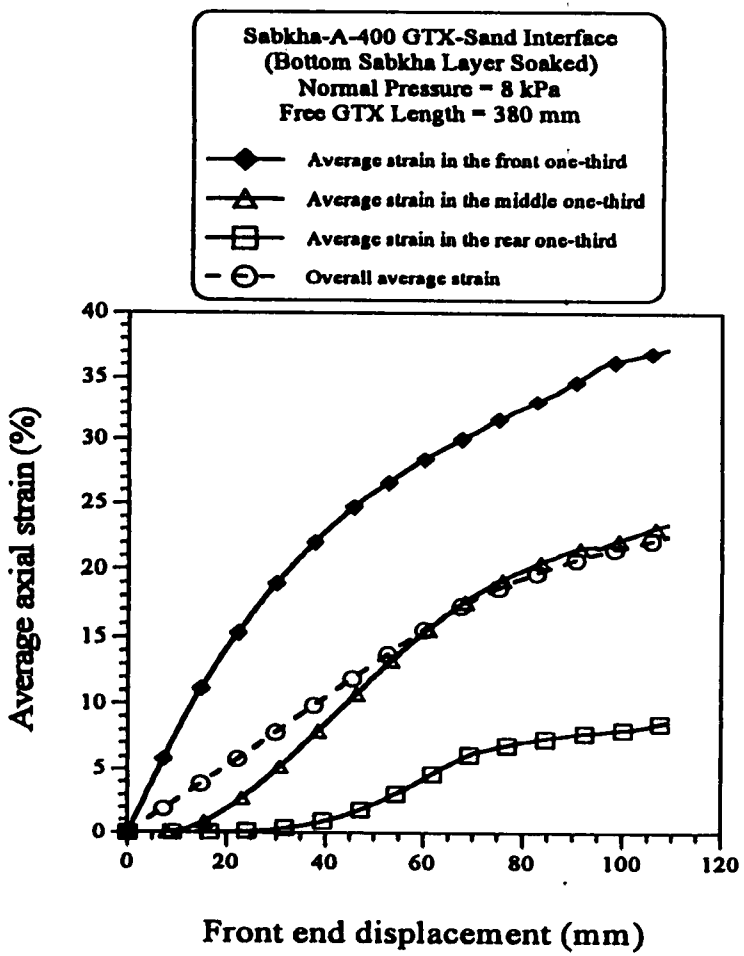

Fig. B1.44: Variation of average axial strain of A-400 geotextile with the front end displacement for sabkha-GTX-sand interface, at 8 kPa normal pressure and 380 mm long geotextile for sabkha layer in the soaked condition

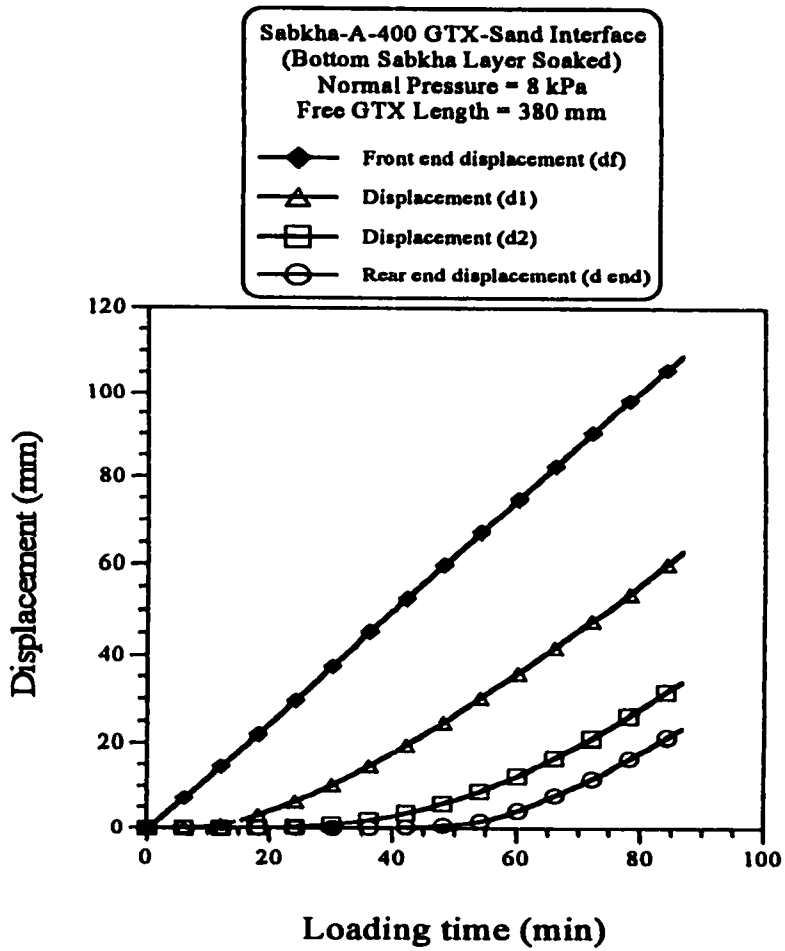

Fig. B1.45: Variation of displacement of A-400 geotextile with loading time for sabkha-GTX-sand interface, at 8 kPa normal pressure, and 380 mm long free geotextile for sabkha layer in the soaked condition

VITA

- Syed Muhammad Ali.
- Born in Lahore, Pakistan.
- Received Bachelor of Science in Civil Engineering from University of Engineering and Technology Lahore, Pakistan in September 1995.
- Worked as a Geotechnical Engineer with National Engineering Services Pakistan (Pvt.) Limited, NESPAK, Lahore, Pakistan from December 1995 to August 1997.
- Completed Master of Science in Civil Engineering from King Fahd University of Petroleum and Minerals, Dhahran, Saudi Arabia in September 1999.